HIGH THROUGHPUT IDENTIFICATION OF RARE CELL POPULATIONS BY FUNCTIONAL PHENOYPING

Syung Hun Han

A DISSERTATION

in Bioengineering

Presented to the Faculties of the University of Pennsylvania

in Partial Fulfillment of the Requirements for the

Degree of Doctor of Philosophy

2020

Co-Supervisor of Dissertation

_____

Daeyeon Lee

Professor of Chemical and Biomolecular Engineering

Co-Supervisor of Dissertation

_____

Junhyong Kim

Professor of Biology

Graduate Group Chairperson

_____

Yale E. Cohen

Professor of Bioengineering

Dissertation Committee

David Issadore, Associate Professor of Bioengineering

Arjun Raj, Professor of Bioengineering

Yongwon Choi, Professor of Pathology and Laboratory Medicine

ACKNOWLEDGMENTS

I would like to express gratitude for all the opportunities, supports, and privileges that made me to this point. I've been extremely privileged by the exceptional level of education that the University of Pennsylvania provided to me, generous emotional and physical support from my friends and colleagues, endless support in both research and personal life from both of my Principal Investigators, Professor Daeyeon Lee and Professor Junhyong Kim, and all the love from my family members.

With my linguistic ability, I probably can never sufficiently thank both of my principal investigators, Professor Daeyeon Lee and Professor Junhyong Kim. Frankly speaking, I personally never pictured myself as a Ph.D. even when I was applying for the Doctoral Program in Bioengineering, and even when I was admitted to it. I have to say that I am exceptionally fortunate to have both professors as my PI. As a co-advised student, I enjoyed exploring both labs and learned lots of diverse research topics from all the group members. Both Professor Daeyeon Lee and Professor Junhyong Kim always guided me toward the appropriate research path and have always cared for me professionally and personally. Again, I am really, sincerely grateful for both of you, Professor Daeyeon Lee and Professor Junhyong Kim.

Thank you so much to my committee members, Professor Yongwon Choi, Professor Arjun Raj, and Professor David Issadore, who have continuously and kindly given highly valuable suggestions, inputs, and very insightful opinions at every committee meeting during my Ph.D. program.

I also would like to thank all of my colleagues, who helped my research a lot. I would also like to thank Dr. Yunhee Jeong and Dr. Matthew Walsh from the Choi lab for continuously working with me on T cell culture protocol. I would also like to thank Jean

Rosario from the Kim lab for helping me with the automated microscopy system setup. I also would like to thank Seung Yub Han, Jihoon Kim, and Catherine Lucey from the Kim lab for helping with computational analysis, sequencing, and cell culture. I would also like to thank Dr. Stephen Fisher, Dr. Erik Nordgren, and Da Kuang from the Kim lab for lots of help in research. I also would like to thank microfluidics subgroup members in Lee lab for continuously working with me to make a breakthrough in many microfluidic-based challenges.

Thank you to Professor Bomyi Lim for advising and assisting in developing the kinetic modeling system and a joyful chat time that relieved my research stress a lot. I also would like to thank Dr. Bang Jin Kim for helping me get through the difficult times in the Ph.D. program with lots of emotional support.

I probably could not have achieved this far without all the support from my family. I thank my father, Sang Woo Han, my mother, Sun Hee Park, my brother, Seung Yub Han, for all the love and support they've given me. My parents were always passionate about education, and with the honesty and tenacity that they've passed down to me, I was able to complete this Ph.D. program.

Lastly, I would like to thank my beautiful wife, Min Ju Lee, and my lovely daughter, Sophia Yesung Han. My wife has always supported my research and helped me to achieve this far by her love. She fed me, made me go to work, made me write a paper, loved me, and took care of me all the time. She gave birth to my beloved daughter, Sophia, so that I can embrace myself to achieve more as a father. Now that I am finishing up my degree, I would like to do the same for her as she completes her Ph.D. program. I would also like to thank my lovely daughter, Sophia, for being a healthy, lovely baby, making me smile and happy, and inspiring me to pursue further. Thank you to everyone.

ABSTRACT

HIGH THROUGHPUT IDENTIFICATION OF RARE CELL POPULATION BY FUNCTIONAL PHENOTYPING

Syung Hun Han

Daeyeon Lee and Junhyong Kim

Identification of rare cell types can enable early detection of disease and enhance the fundamental understanding of cellular processes. Most current approaches to identify rare cell populations rely on static phenotyping. Although static phenotyping can readily differentiate cells, these methods cannot fully uncover individual cells' dynamic heterogeneity. Cell-to-cell heterogeneity in metabolic profiles has recently been suggested as a critical indicator for their potential cell fate decision. The flexibility of metabolic reprogramming has been raised as a requirement for memory T cell formation, and a similar notion applies to the cancer cell metastasis. It suggests that metabolic profiling, which is part of functional phenotyping, can give a valuable insight into the disease cure and prevention. Such a metabolomics study is currently highly limited due to inadequate research tools. Recently, several approaches have been developed to enable functional phenotyping and now allow some basic single-cell level functional phenotyping. However, these approaches either lack throughput or selective recoverability or analytical and monitoring system.

This thesis presents a microfluidic-based device that allows rare cell population identification by on-chip dynamic functional phenotyping and analysis, followed by highly

selective recovery of cells for subsequent transcriptomic study. Using this system, we investigate a seemingly homogeneous static phenotypic cell population and de-cluster the subpopulation based on its distinctive dynamic functional phenotype. The high-throughput dynamic monitoring of the individual cell and functional probe's reactions is computationally analyzed using a machine learning technique. The subpopulations are subsequently sorted. Using a novel photoactivated selective recovery (PHASR) membrane, target cells are precisely retrieved, and single-cell level RNA sequencing is conducted. The individual transcriptomic profile is studied in parallel to the observed functional phenotype to investigate the relationship between metabolomics and transcriptomics. Kinetic modeling enables the demultiplexing of simple metabolic profiles into well-defined biological processes. With single-cell level RNA sequencing and high-throughput metabolic profiling, a valuable correlation is established between metabolomics and transcriptomics. Single-cell level heterogeneity in the metabolic profile can be related to the gene expression difference.

This thesis shows a successful demonstration of capability for high throughput single-cell level functional phenotyping, computational kinetic modeling system that can decipher the observed functional phenotype to more meaningful biological reaction rates, high-throughput and high-selective recovery microfluidic system that allows single-cell RNA sequencing, and the establishment of the relationship between the transcriptome and functional phenotype. We believe this work can positively impact the fields of single-cell study, microfluidics, and image-based computational analysis.

TABLE OF CONTENTS

LIST OF TABLES

LIST OF FIGURES

CHAPTER 1

INTRODUCTION

1.1. SIGNIFICANCE

Recent advances in single-cell RNA sequencing technology revealed unexpected heterogeneity within a single population of cells.[1] A cell population with identical genomic DNA has been previously assumed as homogeneous.[2] Surprisingly, a single-cell population of near genetic identity under the same microenvironment showed significant variance in gene expression and phenotypes.[3,4] Such heterogeneity was beyond the variation that can be explained by the degree of genetic variation.[3] Before single-cell RNA sequencing results, scientists have been working with population-level studies partly due to the belief that it is unnecessary to conduct a single-cell level study and partly due to the technical difficulty.[5] With the advance of sequencing technologies, single-cell level RNA sequencing became feasible, and scientists were able to discover the heterogeneity within the population of cells with identical genomic DNA.[6–8] One recent study showed that the identical cell population treated with siRNA exhibited a different gene expression level from individual cells.[1] As shown by many studies, the cell population's mean gene expression level cannot serve as an accurate representation of multiple cells' gene expression. Such misrepresentation suggests that the population-level study can mask the underlying individual heterogeneity. Pooled average data of heterogeneous cells is not only masking individual single-cell heterogeneity but also can be misleading.

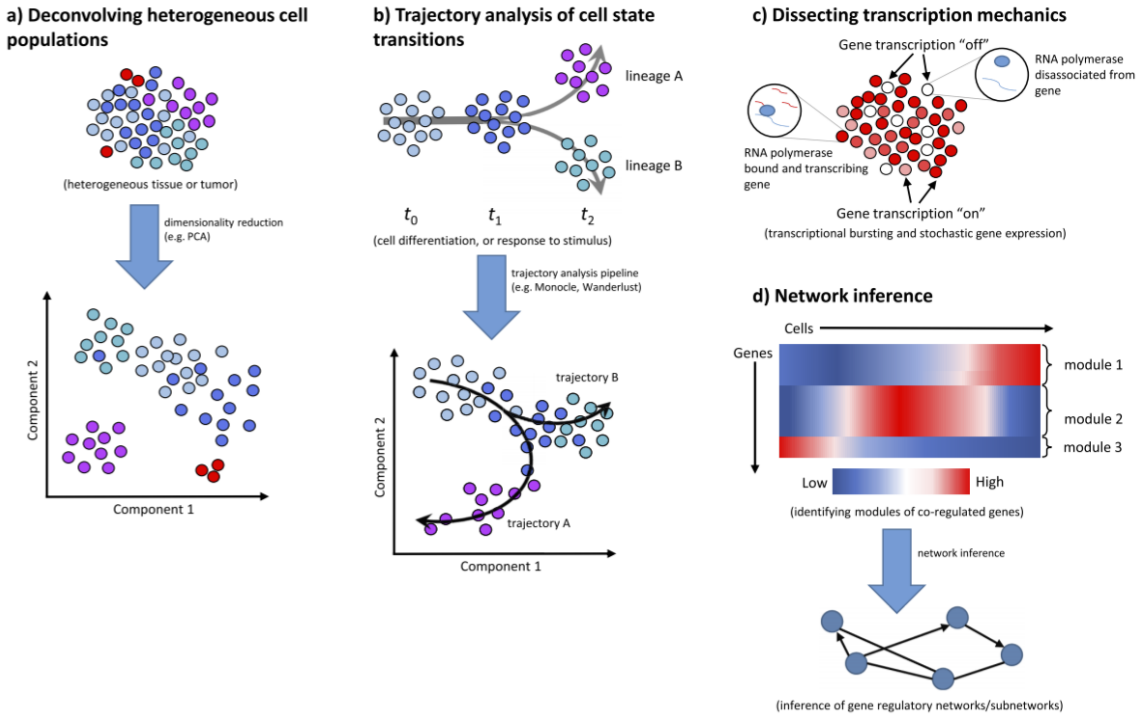

Figure 1.1. Single Cell Heterogeneity, Subsets, and Trajectories. With sufficient single-cell level resolution data, the scRNA-seq result can divulge subsets of an identical population. With dynamic observation added, it can also unveil the trajectories of differentiation. Adapted from Liu al.[9]

Since then, numerous biologists, immunologists, and pathologists have highlighted the potentials of a single-cell level study to unveil the cause of heterogeneity and to harness the inherent heterogeneity for potential clinical purposes.[5,10–15] The motif and driving mechanism for single-cell heterogeneity have not been fully explored yet. Further in-depth study of single-cell heterogeneity is needed to answer all the mysteries around the single-cell heterogeneity and potentially take advantage of inherent heterogeneity.[4] Population-level studies, which has been a standard so far, do not have sufficient data resolution to be de-multiplexed into millions of individual cellular signals. On the contrary, high-throughput observations of single-cells can be aggregated, mixed, and averaged to show population-level behaviors. As scientific instruments' capacity

enhances, it is now highly recommended to conduct higher resolution studies for better understanding, as shown in **Figure 1.1**. With enhanced resolution of studies, it is possible to unveil the seemingly homogeneous population into distinctive subsets and fit the subsets to trajectories. Dynamic high-throughput single-cell observation not only allows researchers to establish the pathway of cellular differentiation, but also allows us to unveil and predict the future trajectories of the cellular differentiation.[2,16] Even though the future trajectory projection cannot be completely accurate, estimates from single cells can effectively narrow down the ranges of the trajectory. It can benefit disease-related researchers, including but not limited to oncologists and vaccine developers.

Single-cell level heterogeneity is still full of mystery in various aspects. Numbers of hypotheses have been raised to explain the origin and the necessity of the single-cell heterogeneity, but none has been proven in a conclusive way.[3,4] Stochastic asymmetric cell division, bet-hedging, cell-to-cell interaction are the examples of previously suggested hypotheses for single-cell heterogeneity. Recent studies suggest that such seemingly negligible and common heterogeneity may be tightly linked to cell fate plasticity.[17–19] More specifically, immunologists recently suggested that the individual cell's metabolism may be the key indicator for the immune cell fate decision or plasticity. A new field of immunometabolism has been established, and scientists have been relentlessly investigating to improve metabolic profiling technology.[20–23] Along with transcriptomics and proteomics, metabolomics is the emerging frontier.[24–29]

This thesis aims to develop a platform that can improve upon the current technologies of single-cell level study, to broaden the types of feasible phenotyping, to build an accurate profiling algorithm, and to potentially offer the flexibility of combining multiple omics profiling. To my best knowledge, no studies have been reported on the

high-throughput single-cell level metabolic profiling that can be combined with the transcriptomic profiles to date. Metabolomics, in conjunction with transcriptomics, can potentially open a new field of multi-omics study for single-cell studies. Hence, the development of the proposed device and the system can bring significant impacts on many fields of studies such as molecular biology, immunology, oncology, and any fields that can harness single-cell heterogeneity and multi-omics investigation.

1.2. CURRENT APPROACHES FOR SINGLE CELL STUDY

Single-cell population study requires isolation and subsequent characterization of rare subpopulations: standard methods include Fluorescence-Activated Cell Sorting (FACS), Magnetic-Activated Cell Sorting (MACS), microfluidic device, and micro-capillary-well array, as shown in **Figure 1.2**.[1,6,17,30–40] All of the methods mentioned above provide great ways for the single-cell level study. Still, since none of them were developed with the intention of the high-throughput single-cell level study, shortcomings exist in all methods. FACS and MACS allow the highest throughput for single-cell level study, but they require expensive antibodies and magnetic beads for the detection phase.[41] Besides, the generally high price of the instrument itself is a handicap for its popular usage. FACS and MACS machines can actively detect, read signals, and separate cells on tens of thousands per-second basis. However, these two only allow static surface phenotyping and do not offer any kind of dynamic phenotyping.[42] Single-cell heterogeneity within an identical population is unlikely to be observed using the surface phenotyping as they will all express the same surface markers. Subsets of the population may express different magnitudes of surface markers such as high and low. However, it is still an uncertain way of differentiating subsets within the population as the

borderline can be highly subjective. In summary, the high cost and inflexibility of assay types are the major shortcomings of the FACS and MACS.

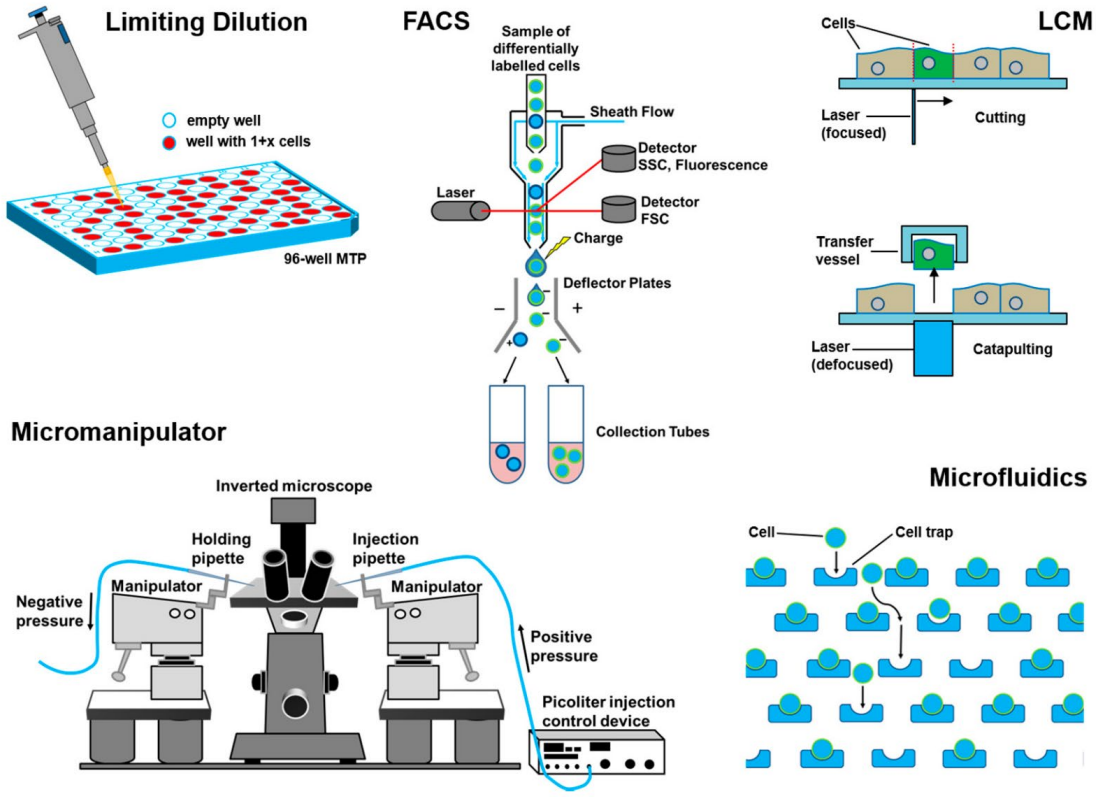

Figure 1.2. Current technologies for single-cell isolation. Current methods for single-cell isolations are limiting dilution, Fluorescence-Activated Cell Sorting (FACS), Laser Capture Microdissection (LCM), micromanipulator, and microfluidics. The highest throughput method is FACS, and the most flexible approach is micromanipulator. Adapted from Gross et al.[43]

On the contrary, LCM and micromanipulator offer the lowest throughput for the single-cell level study.[43] Still, at the same time, they offer the highest degree of experimental flexibility for all single-cell level research. As these methods entirely separate a single cell from the bulk and place it into an individual chamber, the researcher can exploit the full range of profiling and even the combination of functional

and surface phenotyping.[2,44] However, since a single cell must be manually separated from the bulk population, the procedure can be highly labor-intensive and time-consuming. The isolation of a single cell allows the researcher to exploit any aspects of the cellular characteristics or phenotype. Still, it comes with severe shortcomings such as increases in the required time and labor and a significantly reduced sensitivity. A higher volume of reagents is needed for individual experiments than any other technologies that use reagents. The higher amount of reaction volume increases the cost of the experiment and decreases the sensitivity threshold. For single-cell level studies, high sensitivity, as well as sufficient throughput, are two of the important requirements.

Limited dilution series is another technique that allows single-cell level study. This approach has been available for use for a long time as it does not require any sophisticated skills or instruments. With advanced fabrication techniques, a microcapillary array, a more advanced version of the limited dilution series, has been developed recently. Microcapillary array is composed of honeycomb-shaped wells that are in the size range of tens of microns. Application of the cell suspension on the microcapillary array results in even-spreading of the liquid into individual wells. The distribution of cells to each well entirely follows the Poisson ratio distribution. Due to the small size of individual wells, the cell suspension remains locked in the wells via surface tension even after removing the bottom sealing wrap. This method offers highly time-efficient single-cell isolation and great flexibility for phenotyping. Although the well size is small enough for highly sensitive functional phenotyping, the overall height of the well is 1 mm, which puts the aspect ratio of the well to 1:250,000. With the dropped sensitivity due to the limited well height fabrication technique, another shortcoming of the

microcapillary array is the downstream processes' flexibility. Individual well must be laser-focused, released and collected to another vial for the follow-up processes, and it can be highly susceptible to contaminations.

Recently, microfluidics has emerged as a powerful platform to enable single cell studies. It offers throughput that is still slightly lower than the FACS and MACS, but is significantly higher than the LCM and micromanipulators. The most significant advantages of microfluidics are flexibility and customizability. Depending on the experimental needs, the system can be fully tailored from the design to the fabrication method to fit the precise needs of the experiment. With all the benefits of the instruments combined, detection and detailed investigation of functionally rare cell populations will greatly benefit from a future platform device that (a) can actively and rapidly compartmentalize single cells, (b) can sensitively interrogate single cells with desired probes for complete single-cell phenotyping, (c) is not limited to surface phenotyping, (d) is equipped with flexibility of downstream processes such as the addition of stimulators, inhibitors and library preparation for sequencing.

In particular, our design focuses on high capacity (tens of thousands of cells), as well as inexpensive device design and fabrication process. The system allows in-depth investigation and correlation of observed functional phenotype with the sequenced transcriptome. The device will provide several advantages, including, but not limited to, forming a completely isolated, yet fully mobile, reaction chamber for a single cell that ensures single-cell level phenotyping and facilitates further manipulation.

1.3. FORMATION OF MEMORY T CELL

The immune system must retain a persistently high number of immune cells of great heterogeneity, which is essential for burst adaptiveness to the changing environment.[45] Therefore, single-cell level heterogeneity must be well utilized by the immune system. An immune response is formulated by the cooperation of various immune cells, depending on the pathogen type.[46] Innate immunity and adaptive immunity interact closely to provide a highly protective, yet tolerant enough, immunity to the host against the hostile environment.[47] Harmonious innate and adaptive immune cells keep the host healthy. In most cases, the immune response involves macrophage, dendritic cells, B cells, and T cells to independently yet interactively work to clear out the pathogen. The T cell is one of the leading players in our immune system. Individual immune cells have their critical roles as the individual function is directly related to other immune cell roles. Antigen-presenting cells like macrophage and dendritic cells continuously inspect the system, and upon infection, the system utilizes all immune cells for swift antigen clearance. For example, the antigen-presenting cell must be first detected by the major histocompatibility complex II (MHC II) and get scanned by the CD4+ helper T cells. This detection calls out for the subsequent downstream processes, such as calling B cells to make a large number of antibodies against the pathogen or recruit macrophage for direct engulfment.

Beyond the heterogeneity of the immune cell types, functional phenotypic heterogeneity was proven to be critical for flawless immunity.[22] In the case of an adaptive immune system, however, the heterogeneity can be limitless. Therefore, a detailed investigation to better understand the single-cell immune system heterogeneity can enhance our immune system knowledge. A recent study also revealed significant

functional heterogeneity in phenotypically homogeneous T cell populations and a potential that the functional phenotypic heterogeneity may serve as a guideline for cell fate decision.[48,49] Importance of functional phenotyping for immune cells has been emphasized significantly from papers on immunometabolism.[21,22] Simple surface phenotyping cannot actively sort subpopulations of specific immune cell types. Detailed functional phenotyping technique at single-cell level is likely to benefit in-depth appreciation of immune cell heterogeneity.[23]

Under the quiescent state, various populations of CD8+ Naïve T cells reside in the system with minimal numbers of individual types.[46,50–53] Upon infection, when the pathogen is detected by the immune system, specific naïve T cell with the corresponding T Cell Receptor (TCR) is activated and differentiates into the CD8+ effector T cells. Upon activation, the naïve T cell goes through significant changes in their metabolic profile. This metabolic reprogramming changes the T cell to utilize the catabolic metabolism instead of the anabolic metabolic pathway of the Krebs cycle.[19,54–57] The functional differences between the naïve T cell and the effector T cell are likely the result of the metabolic reprogramming.[20,58,59] The effector T cell concentrates on vigorous proliferation via glycolysis, which is the main pathway of metabolism for most cancer cells. The metabolic reprogramming may be necessary as oxygen can be the bottleneck for such rapid expansion. In return, these metabolic reprogramming may change the metabolic pathway of the effector T cell, wholly or partially. It is still unknown whether the metabolic change makes the effector T cell solely utilize the Warburg metabolism and shut off the aerobic metabolic pathway entirely or partially.[60]

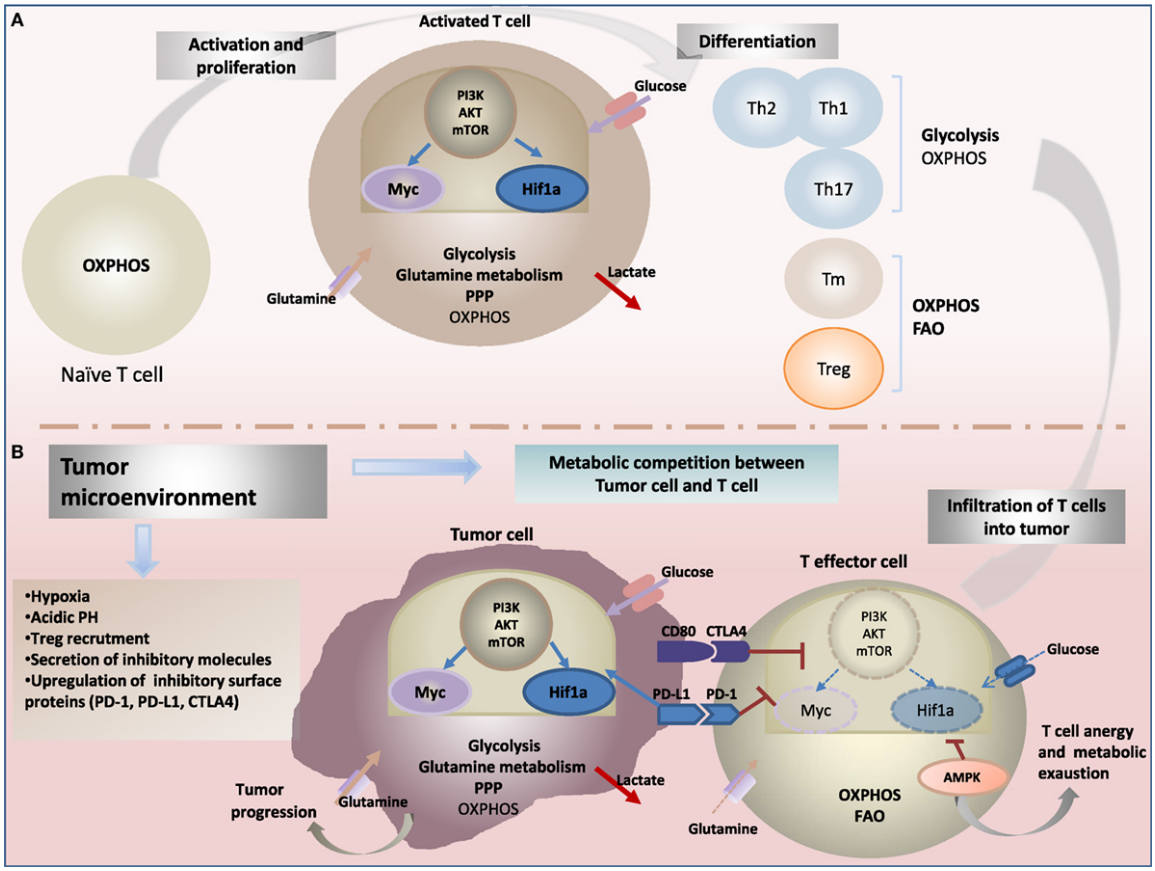

Figure 1.3. Metabolic pathways of naive, effector, and memory T cells. Illustration of various metabolic profiles and the metabolic reprogramming the T cells go through for the differentiation. Adapted from Kouidhi et al.[61]

Once the effector T cells reach an appropriate level of expansion, they effectively clear the pathogen out of the system. A highly expanded population of effector T cells is burdensome once the system is clean. As the necessity drops, most of the effector T cells die by apoptosis to prevent unnecessary glucose waste. Not all of the effector T cells die by apoptosis, and a small portion of the effector T cells further differentiate themselves.[53,62–73] This secondary differentiation is achieved by another metabolic reprogramming that switches the effector T cells' metabolic pathway again. These secondary differentiated T cells are memory T cells that mainly live on aerobic quiescent

metabolic pathways like normal cells. As a result, memory T cells goes through two rounds of metabolic reprogramming either partially or wholly, as shown in **Figure 1.3**.

Since it has to go through the two successful metabolic reprogrammings, the memory T cell populations' precursor may possess a unique metabolic profile. The subsidiary metabolic pathway profiles are likely to be a crucial functional phenotype along with the primary metabolic pathway profile. Fatty acid oxidation is another crucial energy-generating pathway. The capability to utilize the fatty acid oxidation was recently proposed to be a required feature to fully differentiate into memory T cells.[64] Using the novel high-throughput functional phenotyping device that we developed, we might closely investigate the various metabolic profiles of the effector T cells and correlate the transcriptomic profiles to unveil the potential cell fate plasticity and the requirement for the secondary differentiation of the effector T cells. Correlating metabolomics and transcriptomics can divulge the hidden driving mechanism of the memory T cell differentiation. Unraveling the hidden mechanism will inform the researchers of which genes or parts of the cells to manipulate for its ultimate and optimal use. For instance, memory T cell formation rate can be enhanced so that a vaccine's dosage can be reduced to minimize the typical side-effects of the vaccines. In other cases, if specific diseases' immunity formation rate is rare, one can artificially enhance the immunity formation rate against it so that the patients can fight off the pathogen within their own immune systems. As the last line of the defense of our body, the ability to manipulate the immune system at will is undoubtedly advantageous for all human beings.

1.4. CANCER CELL METABOLISM

A new cell population has been added in this dissertation as a potential target cell population due to the unexpected pandemic situation that prevented experiments on primary T cells. As primary cells like the effector T cells require animal facility operation, it became difficult to get sustainable supplies of the effector T cells for the parts of the thesis. As a result, an easily culturable cell line was chosen for the experiments' sustainable living cell supply. EL4 cell line is a mouse lymphoma cell line, which was chosen for the several reasons. Cancer cells are also highly heterogeneous by their nature, partly due to their high genetic mutation rates and partly due to inevitable single-cell level heterogeneity.

Cancer is one of the diseases that many scientists have tackled to conquer it as its occurrence rate and fatality rate make it one of the major diseases that kill a lot of people. Just like the T cell populations, cancer cells go through secondary differentiation, a metastasis.[58,74,75] Epithelial-like cancer cells differentiate into mesenchymal-like cancer cells and become circulating tumor cells. This circulating tumor cell can go through another metastasis and become mesenchymal-like cancer cells that spread to all the other parts of the body. Cancer by itself is invasive and life-threatening, and the ability to metastasis makes it a more deadly disease as it can theoretically spread to anywhere, making it impossible to be cleanly removed by surgical methods. As shown in **Figure 1.4**, a cancer cell must undergo several metabolic reprogramming steps to adapt to various microenvironments. Only a small portion of the primary cancer cell succeeds with metabolic reprogramming and make the metastasis happen, and the same occurs for the reverse metastasis at the new loci. The success rate of twice metabolic reprogramming might be comparable to the memory T cell populations' formation rate.

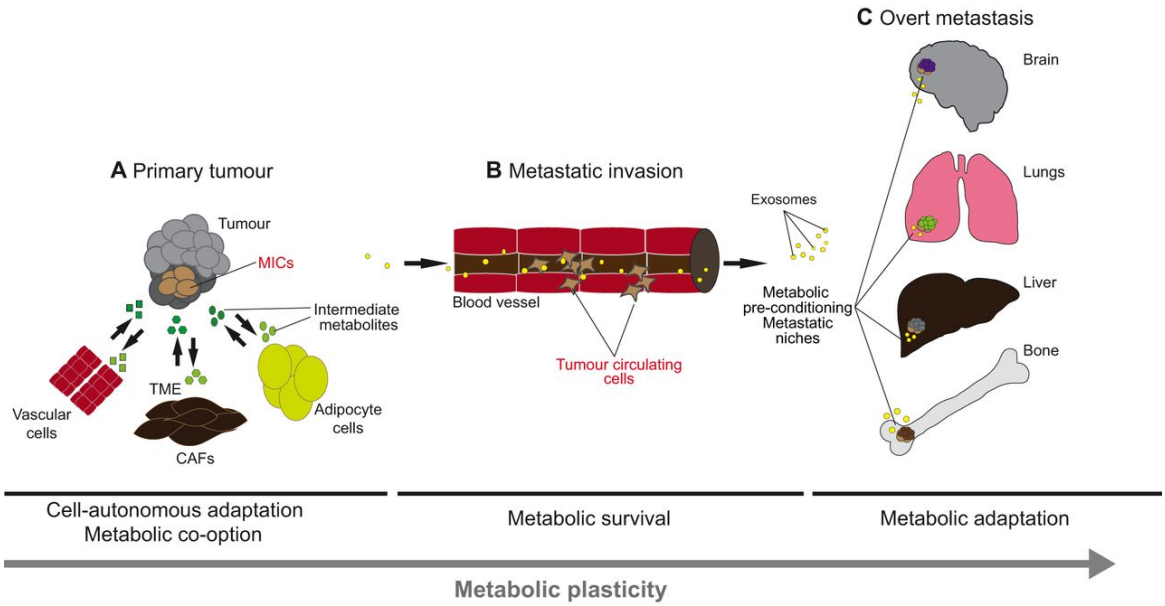

Figure 1.4. Metabolic reprogramming and adaptation of cancer cells. This figure shows the metabolic plasticity is increasing with the cancer metastasis differentiation. It goes through several metabolic reprogramming to spread itself to various loci of the body. Adapted from Pascual et al.[74]

Furthermore, detailed metabolomics of cancer cells may allow one to envision the precursors of the cells that have a higher chance of metastasis. Co-investigation of metabolomics and transcriptomics can also bring a new insight into which gene expression is necessary for metabolic reprogramming. This new insight can potentially guide new therapeutic developments for metastasis suppression to patients. Such discovery can also allow scientists to potentially suppress the cancerous region's specific metabolic pathway to prevent further metastasis and cancer spread.

1.5. MICROFLUIDICS FOR FUNCTIONAL PHENOTYPING

Microfluidics, without dispute, offers the most versatile and custom-tailored experimental setup for most types of research. Microfluidics has evolved to a great extent over the last few decades in areas such as throughput, solvent compatibility, ease

of fabrication, etc.[76,77] Polydimethylsiloxane (PDMS) microfluidics is the most conventional and the most widely-used microfluidics chip in the field due to its ease of moldiness, optical transparency that allows easy visualization, and the cheap fabrication cost.

Fabrication of microfluidic devices is relatively simple as long as the facility with the appropriate instrument is in the vicinity. However, a cleanroom facility is required if a highly sophisticated device design needs to be imprinted immaculately. Only a UV light source, a spin coater, and hot plates are needed for conventional microfluidic device fabrications. The simulation software that can accurately predict the fluid mechanics within the microfluidic devices has also evolved significantly to minimize trial and error of the multiple device designs and fabrications.

Microfluidics can effectively and effortlessly isolate the cells that are distinctive in their physical characteristics from a pool of cells even without fluorescent or magnetic markers.[36,78] Using multiple pillars and a highly tuned flow rate, microfluidic devices can separate cells of distinctively different sizes. Such a size-based separation technique has been continuously improving. Many devices have been developed that co-utilizes sheath-flow based size separation and magnetic field based size separation for better size separation control. Along with the size-based separation, various physical characteristics assessment tools have been developed using microfluidics, such as deformability testing.[79] Cellular deformability is an important characteristic that may be vital to its function. For cells that must stretch and be elastic, one of the functional heterogeneities among the Actin populations is elasticity, as it is highly correlated with branching capability.[80] Recent study also showed that the cell's deformability is predictive of metabolic profile and successfully sorted out cancer cell subpopulation

based on glycolysis differences.[81] It is a very innovative method to correlate the cells' physical characteristics with metabolomics and to provide excellent throughput as it does not involve dynamic observation. Nonetheless, the approach lacks the choice for metabolomics study; it cannot be extended to other metabolic profiles such as oxygen consumption and fatty acid consumption.

1.6. CONCLUSION

It is vital to study single-cell level heterogeneity as it hides lots of mysteries from the researcher. Unraveling these hidden mechanisms can allow scientists to understand mother nature more and potentially utilize it for the living organism's well-being. There are two target cell populations in this thesis: primary T cells and mouse lymphoma cell line. Unfortunately, not many studies have been conducted with the primary T cell, as the initial phase of the thesis used mouse lymphoma cell line for the ease of culture, and the later phase of the thesis also had to use mouse lymphoma cell line due to the unexpected pandemic situation. However, the mouse lymphoma cell line study might be positively correlated with T cells, although not precisely, in a way to show the correlations between the metabolomics and the transcriptomics. The current technologies available for single-cell studies all have some extent of shortcomings that prevent truly high-throughput functional phenotyping of single cells. Improving and innovating new instruments or devices for better research is one of the unremitting goals of researchers. This thesis proposes utilizing microfluidic devices to tackle single-cell related metabolic profiling issues of the current technologies to provide a new innovative single-cell level high-throughput functional phenotyping device. Not only limited to the microfluidic device fabrication, but this thesis also proposes to develop a complete and

automated system that automatically conduct dynamic observation and perform computational analyses of the observed profiles. The novel and innovative device will also have unique functionality built-in for highly selective recovery of the target cell for downstream sequencing analysis.

1.7. REFERENCES

1. Bertozzi CR, Francis MB, Hsiao SC, et al. Integrated microfluidic bioprocessor for single-cell gene expression analysis. *Proc Natl Acad Sci*. 2008;105(51):20173-20178. doi:10.1073/pnas.0806355106

2. Hwang B, Lee JH, Bang D. Single-cell RNA sequencing technologies and bioinformatics pipelines. *Exp Mol Med*. 2018;50:96. doi:10.1038/s12276-018-0071-8

3. Ackermann M. REVIEWS A functional perspective on phenotypic heterogeneity in microorganisms. *Nat Publ Gr*. 2015;13(8):497-508. doi:10.1038/nrmicro3491

4. Dueck H, Eberwine J, Kim J. Variation is function: Are single cell differences functionally important?: Testing the hypothesis that single cell variation is required for aggregate function. *BioEssays*. 2016;38(2):172-180. doi:10.1002/bies.201500124

5. Yuan G-C, Cai L, Elowitz M, et al. Challenges and emerging directions in single-cell analysis. *Genome Biol*. 2017;18(1):84. doi:10.1186/s13059-017-1218-y

6. Sarkar S, Cohen N, Sabhachandani P, Konry T. Phenotypic drug profiling in droplet microfluidics for better targeting of drug-resistant tumors. *Lab Chip*. 2015;15(23):4441-4450. doi:10.1039/c5lc00923e

7. Balagaddé FK, You L, Hansen CL, Arnold FH, Quake SR. Microbiology: Long-term monitoring of bacteria undergoing programmed population control in a microchemostat. *Science (80-)*. 2005;309(5731):137-140. doi:10.1126/science.1109173

8. Hatch AC, Fisher JS, Tovar AR, et al. 1-Million droplet array with wide-field fluorescence imaging for digital PCR. *Lab Chip*. 2011;11(22):3838-3845. doi:10.1039/c1lc20561g

9. Trapnell C, Liu S. Single-cell transcriptome sequencing: Recent advances and remaining challenges. *F1000Research*. 2016;5:182. doi:10.12688/f1000research.7223.1

10. Lyu F, Blauch LR, Tang SKY. *Quantifying Phenotypes in Single Cells Using*

Droplet Microfluidics. Vol 148. 1st ed. Elsevier Inc.; 2018. doi:10.1016/bs.mcb.2018.09.006

11. Sinha N, Subedi N, Tel J. Integrating Immunology and Microfluidics for Single Immune Cell Analysis. 2018;9(October):1-16. doi:10.3389/fimmu.2018.02373

12. Kurd NS, He Z, Louis TL, et al. Early precursors and molecular determinants of tissue-resident memory CD8 $^{+}$ T lymphocytes revealed by single-cell RNA sequencing. *Sci Immunol*. 2020;5(47):eaaz6894. doi:10.1126/sciimmunol.aaz6894

13. Savas P, Virassamy B, Ye C, et al. Single-cell profiling of breast cancer T cells reveals a tissue-resident memory subset associated with improved prognosis. *Nat Med*. 2018;24(7):986-993. doi:10.1038/s41591-018-0078-7

14. Jackson-Holmes EL, McDevitt TC, Lu H. A microfluidic trap array for longitudinal monitoring and multi-modal phenotypic analysis of individual stem cell aggregates. *Lab Chip*. 2017;17(21):3634-3642. doi:10.1039/c7lc00763a

15. Ng EX, Miller MA, Jing T, Chen CH. Single cell multiplexed assay for proteolytic activity using droplet microfluidics. *Biosens Bioelectron*. 2016;81:408-414. doi:10.1016/j.bios.2016.03.002

16. Kimmerling RJ, Lee Szeto G, Li JW, et al. A microfluidic platform enabling single-cell RNA-seq of multigenerational lineages. *Nat Commun*. 2016;7:1-7. doi:10.1038/ncomms10220

17. Kunz DJ, Gomes T, James KR. Immune cell dynamics unfolded by single-cell technologies. *Front Immunol*. 2018;9(JUN):1-8. doi:10.3389/fimmu.2018.01435

18. Papalexi E, Satija R. Single-cell RNA sequencing to explore immune cell heterogeneity. *Nat Publ Gr*. 2017;18(1):35-45. doi:10.1038/nri.2017.76

19. Das A, Sinha M, Datta S, et al. Monocyte and Macrophage Plasticity in Tissue Repair and Regeneration. *Am J Pathol*. 2015;185(10):2596-2606. doi:10.1016/j.ajpath.2015.06.001

20. Miller A, Nagy C, Knapp B, et al. Exploring Metabolic Configurations of Single Cells within Complex Tissue Microenvironments. *Cell Metab*. 2017;26(5):788-800.e6. doi:10.1016/j.cmet.2017.08.014

21. O'Neill LAJ, Kishton RJ, Rathmell J. A guide to immunometabolism for immunologists. *Nat Rev Immunol*. 2016;16(9):553-565. doi:10.1038/nri.2016.70

22. O'Neill LAJ, Pearce EJ. Immunometabolism governs dendritic cell and macrophage function. *J Exp Med*. 2016;213(1):15-23. doi:10.1084/jem.20151570

23. Artyomov MN, Van den Bossche J. Immunometabolism in the Single-Cell Era. *Cell Metab*. October 2020. doi:10.1016/j.cmet.2020.09.013

24. Clarke CJ, Haselden JN. Metabolic profiling as a tool for understanding mechanisms of toxicity. *Toxicol Pathol*. 2008;36(1):140-147.

doi:10.1177/0192623307310947

25. Bathe OF, Farshidfar F. From Genotype to Functional Phenotype: Unraveling the Metabolomic Features of Colorectal Cancer. 2014:536-560. doi:10.3390/genes5030536

26. Teslaa T, Teitell MA. Techniques to monitor glycolysis. In: *Methods in Enzymology*. Vol 542. Academic Press Inc.; 2014:91-114. doi:10.1016/B978-0-12-416618-9.00005-4

27. Sriyudthsak K, Shiraishi F, Hirai MY. Mathematical modeling and dynamic simulation of metabolic reaction systems using metabolome time series data. *Front Mol Biosci*. 2016;3(MAY):15. doi:10.3389/fmolb.2016.00015

28. Catchpole G, Platzer A, Weikert C, et al. Metabolic profiling reveals key metabolic features of renal cell carcinoma. *J Cell Mol Med*. 2011;15(1):109-118. doi:10.1111/j.1582-4934.2009.00939.x

29. Kumar R, Ghosh M, Kumar S, Prasad M. Single Cell Metabolomics: A Future Tool to Unmask Cellular Heterogeneity and Virus-Host Interaction in Context of Emerging Viral Diseases. *Front Microbiol*. 2020;11:1152. doi:10.3389/fmicb.2020.01152

30. Han A, Glanville J, Hansmann L, Davis MM. Linking T-cell receptor sequence to functional phenotype at the single-cell level. *Nat Biotechnol*. 2014;32(7):684-692. doi:10.1038/nbt.2938

31. Sarkar S, Sabhachandani P, Stroopinsky D, et al. Dynamic analysis of immune and cancer cell interactions at single cell level in microfluidic droplets. *Biomicrofluidics*. 2016;10(5). doi:10.1063/1.4964716

32. Sarkar S. T Cell Dynamic Activation and Functional Analysis in Nanoliter Droplet Microarray. *J Clin Cell Immunol*. 2015;06(03). doi:10.4172/2155-9899.1000334

33. Sarkar S, Cohen N, Sabhachandani P, Konry T. Phenotypic drug profiling in droplet microfluidics for better targeting of drug-resistant tumors. *Lab Chip*. 2015;15(23):4441-4450. doi:10.1039/c5lc00923e

34. Donnenberg AD, Donnenberg VS. Rare-Event Analysis in Flow Cytometry. *Clin Lab Med*. 2007;27(3):627-652. doi:10.1016/j.cll.2007.05.013

35. Kuang Y, Biran I, Walt DR. Simultaneously monitoring gene expression kinetics and genetic noise in single cells by optical well arrays. *Anal Chem*. 2004;76(21):6282-6286. doi:10.1021/ac049053f

36. Karabacak NM, Spuhler PS, Fachin F, et al. Microfluidic, marker-free isolation of circulating tumor cells from blood samples. *Nat Protoc*. 2014;9(3):694-710. doi:10.1038/nprot.2014.044

37. Zhou Y, Basu S, Wohlfahrt KJ, et al. A microfluidic platform for trapping, releasing and super-resolution imaging of single cells. *Sens Actuators B Chem*.

2016;232:680-691. doi:10.1016/j.snb.2016.03.131

38. Rettig JR, Folch A. Large-scale single-cell trapping and imaging using microwell arrays. *Anal Chem*. 2005;77(17):5628-5634. doi:10.1021/ac0505977

39. Lecault V, Vaninsberghe M, Sekulovic S, et al. High-throughput analysis of single hematopoietic stem cell proliferation in microfluidic cell culture arrays. *Nat Methods*. 2011;8(7):581-589. doi:10.1038/nmeth.1614

40. Hondroulis E, Movila A, Sabhachandani P, et al. A droplet-merging platform for comparative functional analysis of m1 and m2 macrophages in response to e. coli-induced stimuli. *Biotechnol Bioeng*. 2017;114(3):705-709. doi:10.1002/bit.26196

41. Segaliny AI, Li G, Kong L, et al. Functional TCR T cell screening using single-cell droplet microfluidics. *Lab Chip*. 2018;18(24):3733-3749. doi:10.1039/C8LC00818C

42. Kim SM, Lee SH, Suh KY. Cell research with physically modified microfluidic channels: A review. *Lab Chip*. 2008;8(7):1015. doi:10.1039/b800835c

43. Gross A, Schoendube J, Zimmermann S, Steeb M, Zengerle R, Koltay P. Technologies for Single-Cell Isolation. *Int J Mol Sci*. 2015;16(8):16897-16919. doi:10.3390/ijms160816897

44. Minakshi P, Kumar R, Ghosh M, et al. Single-cell proteomics: Technology and applications. In: *Single-Cell Omics: Volume 1: Technological Advances and Applications*. Elsevier; 2019:283-318. doi:10.1016/B978-0-12-814919-5.00014-2

45. Lim B, Reddy V, Hu X, et al. Magnetophoretic circuits for digital control of single particles and cells. *Nat Commun*. 2014;5(1):3846. doi:10.1038/ncomms4846

46. Miller CH, Klawon DEJ, Zeng S, Lee V, Socci ND, Savage PA. Eomes identifies thymic precursors of self-specific memory-phenotype CD8+ T cells. *Nat Immunol*. April 2020:1-11. doi:10.1038/s41590-020-0653-1

47. Zhang L, Romero P. Metabolic Control of CD8 + T Cell Fate Decisions and Antitumor Immunity. *Trends Mol Med*. 2018;24(1):30-48. doi:10.1016/j.molmed.2017.11.005

48. Raj A, Rifkin SA, Andersen E, Van Oudenaarden A. Variability in gene expression underlies incomplete penetrance. *Nature*. 2010;463(7283):913-918. doi:10.1038/nature08781

49. Ma C, Fan R, Ahmad H, et al. A clinical microchip for evaluation of single immune cells reveals high functional heterogeneity in phenotypically similar T cells. *Nat Med*. 2011;17(6):738-743. doi:10.1038/nm.2375

50. Bradley A, Hashimoto T, Ono M. Elucidating T cell activation-dependent mechanisms for bifurcation of regulatory and effector T cell differentiation by multidimensional and single-cell analysis. *Front Immunol*. 2018;9(JUL).

doi:10.3389/fimmu.2018.01444

51. Crespo J. Naïve T Cell Functional Heterogeneity. 2018.

52. Guo X, Zhang Y, Zheng L, et al. Global characterization of T cells in non-small-cell lung cancer by single-cell sequencing. *Nat Med*. 2018;24(7):978-985. doi:10.1038/s41591-018-0045-3

53. Gerlach C, van Heijst JWJ, Swart E, et al. One naive T cell, multiple fates in CD8 + T cell differentiation. *J Exp Med*. 2010;207(6):1235-1246. doi:10.1084/jem.20091175

54. Italiani P, Boraschi D. From monocytes to M1/M2 macrophages: Phenotypical vs. functional differentiation. *Front Immunol*. 2014;5(OCT):1-22. doi:10.3389/fimmu.2014.00514

55. Schulz C, Perdiguero EG, Chorro L, et al. A lineage of myeloid cells independent of myb and hematopoietic stem cells. *Science (80-)*. 2012;335(6077):86-90. doi:10.1126/science.1219179

56. Ma X, Lin WY, Chen Y, et al. Structural basis for the dual recognition of helical cytokines IL-34 and CSF-1 by CSF-1R. *Structure*. 2012;20(4):676-687. doi:10.1016/j.str.2012.02.010

57. Hayashi SI, Yamane T, Miyamoto A, et al. Commitment and differentiation of stem cells to the osteoclast lineage. *Biochem Cell Biol*. 1998;76(6):911-922. doi:10.1139/o98-099

58. Ortmayr K, Dubuis S, Zampieri M. Metabolic profiling of cancer cells reveals genome-wide crosstalk between transcriptional regulators and metabolism. doi:10.1038/s41467-019-09695-9

59. Ortmayr K, Dubuis S, Zampieri M. Metabolic profiling of cancer cells reveals genome-wide crosstalk between transcriptional regulators and metabolism. doi:10.1038/s41467-019-09695-9

60. Muroski ME, Miska J, Chang AL, et al. Fatty Acid Uptake in T Cell Subsets Using a Quantum Dot Fatty Acid Conjugate. *Sci Rep*. 2017;7(1):1-11. doi:10.1038/s41598-017-05556-x

61. Kouidhi S, Elgaaied AB, Chouaib S. Impact of metabolism on T-cell differentiation and function and cross talk with tumor microenvironment. *Front Immunol*. 2017;8(MAR):1. doi:10.3389/fimmu.2017.00270

62. Araki K, Turner AP, Shaffer VO, et al. mTOR regulates memory CD8 T-cell differentiation. *Nature*. 2009;460(7251):108-112. doi:10.1038/nature08155

63. Pearce EL, Walsh MC, Cejas PJ, et al. Enhancing CD8 T-cell memory by modulating fatty acid metabolism. *Nature*. 2009;460(7251):103-107. doi:10.1038/nature08097

64. van der Windt GJW, Pearce EL. Metabolic switching and fuel choice during T-cell

differentiation and memory development. *Immunol Rev*. 2012;249(1):27-42. doi:10.1111/j.1600-065X.2012.01150.x

65. Sarkar S, Kalia V, Haining WN, Konieczny BT, Subramaniam S, Ahmed R. Functional and genomic profiling of effector CD8 T cell subsets with distinct memory fates. *J Exp Med*. 2008;205(3):625-640. doi:10.1084/jem.20071641

66. Arens R, Schoenberger SP. Plasticity in programming of effector and memory CD8+ T-cell formation. *Immunol Rev*. 2010;235(1):190-205. doi:10.1111/j.0105-2896.2010.00899.x

67. Prlic M, Bevan MJ. Immunology: A metabolic switch to memory. *Nature*. 2009;460(7251):41-42. doi:10.1038/460041a

68. Buchholz VR, Gräf P, Busch DH. The smallest unit: Effector and memory CD8+ T cell differentiation on the single cell level. *Front Immunol*. 2013;4(FRB):31. doi:10.3389/fimmu.2013.00031

69. Buck MD, O'Sullivan D, Pearce EL. T cell metabolism drives immunity. *J Exp Med*. 2015;212(9):1345-1360. doi:10.1084/jem.20151159

70. Chang JT, Wherry EJ, Goldrath AW. Molecular regulation of effector and memory T cell differentiation. *Nat Immunol*. 2014;15(12):1104-1115. doi:10.1038/ni.3031

71. Choi SW, Gerencser AA, Nicholls DG. Bioenergetic analysis of isolated cerebrocortical nerve terminals on a microgram scale: Spare respiratory capacity and stochastic mitochondrial failure. *J Neurochem*. 2009;109(4):1179-1191. doi:10.1111/j.1471-4159.2009.06055.x

72. Crotty S, Johnston RJ, Schoenberger SP. Effectors and memories: Bcl-6 and Blimp-1 in T and B lymphocyte differentiation. *Nat Immunol*. 2010;11(2):114-120. doi:10.1038/ni.1837

73. Fabre S, Lang V, Harriague J, et al. Stable Activation of Phosphatidylinositol 3-Kinase in the T Cell Immunological Synapse Stimulates Akt Signaling to FoxO1 Nuclear Exclusion and Cell Growth Control. *J Immunol*. 2005;174(7):4161-4171. doi:10.4049/jimmunol.174.7.4161

74. Pascual G, Domínguez D, Benitah SA. The contributions of cancer cell metabolism to metastasis. *DMM Dis Model Mech*. 2018;11(8). doi:10.1242/dmm.032920

75. Pavlova NN, Thompson CB. The Emerging Hallmarks of Cancer Metabolism. *Cell Metab*. 2016;23(1):27-47. doi:10.1016/j.cmet.2015.12.006

76. Jeong HH, Han SH, Yadavali S, Kim J, Issadore D, Lee D. Moldable Perfluoropolyether-Polyethylene Glycol Networks with Tunable Wettability and Solvent Resistance for Rapid Prototyping of Droplet Microfluidics. *Chem Mater*. 2018;30(8):2583-2588. doi:10.1021/acs.chemmater.7b05043

77. Jeong HH, Yelleswarapu VR, Yadavali S, Issadore D, Lee D. Kilo-scale droplet

generation in three-dimensional monolithic elastomer device (3D MED). *Lab Chip*. 2015;15(23):4387-4392. doi:10.1039/c5lc01025j

78. Lim H, Back SM, Hwang MH, Lee D-H, Choi H, Nam J. Sheathless High-Throughput Circulating Tumor Cell Separation Using Viscoelastic non-Newtonian Fluid. *Micromachines*. 2019;10(7):462. doi:10.3390/mi10070462

79. Urbanska M, Muñoz HE✉. A comparison of microfluidic methods for high-throughput cell deformability measurements. *Nat Methods*. doi:10.1038/s41592-020-0818-8

80. Pujol T, Du Roure O, Fermigier M, Heuvingh J. Impact of branching on the elasticity of actin networks. *Proc Natl Acad Sci U S A*. 2012;109(26):10364-10369. doi:10.1073/pnas.1121238109

81. Zielke C, Pan CW, Gutierrez Ramirez AJ, et al. Microfluidic Platform for the Isolation of Cancer-Cell Subpopulations Based on Single-Cell Glycolysis. doi:10.1021/acs.analchem.9b05738

CHAPTER 2

RESEARCH OVERVIEW

2.1. SPECIFIC AIMS

The thesis's overall goal is to develop a novel high-throughput functional phenotyping device to gain insight into the potential origin of the functional phenotypic heterogeneity of the primary immune cell and the cancer cell, specifically T cell and EL4 cells. Little is known regarding the driving force and motive of single-cell heterogeneity. Before single cell level RNA sequencing, single cells of genetic identity was assumed to have functional homogeneity; yet, recent studies showed a significant variance of functional phenotypes among genetically identical cell populations under the same environment.[1,2] Immune system maintains a large number of immune cells for active protection. Persistency is essential to keep up the health condition daily, and swiftness is also required to adapt to sudden infections. Functional heterogeneity of immune cells, which is contributed not only by the various types of immune cells but also by the single-cell level heterogeneity, makes such flexibility possible.[3,4] Recent studies have revealed the importance of functional heterogeneity of immune cells and the potential correlation between metabolomics and cell fate plasticity.[5–8] As a novel approach, combined investigation of metabolomics, cell fate decision, and transcriptomics can potentially provide valuable and powerful knowledge. Correlations divulged from the study can be a vital starting point for any multi-omics study conducted in the future. Correlations established from this thesis can provide great insight to immunologists and therapeutical industries such as precursor cell identification via metabolic profiling and artificial

manipulation of patients' immune systems to promote or demote the growth of cells of specific metabolic profiles or transcriptomic profiles.

Single-cell level heterogeneity was discovered recently, and as a result, the importance of the single-cell level research has been recently highlighted. Due to the short history of research needs, current single-cell level research equipment is excellent but not impeccable. The state-of-the-art technology like Fluorescence-Activated Cell Sorting (FACS) facilitates extremely high-throughput single-cell sorting but is limited to only surface phenotyping.[9,10] Surface phenotyping can sort out subpopulations of genetically identical cell populations based on the expression levels of the cluster of differentiation, CD, but it is incapable of any subpopulation separation based on their functional phenotype. As surface phenotyping requires the knowledge of target surface phenotype, cell population isolation without a known target surface phenotype is impossible. Functional phenotyping requires isolated, stationary single-cell, and it can be most efficiently achieved through microfluidics as it is specialized for single-particle handling within a pico-liter droplet.[11,12] Besides, droplet microfluidics can add on a flexible and automated downstream process within the isolated mobile droplet.[13,14] In-droplet processes significantly reduce the risk of contamination, which is critical for any single-cell analysis.[15] Therefore, the development of a platform device that can rapidly isolate and investigate functional phenotypic heterogeneity of rare cell populations and also capable of the flawless complex downstream process is expected to benefit all researchers conducting the single-cell level study.

This thesis involves developing a novel single-cell level high throughput functional phenotyping device with a built-in metabolic profile analysis algorithm and a novel structural improvement for highly selective recovery of the target after metabolic

profiling. It will have the capability to investigate tens of thousands of single cells in a single chip and rapidly analyze individual metabolic profiles for subset clustering based on the observed metabolic profiles. A separate, follow-up modeling system can also demultiplex the observed metabolic profiles to biologically meaningful rate constants. Target cells from each cluster of metabolic profiles are processed for transcriptomic profiling, which is correlated to the previously observed metabolic profiles for the multi-omics level single-cell investigation. A combined thesis aims will show an unprecedented correlation between metabolomics and transcriptomics. We believe such an approach will positively impact many scientific fields and benefit future studies in those fields.

Aim 1: Develop a high-throughput microfluidic device capable of rare cell population detection by functional phenotyping and a coupled system for metabolic profile analysis.

Hypothesis: Genetically identical single cell populations are composed of subpopulations of cells with different metabolic profiles, beyond the extent to which the cell cycle difference can be attributed.

Many microfluidic devices have been developed for highly efficient separation of a target cell population from a heterogeneous cell pool.[16,17] Some devices have been developed to almost resemble the Fluorescence-Activated Cell Sorting machine. Nonetheless, metabolic profiling has not been fully exploited in the field of microfluidics.[14,18,19] Metabolic profiling requires highly contained isolation of single cells for correct metabolomics studies, and microfluidics fits well with such a requirement. As many biologists and immunologists have suggested, genetically identical cell populations

are expected to differ in their metabolic profiles. The microfluidic device approach is likely to succeed as a small droplet generation enhances the signal to noise ratio of the metabolic signal readout. To ensure an accurate single-cell metabolomics study, cells are separated from the functional probe before the droplet formation. The inner content of the droplet is tightly contained via surfactants that minimize the cross-talk among droplets.[20–22] The fluorescent nutrient analogue allows accurate measurement of single-cell nutrition uptake and metabolism.[23–26] Dynamic observation of multiples of single-cell over an extended time is analyzed via ImageJ macro, Python codes, and MATLAB codes for quantitative measurement and comparison of metabolic profiles. A kinetic modeling system is also constructed to demultiplex the metabolic profiles into biologically meaningful constant rates. A combination of proposed studies will result in the development of a novel high-throughput microfluidic device capable of functional phenotyping, metabolic profile analysis and comparison, and systematic algorithm to convert a simple metabolic profile to a complex mix of biological reactions.

Aim 2: Develop an innovative microfluidic device with a stationary array that fully supports high-throughput dynamic observation while enabling highly selective recovery of the target.

Hypothesis: Stimuli-responsive layer that is optically transparent within the visible spectrum can enable both high-throughput dynamic observation and highly selective recovery of the target.

Droplets generated via microfluidics can be stationed quickly through many methods. However, the selective recovery of droplets from the stationary array remains

a difficult challenge for many microfluidics researchers. A stimuli-responsive polymer layer embedded into stationary array microfluidics can facilitate the actuation of specific droplet recovery spots. The fabrication of the stimuli-responsive layer is much simpler than the multiple thin layer alignment and bonding. This stimuli-responsive layer can also remove the necessity of multiples of the peripheral equipment for the highly selective recovery of the droplets. A regular polymer layer with photoacoustic dye for added sensitivity to a specific wave spectrum is expected to facilitate the droplet push-out recovery.[27–29] Such a photo-responsive layer can be embedded within the Polydimethylsiloxane (PDMS) stationary observation chamber through a surface tuning.[30] Photoacoustic dye outside the visible spectrum toward the IR spectrum ensures a complete open light spectrum for any metabolic profiling and harmless effect on the cells. The addition of plasticizer also guarantees minimal effect from any heat damage. This development can actively recover the droplet of interest from the closed microfluidics device without a harmful effect on the remaining cells while providing full flexibility of the metabolomics investigation.

Aim 3: Investigate the transcriptomic profiles of the metabolic profiled single cells and establish the correlation between metabolomics and transcriptomics.

Hypothesis: Metabolic profile difference and transcriptomic profile difference have significant correlations among genetically identical cell populations.

Differences in the metabolic profiles can come from a blend of various factors ranging from the difference in the cell cycle to the difference in gene expression level. Regardless of the difference in the cell cycle state, the metabolic profile must correlate

with its transcriptomic profile.[31–33] Single-cell RNA sequencing data from this thesis can be cross investigated with the already measured metabolic profiles. Parallel comparison of the transcriptomics and metabolomics must reveal a positive or negative correlation, especially from the metabolism-related genes. Moreover, ribosomal protein expression levels also can be compared with the metabolic profiles. Metabolism-related gene expression profile combined with the metabolism-related ribosomal protein expression profile can reveal valuable information on a multi-omics study using microfluidics at the single-cell level.

2.2. THESIS OUTLINE

Chapter 1 provided an overview of the research background, including the significance of the thesis, current approaches for the single-cell level investigation, memory T cell formation mechanism and the importance of metabolic profiling the effector T cells, how the functional phenotyping of the cancer cells can be correlated with the T cell functional phenotyping and current microfluidics approach for the functional phenotyping assays. It summarizes the potential correlation of metabolomics and transcriptomics and suggests the multi-omics profiling of single cells in high-throughput via the novel device the thesis proposes to develop. Chapter 3 consists of a highly focused summary of the droplet microfluidics and current stationary array formation of water-in-oil droplets within the microfluidics. It provides a mini-review of the available methods in the field and perspectives regarding how to implement it for the enhanced utilization for single-cell level studies.

Chapter 4 describes the scientific work proposed in Aim 1, describing the development of the microfluidic devices that co-encapsulate single cell and functional

probe within a droplet, an automated microscopy and analysis algorithm that analyzes and clusters the cell subpopulation based on the metabolic profiles, and a kinetic modeling algorithm that converts metabolic profile to concrete biological processes. Chapter 5 describes the scientific work proposed in Aim 2, describing the novel stimuli-responsive microfluidic device's invention for highly selective recovery of the target droplet from the closed microfluidic device. Chapter 6 describes the scientific work proposed in Aim 3, investigating the metabolic profile and the transcriptomic profile of individual cells for multi-omics study.

Chapter 7 summarizes the work presented within the thesis and discusses the overall impact of this thesis on the research fields conducting a single-cell level study. Current limitations and future direction of this thesis that can further expand the knowledge of the correlation of metabolomics and transcriptomics will also be described.

2.3. REFERENCES

1. Dueck H, Eberwine J, Kim J. Variation is function: Are single cell differences functionally important?: Testing the hypothesis that single cell variation is required for aggregate function. *BioEssays*. 2016;38(2):172-180. doi:10.1002/bies.201500124
2. Ackermann M. REVIEWS A functional perspective on phenotypic heterogeneity in microorganisms. *Nat Publ Gr*. 2015;13(8):497-508. doi:10.1038/nrmicro3491
3. Chang JT, Wherry EJ, Goldrath AW. Molecular regulation of effector and memory T cell differentiation. *Nat Immunol*. 2014;15(12):1104-1115. doi:10.1038/ni.3031
4. Kurd NS, He Z, Louis TL, et al. Early precursors and molecular determinants of tissue-resident memory CD8 $^{+}$ T lymphocytes revealed by single-cell RNA sequencing. *Sci Immunol*. 2020;5(47):eaaz6894. doi:10.1126/sciimmunol.aaz6894
5. Buck MD, O'Sullivan D, Pearce EL. T cell metabolism drives immunity. *J Exp Med*. 2015;212(9):1345-1360. doi:10.1084/jem.20151159
6. Kouidhi S, Elgaaied AB, Chouaib S. Impact of metabolism on T-cell differentiation

and function and cross talk with tumor microenvironment. *Front Immunol*. 2017;8(MAR):1. doi:10.3389/fimmu.2017.00270

7. Miller A, Nagy C, Knapp B, et al. Exploring Metabolic Configurations of Single Cells within Complex Tissue Microenvironments. *Cell Metab*. 2017;26(5):788-800.e6. doi:10.1016/j.cmet.2017.08.014

8. Zhang L, Romero P. Metabolic Control of CD8 + T Cell Fate Decisions and Antitumor Immunity. *Trends Mol Med*. 2018;24(1):30-48. doi:10.1016/j.molmed.2017.11.005

9. Donnenberg AD, Donnenberg VS. Rare-Event Analysis in Flow Cytometry. *Clin Lab Med*. 2007;27(3):627-652. doi:10.1016/j.cll.2007.05.013

10. Kunz DJ, Gomes T, James KR. Immune cell dynamics unfolded by single-cell technologies. *Front Immunol*. 2018;9(JUN):1-8. doi:10.3389/fimmu.2018.01435

11. Wang W, Yang C, Liu Y, Li CM. On-demand droplet release for droplet-based microfluidic system †. *Lab Chip*. 2010;10:559-562. doi:10.1039/b924929j

12. Golberg A, Linshiz G, Kravets I, et al. Cloud-Enabled Microscopy and Droplet Microfluidic Platform for Specific Detection of Escherichia coli in Water. Brody JP, ed. *PLoS One*. 2014;9(1):e86341. doi:10.1371/journal.pone.0086341

13. Abate AR, Hung T, Mary P, Agresti JJ, Weitz DA. High-throughput injection with microfluidics using picoinjectors. *Proc Natl Acad Sci*. 2010;107(45):19163-19166. doi:10.1073/pnas.1006888107

14. Demaree B, Weisgerber D, Lan F, Abate AR. An Ultrahigh-throughput Microfluidic Platform for Single-cell Genome Sequencing. *J Vis Exp*. 2018;(135):1-13. doi:10.3791/57598

15. Leung K, Zahn H, Leaver T, et al. A programmable droplet-based microfluidic device applied to multiparameter analysis of single microbes and microbial communities. *Proc Natl Acad Sci*. 2012;109(20):7665-7670. doi:10.1073/PNAS.1106752109

16. Karabacak NM, Spuhler PS, Fachin F, et al. Microfluidic, marker-free isolation of circulating tumor cells from blood samples. *Nat Protoc*. 2014;9(3):694-710. doi:10.1038/nprot.2014.044

17. Lim H, Back SM, Hwang MH, Lee D-H, Choi H, Nam J. Sheathless High-Throughput Circulating Tumor Cell Separation Using Viscoelastic non-Newtonian Fluid. *Micromachines*. 2019;10(7):462. doi:10.3390/mi10070462

18. Abate AR, Chen CH, Agresti JJ, Weitz DA. Beating Poisson encapsulation statistics using close-packed ordering. *Lab Chip*. 2009;9(18):2628-2631. doi:10.1039/b909386a

19. Agresti JJ, Antipov E, Abate AR, et al. Ultrahigh-throughput screening in drop-based microfluidics for directed evolution. *Proc Natl Acad Sci U S A*.

2010;107(9):4004-4009. doi:10.1073/pnas.0910781107

20. Pan M, Rosenfeld L, Kim M, et al. Fluorinated Pickering Emulsions Impede Interfacial Transport and Form Rigid Interface for the Growth of Anchorage-Dependent Cells. 2014. doi:10.1021/am506443e

21. Pan M, Kim M, Blauch L, Tang SKY. Surface-functionalizable amphiphilic nanoparticles for pickering emulsions with designer fluid-fluid interfaces. *RSC Adv*. 2016;6(46):39926-39932. doi:10.1039/c6ra03950b

22. Lyu F, Blauch LR, Tang SKY. *Quantifying Phenotypes in Single Cells Using Droplet Microfluidics*. Vol 148. 1st ed. Elsevier Inc.; 2018. doi:10.1016/bs.mcb.2018.09.006

23. Yoshioka K, Takahashi H, Homma T, et al. A novel fluorescent derivative of glucose applicable to the assessment of glucose uptake activity of Escherichia coli. *Biochim Biophys Acta - Gen Subj*. 1996. doi:10.1016/0304-4165(95)00153-0

24. Dinuzzo M, Giove F, Maraviglia B, Mangia S. Glucose metabolism down-regulates the uptake of 6-(N-(7-nitrobenz-2-oxa-1, 3-diazol-4-yl)amino)-2-deoxyglucose (6-NBDG) mediated by glucose transporter 1 isoform (GLUT1): Theory and simulations using the symmetric four-state carrier model. *J Neurochem*. 2013;125(2):236-246. doi:10.1111/jnc.12164

25. Wüstner D, Christensen T, Solanko L, Sage D. Photobleaching Kinetics and Time-Integrated Emission of Fluorescent Probes in Cellular Membranes. *Molecules*. 2014;19(8):11096-11130. doi:10.3390/molecules190811096

26. Furlong ST, Thibault KS, Morbelli LM, Quinn JJ, Rogers RA. Uptake and compartmentalization of fluorescent lipid analogs in larval Schistosoma mansoni. *J Lipid Res*. 1995;36(1):1-12.

27. Han SH, Choi Y, Kim J, Lee D. Photoactivated Selective Release of Droplets from Microwell Arrays. *ACS Appl Mater Interfaces*. 2020;12(3):3936-3944. doi:10.1021/acsami.9b17575

28. Rajendrakumar SK, Chang NC, Mohapatra A, et al. A lipophilic IR-780 dye-encapsulated zwitterionic polymer-lipid micellar nanoparticle for enhanced photothermal therapy and NIR-based fluorescence imaging in a cervical tumor mouse model. *Int J Mol Sci*. 2018;19(4):1-15. doi:10.3390/ijms19041189

29. Taratula O, Schumann C, Duong T, Taylor KL, Taratula O. Dendrimer-Encapsulated Naphthalocyanine as a Single Agent-Based Theranostic Nanoplatform for Near-Infrared ... single agent-based theranostic nanoplatform. 2014;(May 2016). doi:10.1039/C4NR06050D

30. Lee M, Zine N, Lopez-martinez MJ, Plaza JA. Integration of PDMS microfilters and micromixers bonded onto APTES-functionalized polymeric films for size sorting and mixing of microparticles. 2014:1-4.

31. Clarke CJ, Haselden JN. Metabolic profiling as a tool for understanding

mechanisms of toxicity. *Toxicol Pathol*. 2008;36(1):140-147. doi:10.1177/0192623307310947

32. Bathe OF, Farshidfar F. From Genotype to Functional Phenotype: Unraveling the Metabolomic Features of Colorectal Cancer. 2014:536-560. doi:10.3390/genes5030536

33. Kumar R, Ghosh M, Kumar S, Prasad M. Single Cell Metabolomics: A Future Tool to Unmask Cellular Heterogeneity and Virus-Host Interaction in Context of Emerging Viral Diseases. *Front Microbiol*. 2020;11:1152. doi:10.3389/fmicb.2020.01152

CHAPTER 3

STATIC ARRAY OF DROPLETS AND ON-DEMAND RECOVERY FOR BIOLOGICAL ASSAYS

Adapted from: Han SH, Kim J, Lee D. Static Array of Droplets and On-Demand Recovery for Biological Assays. *Biomicrofluidics*. 2020;14(5):051302. doi:10.1063/5.0022383

3.1. INTRODUCTION

The field of microfluidics has evolved rapidly over the last few decades in an ongoing effort to transform the bulky, expensive, complex analytical systems into coin-sized, inexpensive, simple devices that can separate, concentrate, induce reactions, add reagents and allow observations to enable analyses of biological samples.[1,2] Droplet microfluidics, which takes advantage of formation of highly uniform emulsion droplets, have emerged as a powerful platform for biological research. It can dramatically facilitate high throughput single cell manipulation and analysis, while using small volume of reagents.

In the last few decades, cell biology community has recognized that a genetically identical population of cells from the same lineage can display a wide range of heterogeneity in their phenotype, gene expression and fate. Such a recognition has led to a strong desire to develop and use advanced methods to observe single cells and perform multi-omics profiling and analyses at the single cell level. Conventional methods of cell observation and manipulations were originally developed to handle large volumes of samples or manipulate a very small number (< 10) of cells. Such systems include multi-well plates, laser catapult micromanipulator, and microcapillary pipette manipulator,

all of which involve laborious and time-consuming procedures that limits their throughput.

In response, new technologies to enable single cell analyses have been developed and commercialized. A prime example is the 10× Genomics® platform, which allows for preparation of multiple sequencing libraries of single cells without the need for micromanipulators or laser catapult manipulators[3]. Although high throughput single cell sequencing is possible, this system does not allow direct observation for phenotyping and sorting of cells based on their phenotype. A common practice to improve specificity of this technology is to pre-sort the single cell population, often through conventional surface marker phenotyping equipment such as fluorescence activated cell sorter (FACS) and magnetic activated cell sorter (MACS). Although these methods offer extremely high throughput and speed, they are typically limited to the use of known surface markers, which can be problematic because heterogeneous single cells are known to possess identical markers and populations with unknown surface markers cannot be sorted using these methods.[4]

One of the biggest advantages of microfluidics is their flexibility and modularity. Microfluidic devices can be specifically tailored and designed to meet the needs for a particular experiment. Droplet microfluidics, in particular, has emerged as a powerful platform that can be engineered to allow extended dynamic phenotyping. Droplets can function as closed reaction chambers that allow generalized phenotyping of individual cells such as metabolite synthesis rate, cell morphology, cell division kinetics, etc.[5] For dynamic observation over extended time, it is critical to trap and observe cell-containing droplets and to recover a subset of the captured droplets for subsequent analyses and processing. The selection of a trapping method for droplet array formation must be

carefully considered, as the releasing method and the selectivity of droplets are largely restricted by which type of trapping method is used. Static arrays can be largely divided into two-dimensional traps and three-dimensional traps. Typically, arrays utilizing two-dimensional traps rely on hydrodynamic force, electric field, magnetic field, or capillary force, whereas arrays using three-dimensional traps rely on pneumatic valves and density difference between continuous and dispersed phases to trap droplets.

3.2. REVIEW OF CURRENT METHODS

Capture method	Selectivity		Throughput	Fabrication Difficulty	Cell Damage	Example
	Capture	Release				
Hydrodynamic	△	△ / ○	High	Low	- / Med	Reference [6–9]
Density-difference	X	X / ○	High	Low	- / Med	Reference [10,12,28]
Pneumatic valve	○	○	Med	High	Low	Reference [14–19]
Surface Acoustic Wave (SAW)	○	○	Low	Med	Low	Reference [21,22]
Electrophoresis	○	○	Low	Med	Low	Reference [23]
Magnetophoresis	△	△	Low	Med	Low	Reference [24,25]
Hydrogel	X	X	High	Low	-	Reference [27]

Table 3.1. Current methods for selective capture and recovery. Summary table of selectivity and throughput for each type of droplet capture method in literature.

This perspective will provide a brief review of selected microfluidic methods for droplet capture, static array formation, and recovery, as well as provide suggestions for potential improvements. In particular, this chapter will focus on droplet trapping and

manipulation methods that are designed to facilitate dynamic, long-term observation and selective recovery of encapsulated samples of living cells. Although numerous methods currently exist, there is still ample room for improvement in selectivity, throughput, and ease-of-use. Key features of highlighted methods are summarized in **Table 3.1**.

Hydrodynamic force-driven droplet trapping is a commonly used approach for droplet capture and static array formation. In general, this approach takes advantage of differences in hydrostatic resistance to enable droplet capture. Examples include static microdroplet arrays, resettable dynamic microarray, trap-and-release microfluidic microarray, and dropspots.[6–9]

The static microdroplet array, as shown in **Figure 3.1-A**, utilizes U-shaped traps to arbitrarily capture flowing droplets while the exhaust channels in the traps both ensure single droplet capture and retention, and serve as release channels for recovery of the captured droplets.[6] This is a simple, yet highly effective droplet capture system that is capable of capturing and releasing hundreds of droplets. Depending on the size of droplets, a simple adjustment of device design (e.g., inter-trap distance, trap size) can optimize droplet capture. With optimized inter-trap distance, the device requires approximately 28,500 μm^2 to capture one droplet, somewhat limiting the throughput of this approach. As is, the device offers non-selective capture and recovery of captured droplets. An additional component in the exhaust channel can potentially allow selective recoverability. For instance, by using hydrogel that responds to external stimuli such as light, it will be possible to generate traps that can catch and release droplets via hydrogel swelling and collapse. Other stimuli dependent manipulations that can actively or passively drive droplets out of the traps can broaden the utility of this type of device.

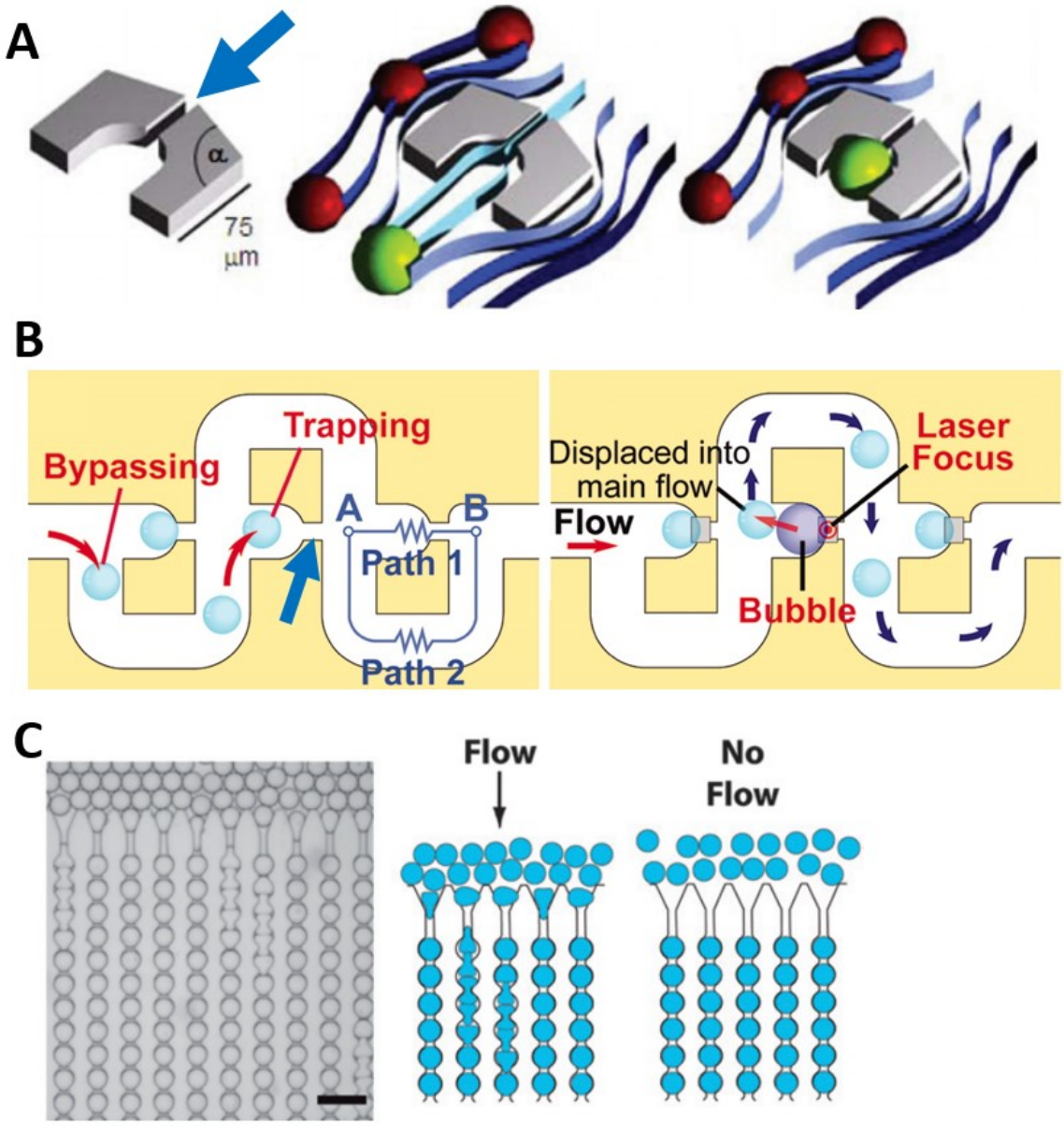

FIGURE 3.1. Hydrodynamic force driven droplet trapping and recovery. Examples of hydrodynamic force driven droplet trapping and recovery methods **A-C**. **A** shows static trapping arrays that trap droplets randomly. Exhaust channels in Figure 3.1-A and 3.1-B are marked with blue arrows. Reprinted with permission from Lab Chip 2009, 9, 692-698, DOI: 10.1039/B813709A. Copyright (2009) Royal Society of Chemistry. **B**

shows sequential droplet trapping into trapping spot and precise recovery of trapped droplet via bubble formation at aluminum pattern, located within the exhaust channel, with laser excitation. Reprinted with permission from PNAS 2007, 104(4), 1146-1151. Copyright (2008) National Academy of Science. **C** shows a highly efficient droplet trapping and monitoring system, Dropspot. Reprinted with permission from Lab Chip 2009, 9, 44, DOI: 10.1039/B809670H. Copyright (2009) Royal Society of Chemistry.

The modified resettable dynamic microarray and the trap-and-release microfluidic microarray share an identical device design for droplet capture as shown in **Figure 3.1-B**. Unlike the static microdroplet array, these microarray systems allow droplets to be captured in the order which they are introduced into the device.[7,8] A droplet traveling through the flow channel enters the first vacant trapping spot. This droplet capture in the trapping spot is due to lower flow resistance in the exhaust channel of the trapping spot compared to that of the main flow channel. A similar phenomenon induces the next droplet to bypass the now occupied trapping spot, flow through the loop channel, and enter the next vacant trapping spot. For the modified resettable dynamic microarray system, recovery is simple; back-flowing releases all captured droplets back into the loop channel. In addition, pillars surrounding the exhaust channel ensure smooth recovery of released droplets without clogging the exhaust channel. This is a semi-selective recovery system; as recovered droplets will exit the channel in the order of capture, delicate backflow with timed collection could, in theory, enable selective recovery of the target droplets; however, such recovery has not been demonstrated. This modified resettable array has been shown to capture up to 10,000 droplets in a single chip, which can be easily scaled up to higher numbers. Timed collection of released droplets can potentially be optimized for high-precision selective recovery; however, without extensive optimization, it will likely result in imperfection. Alternatively, the resettable dynamic microarray can incorporate ad-hoc barcode or quantum-dot in the

droplets, to improve selectivity; however, this approach would need to add a separation step to enable selective recovery or analysis.

Selectivity of the modified resettable array has been improved by adding metal patterns on the exhaust channels to push droplets out of the traps as shown in **Figure 3.1-B**.[8] The trap-and-release microfluidic microarray utilizes a focused laser to heat an aluminum pattern to 132°C and create a bubble which pushes the droplet out of the trapping spot into the mainstream within 300 msec. The device is relatively simple to fabricate and provides excellent selectivity with a short response time and can process up to 10,000 droplets. However, although heating and bubble generation take place in less than a second, even a brief exposure to high temperature can damage biological samples encapsulated in the droplets. To mitigate this heat-induced damage, the exhaust pattern can be replaced with a hydrogel that swells upon a small temperature increase to minimize heat-induced damage. Alternatively, a buffer spot or a thin stimuli responsive layer (e.g., hydrogel) can be placed between the trapping spot and the aluminum pattern such that heating generates a bubble which in turn expands the buffer spot and pushes out the captured droplet.

The dropspot, as shown in **Figure 3.1-C**, is a simple pea-in-a-pod shaped microfluidic device that captures a droplet in an array of circular chambers connected by narrow constrictions. This system mainly depends on droplets pushing preceding droplets to fill the chambers. Due to the simple chamber geometry and trapping algorithm, it can trap a large number of droplets within a single chip. A dropspot that can trap 64,000 droplets has been reported.[9] Similar to the resettable dynamic microarray, the dropspot allows semi-selective recovery of target samples, as droplets are released

in the order they were captured. Although manual collection of droplets in target position is possible, it is highly inefficient and error prone.

One of the most high-throughput methods for droplet capture uses the intrinsic difference in density between the droplet and the continuous phase. As droplet microfluidics typically uses an aqueous phase and an oil phase, a density difference between the two phases inevitably exists. For example, in an experiment using fluorocarbon oil such as FC-40 or HFE-7500 as the continuous phase, aqueous droplets (density ~ 1 g/mL) are significantly lighter than the continuous phase (density of FC-40 = 1.85 g/mL; density of HFE-7500 = 1.61 g/mL). Under these conditions, a floating droplet array (FDA) can capture droplets nonspecifically.[10] Although the intrinsic density differences between the phases make the system simple to implement, the system cannot be used if the density difference is negligible.

The floating droplet array (FDA) system, as shown in **Figure 3.2-A**, can operate at a trapping efficiency of approximately 20%, which can be slightly increased by ceasing droplet generation when 40% of the wells are filled to minimize the number of droplets that bypass the wells without getting trapped.[10] The trapping efficiency can be further enhanced by changing the flow rates and droplet size, and by varying the dimension of and spacing between trapping wells. In some cases, the buoyancy force, resulting from the density differences, may be too small for droplets to overcome the flow inertia if the continuous flow rate is too high. In such a case, additional oil drainage system may need to be introduced prior to the FDA to reduce the total flow rate and increase the overall volume fraction of droplets in the flow.[11] With optimized droplet flow speed, well size, well depth and droplet generation time, up to 95% capture efficiency can be achieved. [12] Besides its simple trapping mechanism, another advantage of the FDA is throughput.

FDA device design has very small dead space within the device resulting in one of the highest throughput systems. The small dead space of the FDA can be attributed to both three-dimensional design and no need for exhaust channels. Although the lack of exhaust channels enables high throughput capture of droplets, droplet recovery is limited to nonspecific recovery. Flipping the chip releases all droplets from the wells, and since recovery is not order-based like the modified resettable dynamic microarray or the dropspot, the process is completely non-selective. To introduce selectivity, droplets must contain barcodes.

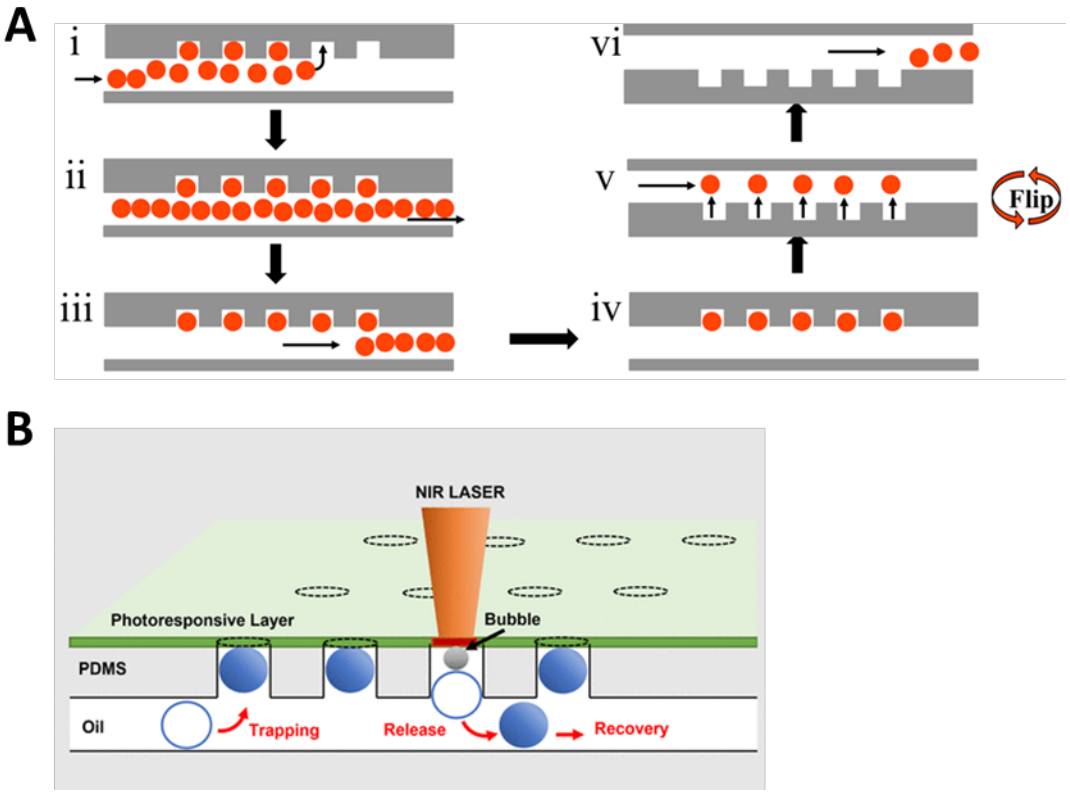

FIGURE 3.2. Density difference driven droplet trapping and recovery. Examples of density-difference driven droplet trapping, and recovery methods **A-B**. **A** (i)-(vi) shows nonspecific trapping and recovery of droplets using density difference between the droplet and the continuous phase. Reprinted with permission from Micromachines 2015, 6(10), 1469-1482. Copyright (2015) Creative Commons Attribution License. **B** shows implementation to A by additional photoresponsive layer for enhanced selective

recoverability of the device. Reprinted with permission from ACS Appl. Mater. Interfaces 2020, 12, 3, 3936-3944. Copyright (2020) American Chemical Society.

Recently, a UV laser-based system that allows selective recovery of droplets from a FDA has been reported.[12] After nonspecific capture, a focused UV laser with pulse energy above 90 μJ with a pulse duration of a few nanoseconds was used to generate heat-induced cavitation bubbles that expel target droplets out of their trap wells. While this system adds a powerful selective recoverability mechanism, the usage of UV laser could potentially damage the encapsulated biological samples (e.g., cells). As an alternative, the top of the wells can be lined with a hydrogel, which can absorb UV and swell to mitigate such a potential damage. More recently, a new device that uses a less harmful near infrared (NIR) laser source in combination with a NIR-responsive layer with a photoacoustic dye has shown to enable selective recovery of droplets with living cells, as shown in **Figure 3.2-B**.[13] A focused NIR laser with pulse energy above 6 mJ and a pulse duration of less than a second was applied on a polystyrene layer containing a photoacoustic dye, which generated heat-induced cavitation bubbles that expelled target droplets out of the wells. Cell viability was not affected by this process. Density difference-driven droplet capture and recovery systems can provide high throughput and selective recovery; however, the approach requires fabrication of three-dimensional devices with multiple layers. Also, an external laser source is needed to enable selective recovery. A system that does not require a high-power laser source and that can be fabricated in a single layer would greatly enhance the implementation of this approach.

Microfluidic devices that use hydrodynamic forces and external stimuli provide the highest throughput and at the same time allow for selective recovery of the captured droplets. Although microfluidics provides great benefits of a closed system, this same isolation makes it difficult to apply an external force to enable on-demand droplet

manipulation. Pneumatic valves are useful tools in such a case as they can exert forces locally on-demand to neighboring microfluidic channels. Vales can be used to reduce channel dimensions, which allows for flow of small sized droplets or complete shut-off of channels, or alter the flow directions. Many studies have used pneumatic valves for selective droplet manipulation as they offer the most intuitive and direct control of droplets.[14–17] Large-scale integration of pneumatic valves, also known as the Quake valve, has shown to enable effective capture and manipulation of 1,000 droplets. A built-in multiplexor effectively reduces the required number of external valves with an innovative scheme utilizing a combinatorial array of binary valve patterns.[18] With pneumatic valves, fully selective droplet capture and recovery is possible. In addition, the pneumatic valve also allows for on-demand droplet merging and mixing.

By far, pneumatic valve-based systems offer the highest degree of control and selectivity for droplet manipulation; as a result, many studies have used the multiplexor-incorporated pneumatic valves to manipulate multiple chambers for biological assays of cells.[19] Recently, a pneumatic valve system was used to achieve controlled droplet discretization and manipulation.[16] Rather than a simple binary on/off system, the pressure on a pneumatic valve was controlled to capture a specific volume of aqueous solution into the traps. Using the same principle, the captured droplet can also be partially released. Partial release followed by partial capture enables mixing of different solutions. While it has the highest degree of controllability, pneumatic valve systems require highly complicated fabrication procedures and numerous peripheral tools for delicate control of individual valves. Currently, pneumatic valve-based systems present high entry barriers to many researchers because of their complexity; however, their adoption can be potentially improved by on-chip incorporation of peripheral equipment to

minimize the number of tools required. For example, manually operable on-chip bi-stable pneumatic valves have been developed to demonstrate on-chip digital flow switching from multiple sources.[20] While challenging, such an effort will enhance the implementation of pneumatic valve-based microfluidic devices.

An example of hybrid capture and release device uses surface acoustic wave (SAW), a popular choice of selective droplet capture and release in microfluidic systems, to achieve selective droplet recovery.[21] In this method, after a droplet is captured by hydrodynamic force, application of pulse SAW induces the generation of a bubble in the coupling channel pushing the droplet out of the chamber. As SAW is a non-invasive force, this method is useful for experiments involving biological samples. However, the throughput of this system is significantly lower than the aforementioned devices. A study demonstrated a selective recovery system composed of 5 traps. Scaling-up this approach requires additional interdigitated transducers (IDT) and coupling channel, which requires a large footprint within the microfluidic chip, limiting the maximum throughput.[21]

A similar system without coupling channels can also offer selective capture with a higher throughput.[22] For example, the device shown in **Figure 3.3-A** captures a small number of droplets (< 10) selectively using SAW, rather than hydrodynamic force. Next, slanted finger interdigitated transducers (SF-IDTs) are used to release droplets by adjusting the position, voltage, and frequency of applied SAW. Trapping and releasing of droplets in different microwells involve fine-tuning of SAW frequency, enabling highly selective capture and release of a target droplet within a chip with a simple design. Furthermore, as the SF-IDT system occupies less space than IDT-coupling, SF-IDT systems have some potential for further scaling-up.

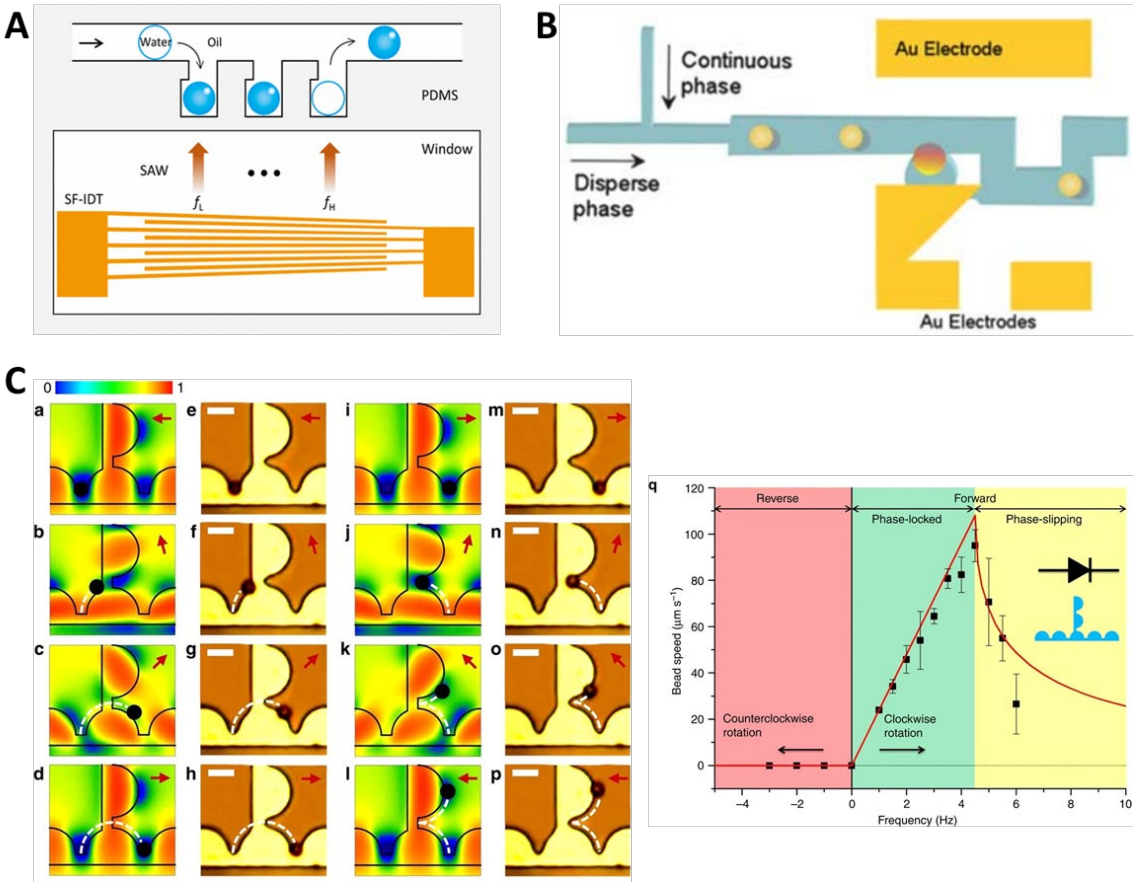

FIGURE 3.3. SAW and electrode assisted droplet trapping and recovery. Example of SAW and electrode assisted droplet trapping and recovery **A-B**. **A** shows Fine SAW frequency tuning allows location specific droplet capturing and recovery. Reprinted with permission from ACS Anal. Chem. 2017, 89, 4, 2211-2215. Copyright (2017) American Chemical Society. **B** shows electrode assisted droplet trapping and recovery using both electric field and dielectrophoresis. Reprinted with permission from Lab Chip 2010, 10, 559-561 DOI: 10.1039/B924929J. Copyright (2010) Royal Society of Chemistry. Example of magnetophoresis assisted droplet trapping and recovery **C**. The potential energy landscape in **a-d** and **i-l** is associated with experimental images in **e-h** and **m-p**. Rotating field in the forward-biased mode uses an external field with angular orientation of φ=180°, 105°, 45° and 0° as shown in **a-d**. Reverse-biased mode uses an external field with an angle of φ=0°, 75°, 135° and 180° as shown in **i-l**. The red arrows indicate instantaneous external field direction and the blue energy minima correspond to the particle location. The velocity and frequency relationship for reverse and forward mode as well as phase-slipping mode is represented in **q**. Reprinted with permission from Lim, B. et al., Nat Commun **5**, 3846 (2014). Copyright © 2014, Springer Nature.

The electrode-based hybrid system, shown in **Figure 3.3-B**, is another method that enables selective capture and release of droplets. A voltage across thin gold electrodes can exert electrohydrodynamic forces on a droplet, enabling selective capture and release.[23] The DC voltage generates a non-uniform electric field that pulls droplets via a hydrodynamic inertial force and captures them into individual chambers. To release the captured droplets, voltage is applied to induce two forces, dielectrophoresis force and Coulomb force, which push droplets to the main continuous phase channel. The device provides great selective capture and recovery, but suffers from complex fabrication protocol and low throughput.

Both the SAW- and the electrode-based systems require built-in or peripheral accessories, which reduces the throughput; the issue of low throughput can be potentially ameliorated by combining a three-dimensional droplet capture array with vertical incorporation of the IDTs or electrodes, which will require novel design and implementation.

Another method of droplet and particle manipulation is through magnetophoresis, which requires the presence of magnetic beads or ferrofluid within the droplets.[24,25] This may increase the cost of an experiment or make the system biologically incompatible. Recently, the possibility of manipulating multiple single magnetic particles using a rotating external field has been demonstrated, as shown in **Figure 3.3-C**.[25] The direction of particle movement can be adjusted from clockwise forward to counterclockwise reverse in semi-circular tracks, and the particle can be forced out of phase-locked condition to the phase-slipping regime, skipping it over to the next track. Although magnetophoresis allows multiplexed manipulation of particles or droplets and precise

trapping and recovery of samples, the system does not allow for fully selective individual target manipulation and is limited by low speed (~ hundred microns per second).

A potentially powerful technology which has not been fully explored or applied to its maximum potential in selective trapping and recovery systems is hydrogels [26]. Hydrogels are highly responsive to external stimuli and can be readily tailored to meet many needs in microfluidics. A hydrogel-based, temperature-responsive actuator has recently been reported [27]. Using patterned chromium and gold bilayers to induce local heating, a thermally responsive hydrogel closes one of binary paths on-demand to achieve flow path divergence. Similar to the aforementioned FDA, multiple droplets in the flow channel can be trapped at specific locations by inducing local heating, making this approach a powerful trap and release mechanism. The fast response rate of 250 msec enables efficient trapping and rapid recovery. The current system uses lower critical solution temperature (LCST) hydrogels which requires cooling below 32 ℃ to induce swelling and heating above 32 ℃ to collapse the hydrogel. This condition limits the capturing and observation to below 32 ℃ which is not ideal for studies involving living cells. An upper critical solution temperature (UCST) hydrogel that swells and collapses above and below a critical temperature, respectively, may be more useful for studies that involve living cells.

Optimal selective trapping and recovery systems require a balance of selectivity, throughput and ease of fabrication. Trade-offs among these factors must be considered when choosing an appropriate system for a specific application. As computational and genomic technologies advance, the demands for high resolution, multiplexed phenotyping, and increased sample size will continuously increase. To satisfy these demands while minimizing cost, biocompatibility issues, and design complexity,

continued developments and innovations in droplet microfluidic technology is critical. In particular, adoption and incorporation of advances in materials science and nanotechnology will enable the next generation microfluidic devices for biological assay and analysis applications. For example, stimuli-responsive materials such as hydrogels that can detect the presence of metabolites could potentially enable autonomous, selective recovery of droplets, eliminating the needs for external control via light or pressure. Recent advances in artificial intelligence, pattern recognition, and machine learning also will be key to processing large data to better understand complex phenomena that are often associated with biological assays. As the biology community shifts its focus toward understanding the role of subcellular components and organelles, methods to capture, separate, and analyze these delicate components using microfluidics will require new approaches and innovations.

3.3. REFERENCES

[1] F. Del Ben, M. Turetta, G. Celetti, A. Piruska, M. Bulfoni, D. Cesselli, W.T.S. Huck, and G. Scoles, Angew. Chemie - Int. Ed. 55, 8581 (2016).

[2] H.H. Jeong, S.H. Han, S. Yadavali, J. Kim, D. Issadore, and D. Lee, Chem. Mater. 30, 2583 (2018).

[3] A. Nathan, Y. Baglaenko, C.Y. Fonseka, J.I. Beynor, and S. Raychaudhuri, Curr. Opin. Immunol. 61, 17 (2019).

[4] N. Xiang, J. Wang, Q. Li, Y. Han, D. Huang, and Z. Ni, Anal. Chem. 91, 10328 (2019).

[5] B. Dura, S.K. Dougan, M. Barisa, M.M. Hoehl, C.T. Lo, H.L. Ploegh, and J. Voldman, Nat. Commun. 6, 5940 (2015).

[6] A. Huebner, D. Bratton, G. Whyte, M. Yang, A.J. Demello, C. Abell, and F. Hollfelder, Lab Chip 9, 692 (2009).

[7] K. Iwai, W.H. Tan, H. Ishihara, and S. Takeuchi, Biomed. Microdevices 13, 1089 (2011).

[8] W.-H. Tan and S. Takeuchi, Proc. Natl. Acad. Sci. 104, 1146 (2007).

[9] C.H.J. Schmitz, A.C. Rowat, S. Köster, and D.A. Weitz, Lab Chip 9, 44 (2009).

[10] L. Labanieh, T. Nguyen, W. Zhao, D.-K. Kang, L. Labanieh, T.N. Nguyen, W. Zhao, and D.-K. Kang, Micromachines 6, 1469 (2015).

[11] M. Kim, C.M. Leong, M. Pan, L.R. Blauch, and S.K.Y. Tang, SLAS Technol. 22, 529 (2017).

[12] A.I. Segaliny, G. Li, L. Kong, C. Ren, X. Chen, J.K. Wang, D. Baltimore, G. Wu, and W. Zhao, Lab Chip 18, 3733 (2018).

[13] S.H. Han, Y. Choi, J. Kim, and D. Lee, ACS Appl. Mater. Interfaces 12, 3936 (2020).

[14] H.-H. Jeong, B. Lee, S.H. Jin, S.-G. Jeong, and C.-S. Lee, Lab Chip 16, 1698 (2016).

[15] T. Thorsen, S.J. Maerkl, and S.R. Quake, Science (80-.). 298, 580 (2002).

[16] S. Padmanabhan, T. Misteli, and D.L. DeVoe, Lab Chip 17, 3717 (2017).

[17] J.H. Choi, S.K. Lee, J.M. Lim, S.M. Yang, and G.R. Yi, Lab Chip 10, 456 (2010).

[18] M.A. Unger, H.P. Chou, T. Thorsen, A. Scherer, and S.R. Quake, Science (80-.). 288, 113 (2000).

[19] K. Leung, H. Zahn, T. Leaver, K.M. Konwar, N.W. Hanson, A.P. Pagé, C.-C. Lo, P.S. Chain, S.J. Hallam, and C.L. Hansen, Proc. Natl. Acad. Sci. 109, 7665 (2012).

[20] A. Chen and T. Pan, Lab Chip 14, 3401 (2014).

[21] R.W. Rambach, P. Biswas, A. Yadav, P. Garstecki, and T. Franke, Analyst 143, 843 (2018).

[22] J.H. Jung, G. Destgeer, J. Park, H. Ahmed, K. Park, H.J. Sung, J. Ho Jung, G. Destgeer, J. Park, H. Ahmed, K. Park, H. Jin Sung, J.H. Jung, G. Destgeer, J. Park, H. Ahmed, K. Park, and H.J. Sung, Anal. Chem. 89, 2211 (2017).

[23] W. Wang, C. Yang, Y. Liu, and C.M. Li, Lab Chip 10, 559 (2010).

[24] B.B. Yellen, R.M. Erb, H.S. Son, R. Hewlin, Jr., H. Shang, and G.U. Lee, Lab Chip 7, 1681 (2007).

[25] B. Lim, V. Reddy, X. Hu, K. Kim, M. Jadhav, R. Abedini-Nassab, Y.-W. Noh, Y.T. Lim, B.B. Yellen, and C. Kim, Nat. Commun. 5, 3846 (2014).

[26] C.B. Goy, R.E. Chaile, and R.E. Madrid, React. Funct. Polym. 104314 (2019).

[27] L. D'Eramo, B. Chollet, M. Leman, E. Martwong, M. Li, H. Geisler, J. Dupire, M. Kerdraon, C. Vergne, F. Monti, Y. Tran, and P. Tabeling, Microsystems Nanoeng. 4, 17069 (2018).

[28] J.R. Rettig and A. Folch, Anal. Chem. 77, 5628 (2005).

CHAPTER 4

KINETIC MODELING OF GLUCOSE UPTAKE AND METABOLISM BY SINGLE CELLS

4.1. INTRODUCTION

A seemingly homogeneous single cell population of identical genomic DNA is surprisingly heterogeneous (Dueck *et al*, 2016). A recent single-cell transcriptomic study revealed extremely valuable heterogeneity that was not detectable with conventional population-level studies (Bertozzi *et al*, 2008; Papalexi & Satija, 2017). The genome is a fixed structure and sequence of information. It does not accurately predict the final phenotype or function as the genome is subject to various downstream processes that impose significant modifications (Dueck *et al*, 2016; Yuan *et al*, 2017). Epigenetic alteration and modification are followed by transcriptional regulation, post-translational modification, and regulation (Bathe & Farshidfar, 2014). These altogether sequentially and synchronously contribute to the phenotype. Therefore, genomic information does not fully predict the final phenotype (MacRae & Vasan, 2016). Many theories have been formulated to explain the origin of such heterogeneity, but there is no single theory that perfectly explains the phenomenon (Ackermann, 2015). Recent studies have continuously emphasized the importance of single-cell level lineage tracing (Kunz *et al*, 2018). Combined studies of phenotyping, transcriptomics, proteomics, and genomics on the single cell level, which refers to single-cell lineage tracing, will allow us to understand more complex molecular biology.

To gain a deeper understanding of all the hidden aspects of the single-cell heterogeneity, a large number of multi-omics studies, in which transcriptomics is combined with proteomics or metabolomics, could play an important role (Nathan *et al*, 2019). Intracellular heterogeneity and surface-level heterogeneity have been well studied using fluorescence-activated cell sorting (Kunz *et al*, 2018). Nevertheless, a few developments have been made on extracellular heterogeneity (Zhang & Romero, 2018). Single-cell level extracellular signal measurement can provide valuable information for single-cell metabolic profiling, which can benefit many fields of science, including biology, immunology, and pathology (Kumar *et al*, 2020).

Among many available technologies, microfluidics has emerged as a powerful platform to enable single-cell isolation and metabolomics study (Kumar *et al*, 2020; Han *et al*, 2020). High flexibility in device design customization, low cost of fabrication and operation, high throughput single-cell isolation, and the capability of single-cell level extracellular signal detection altogether make microfluidic the preferred choice for single-cell metabolomics study (Utharala *et al*, 2018; Minakshi *et al*, 2019; Gross *et al*, 2015).

In addition to the needs for the metabolic profiling, the kinetic modeling of the metabolic profiles observed is also extremely valuable, since the observed metabolic profiles can merely tell the amount of nutrient consumption over the measurement time window. Although the amount of relative consumption over time is a valuable metabolic profile, it lacks temporal resolution. Thus, high temporal resolution metabolic profile combined with kinetic modeling that can accurately explain the time evolution of metabolic profile is expected to enhance single-cell metabolomics studies. A kinetic model that can accurately unravel and deconvlute the mingled kinetics of the dynamic metabolic profiles will allow a simplified understanding of single-cell metabolism.

To achieve the goal of high-dimensional metabolic profiling and analysis, this study utilizes co-encapsulation of a single cell and fluorescent form of nutrient analogue using high-throughput droplet generation to monitor and investigate a large number of metabolic profiles for individual single cells. In addition, specifically tailored computational analysis allows automated single-cell metabolic profiling and clustering followed by kinetic modeling. We develop an analytical kinetic model that can interpret and decipher the possible mechanism behind complex single-cell functional profiles. The kinetic model developed in this work utilizes a differential equation to deconvolute the observed metabolic profile into time and kinetic constants that are relevant to the rates of nutrient uptake and consumption. We believe that this will benefit many studies involved in cellular metabolism, and it can potentially bring a significant impact on cell diet studies.

4.2. RESULTS

Cultured mouse lymphoma cell-line, EL4, and fluorescent glucose analogue, either 2-(N-(7-Nitrobenz-2-oxa-1,3-diazol-4-yl)Amino)-2-Deoxyglucose (2-NBDG) or 6-(N-(7-Nitrobenz-2-oxa-1,3-diazol-4-yl)Amino)-6-Deoxyglucose (6-NBDG), are co-encapsulated into individual droplets using a microfluidic device with flow-focus junction as shown in **Fig 4.1-A** and **Fig 4.1-B**. The microfluidic device is designed specifically to ensure contactless, perfectly parallel laminar flow of both the cell suspension and the functional probe prior to the droplet formation, as demonstrated in **Fig 4.1-C**; this ascertains the signal from the functional probe is solely from the cell

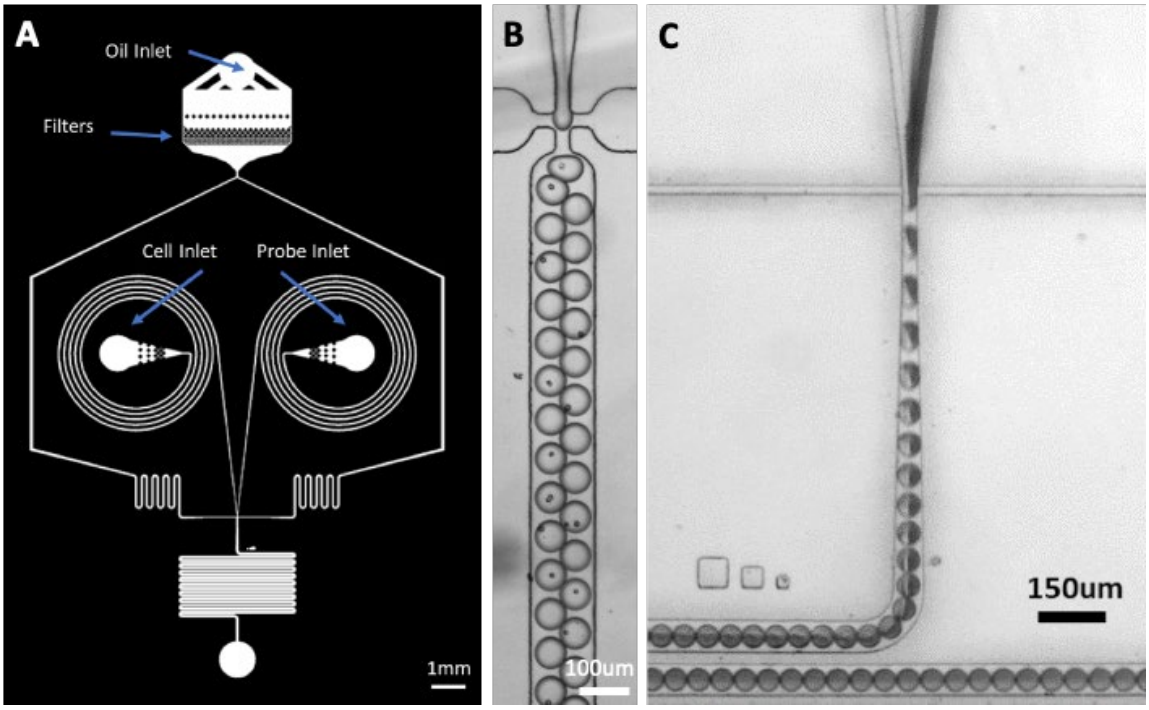

Figure 4.1 - Demonstration of droplet generation co-encapsulating single cell and functional probe. (A) Modified design of conventional microfluidic device design to ensure co-encapsulation of the functional probe and cell suspension. (B) Demonstration of a single cell and functional probe co-encapsulated droplet formation. (C) Food-dye assisted demonstration of laminar flow between the functional probe and cell suspension prior to droplet formation. Scale bars are notated for its own scale.

within the same droplet. Two aqueous inlets join less than 100 μm before the flow-focus junction and get mixed after droplet formation. To prevent droplet coalescence, we use the 1:1 mixture of two types of surfactants. The EA surfactant is a commercially available tri-block copolymer composed of perfluoropolyether (PFPE) and polyethylene glycol (PEG) blocks. It is most widely used in emulsion stabilization in fluorinated oils like FC-40 and HFE-7500. Functionalized SiO_2 nanoparticle surfactants, a relatively new type of surfactant, have been proven to minimize crosstalks between droplets. A 1:1 mixture of high concentration EA-surfactant (5% in HFE-7500) and standard concentration SiO_2 (2% in HFE-7500) nanoparticle surfactants successfully stabilizes droplet with minimal adhesion between droplets, a known shortcoming of SiO_2 nanoparticle surfactants.

Droplet sizes can be adjusted from 30 μm to 60 μm in diameter. This study uses 50 μm diameter droplets as they provide the optimized signal to background ratio within the droplets. Generated droplets are trapped into the observation chamber using the density difference between the continuous phase and the droplets; the density of droplets is approximately 1 g/ml, and the density of the HFE-7500 phase is approximately 1.6 g/ml. Trapping of droplets is required for the time lapse metabolic profiling.

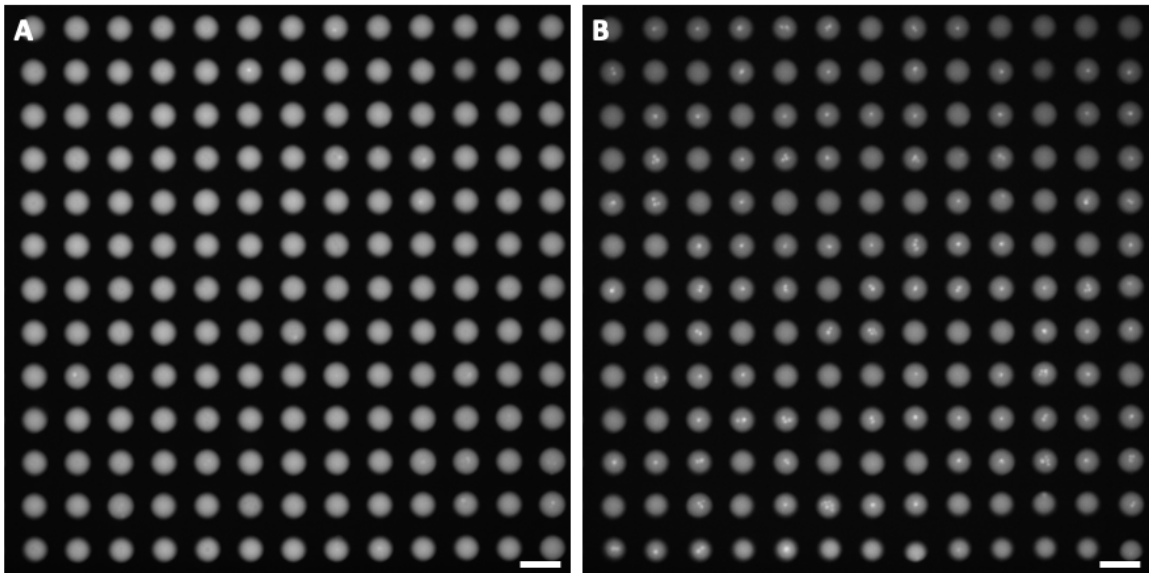

Figure 4.2 - Time-lapse imaging of static array of droplets over 4 hours. Droplets contain mouse lymphoma EL4 cells and 2-NBDG glucose analogue. (A) Image from t = 0 of the dynamic observation and (B) image from t = 4 hrs of the dynamic observation. As cells uptake co-encapsulated glucose analogue, the fluorescence intensity from the cell is greater than the environment. Scale bars are 100 μm.

A static array of droplets containing glucose analogue with or without cells are monitored dynamically for 4 hours. **Fig 4.2-A** and **Fig 4.2-B** represent images taken of the same droplets at t = 0 and t = 4 hrs, respectively. As the cell is co-encapsulated with the fluorescent glucose analogue, the cellular nutrient uptake increases the intracellular fluorescence intensity while decreasing the extracellular fluorescent intensity of the

droplet. The live cell imaging solution (LCIS) ensures cell viability for a minimum of 4 hours at room temperature conditions. Thus, we are confident that the cells are healthy and viable with the current environmental condition of 37ºC, 5% CO_2, and 95% humidity. We previously confirmed that encapsulated cells remain viable up to 8 hours using the live/dead viability assay.

The observation chamber is approximately 1.5 cm by 4 cm in dimension; multiple position acquisitions are necessary to obtain the entire chip's time-series data. We coded for the zig-zag stage movement to ensure the shortest travel length to maximize the temporal resolution. The cells are stained with CellTrace Violet to differentiate droplets with a single cell, multiple cells, and no cell. Multiple cells encapsulated droplets are filtered out by thresholding the size and circularity from DAPI-filter acquired images. As noted in the Materials and Methods section, time-lapse image acquisitions are fully automated using the MetaMorph journal and can be found in the APPENDIX.

Using ImageJ particle analysis, individual droplet information and cell information is extracted. The ImageJ particle analysis is slightly modified in an effort to capture top 0.5% intensity average value from individual droplets, and the modified ImageJ package can be found in the APPENDIX. Top 0.5% intensity average extraction is not required, but it is recommended as simple maximum intensity extraction from the droplet can be more spurious; since the cell is occupying roughly 0.5% of the pixel area of the droplet, an average of intensity profiles can potentially pick up total fluorescence signal from the cell. ImageJ extracted particle analysis files are exported to MATLAB to align the time series data based on spatially sorted individual droplets. The MATLAB code for spatially sorting individual droplets and filtering out single-cell encapsulating droplets to acquire single-cell time series data can also be found in the APPENDIX.

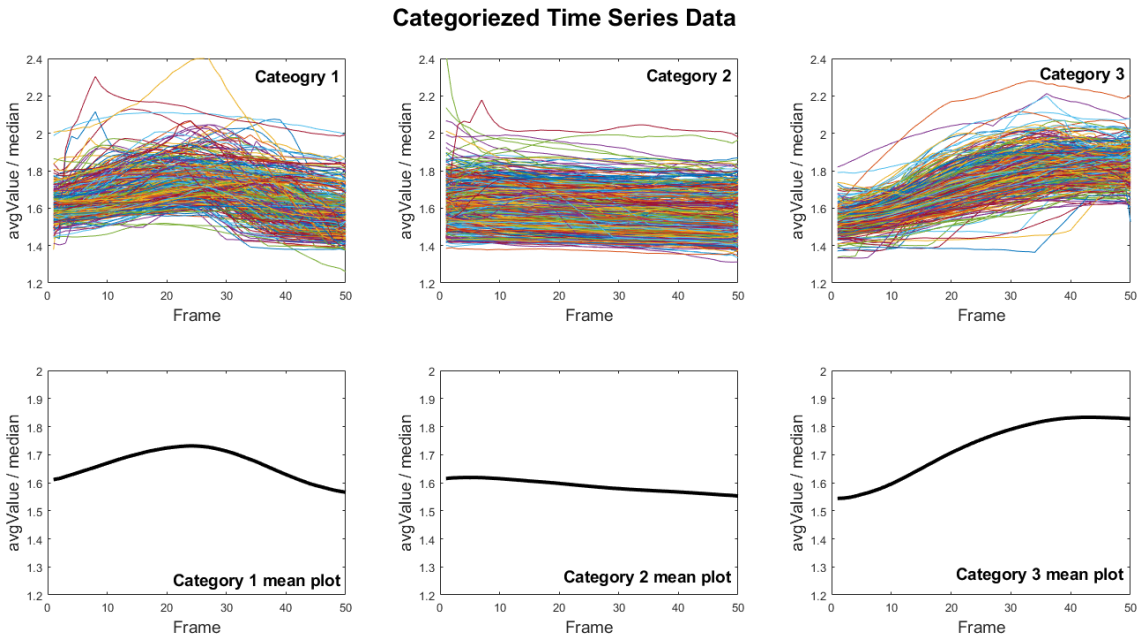

Figure 4.3 - Demonstration of categorization of time series data using Dynamic Time Warping. Metabolic profiles are divided into three categories, and randomly selected five hundred lines are plotted on top. The averaged single line plots of the corresponding category are plotted on the bottom. Y-axis represents the top 0.5% intensity average value divided by the median of the corresponding droplet, and the x-axis represents the frame number of the time series. Each frame represents 4 minutes.

The extracted time-lapse data can be easily categorized using various clustering methods such as principal component analysis (PCA), diffusion mapping (DM), and dynamic time warping (DTW) as demonstrated in **Fig 4.3**. It shows DTW based time series data clustering; the top three plots show randomly picked 100 plots from each cluster, and the bottom three plots show averaged single line plot of the corresponding cluster. Regardless, clustered data dimensions such as PCA components 1, 2, or DM components 1, 2 lack physiological meaning. To further understand the cellular function and metabolic profile that we observe, this study develops a kinetic model that can bestow physiological characteristics to an individual profile. Michaelis-Menten equation

was used as the original backbone of the system for kinetic modeling. Michaelis-Menten kinetics equation is as follows:

$$\mathbf{E} + \boldsymbol{S} \underset{k_f}{\overset{k_r}{\rightleftharpoons}} \boldsymbol{ES} \xrightarrow{k_{cat}} \boldsymbol{E} + \boldsymbol{P} \tag{1}$$

The equation is modified to describe the glucose uptake and metabolism :

$$\mathbf{L}_{out} + \boldsymbol{R} \underset{k_f}{\overset{k_r}{\rightleftharpoons}} \boldsymbol{LR} \xrightarrow{k_{in}} \boldsymbol{R} + \boldsymbol{L}_{cytosol} \tag{2}$$

Instead of enzyme, substrate, and product, our system is described with L_{out}, R, LR, $L_{cytosol}$, k_f, k_r, and k_{in}, representing ligand outside the cell, receptor, ligand-receptor complex, a ligand in the cytosol, forward reaction rate, reverse reaction rate and internalizing rate, respectively. A ligand can be any type of glucose analogue: 2-NBDG (2-(N-(7-Nitrobenz-2-oxa-1,3-diazol-4-yl)Amino)-2-Deoxyglucose) and 6-NBDG (6-(N-(7-Nitrobenz-2-oxa-1,3-diazol-4-yl)Amino)-6-Deoxyglucose), and the receptor is GLUT1 transport pathway. x-NBDGs, either 2-NBDG or 6-NBDG, bind with the GLUT1 transport pathway and form the ligand-receptor complex, LR, then is internalized, representing $L_{cytosol}$, and leaving empty GLUT1 receptor available for next ligand binding. In addition to equation (2), additional equations are added to describe potential molecular processes.

$$\emptyset \xrightarrow{\mathbf{k_{de\ novo}}} \mathbf{R_{de\ novo}} \tag{3}$$

$$\emptyset \xrightarrow{\mathbf{k_{de\ novo}}} \mathbf{L_{de\ novo}} \tag{4}$$

$$\mathbf{L_{cytosol}} \xrightarrow{\mathbf{k_{con}}} \emptyset \tag{5}$$

The three equations above are added to describe the appearance of a new GLUT1 transport molecule and newly accessible ligand by the new de novo receptor.

Previous studies support de novo GLUT1 transport components translocation onto the cell surface (Olsen *et al*, 2014; Dallner *et al*, 2006). The de novo ligand assumption follows the de novo receptor assumption. This corresponding de novo ligand appearance accounts for the minimal distance required for the ligand and receptor to interact. Ligands within the droplet are subject to the Brownian diffusion, and we assume that not every ligand is readily accessible by every receptor (Ju *et al*, 2015). In addition to the de novo appearance of receptor and ligand on the surface of the cell membrane, equation (5) is added to account for metabolic breakdown of the internalized glucose analogue, which occurs at the rate of k_{con}. The rate of k_{con} is under the assumption that the endocytosed 2-NBDG is subsequently converted into a non-fluorescent form of derivative, 2-NBDG 6-phosphate by hexokinase.(Yoshioka *et al*, 1996) Four equations (2)-(5) are combined and converted as ordinary differential equations for computational optimization via MATLAB.

$$\frac{\mathbf{d}[\mathbf{L_{out}}]}{\mathbf{dt}} = -\boldsymbol{k_f}[\boldsymbol{L_{out}}][\boldsymbol{R}] + \mathbf{k_r}[\boldsymbol{LR}] + \boldsymbol{A_i sech^2(t - T_i)} \tag{6}$$

$$\frac{\mathbf{d}[\boldsymbol{R}]}{\mathbf{dt}} = -\boldsymbol{k_f}[\boldsymbol{L_{out}}][\boldsymbol{R}] + \mathbf{k_r}[\boldsymbol{LR}] + \boldsymbol{k_{in}}[\boldsymbol{LR}] + \boldsymbol{A_i sech^2(t - T_i)} \tag{7}$$

$$\frac{\mathbf{d}[\boldsymbol{LR}]}{\mathbf{dt}} = \boldsymbol{k_f}[\boldsymbol{L_{out}}][\boldsymbol{R}] - \mathbf{k_f}[\boldsymbol{LR}] - \boldsymbol{k_{in}}[\boldsymbol{LR}] \tag{8}$$

$$\frac{\mathbf{d}[\mathbf{L_{cytosol}}]}{\mathbf{dt}} = \mathbf{k_{in}}[\boldsymbol{LR}] - \boldsymbol{k_{con}}[\boldsymbol{L_{cytosol}}] \tag{9}$$

The above four equations (6)-(9) are all of the ordinary differential equations used in MATLAB for kinetic modeling. T_i and A_i in Eq (6) and Eq (7) equation denote the timing and magnitude of de novo ligand and receptor appearance in the system. The

hyperbolic secant terms are also used to account for the de novo ligand and receptor's sudden pulse-like appearance. Four MATLAB scripts, composed of one main script and three subsidiary scripts, are used in this study. The main script reads out the data, creates pseudo-data for kinetic modeling, and runs ODE solver while continuously referring to the three subsidiary scripts until the exit condition is met.

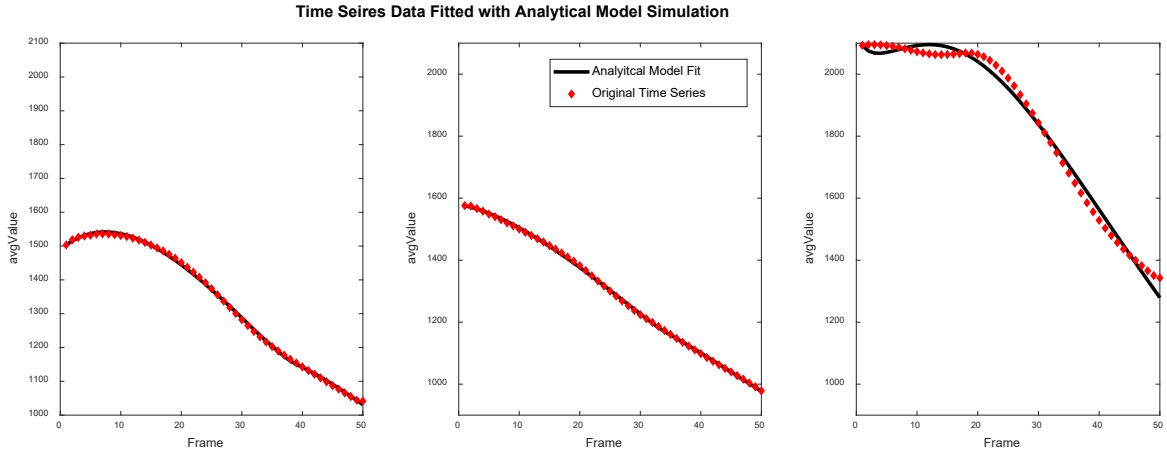

Figure 4.4 - Comparison of the original time series data with the model line generated by the kinetic modeling. Three randomly selected time series and its corresponding analytical model simulation data are plotted. Red diamond plots are original time-series data, and the black line is generated via analytical model simulation. Y-axis represents the top 0.5% intensity average value of the droplet, and the X-axis represents the frame number of the time series.

Using the sum of squared errors, the best intercept line is calculated with the ODE solver. Prior to ODE solving, data are soothed with MATLAB smooth function via a robust version of local regression using weighted linear least squares and a 2nd-degree polynomial model with a 2% span of a total number of data points. As a non-stiff problem, ODE45 solver, built-in to MATLAB, is used for the speed and accuracy of the kinetic modeling; other types of ODE solver such as ODE15s and ODE113 were tested, but ODE45 showed the highest time efficiency and accuracy. A total of 36,440 single cell metabolic profiles were fitted for kinetic modeling. Due to the large quantity of kinetic

modeling, multi-core clusters are utilized to shorten the model fitting time. The kinetic modeling system's precision was tested by visually comparing the original time series to the model line generated using the parameters calculated by the system, as shown in **Fig 4.4**. The simulation line fits well with the original time series data, supporting the kinetic modeling system's precision.

In order to further validate the kinetic model, two separate experiments involving a different type of glucose analogue were conducted using 2-NBDG and 6-NBDG. Both 2-NBDG and 6-NBDG are similar fluorescent forms of glucose analogues, but they differ in the fluorescent molecule attachment positions. Upon internalization, 2-NBDG can be modified to 2-NBDG 6-Phosphate by hexokinase, but due to the modification at 6^{th} position, 6-NBDG cannot be further converted by the hexokinase, resulting in accumulation of the internal 6-NBDG molecules.

	2-NBDG exp		**6-NBDG exp**		**Wilcoxon Rank-Sum Test**			
	Mean	Std Error	Mean	Std Error	p-value	h-value	Z-stat value	Rank-Sum value
$\mathbf{A_1}$	3.104	0.002	19.483	0.004	0.00E+00	1.00	-77.73	3.01E+08
$\mathbf{A_2}$	4.247	0.002	26.768	0.006	0.00E+00	1.00	-67.83	3.11E+08
$\mathbf{A_3}$	3.941	0.002	30.091	0.007	0.00E+00	1.00	-64.54	3.14E+08
$\mathbf{k_f}$	2.385	0.001	5.701	0.003	0.00E+00	1.00	-61.90	3.17E+08
$\mathbf{k_r}$	2.795	0.002	247.687	0.023	0.00E+00	1.00	-42.29	3.36E+08
$\mathbf{k_{in}}$	0.029	0.000	2.855	0.000	0.00E+00	1.00	-75.33	3.03E+08
$\mathbf{k_{con}}$	0.038	0.000	0.019	0.000	0.00E+00	1.00	131.54	5.09E+08

Table – 4.1. Parameters were acquired from kinetic modeling for separate x-NBDG experiments and statistical analysis. 2-NBDG and 6-NBDG experiments are conducted, and kinetic modeling parameters are shown in means and standard errors. Wilcoxon Rank-Sum test was conducted on each parameter from kinetic modeling. The statistical results, p-value, h-value, z-statistics value, and rank-sum value are reported.

Experimental data of x-NBDGs (2-NBDG and 6-NBDG) are all fitted into the kinetic modeling, and the results are shown in **Table 4.1**. For comparison of the parameters from each experiment, mean and standard error values are provided. For

statistical analysis, normal distribution of the 2-NBDG and 6-NBDG experiment parameters was tested using MATLAB's built-in function of Kolmogorov-Smirnov test, and since all were deemed to be non-normal, nonparametric statistical analysis of Wilcoxon Rank-Sum test was conducted to compare the kinetic modeling parameters from each experiment statistically. The p-values for all parameters are much less than 0.05, resulting in the rejection of null-hypothesis of identity between 2-NBDG and 6-NBDG reaction rates in all cases. The kinetic modeling parameter values are all significantly greater in the 6-NBDG experiment, except for the k_{con}, the consumption rate. The unmetabolizable 6-NBDG can explain all of the significant differences. Since 6-NBDG cannot be metabolized, the free 6-NBDG molecule continuously binds to the GLUT1 and unbind, gets internalized, binds to the intracellular side of GLUT1, then unbinds again continuously in an effort to acquire a metabolizable glucose source. The consumption rate, k_{con}, is expected to be zero in the 6-NBDG experiment, but it was only half the 2-NBDG experiment rate. Since it is hard to distinguish the fluorescence intensity decrease from metabolic breakdown and photobleaching, the modeling system's consumption rate must be a complex combination of the photobleaching and the metabolic breakdown rate. The kinetic modeling of the 2-NBDG experiment and 6-NBDG experiment shows that the modeling system can distinguish the difference in the metabolic profile posed by the change of the nutrient, glucose analogue.

	Category 1	**Category 2**	**Category 3**	**Wilcoxon Rank-Sum Test p-value**		
	Mean	Mean	Mean	Cat 1 & 2	Cat 1 & 3	Cat 2 & 3
A_1	4.257	2.369	3.361	0.000	0.000	0.037
A_2	10.028	2.987	3.922	0.000	0.000	0.000
A_3	8.727	2.888	2.696	0.000	0.000	0.000
k_f	5.422	1.534	2.800	0.000	0.000	0.000
k_r	1.881	1.738	3.224	0.000	0.018	0.000

k_{in}	0.025	0.017	0.015	0.000	0.000	0.000
k_{con}	0.044	0.042	0.043	**0.556**	**0.240**	**0.312**

Table – 4.2. Average parameter values for individual categories of the 2-NBDG experiment. Category numbering is identical to those in **Fig 4.3**. Wilcoxon Rank-Sum test p-values show a significant difference in parameters between categories. Statistically insignificant parameters between categories are highlighted in bold.

Ultimately, the kinetic system can give valuable physiological insight to rationalizing a metabolic profile observed from each category. As shown in **Table 4.2**, parameters from individual categories are all significantly different from each other except for the metabolic breakdown rate, k_{con}. The ligand-receptor binding and unbinding rates and the internalization rates are all significantly different among categories. We can potentially characterize Category 1 population from the kinetic modeling parameter as the ones with high affinity and fast GLUT1 transport pathway, evidenced by their highest k_f and k_{in} rates. On the other hand, the Category 2 population can be characterized as the ones with the GLUT1 pathway that binds with glucose analogue with the least affinity: the lowest k_f rate.

4.3. DISCUSSION

Michaelis-Menten equation inspired kinetic model can generate a model line with high accuracy compared to the original time series data and can decipher the underlying processes contributing to the cellular metabolic profiles. This study demonstrates the capability of dynamic metabolic profiling of approximately 12,000 single cells within a 3-hour time window with a temporal resolution of 4 minutes. Relatively plain categorization of the metabolic profiles gained valuable physiological meanings from the follow-up kinetic modeling. The system showed that it can construct a simulation kinetics that accurately resembles the observed metabolic profiles using the Michaelis-Menten

equation driven ordinary differential equations. The kinetic modeling system developed in this study also demonstrated the ability to distinguish the metabolic difference affected by the nutrient source change. We compared kinetic modeling parameters obtained from x-NBDGs experiments and showed the difference between two different substrates. The 6-NBDG experimental data's k_{con} is lower than that of 2-NBDG experimental data, and we believe it accounts for the indigestibility of the 6-NBDG. Further analysis of the kinetic modeling with comparison to the metabolic profile categorization, in addition, showed that we can potentially understand more regarding the reason for the observed metabolic patterns.

The quality of metabolic profiling can further be improved in the future by increasing the temporal resolution by adopting a higher resolution photon-sensitive microscope camera. In addition, incorporation of a functional probe, which has identical photo-quench characteristics as the fluorescent glucose analogue, can significantly help with decomposing the consumption rate into separate consumption rates and photobleaching rates. This will increase the accuracy of the consumption rate calculation without adding a weight on the computational side.

4.4. METHODS

Reagents

Polydimethylsiloxane (PDMS) was purchased from Dow Corning Corp, MI, USA. HFE-7500 oil containing 5% EA-surfactant (FluoSurf) and HFE-7500 oil containing functionalized SiO_2 nanoparticle surfactant (Fluoro-Phase) was purchased from Dolomite Microfluidics, United Kingdom. Trichloro(1H,1H,2H,2H-perfluorooctyl)silane (PFOTS) were purchased from Sigma-Aldrich, MO, USA. 2-NBDG (2-(N-(7-Nitrobenz-2-oxa-1,3-

diazol-4-yl)Amino)-2-Deoxyglucose), 6-NBDG (6-(N-(7-Nitrobenz-2-oxa-1,3-diazol-4-yl)Amino)-6-Deoxyglucose) Live Cell Imaging Solution (LCIS), RPMI 1640 media, Fetal Bovine Serum (FBS), Penicillin-Streptomycin (10,000U/mL), 100x (4-(2-hydroxyethyl)-1-piperazineethanesulfonic acid) HEPES, 100x GlutaMAX supplement, 2-Mercaptoethanol, Ficoll and CellTrace Violet were purchased from Thermo Fisher Scientific, MA, USA. Fluorinert FC-40 oil was purchased from Sigma Aldrich, MO, USA. 3M Novec 7500 Engineering fluid was purchased from 3M, MN, USA.

Device Fabrication

Two device masks, one for droplet generator and the other for the droplet observation chamber, are designed using AutoCAD 2019 and printed by CAD/Art Service, Inc. (CA, USA). The droplet generator uses a conventional flow-focusing junction design with a single oil inlet, two aqueous phase inlets, and a single outlet. Two aqueous phase inlets merge just before the flow-focusing junction. The master mold for the droplet generator is fabricated on a 3” silicon wafer (University Wafer Inc, MA, USA), and the master mold for the droplet observation chamber is fabricated on a 4” silicon wafer using the conventional soft lithography technique. The master molds are all fabricated inside a cleanroom in the Quattrone Nanofabrication Center of the Singh Center of Nanotechnology at the University of Pennsylvania. A positive photoresist SU-8 3050 (MicroChem, MA, USA) is used. The molds' thickness is controlled by adjusting the rotation speed of spin coating in conjunction with the UV exposure time under a mask aligner (SUSS Microtec, Garching, Germany). To produce the master for the droplet observation chamber, a multi-layer mold fabrication method is employed. Multi-layer mold fabrication skips mold development after initial post-bake and proceeds with spin-coating of the second photoresist layer. The master mold for the droplet observation

chamber has a flow channel height of 60 μm and the well height of 50 μm. The droplet generator mold is fabricated via the single-layer soft lithography technique with the channel height of 40 μm. Fabricated master molds are subsequently silanized with trichloro(1H,1H,2H,2H-perfluorooctyl)silane (PFOTS) to facilitate the detachment of cured polydimethylsiloxane (PDMS). Polydimethylsiloxane (PDMS) precursor is prepared by mixing the base and curing agents of Sylgard 184 (Dow Corning Corp, MI, USA) in a 10:1 ratio and is degassed in a vacuum chamber for 30 minutes. The degassed PDMS mixture is poured onto the master molds. The thicknesses of poured PDMS for the droplet generator and the observation chamber is 3 mm and 1 mm, respectively.

All molds are placed in an aluminum foil pan and degassed for another 30 minutes. After degassing, the top flow channel mold and the droplet generator mold are kept in an oven for 4 hours at 65 °C. Both the droplet generator and the observation chamber PDMS are, separately, bonded to a plain 1x3” glass slide using a conventional oxygen plasma treatment. The bonded devices are placed in an 80 °C oven for 2 hours to allow complete bonding.

EL4 Cell Culture and Preparation

EL4 mouse lymphoma cells are suspended in cRPMI media made by mixing RPMI 1640 media with 10% Fetal Bovine Serum, 100x (4-(2-hydroxyethyl)-1-piperazineethanesulfonic acid) HEPES, 100x GlutaMAX supplement, 100x Penicillin-Streptomycin and 1,000x 2-mercaptoethanol. Cells are suspended in a pre-warmed media at a concentration of 200,000 cells/mL for a total volume of 20 mL. The suspension is then transferred to a T-75 flask and incubated at 37 °C, 5% CO_2

incubator. For every two to three days, cell concentration was measured using a hemocytometer, and 4 million cells are suspended in fresh media up to 20 mL. Prior to the droplet generation, 10 million cells are transferred to a 50 mL conical tube, and dead cells are separated using density gradient, Ficoll. After removing the supernatant, cells are suspended in 1mL of pre-warmed Live Cell Imaging Solution, and 4 µL of 5 mM CellTrace Violet is added. After mixing by gentle pipetting, the suspension is incubated at 37 °C for 20 minutes. Subsequently, 12 mL of Live Cell Imaging Solution is added, mixed, and centrifuged at 200g for 5 minutes. The supernatant is removed, and the cell is resuspended in Live Cell Imaging Solution with a density of 1.8×10^7 cells/ml.

Droplet Generation and Trapping

The droplet generator and the observation chamber are silanized with a 2% PFOTS solution in HFE-7500 oil for 5 minutes following plasma treatment. Both devices are flushed with neat HFE-7500. The droplet generator is then connected with three PTFE tubings, each connected to a syringe: one filled with a 1:1 mixture of FluoSurf and Fluoro-Phase, the other filled with functional dye in LCIS, and the last filled with cell suspension in LCIS. Aqueous phase flow rates are set at 150 µL/hr, and the oil phase flow rate is set at 300 µL/hr. Once droplet generation stabilizes, the droplet generator outlet is connected to the observation chamber's inlet via PTFE tubings. Droplets generated from the droplet generator travel through a PTFE tubing and enter the bottom trap channel of the PHASR device. Before connection, the observation chamber is flushed with neat HFE-7500 until air bubbles within the device are entirely removed. With >60% of the wells filled with droplets, the droplet injection tubing is disconnected, and neat FC-40 oil is injected slowly to fill the remaining wells with the droplets. The oil

phase's flow rate is increased to 500 µL/hr to remove un-trapped droplets from the channel. Upon clearing of un-trapped droplets from the observation chamber channel, the observation chamber is disconnected from the PTFE tubings, and both the inlet and outlet of the observation chamber are sealed with the adhesive seal tabs from the Grace BioLabs, OR, USA, to prevent the evaporation of the continuous phase.

Dynamic Observation and Data Analysis

The observation chamber is then placed onto the stage of an inverted microscope for time-lapse imaging. The microscope specification used in the experiment is as follows. The main body is Zeiss Axio Observer 7 with a motorized Z step motor equipped with Zeiss motorized scanning stage 130 x 100 step (X and Y movement), Illuminator microLED 2 transmitted-light illumination condenser with shutter. It is also equipped with Colibri 5 Type RGB-UV fluorescence light source with 90 HE LED filter sets, motorized 6x reflector turret with shutter. PlanApo 10x air objective with 0.45 NA, with a working distance of 2.0, is used in the experiment. The microscope body, stage, and objective were all purchased from Carl Zeiss Microscopy, LLC., NY, USA. For the camera, Andor Zyla 4.2 sCMOS camera was purchased from Oxford Instruments, MA, USA. A digital cage-type microscope incubator was custom-built to have an active temperature, CO_2, and humidity control within the gas chamber with a 1 x 3-inch glass slide insert and was purchased from Okolab, NA, Italy. For the operation of all devices, MetaMorph microscopy automation and image analysis software used in the experiment was purchased from Molecular Devices, LLC., CA, USA. For data analysis, MATLAB from Mathworks, MA, USA, was used under an educational student license.

The environmental chamber is turned on at least 2 hours in advance to make a favorable environment of 37 ºC with 95% humidity and 5% CO_2 concentration. A custom

coded MetaMorph journal is used to automatically maneuver the stage to multiple positions and acquire multiple images with pre-set exposure conditions. Once the device is locked onto the stage, custom-coded MetaMorph journals execute automated acquisitions over time. 6% UV intensity, 6% Brightfield intensity, 15% GFP intensity is used with an exposure time of 10 msec, 10 msec, and 15 msec, respectively. Brightfield imaging can be skipped, but a single loop of brightfield imaging is recommended to backtrack clean imaging condition at every position. DAPI imaging loop follows the brightfield imaging loop to identify CellTrace Violet stained cells' location at each position. Fifty loops of GFP imaging is conducted in this experiment. Upon acquisition, image files are organized into corresponding folders via PyCharm, developed by JetBrains. The PyCharm code for image file organization can be found in the APPENDIX. Acquired images are analyzed using ImageJ particle analysis. Images are imported as image sequences per each position, and the time-lapse data of individual droplets are extracted via ImageJ particle analysis. A modified version of the ImageJ particle analysis is used in the study, and the full package can be found in the APPENDIX. The modified ImageJ package is executed with IntelliJ IDEA, developed from JetBrains. The modified ImageJ particle analysis allows the top 0.5% intensity average extraction from individual droplets over time-lapse data. This top 0.5% intensity profile more accurately depicts the cell's total fluorescence signal as the cell occupies roughly 0.5% of the droplet area.

Extracted data are subsequently sorted by individual droplets using MATLAB code. Since ImageJ particle analysis over time-lapse data does not guarantee consistent numbering of the same droplet over the time, MATLAB code analyzes the droplet center X, and Y coordinate then numbers individual droplet and re-organizes the ImageJ extracted data. Individual cell positions are also analyzed using the DAPI loop ImageJ

particle analysis data. Based on the cell size and shape, such as roundness, each droplet is categorized for containing no cell, single cell, or multiple cells. Using single-cell containing data, principal component analysis (PCA) is conducted via MATLAB and stored separately. MATLAB code for data processing is available in the APPENDIX. Also, Dynamic Time Warping (DTW) clustering method is conducted via R and its built-in "tsclust" package. Processed data is subsequently uploaded to cluster for batch processing of MATLAB analytical model fitting. Model fitting code utilizes MATLAB's built-in "fmincon" function with an ODE45 ordinary differential equation solver. Four separate code files are used to optimize the model fitting to the original time series data. The full script and code can be found in the APPENDIX. For statistical analysis, MATLAB's built-in Kolmogorov-Smirnov test was conducted to check the data's normal distribution. Due to non-normal distributed kinetic modeling parameters, nonparametric statistical analysis, the Wilcoxon Rank-Sum test, was conducted via MATLAB.

4.5. REFERENCES

Ackermann M (2015) REVIEWS A functional perspective on phenotypic heterogeneity in microorganisms. *Nat. Publ. Gr.* **13:** 497–508 Available at: http://dx.doi.org/10.1038/nrmicro3491

Bathe OF & Farshidfar F (2014) From Genotype to Functional Phenotype: Unraveling the Metabolomic Features of Colorectal Cancer. **:** 536–560

Bertozzi CR, Francis MB, Hsiao SC, Thaitrong N, Douglas ES, Toriello NM & Mathies RA (2008) Integrated microfluidic bioprocessor for single-cell gene expression analysis. *Proc. Natl. Acad. Sci.* **105:** 20173–20178 Available at: http://www.pnas.org/content/105/51/20173.abstract%5Cnhttp://www.pnas.org/content/105/51/20173.full.pdf

Dallner OS, Chernogubova E, Brolinson KA & Bengtsson T (2006) β_3 -Adrenergic Receptors Stimulate Glucose Uptake in Brown Adipocytes by Two Mechanisms Independently of Glucose Transporter 4 Translocation. *Endocrinology* **147:** 5730–5739 Available at: https://academic.oup.com/endo/article-lookup/doi/10.1210/en.2006-0242 [Accessed July 19, 2020]

Dueck H, Eberwine J & Kim J (2016) Variation is function: Are single cell differences

functionally important?: Testing the hypothesis that single cell variation is required for aggregate function. *BioEssays* **38:** 172–180
Gross A, Schoendube J, Zimmermann S, Steeb M, Zengerle R & Koltay P (2015) Technologies for Single-Cell Isolation. *Int. J. Mol. Sci.* **16:** 16897–16919 Available at: http://www.mdpi.com/1422-0067/16/8/16897 [Accessed July 15, 2020]
Han SH, Choi Y, Kim J & Lee D (2020) Photoactivated Selective Release of Droplets from Microwell Arrays. *ACS Appl. Mater. Interfaces* **12:** 3936–3944
Ju L, Qian J & Zhu C (2015) Transport regulation of two-dimensional receptor-ligand association. *Biophys. J.* **108:** 1773–1784 Available at: /pmc/articles/PMC4390815/?report=abstract [Accessed July 19, 2020]
Kumar R, Ghosh M, Kumar S & Prasad M (2020) Single Cell Metabolomics: A Future Tool to Unmask Cellular Heterogeneity and Virus-Host Interaction in Context of Emerging Viral Diseases. *Front. Microbiol.* **11:** 1152 Available at: www.frontiersin.org [Accessed July 15, 2020]
Kunz DJ, Gomes T & James KR (2018) Immune cell dynamics unfolded by single-cell technologies. *Front. Immunol.* **9:** 1–8
MacRae CA & Vasan RS (2016) The future of genetics and genomics. *Circulation* **133:** 2634–2639 Available at: https://www.ncbi.nlm.nih.gov/pmc/articles/PMC6188655/ [Accessed July 15, 2020]
Minakshi P, Kumar R, Ghosh M, Saini HM, Ranjan K, Brar B & Prasad G (2019) Single-cell proteomics: Technology and applications. In *Single-Cell Omics: Volume 1: Technological Advances and Applications* pp 283–318. Elsevier
Nathan A, Baglaenko Y, Fonseka CY, Beynor JI & Raychaudhuri S (2019) Multimodal single-cell approaches shed light on T cell heterogeneity. *Curr. Opin. Immunol.* **61:** 17–25 Available at: https://linkinghub.elsevier.com/retrieve/pii/S0952791519300469 [Accessed August 26, 2019]
Olsen JM, Sato M, Dallner OS, Sandström AL, Pisani DF, Chambard JC, Amri EZ, Hutchinson DS & Bengtsson T (2014) Glucose uptake in brown fat cells is dependent on mTOR complex 2-promoted GLUT1 translocation. *J. Cell Biol.* **207:** 365–374 Available at: /pmc/articles/PMC4226734/?report=abstract [Accessed July 19, 2020]
Papalexi E & Satija R (2017) Single-cell RNA sequencing to explore immune cell heterogeneity. *Nat. Publ. Gr.* **18:** 35–45 Available at: http://dx.doi.org/10.1038/nri.2017.76
Utharala R, Tseng Q, Furlong EEMM & Merten CA (2018) A Versatile, Low-Cost, Multiway Microfluidic Sorter for Droplets, Cells, and Embryos. *Anal. Chem.* **90:** 5982–5988 Available at: https://pubs.acs.org/doi/10.1021/acs.analchem.7b04689. [Accessed June 6, 2019]
Yoshioka K, Saito M, Oh KB, Nemoto Y, Matsuoka H, Natsume M & Abe H (1996) Intracellular fate of 2-NBDG, a fluorescent probe for glucose uptake activity, in Escherichia coli cells. *Biosci. Biotechnol. Biochem.* **60:** 1899–901 Available at: http://www.ncbi.nlm.nih.gov/pubmed/8987871
Yuan G-C, Cai L, Elowitz M, Enver T, Fan G, Guo G, Irizarry R, Kharchenko P, Kim J, Orkin S, Quackenbush J, Saadatpour A, Schroeder T, Shivdasani R & Tirosh I (2017) Challenges and emerging directions in single-cell analysis. *Genome Biol.* **18:** 84 Available at: http://www.ncbi.nlm.nih.gov/pubmed/28482897%0Ahttp://www.pubmedcentral.nih.gov/articlerender.fcgi?artid=PMC5421338
Zhang L & Romero P (2018) Metabolic Control of CD8 + T Cell Fate Decisions and

Antitumor Immunity. *Trends Mol. Med.* **24:** 30–48 Available at: http://dx.doi.org/10.1016/j.molmed.2017.11.005

CHAPTER 5

PHOTOACTIVATED SELECTIVE RELEASE OF DROPLETS FROM MICROWELL ARRAYS

Adapted from: Han SH, Choi Y, Kim J, Lee D. Photoactivated Selective Release of Droplets from Microwell Arrays. *ACS Appl Mater Interfaces*. 2020;12(3):3936-3944. doi:10.1021/acsami.9b17575

5.1. INTRODUCTION

Droplet microfluidics has enabled rapid production of highly uniform emulsion droplets with a wide range of applications. In particular, individual microfluidic droplets can be used as micro-chambers, making them a versatile platform to perform rapid high throughput assays while significantly reducing the volume of reagents required.[1–4] Compared to conventional multi-well plate-based assays, the required reagent volume can be reduced by three to five orders of magnitude and the per-sample manipulation time can also be reduced by up to ten-folds.[1,5–7] Several applications including single cell gene regulation, nuclear division and metabolism study require culturing of cells or monitoring dynamic events within droplets for extended periods from hours to days. Various types of static array devices have been developed for such applications which allow for real time dynamic observation of events that occur within the droplets.[8–12]

For a number of applications that involve trapping droplets in a microwell array for extended periods, it is highly beneficial and desirable to recover droplets following the observation. For example, selective release of droplets that contain a single or multiple cell that show a rare phenotype could enable single cell sequencing and potentially uncover the molecular basis of such a phenotype. A handful of methods have been

developed for the selective recovery of droplets from a microwell array. The recovery methods depend highly on the trapping methods that are used for dynamic monitoring or droplet incubation.[8,13–19] In case of the so-called pea-in-a-pod device, where droplets are guided through and physically trapped in a corrugated channel, selective recovery is not possible without using some type of barcode or labels within each droplets; such post-hoc selection from barcode is inefficient if the phenotype is rare.[25] For a device with microwell arrays that captures droplets by density difference, droplets can be released by simply flipping the device; however, this method is non-specific, and does not enable selective recovery.[20,21] Currently, the most effective method for selective recovery of droplets is based on mechanical actuation using pneumatic valves.[10,13,14,22] Mechanical actuation can trap and release droplets in both 2-dimensional and 3-dimensional arrays with considerable accuracy and precision. However, the applicability of this approach is potentially limited by the fact that the number of valves must at least match the number of microwells. This would require a rather complicated device fabrication process and also require sophisticated equipment to control and deliver pressure to the necessary set of valves to enable selective release. Due to these limitations, the capacity for capture and selective release based on this approach has been limited to a few hundreds, whereas many high capacity applications including rare cell phenotyping require monitoring at least a few thousand droplets.

In this report, we develop a method to capture and selectively release droplets from a microwell array by combining a photoresponsive layer with the conventional microfluidic device fabrication technique. The photoresponsive layer, made of a glassy polymer, polystyrene, a photoresponsive dye and a plasticizer, is sandwiched in between the microwell array and a PDMS slab with or without a top flow channel that is

used to apply positive or negative pressure. The glass transition temperature and absorption spectra of the photoresponsive layer can be engineered to address a variety of experimental needs. Furthermore, the incorporation of the photoresponsive layer minimally alters the chip fabrication process and the selective recovery of samples can be performed without relying on a large number of supporting instruments. Previous studies have incorporated aluminum patterns that serve as heating blocks into a device or used focused UV laser to heat the oil interface adjacent to the droplet to release droplets.[14,23] We use NIR laser which is far less harmful to biological molecules and cells than UV laser. We demonstrate photoactivated selective release (PHASR) of droplets from a photoresponsive layer-embedded array consisting of 4,400 microwells which we believe is the largest capacity reported for dynamic observation with selective recovery to date. With slight modification on the laser intensity and the focal plane, we show that two different ways of recovery are possible. High intensity focused laser on the photoresponsive layer allows release-up recovery of the droplet whereas low intensity focused laser on the photoresponsive layer-oil interface induces push-down recovery of droplets. Moreover, this method does not require any extra instruments that scale with the number of microwells. Thus, we anticipate that the PHASR method enabled in this high-capacity system will benefit many research fields utilizing phenotyping in combination with genotyping such as molecular biology and immunology.

5.2. EXPERIMENTAL METHODS

ABBREVIATIONS

PHASR, photoactivated selective release; PDMS, polydimethylsiloxane; PS, polystyrene; SiNc, silicon 2,3-naphthalocyanine bis(trihexylsilyloxide); IR-780, infra-red-

780 iodide; DEGD, di(ethylene glycol) dibenzoate; NIR, near-infrared; UV, ultraviolet; T_g, glass transition temperature; FTIR, Fourier Transform Infrared Radiometer; PFOTS, trichloro(1H,1H,2H,2H-perfluorooctyl)silane;

Reagents

Polystyrene (PS) with MW of 192,000, trichloro(1H,1H,2H,2H-perfluorooctyl)silane (PFOTS), di(ethylene glycol) Dibenzoate (DEGD), IR-780 iodide (IR-780) and silicon 2,3-naphthalocyanine bis(trihexylsilyloxide) (SiNc) were purchased from Sigma-Aldrich, MO, USA. Polydimethylsiloxane (PDMS) was purchased from Dow Corning Corp, MI, USA. FC-40 oil containing 2% EA-surfactant (Pico-surf) was purchased from Dolomite Microfluidics, United Kingdom. EL4 (ATCC TIB-39) mouse lymphoma cell line, ATCC-formulated Dulbecco's Modified Eagle's medium and horse serum were purchased from American Type Cell Culture, VA, USA. Live/Dead mammalian cell viability assay kit was purchased from Thermo Fisher Scientifics, MA, USA.

Device Fabrication

The device masks are designed using AutoCAD 2018 and printed by CAD/Art Service, Inc. (CA, USA). A master mold is fabricated on a 3" silicon wafer (University Wafer Inc, MA, USA) using the conventional soft lithography technique. The master molds are all fabricated inside a cleanroom in the Quattrone Nanofabrication Center of the Singh Center of Nanotechnology at the University of Pennsylvania. A positive photoresist KMPR-1050 (MicroChem, MA, USA) is used and the thickness of the molds is controlled by adjusting the rotation speed of spin coating in conjunction with the UV exposure time under a mask aligner (SUSS Microtec, Garching, Germany). To produce

the master for the bottom trap channel, a multi-layer mold fabrication method is employed. Multi-layer mold fabrication skips mold development after initial post-bake and proceeds with spin-coating of the second photoresist layer. Top flow channel and droplet generator molds are fabricated via the single layer soft lithography technique. Fabricated master molds are subsequently silanized with trichloro(1H,1H,2H,2H-perfluorooctyl)silane (PFOTS) to facilitate the detachment of cured polydimethylsiloxane (PDMS). Polydimethylsiloxane (PDMS) precursor is prepared by mixing the base and curing agents of Sylgard 184 (Dow Corning Corp, MI, USA) in a 10:1 ratio and is degassed in a vacuum chamber for 30 minutes.

The degassed PDMS mixture is poured onto the master molds. The thicknesses of poured PDMS for the droplet generator and top flow channel are ~ 3 mm ~ 1 mm, respectively. The thickness of poured PDMS for the bottom trap channel is just enough to completely cover the channel structures. All molds are placed in an aluminum foil pan and degassed for another 30 minutes. After degassing, the top flow channel mold and the droplet generator mold are kept in an oven for 4 hours at 65 °C. The droplet generator PDMS is bonded to a plain glass slide using a conventional oxygen plasma treatment. A thin clear polyester film is slowly placed on top of the uncured PDMS on the bottom trap channel while minimizing bubble formation. A 2x3” glass slide is placed on top of the film and then binder clips and a 3-prong clamp are used to apply compressive pressure onto the sandwiched layers of glass slide, polyester film, PDMS solution and the wafer with the bottom trap channel mold. The clamped device is left at room temperature for 1 hour to allow uncured PDMS to completely squeeze out and then placed in an 80 °C oven for 2 hours. Fully cured bottom trap channel PDMS is peeled off from the master mold under ethanol. The polyester film is left on the bottom trap

channel. Other PDMS layers are peeled and prepared using the standard. The base of bottom trap channel is taped with scotch tape to keep the surface clean.

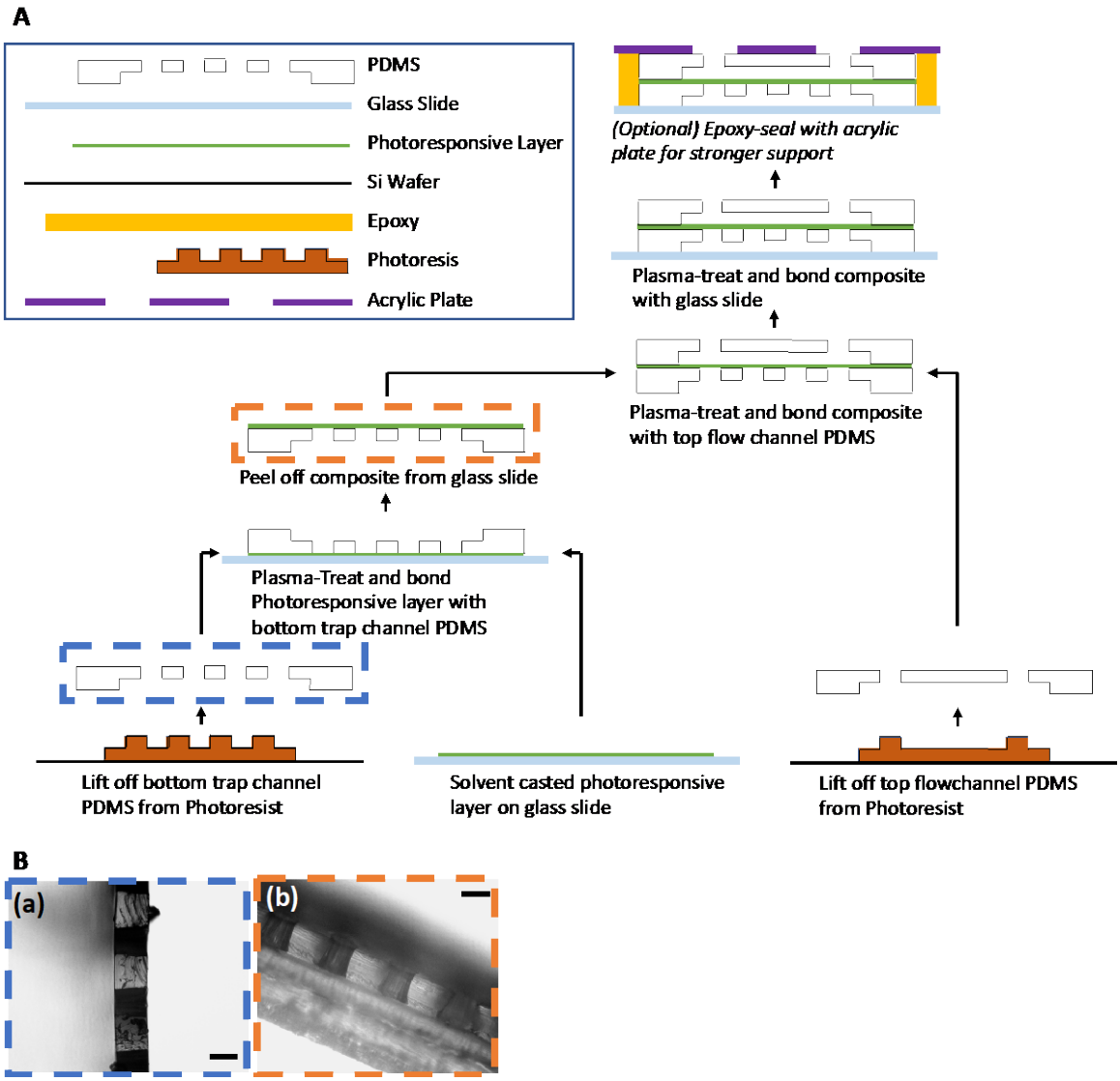

Figure 5.1. PHASR device fabrication protocol. (A) Fabrication protocol for the PHASR device. The first composite laminate is prepared by bonding the photoresponsive layer with the bottom PDMS trap channel and the second composite laminate is prepared by bonding the first composite with the top PDMS flow channel, and the final device is prepared by bonding the second composite to a glass slide. (B) Images of (a) bottom PDMS trap channel showing wells with open-top structure and (b) bottom PDMS trap channel with a photoresponsive layer; the photoresponsive layer covers the microwell array. Images of parts in (A) enclosed with dotted boxes are shown in (B)

The photoresponsive layer is fabricated using polystyrene (PS) of MW 192,000 and di(ethylene glycol) Dibenzoate (DEGD) with IR-780 iodide (Sigma-Aldrich, MO, USA). Two dyes are tested in the study with target actuation spectra in near infrared region: IR-780 and silicon 2,3-naphthalocyanine bis(trihexylsilyloxide) (SiNc). To render PS responsive to near-infrared (NIR) light, we use a photoacoustic dye such as IR-780 iodide (MW ~667g/mol) or silicon 2,3-naphthalocyanine bis(trihexylsilyloxide) (SiNc) (MW ~1,340g/mol). Both are well known photoacoustic dyes in the range of NIR with extinction coefficients greater than 250,000 $M^{-1}cm^{-1}$. In 10 ml of chloroform, 5 wt.% PS, 1.45 wt.% DEGD and 0.1 wt.% IR-780 are added. The glass transition temperature of PS is 90 - 100 °C, which likely is too high for use in the proposed scheme. To ensure that PS responds to light at a more reasonable temperature such that the generated heat would not damage the encapsulated molecules or cells, we add a plasticizer, di(ethylene glycol) dibenzoate (DEGD) (MW ~314g/mol). DEGD is added to the PS solution at 1.45 wt% which is equivalent to 29 wt% of the mass of PS. In addition to 1.45 wt.% of DEGD which lowers the glass transition temperature of the polymer, IR-780 at its solubility limit in chloroform (0.1 wt.%) is added. The solution is left in a mixer and sonicating bath for 1 hour each. Subsequently, the solution is filtered through a 5 μm PTFE syringe filter. The solution is stored in a tightly sealed vial with aluminum foil covering to prevent photobleaching of the photoacoustic dye. A thin photoresponsive layer is prepared using a flow coater. A clean glass slide is placed on a doctor blade coater (NRT100, ThorLab, NJ, USA). Approximately 2 ml of the photoacoustic solution is evenly cast on 2” x 3” glass slides using coating speed of 20 mm/sec and acceleration of 1 mm/sec^2.

The chip assembly process starts with bonding of the bottom trap channel PDMS with the photoresponsive layer. The overview of the fabricated device and fabrication step protocol is schematically shown in **Figure 5.1A**. The vacuum dried photoacoustic layer on a glass slide and the top of the bottom trap channel are oxygen plasma treated at 50 Watts for 45 seconds (SCE 110, Anatech Ltd, MI, USA) and bonded together as shown in **Figure 5.1B-(b)**. The bonded device is left undisturbed for 2 hours to ensure bonding, then the device is carefully peeled off from the glass slide. This bonding between the photoresponsive layer and the bottom trap channel PDMS is irreversible and thus these layers cannot be easily separated. The inlets and outlets for the composite of bottom trap channel and photoresponsive layer and the top flow channel are punched using a 1.0 mm disposable biopsy punch (Integra Miltex, NJ, USA). The base side of the top flow channel is bonded onto the photoresponsive layer using the same oxygen plasma treatment and stored for additional 2 hours; this bonding requires alignment of the bottom trap channel structure to the top flow channel structure and can be performed with high fidelity under a mask aligner or stereoscope. In case of weak bonding between the photoresponsive layer and the top flow channel device, treatment of 5 v/v% (3-Aminopropyl)triethoxysilane (APTES) on the photoresponsive layer following plasma treatment is recommended. After removing the scotch tape, the base of the bottom trap channel is bonded to a glass slide. To enable use under a high-pressure flow system, 1/16” clear acrylic plate can be custom-tailored (PLS 4.75, Universal Laser Systems, AZ, USA) and bonded with the base glass slide using 5-min epoxy.

Cell Culture

EL4 (ATCC TIB-39) mouse lymphoma cell line was purchased from American Type Cell Culture, VA, USA. Thawed cell pellet is suspended in ATCC-formulated

Dulbecco's Modified Eagle's Medium supplemented with horse serum final concentration of 10%. The cell suspension is seeded in a Corning T-75 flask at density of 1.5 x 10^5 cells/ml with total volume of 20 ml. The seeded flask is incubated at 37 °C with 5% CO_2 concentration for 48 hours. The cell suspension is mixed with serological pipette to form homogeneous suspension and the concentration is measured using a hemocytometer. The cell suspension is centrifuged at 90 rcf for 10 minutes without break and supernatant is removed. The cell pellet is resuspended in a growth medium to density of 1.2 x 10^7 cells/ml.

Droplet Generation and Trapping

A droplet generator made with PDMS is silanized with 2% PFOTS solution in FC-40 oil for 5 minutes following plasma treatment. The device is flushed with neat FC-40 oil then connected with two PTFE tubings, each connected to a syringe, one filled with FC-40 containing 2 wt% EA-surfactant and the other filled with aqueous solution with or without dye. The EA surfactant is a commercially available tri-block copolymer composed of perfluoropolyether (PFPE) and polyethylene glycol (PEG) blocks and is most widely used in emulsion stabilization in fluorinated oils like FC-40 and HFE-7500. An aqueous dye such as dimethyl blue can be added to facilitate the visualization of the droplets. Flow rates of 250 µL/hr and 200 µL/hr are used for oil and aqueous phases, respectively. For cell viability assay, cell suspension with density of 1.2 x 10^7 cells/ml and Live/Dead mammalian cell viability assay kit (Thermo Fisher Scientifics, MA, USA) are used as aqueous phases. Aqueous phases are separately introduced into the droplet generator. For the Live/Dead mammalian cell viability assay, the concentrations of EthD-1 and calcein AM are adjusted to 8 µM and 4 µM, respectively, to produce the final concentrations of 4 µM and 2 µM in droplets. Prior to the droplet introduction, the

PHASR device is flushed with neat FC-40 for 2 minutes to remove air bubbles within the device. In addition, the FC-40 oil phase with 2 % PFOTS is flown into the PHASR device to make the channel hydrophobic and prevent droplet adhesion to the channel wall. Droplets generated from the droplet generator travel through a PTFE tubing and enter the bottom trap channel of the PHASR device. With >60% of the wells filled with droplets, the droplet injection tubing is disconnected, and neat FC-40 oil is injected slowly to fill remaining wells with the droplets. Flow rate of the oil phase is increased to 500 µL/hr to remove un-trapped droplets from the channel.

Selective Release of Droplets

All selective release and recovery experiments are conducted at the Vision Research Center of the University of Pennsylvania. To selectively release droplets, we use a home-built two-photon microscope, since the two-photon microscope ensures precise targeting of a specific location within the PHASR device with minimal off-target effects. The mode-locked Titanium:Sapphire ($Ti:Al_2O_3$) laser (Chameleon, Coherent, Santa Clara, CA) is used as an excitation source with the wavelength of 780 nm for IR-780-based photoresponsive layers. The laser has output power of 3.37 Joule/s at 780 nm wavelength, and the pass-through percent of the power is calculated to be roughly 20% of the output. The laser source is Spectra Physics Mai Tai HP 1020 pulsed laser, equipped with DeepSee automated group velocity dispersion compensation. The laser repetition rate is 80 MHz at 800 nm wavelength; the duration of a pulse is less than 100 fsec with the peak power greater than 300 kW. Under 60x water-immersion objective, 5% intensity corresponds to 73.9 $J/s \cdot cm^2$ exposure intensity. In case of a SiNc-based photoresponsive layer, the wavelength is tuned to 775 nm. Several parameters such as laser intensity, laser power, scanning resolution and scanning rate affect the

performance of the PHASR device. To represent the laser exposure in a single parameter, we first calculate the total energy exposure rate in the unit of Watt/cm^2 and multiply this value by the exposure time to determine the total exposure energy per unit area in the unit of J/cm^2. We test ranges of exposure intensity and time for each photoresponsive layer and determine that the exposure energy of 155.03 J/cm^2 is necessary to release 50 μm droplets from 50 μm depth wells using the 17 μm IR-780-based photoresponsive layer. The target is identified within the field of view using a low magnification objective such as 4x or 10x, and then the objective is replaced with a 60x water-immersion objective to zoom-in on the target. The schematics of droplet trapping and release via the two mechanisms are shown in **Figure 5.2B** and **Figure 5.2C**. Depending on the method of recovery, the focal plane is set either at the top of the photoresponsive layer to induce hole formation or at the base for bubble formation. Droplets released from the microwell array are recovered by flowing oil through the channel.

5.3. RESULTS AND DISCUSSION

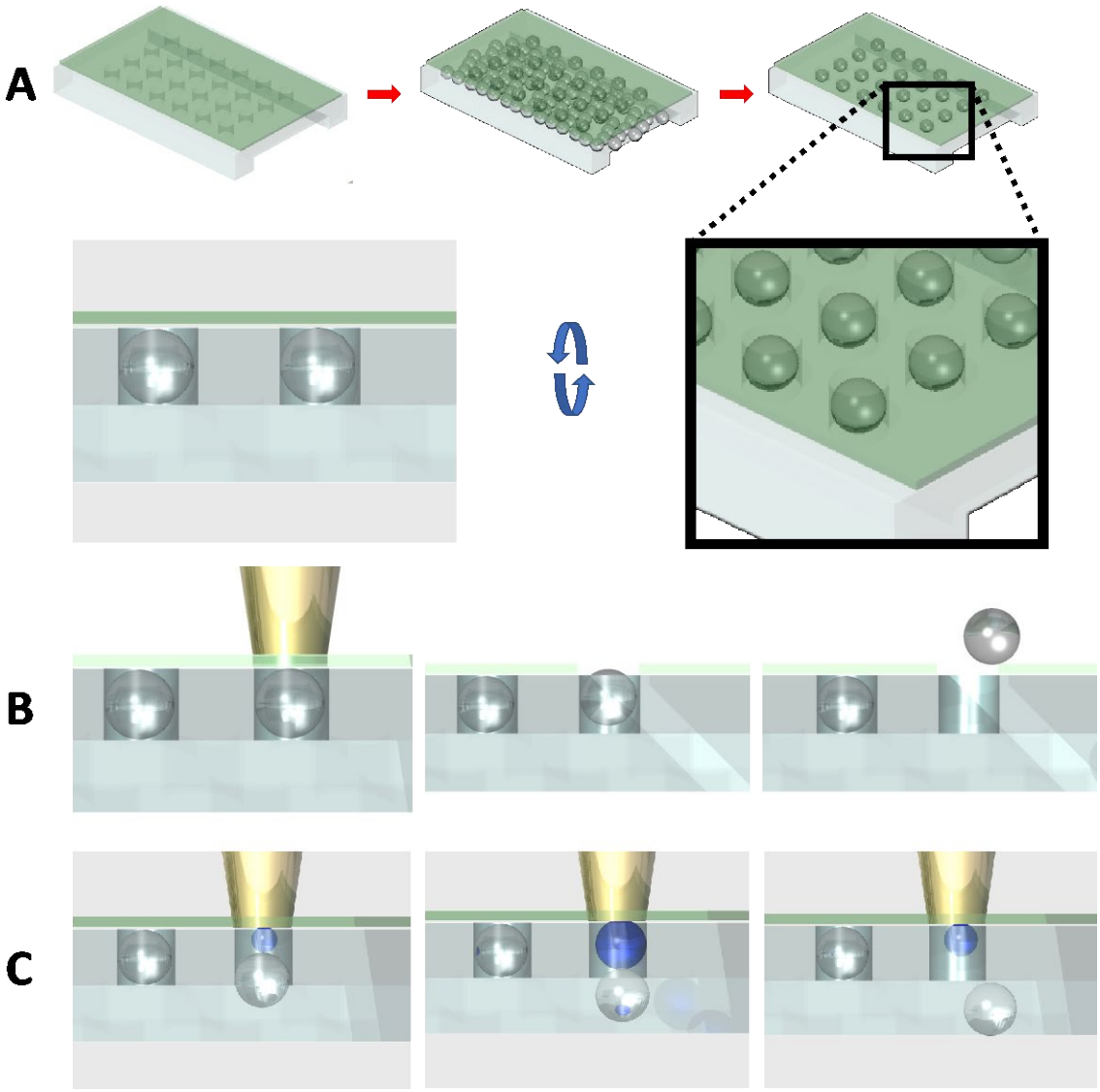

Figure 5.2. PHASR device overview. (A) Droplet static array formation by density difference. The higher density of the oil phase drives trapping of aqueous droplets in wells. (B) NIR laser irradiation on the top of the photoresponsive layer heats and punctures the layer, allowing droplet to float through the opening and into the top flow channel for release-up recovery. (C) NIR laser exposure on the bottom of the photoresponsive layer creates a bubble which pushes out the droplet toward the bottom trap channel for push-down recovery.

Droplet microfluidics can readily isolate cells, particles and even single molecules into individual droplets which can subsequently be arranged into an array that enables

monitoring of dynamic events such as cell response to external stimuli or (bio)chemical reactions. Photoresponsive-layer enabled photoactivated selective release (PHASR) of droplets from a microwell array, we explore in this study, is schematically illustrated in **Figure 5.2**. We use density difference between continuous and dispersed phases to trap droplets into a microwell array as shown in **Figure 5.2A**. The trapping efficiency of using this method is approximately 20%, which agrees well with a previous report.[24] The trapping efficiency can be improved drastically (up to 90%) by slightly tilting the chip back and forth [23]. The trapping efficiency can vary greatly depending on the droplet velocity and the volume fraction of the droplets in the emulsion suspension. This method is advantageous over other methods of droplet trapping because of the ease of device fabrication. The target droplets for further investigation can be identified through optical measurements of individual cells in the microwell array. These measurements can be taken over time, for example, using physiological reporter probes. The microwell array is fully compatible with an environmental chamber capable of full gas and humidity control. Once the targets are identified, they can be released from the microwell array using two different methods as illustrated in **Figure 5.2B** and **Figure 5.2C**. High intensity short burst light can be focused onto the photoresponsive layer to induce rupture of the photoresponsive layer over specific microwells that contain the target droplets (**Figure 5.2B**); droplets can float through the pore and escape the microwell or they can be pushed downward and released by applying positive pressure from the top flow channel. If moderate intensity light is focused onto the photoresponsive layer above a selected well, this will lead to bubble formation which in turn pushes out the droplet from the array as illustrated in **Figure 5.2C**. We believe the bubble formation upon laser exposure is likely a result of cavitation in the oil phase. [25] In case of the layer-rupture induced release-up recovery, the order of droplet release can be random as there is little concern

for recapturing of droplets, whereas in the case of the push-down release, the droplets should be released sequentially in the direction of the flow to prevent droplets from being recaptured by empty microwells.

The device fabrication involves fabrication of three individual layers – the bottom trap channel consisted of a microwell array made of polydimethylsiloxane (PDMS), the middle photoresponsive layer made of polystyrene (PS) and the top PDMS slab with or without a top flow channel - followed by their sequential bonding as shown in **Figure 5.1**. To enable release of droplets through a punctured photoresponsive layer, the bottom trap PDMS channel must have an open-top structure. Even a thin layer of PDMS on the top of each microwell will not allow release of droplets through the punctured photoresponsive layer. To ensure complete open-top structure in the PDMS channel, uncured PDMS, poured on the master, is compressed between a polyester film and the hard master using a 3-prong laboratory clamp, applying pressure of approximately 7 kPa. Given sufficient time, uncured PDMS squeezes out of the space between the polyester film and the patterned photoresist completely. A minimum of 1 hour is used to ensure that the microwell array layer has an open-top structure as shown in **Figure 5.1B-(a)**. Although our demonstration of selective release will be performed with a PHASR device with 4,400 wells, we can readily fabricate a PDMS microwell array with up to 40,000 open-top wells. Solvent-cast photoresponsive layer serves as the top surface (i.e., ceiling) of the bottom trap channel PDMS layer with open-top microwells as shown in **Figure 5.1B-(b)**. To enable layer-rupture induced release-up recovery, we add a PDMS slab with a top flow channel atop the photoresponsive layer. The push-down release device does not require such a top flow channel structure. Layers are bonded

via oxygen plasma treatment, and optional epoxy-based sealing can be added for systems that deal with high pressure flows.

The most essential component of this PHASR device is the photoresponsive layer. We chose to use a glassy thermoplastic polymer, polystyrene (PS) as the base material for this purpose. PS is chosen because free standing films of PS can be readily prepared by using highly entangled PS.[26] Moreover, its thermomechanical properties can be engineered by incorporating a plasticizer. These dyes also have high solubility in good solvents for PS such as chloroform and tetrahydrofuran. Although the quantum yields for these two dyes have not been reported, dyes with similar structures such as IR-800 have quantum yields of 0.034[33,34], indicating that much of the absorbed energy is dissipated via thermal mechanisms, leading to heat generation.

The polymer solution along with the plasticizer and one of the two photoacoustic dyes remains clear and optically transparent during preparation, indicating high solubility of the three components in chloroform. The doctor-blade method is used to coat the solution onto a clean glass slide. The film is dried under vacuum to completely remove the solvent, leading to the formation of an optically transparent and slightly green solid film. The addition of DEGD reduces the glass transition temperature (T_g) of PS significantly to 33 ℃, and the addition of the photosensitive dye does not significantly change the T_g as seen in **Figure 5.3**.[35] The suppression of 60 ℃ in T_g agrees well with previously reported results.[27] This study mainly uses a photoresponsive layer with T_g of 33 ℃ to minimize the potential heat damage on living cells in droplets. If the device requires incubation or imaging at 37 ℃, the composition of photoresponsive layer can be easily adjusted to achieve T_g of ~ 40 ℃.

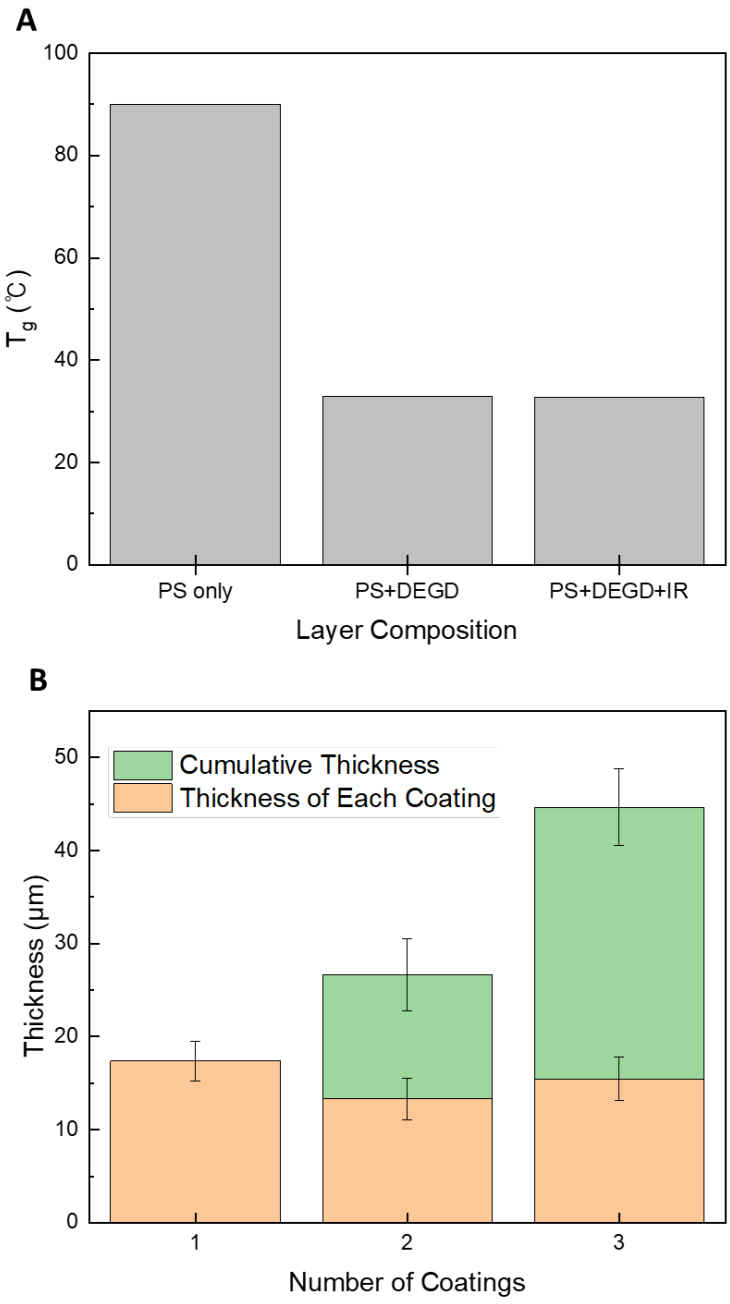

Figure 5.3. Characteristics of photoresponsive layer with IR-780 dye. (A) T_g PS layer, PS layer with DEGD and PS layer with DEGD and IR-780 dye measured via dynamic mechanical analysis (DMA). (B) Thickness of photoresponsive layer as a function of the number of flow coating as determined by profilometry.

Since thin photoresponsive layers would be advantageous in the rupture-induced release-up recovery method, we test layer thicknesses ranging from 100 nm to 30 μm and find that layers with thickness less than 15 μm result in unreliable fabrication due to layer deterioration during either plasma treatment or peel-off process. We determine that the minimum thickness that results in highly reliable device fabrication (success rate >90%) to be approximately 17 μm. The solution concentration of PS and the blade coating condition (gap height = 200 μm, speed of blade translation = 20 mm/sec, polymer concentration = 5 wt%) are thus adjusted to give a 17 μm PS film. The thickness of the PS layer can be increased in ~14 μm increments with additional coatings as shown in **Figure 5.3**.

We also assess the optical properties of the layer as shown in **Figure 5.4**. The FTIR spectra of the layers confirm the incorporation of DEGD as can be seen by the peaks at 1,110 cm^{-1}, 1,280 cm^{-1} and 1,720 cm^{-1} which correspond to the secondary alcohol C-O, aromatic ester C-O and carboxylic acid C=O, respectively, of DEGD. More importantly, the UV-visible (UV-Vis) spectra show that the addition of the photoacoustic dye IR-780 significantly increases the light absorption in the range of 700-900 nm wavelength while maintaining a large window of transparency in the visible range, which is important to ensure direct monitoring of droplets using optical and/or fluorescence microscopy. If maximum fluorescence signal is necessary, an inverted microscope can be used to minimize the light-path absorption from the photoresponsive layer.

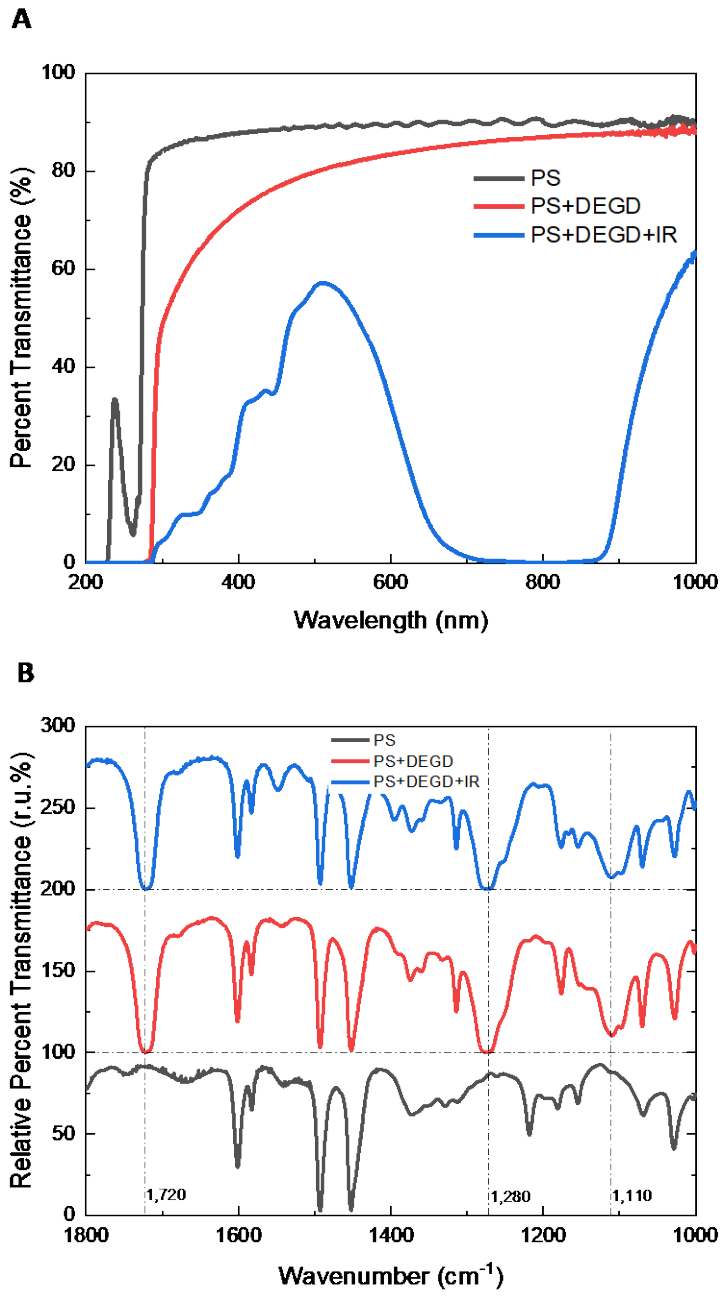

Figure 5.4. Optical characterization of photoacoustic dye-incorporating PS layer. (A) UV-Vis spectra of PS layer, PS layer with DEGD and PS layer with DEGD and IR-780. Suppressed transmittance region is highlighted with a red box. (B) FTIR spectra of PS layer, PS layer with DEGD and PS layer with DEGD and IR-780 dye. Three spectra are offset by 100% for peak visualization.

The key feature of the PHASR device is the capability to specifically and locally heat the photoresponsive layer to puncture the photoresponsive layer or push out the

targets from the selected microwells. With two different photoacoustic dyes, we test the ranges of parameters that enable selective release. IR-780 dye is used primarily in this study because of its low cost and commercial availability. A home-built two photon confocal microscope is used in the study which can deliver highly focused light to a well-defined region. We set the exposure wavelengths at 775 nm and 780 nm for SiNc- and IR-780-incorporated layers, respectively. The highest number of microwell arrays we have successfully incorporated in a PHASR device is 44,000, although all of the demonstrations in this paper are based on PHASR devices with 4,400 microwells.

The effects of laser intensity and scanning parameters on the integrity of the photoresponsive layers are shown in **Figure 5.5**. The exposure area with 60× water-immersion objective and 5× optical zoom is 50 μm by 50 μm, which is close to the size of each well (60 μm in diameter). Depending on the exposure condition and the focal plane, either punctured layer or bubble generation is seen. In order to prevent droplet rupture from the laser exposure, continuous phase with minimum of 2% EA surfactant must be used. In addition, focusing the laser onto the droplet must be prevented. Energy exposure of 1,240.22 J/cm^2 is necessary to create holes in the IR-780-incorporated photoresponsive layer with T_g of 33 ℃. The photoacoustic dye in the photoresponsive layer undergoes photobleaching upon photoactivation as seen by the color change from green to orange around the irradiated region in **Figure 5.5B**, **Figure 5.5C** and **Figure 5.5D**. The extent of photobleaching, which can be assessed by the area of photobleached region that extends beyond the irradiated area, increases as the intensity and irradiation time are increased. This indicates that these devices cannot be used repeatedly. Given the reliability of the fabrication process and the consistent release using the same parameters, new PHASR devices can be prepared readily for each set

of experiment. This approach also minimizes the possibility of cross contamination. Among the two factors, the exposure time seems to have a bigger influence on the extent of photobleaching than the light intensity.

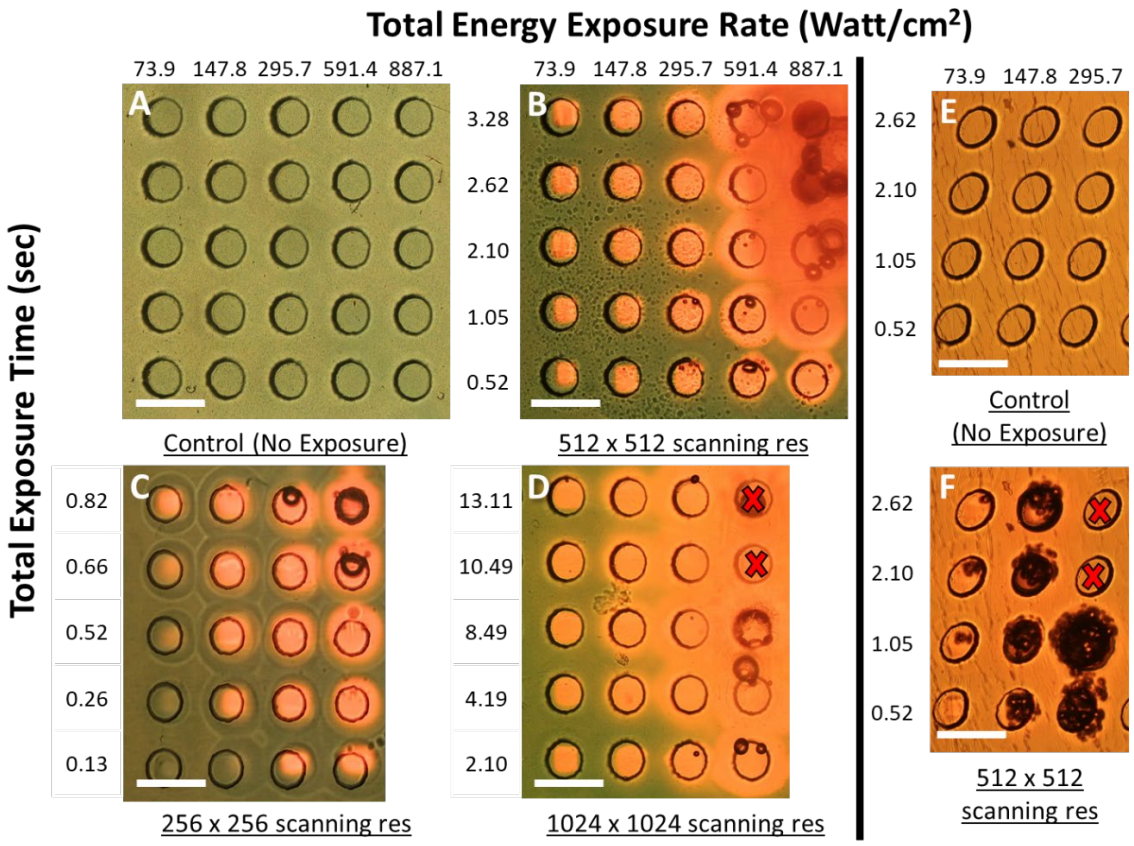

Figure 5.5. Effects of exposure time, resolution and laser intensity on the photoresponsive layer. Five exposure times in the ranges between 0.52s and 3.28s, 0.13s and 0.82s, and 2.10s and 13.11s correspond to scanning time of 2, 4, 8, 10, and 12.5 µs/Pix under specified scanning resolution. (A-D) Response of a 17 µm layer with 5% PS, 1.45% DEGD and 0.1% IR-780. (A) 5x5 microwells with the 17 µm photoresponsive layer. (B,C,D) Effect of light exposure intensity and time on the photoresponsive layer using 512x512 scanning resolution, 256x256 scanning resolution, 1024x1024 scanning resolution, respectively. Wells with red X marks in (D) were not exposed. (E-F) 17 µm photoresponsive layer with 5% PS, 0.45% DEGD, 0.025% IR-780. (E) High T_g photoresponsive layer with 3x4 microwells. (F) Effect of light exposure intensity and time on photoresponsive layer with high T_g using 512x512 scanning resolution. Wells with red X marks in (F) were not exposed. Scale bars are 120 µm.

We also test the effect of the T_g of the photoresponsive layer on hole formation under NIR irradiation. By reducing the concentration of DEDG to 9 wt% of PS, the T_g can be increased to 68 °C. Interestingly, holes can be formed in this photoresponsive layer with a relatively low exposure energy of 77.51 J/cm^2 as seen in **Figure 5.5**. This result indicates that a lower T_g does not necessarily mean that a lower intensity laser and/or a shorter irradiation time is needed to puncture the photoresponsive layer and that the brittleness of the photoresponsive film may play a crucial role in determining the irradiation parameters that induce pore formation.

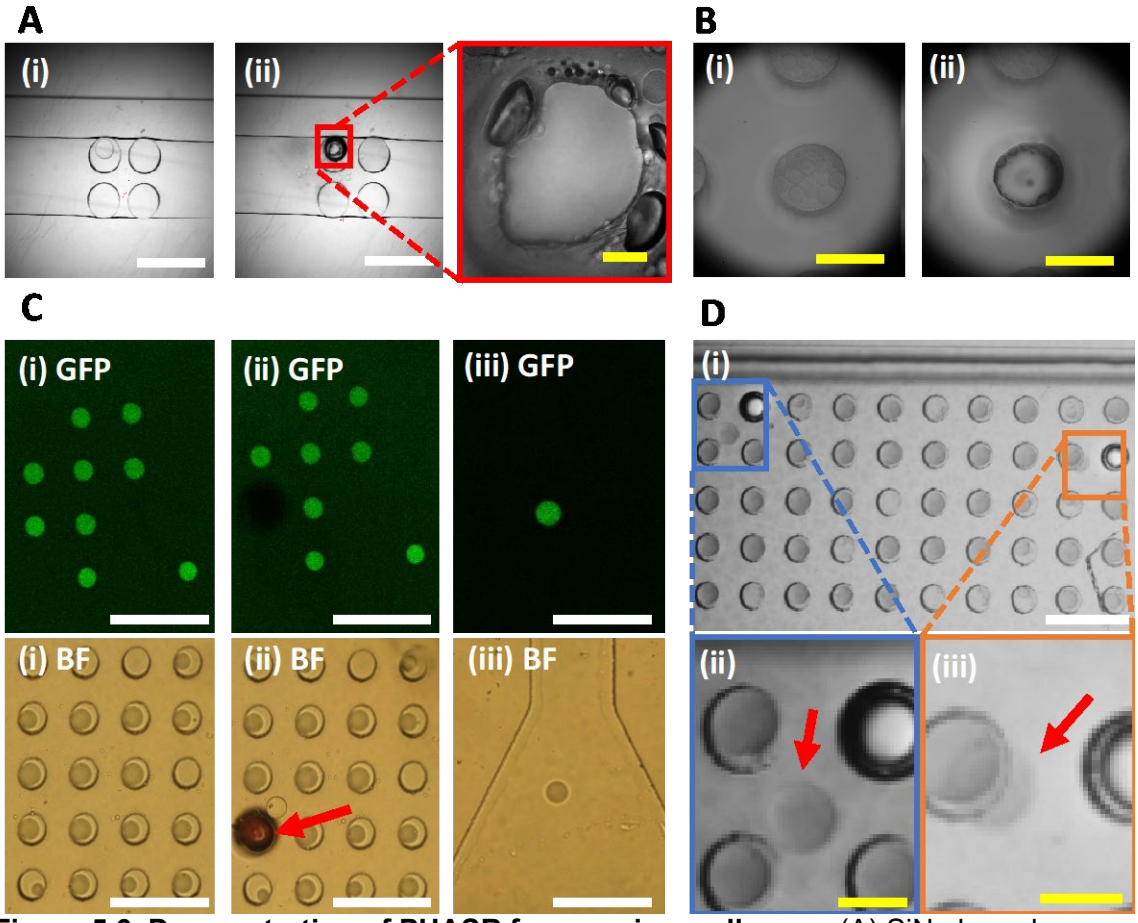

Figure 5.6. Demonstration of PHASR from a microwell array. (A) SiNc-based PHASR via formation of a hole from a 2 x 2 microwells with total exposure energy of 727.34 J/cm^2. (B) IR-780-based PHASR via formation of hole with total exposure energy of 5,425.96 J/cm^2. (C) (i) Device with trapped droplets under fluorescence and bright

field modes, (ii) device under fluorescence and bright field modes after the total exposure energy of 620.11 J/cm^2. A bubble, indicated with red arrow, forms within the well and pushes out the droplet which was trapped in the well to the top right. (iii) Released droplet pushed to a nearby outlet under fluorescence and bright field modes. (D) (i) Multiple droplet release demonstration. (ii) Magnified view of the first released droplet from the blue box of (i) marked with a red arrow. (iii) Magnified view of the second released droplet from the orange box of (i) marked with a red arrow. White scale bars represent 200 μm and yellow scale bars represent 60 μm.

Once the parameters for reliable recovery of droplets are identified, these parameters can be reproducibly used under the same experimental conditions (i.e., photoresponsive layer thickness, composition, focal plane of laser and continuous phase composition). We fabricate 25 PHASR devices using the optimized parameters and observed recovery of selected droplets from all 25 devices using the same exposure parameters, demonstrating high reproducibility of the approach. We observe that laser exposure over the minimum level generally result in significant photobleaching of the photoresponsive layer.

The focal plane of focused laser with respect to the plane of the photoresponsive layer also plays an important role in determining the mode of droplet release from microwells. When the focal plane is set to the top or middle of the photoresponsive layer with exposure energy of 242.23 J/cm^2 under the scanning resolution of 256 x 256 or 310.06 J/cm^2 under the scanning resolution of 512 x 512, the photoacoustic dye induces local heating within the film, leading to the formation of hole(s) in the photoresponsive layer as seen in **Figure 5.6A** and **Figure 5.6B**. Minimum of 242.23 J/cm^2 is required to create a hole in both SiNc and IR-780 based layers with a T_g of 33 ℃. The minimum exposure energy must be adjusted to ensure the formation of a pore large enough for a droplet to rise through. In contrast, when the focal plane is set to the base of the photoresponsive layer, 77.51 J/cm^2 exposure energy is required to create bubble formation that can be used to push out the droplets. This bubble pushes the droplet out

of the well to the bottom trap channel as shown in **Figure 5.6C-(ii)**. We successfully recover the released droplet from **Figure 5.6C-(ii)** by continuously flowing continuous phase to guide the droplet to outlet as shown in **Figure 5.6C-(iii)**. This result indicates that when a low intensity light is focused on the base side of the photoresponsive layer, heat is dissipated into the oil and induces bubble formation. The bubble eventually disappears upon cooling, and its dissolution can be expedited by continuously flowing the oil phase. Although push-down release introduces a possibility of re-capture, continuous flow in the bottom trap channel can minimize such an occurrence. For layer-rupture induced release-up recovery, laser intensity should be kept high and laser should be precisely positioned to the target microwell arrays to prevent bubble formation which could induce push-down release of droplets due to local heating.

In addition, we demonstrate biocompatibility of the PHASR by generating droplets with EL4 cells co-encapsulated with the Live/Dead mammalian cell viability assay probe as shown in **Figure 5.7. Figure 5.7A** shows a microwell array occupied by aqueous droplets either with or without cells. We merge images from the green fluorescent channel and the brightfield channel to clearly show droplets containing live cells. We recover a droplet that contain four cells which is arbitrarily chosen for demonstration. After being released from the well via the push-down mechanism, the target droplet (marked with a red arrow in **Figure 5.7B**) shows that four cells are still alive after selective release. **Figure 5.7D** and **Figure 5.7E** shows continued viability of the cells as the droplet is being guided toward the outlet and is merged with a growth medium to recover the cells.

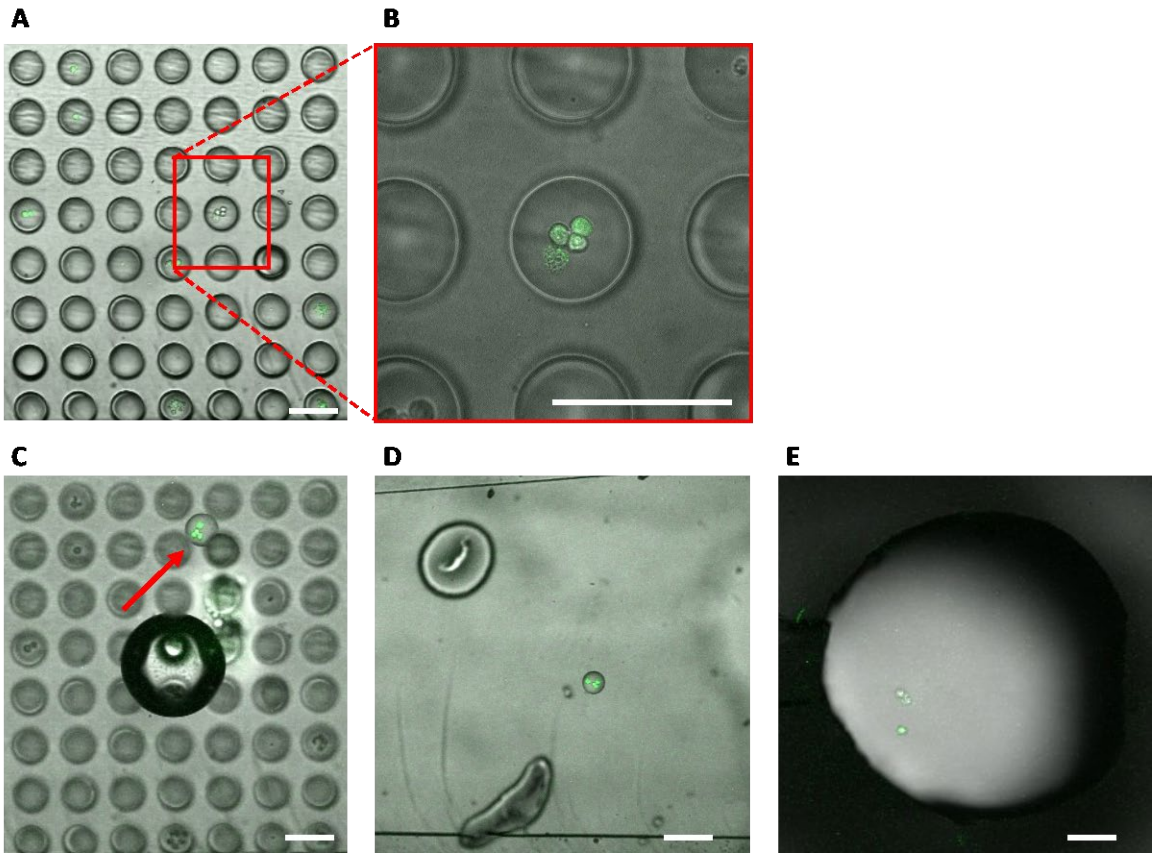

Figure 5.7. Demonstration of selective recovery of droplets from the PHASR device. GFP and brightfield images are merged to clearly show droplets with viable cells. (A) Wide field view of arrays containing some empty droplets and some live cell-containing droplets. (B) Magnified view of a droplet with 4 live cells. (C) The four cells in the released droplet, marked with a red arrow, exhibit green fluorescence indicating that they are alive. (D) Released droplet being pushed toward the outlet showing viable cells. (E) Recovered droplet at the outlet. The droplet is merged with a growth medium and the four cells maintain their viability. Scale bars represent 100 μm.

Although exact temperature measurement is difficult to make, the facts that droplets do not evaporate and cells survive indicate that thermal impact on the droplets and encapsulated materials/cells is minimal.

Upon PHASR, the continuous flow of the oil phase guides the released droplets to the outlet of the PHASR device for their recovery. Using the proposed method, we are able to release approximately one droplet per second. By automating the stage

translation and light irradiation, it will be possible to further accelerate the recovery of identified targets from microwells.

5.4. CONCLUSION

In summary, we have demonstrated that droplets can be captured and selectively released with high speed and precision by incorporating a photoresponsive layer into a microwell device. The properties of the photoresponsive layer can be tailored by changing the plasticizer concentration, photoacoustic dye and thickness to meet the specific requirements for the samples encapsulated in the droplets. We also show that droplets can be released by inducing rupture of the photoresponsive layer or by inducing bubble formation in the microwells. Our results demonstrate that the PHASR device is a powerful platform that enables high capacity assays that require extended incubation of droplets and recovery of analytes from a subset of captured droplets. Although our work focuses on using the photoresponsive layer for PHASR of droplets from a microwell array, we believe the photoresponsive layer could potentially be useful for other applications that require site-specific heating in various micro total analysis systems.

5.5. REFERENCES

1. Dittrich PS, Manz A. Lab-on-a-chip: Microfluidics in drug discovery. *Nat Rev Drug Discov*. 2006;5(3):210-218. doi:10.1038/nrd1985

2. Zhou Y, Basu S, Wohlfahrt KJ, et al. A microfluidic platform for trapping, releasing and super-resolution imaging of single cells. *Sens Actuators B Chem*. 2016;232:680-691. doi:10.1016/j.snb.2016.03.131

3. Pompano RR, Liu W, Du W, Ismagilov RF. Microfluidics Using Spatially Defined Arrays of Droplets in One, Two, and Three Dimensions. *Annu Rev Anal Chem*. 2011;4(1):59-81. doi:10.1146/annurev.anchem.012809.102303

4. Huang N-T, Hwong Y-J, Lai RL. A microfluidic microwell device for immunomagnetic single-cell trapping. *Microfluid Nanofluidics*. 2018;22(2):16. doi:10.1007/s10404-018-2040-x

5. Agresti JJ, Antipov E, Abate AR, et al. Ultrahigh-throughput screening in drop-based microfluidics for directed evolution. *Proc Natl Acad Sci U S A*. 2010;107(9):4004-4009. doi:10.1073/pnas.0910781107

6. Fallah-Araghi A, Baret J-CC, Ryckelynck M, Griffiths AD. A completely in vitro ultrahigh-throughput droplet-based microfluidic screening system for protein engineering and directed evolution. *Lab Chip*. 2012;12(5):882-891. doi:10.1039/c2lc21035e

7. Guo MT, Rotem A, Heyman JA, Weitz DA. Droplet microfluidics for high-throughput biological assays. *Lab Chip*. 2012;12(12):2146-2155. doi:10.1039/c2lc21147e

8. Huebner A, Bratton D, Whyte G, et al. Static microdroplet arrays: A microfluidic device for droplet trapping, incubation and release for enzymatic and cell-based assays. *Lab Chip*. 2009;9(5):692-698. doi:10.1039/b813709a

9. Sun M, Bithi SS, Vanapalli SA. Microfluidic static droplet arrays with tuneable gradients in material composition. *Lab Chip*. 2011;11(23):3949. doi:10.1039/c1lc20709a

10. Jeong H-H, Lee B, Jin SH, Jeong S-G, Lee C-S. A highly addressable static droplet array enabling digital control of a single droplet at pico-volume resolution. *Lab Chip*. 2016;16(9):1698-1707. doi:10.1039/C6LC00212A

11. Rousset N, Monet F, Gervais T. Simulation-assisted design of microfluidic sample traps for optimal trapping and culture of non-adherent single cells , tissues , and spheroids. *Sci Rep*. 2017;7(February):1-12. doi:10.1038/s41598-017-00229-1

12. Wang H-Y, Bao N, Lu C. A microfluidic cell array with individually addressable culture chambers. *Biosens Bioelectron*. 2008;24(4):613-617. https://linkinghub.elsevier.com/retrieve/pii/S0956566308002534. Accessed June 5, 2019.

13. Iwai K, Tan WH, Ishihara H, Takeuchi S. A resettable dynamic microarray device. *Biomed Microdevices*. 2011;13(6):1089-1094. doi:10.1007/s10544-011-9578-7

14. Tan W-H, Takeuchi S. A trap-and-release integrated microfluidic system for dynamic microarray applications. *Proc Natl Acad Sci*. 2007;104(4):1146-1151. doi:10.1073/pnas.0606625104

15. Leung K, Zahn H, Leaver T, et al. A programmable droplet-based microfluidic device applied to multiparameter analysis of single microbes and microbial communities. *Proc Natl Acad Sci*. 2012;109(20):7665-7670. doi:10.1073/PNAS.1106752109

16. Wang W, Yang C, Liu Y, Li CM. On-demand droplet release for droplet-based microfluidic system †. *Lab Chip*. 2010;10:559-562. doi:10.1039/b924929j

17. Park J, Jung JH, Park K, et al. On-demand acoustic droplet splitting and steering in a disposable microfluidic chip. *Lab Chip*. 2018;18(3):422-432. doi:10.1039/c7lc01083d

18. Padmanabhan S, Misteli T, DeVoe DL. Controlled droplet discretization and manipulation using membrane displacement traps. *Lab Chip*. 2017;17(21):3717-3724. doi:10.1039/C7LC00910K

19. Rambach RW, Biswas P, Yadav A, Garstecki P, Franke T. Fast selective trapping and release of picoliter droplets in a 3D microfluidic PDMS multi-trap system with bubbles. *Analyst*. 2018;143(4):843-849. doi:10.1039/C7AN01100H

20. Labanieh L, Nguyen T, Zhao W, et al. Floating Droplet Array: An Ultrahigh-Throughput Device for Droplet Trapping, Real-time Analysisand Recovery. *Micromachines*. 2015;6(10):1469-1482. doi:10.3390/mi6101431

21. Schmitz CHJ, Rowat AC, Köster S, Weitz DA. Dropspots: A picoliter array in a microfluidic device. *Lab Chip*. 2009;9(1):44-49. doi:10.1039/b809670h

22. Melin J, Quake SR. Microfluidic Large-Scale Integration: The Evolution of Design Rules for Biological Automation. *Annu Rev Biophys Biomol Struct*. 2007;36(1):213-231. doi:10.1146/annurev.biophys.36.040306.132646

23. Segaliny AI, Li G, Kong L, et al. Functional TCR T cell screening using single-cell droplet microfluidics. *Lab Chip*. 2018;18(24):3733-3749. doi:10.1039/C8LC00818C

24. Labanieh L, Nguyen TN, Zhao W, Kang D-K. Floating Droplet Array: An Ultrahigh-Throughput Device for Droplet Trapping, Real-time Analysis and Recovery. *Micromachines*. 2015;6(10):1469-1482. doi:10.3390/mi6101431

25. Chiou P-Y, Wu T-H, Park S-Y, Chen Y. Pulse laser driven ultrafast micro and nanofluidics system. *Biosensing III*. 2010;7759(August 2010):77590Z. doi:10.1117/12.861757

26. Polystyrene. https://polymerdatabase.com/polymers/polystyrene.html. Accessed

June 6, 2019.

27. Csernica J, Brown A. Effect of Plasticizers on the Properties of Polystyrene Films W. *J Chem Educ*. 1999;76(11):9-11. doi:10.1021/ed076p1526

CHAPTER 6

CORRELATION BETWEEN METABOLIC PROFILE AND TRANSCRIPTOMIC PROFILE AT THE SINGLE CELL LEVEL

6.1. INTRODUCTION

Recent single-cell level RNA sequencing revealed unexpected heterogeneity among a clonal population.[1] Genetically identical monoclonal population showed significant heterogeneity beyond the degree of genetic variation.[2] Several hypotheses have been formulated to describe the origin of the cell-to-cell heterogeneity and the necessity.[3,4] Cell-to-cell heterogeneity can arise from mechanisms as simple as the asymmetric cell division and as complicated as the cell-to-cell communication-based crowd control.[5,6] For any reason above, heterogeneity among identical cell populations has been observed, and it has been suggested to be positively correlated with the cell state transitions.[7–10]

Recent studies in immunology have suggested that the metabolic profile may be a crucial indicator for the further cell state transition in several immune cells.[11–13] In the case of CD8+ cytotoxic T cells, under quiescent state, naïve T cells with heterogeneous T cell receptor (TCR) reside in the system peacefully.[14,15] When a pathogen is detected, the naïve T cells reprogram their metabolic pathway and differentiate into the effector T cells.[16,17] Such initial metabolic reprogramming is essential for the effector T cell to proliferate vigorously. Initial metabolic reprogramming guides T cell to depend on the anaerobic glycolysis, just like the cancer cells, to overcome the limited supply of oxygen.[18,19] The vastly proliferated effector T cells mostly die by apoptosis once the

pathogen is cleared out of the system. However, a small portion of the effector T cells further differentiates into memory T cells. The secondary metabolic reprogramming accompanies this secondary differentiation.[20–22] This secondary differentiation alters the memory T cells' metabolic pathway to the normal aerobic metabolism. It is unknown whether the memory T cell's precursor retains the fatty acid oxidation (FAO) pathway as an effector T cell or shuts off the FAO pathway and switches back on when it becomes the memory T cell.[23] Nonetheless, the flexibility for double metabolic reprogrammings is likely a requirement for the memory T cell formation. Identification of the effector T cells' subpopulation with distinctive metabolic profiles directly linked to the memory T cell formation can benefit many immunotherapy studies by allowing active manipulation of the immune system for the natural immunity formation against diseases.

A similar phenomenon can also be found in cancer metabolism. Cancer has been the leading cause of death worldwide for decades, and it will continue to be the deadliest disease for the foreseeable future.[24] Its onset occurs in a vital organ and silently compromises the entire organ. Cancer cells can move to a different organ through a process known as metastasis. Early detection of cancer is crucial because it can save the initially infected organ and prevent metastasis.[25] Metastasis of cancer makes it extremely difficult to treat and continuously poses a risk to the patient.[26] For metastasis to occur, epithelial-like cancer cells differentiate into mesenchymal-like cancer cells and become circulating tumor cells (CTC).[24] Circulating tumor cells can go through another metastasis and become mesenchymal-like cancer cells at different loci and become epithelial-like cancer cells. This metastasis effectively allows the spread of the cancers to any part of the host. Like the memory T cells, metastasis cancer cells have to continuously adapt to different metabolic environments and undergo several

metabolic reprogramming steps to adapt to various microenvironments. The cancer cells' metabolic plasticity study can significantly enhance the prevention and treatment of cancer metastasis. The subpopulations with a higher risk of metastasis can show different metabolic profiles correlated to its metabolism-related different gene expression levels.

Distinctive metabolic profiles of a subpopulation of an identical cell population can arise from the single-cell heterogeneity and cell cycle state differences. Since metabolic reprogramming is deeply related to the cellular function for further differentiation, an in-depth investigation of metabolomics combined with the single cancer cells' transcriptomics can enhance our current understanding of the correlation between metabolomics and transcriptomics. The positive correlation of metabolomics and transcriptomics can serve as a vital starting point for the metabolomics study in the T cell since it resembles various aspects of metabolic reprogramming. In this chapter, using the microfluidic device described in Chapter 4 and 5, single-cell level transcriptomics is correlated with the previously observed metabolic profiles. The novel parallel investigation of metabolomics and transcriptomics for cancer cells reveals metabolic profile heterogeneity among the genetically identical population and the relationship between metabolomics and transcriptomics. We believe our approach represent a step forward in the fields of multi-omics study and single-cell study.

6.2. RESULTS

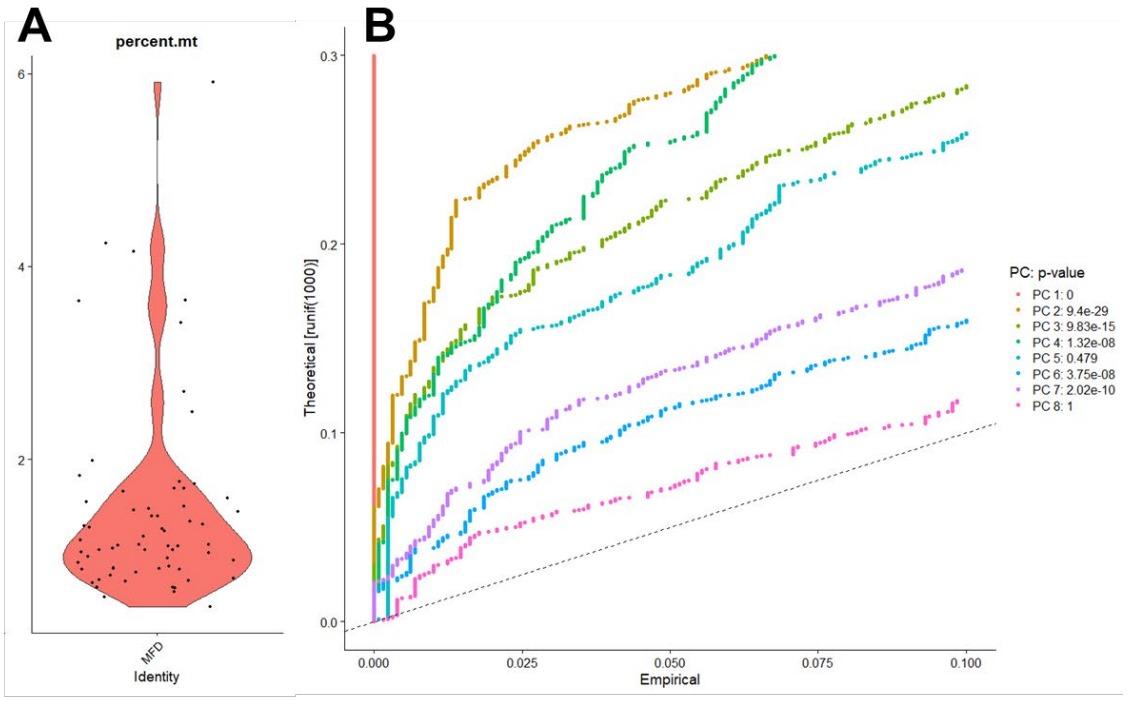
A
percent.mt
6
4
2
MFD
Identity
B
0.3
0.2
0.1
0.0
Theoretical [runif(1000)]
0.000
0.025
0.050
0.075
0.100
Empirical
PC: p-value
PC 1: 0
PC 2: 9.4e-29
PC 3: 9.83e-15
PC 4: 1.32e-08
PC 5: 0.479
PC 6: 3.75e-08
PC 7: 2.02e-10
PC 8: 1

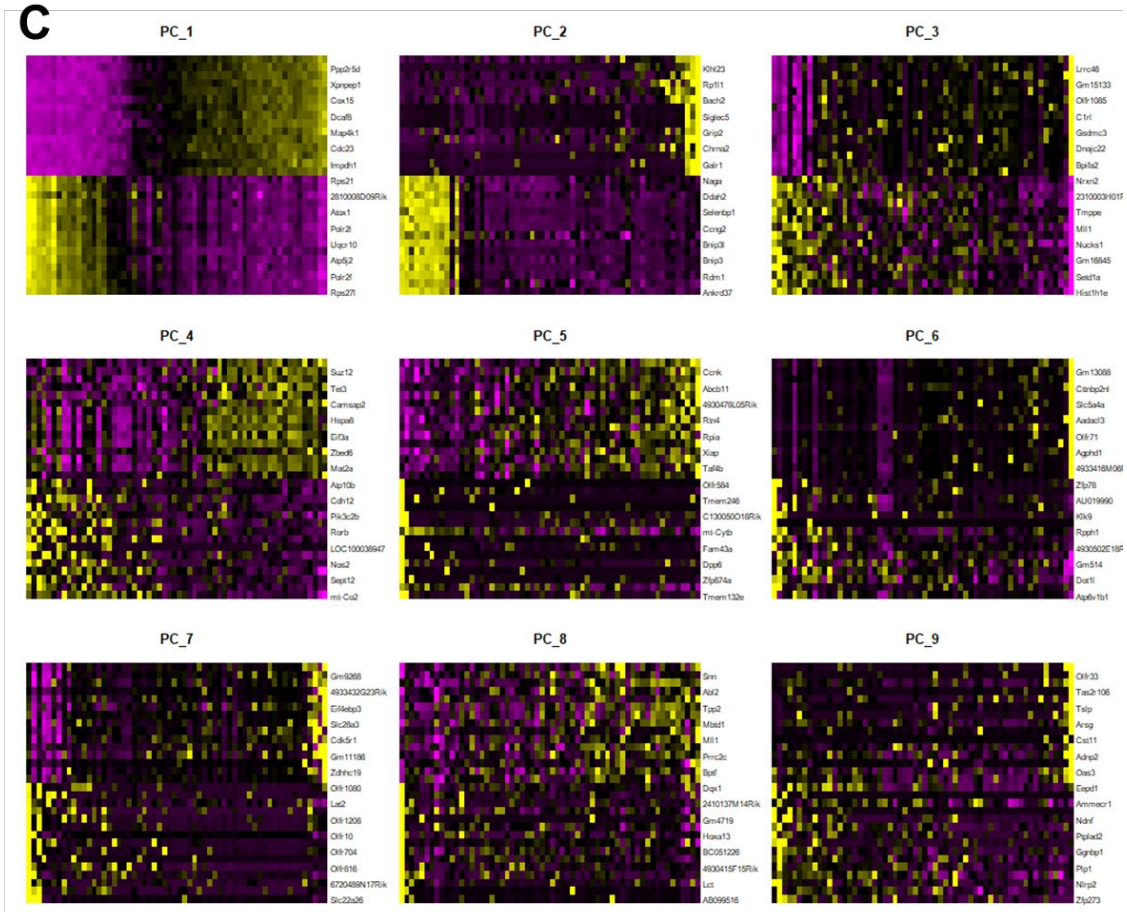
C
PC_1
PC_2
PC_3
PC_4
PC_5
PC_6
PC_7
PC_8
PC_9

Figure 6.1. scRNA-seq quality control and significant principal components. (A) shows the quality of the scRNA-seq through the percent mitochondrial count over the exonic counts. (B) shows the Jackstraw plot to determine the significant principal component numbers, and (C) shows the heatmap of each principal component's features.

Overall experimental setup and method are similar to the ones from **Chapter 4** and **Chapter 5**. For droplet generation, two aqueous streams join at a low angle (< 20°), roughly 100 μm before the flow-focusing junction, to ensure the parallel laminar flows of both phases before the droplet formation. Laminar flow of short distance guarantees that the functional probe's signal is solely corresponding to the encapsulated single-cell only. Upon droplet generation, the droplets are introduced into the full-size photoactivated selective release (PHASR) device. The full-size PHASR device fabrication protocol is a slightly modified from **Chapter 5**. One challenge with scale-up is the rupture of bottom channel PDMS slab/ photoresponsive layer bilayer. Depending on the photoresponsive layer's plasticity and flexibility, exposure of the the bilayer to the vacuum environment for the secondary oxygen plasma treatment for subsequent bonding with the top layer either caused the collapse of the photoresponsive layer or its rupture. Thus, the rupture-based release-up recovery method is abandoned for the scale-up device to remove the fabrication issue. The top PDMS channel layer is replaced with a plain PDMS slab, and the flat top layer is bonded with the photoresponsive layer before the bottom channel PDMS slab.

A cycle of brightfield and UV exposure precedes metabolic profiling to acquire information on individual droplets. UV exposure is necessary as it activates a fluorescence signal from the CellTrace Violet. This signal allows us to distinguish empty droplets, single-cell containing droplets, and multiple-cells containing droplets. Also, it serves as a checkpoint for cell containment after droplet formation. The photoacoustic

dye used in the fabrication of the photoresponsive layer is reactive to the 780 nm wavelength. To accurately focus such a long wavelength, a two-photon laser is required. As noted from **Chapter 5**, the specific photoacoustic dye is selected to minimize the potential damage to the cell along with an effort to bypass the visible range as much as possible such that a wide variety of functional probes can be used.

Cells encapsulated in droplets are observed using automated microscopy. The clusters of the metabolic profiles for glucose uptake and consumption are subsequently categorized using the shape-based dynamic time warping (DTW) clustering method. Droplets are retrieved using two-photon microscopy and broken using a demulsifier. Cells are identified using fluorescence microscopy and processed through the SMART-Seq protocol and the Nextera XT library preparation protocol. A total of 65 cells are retrieved individually. Library prepared samples are pooled then sequenced. Sequenced data are processed through the Kim lab's proprietary pipeline for demultiplexing and alignment. The final exonic count and mitochondrial count data and the previously observed metabolic profiles are used for the downstream analysis and comparison. For single-cell RNA sequencing analysis, the Seurat package in R is used.

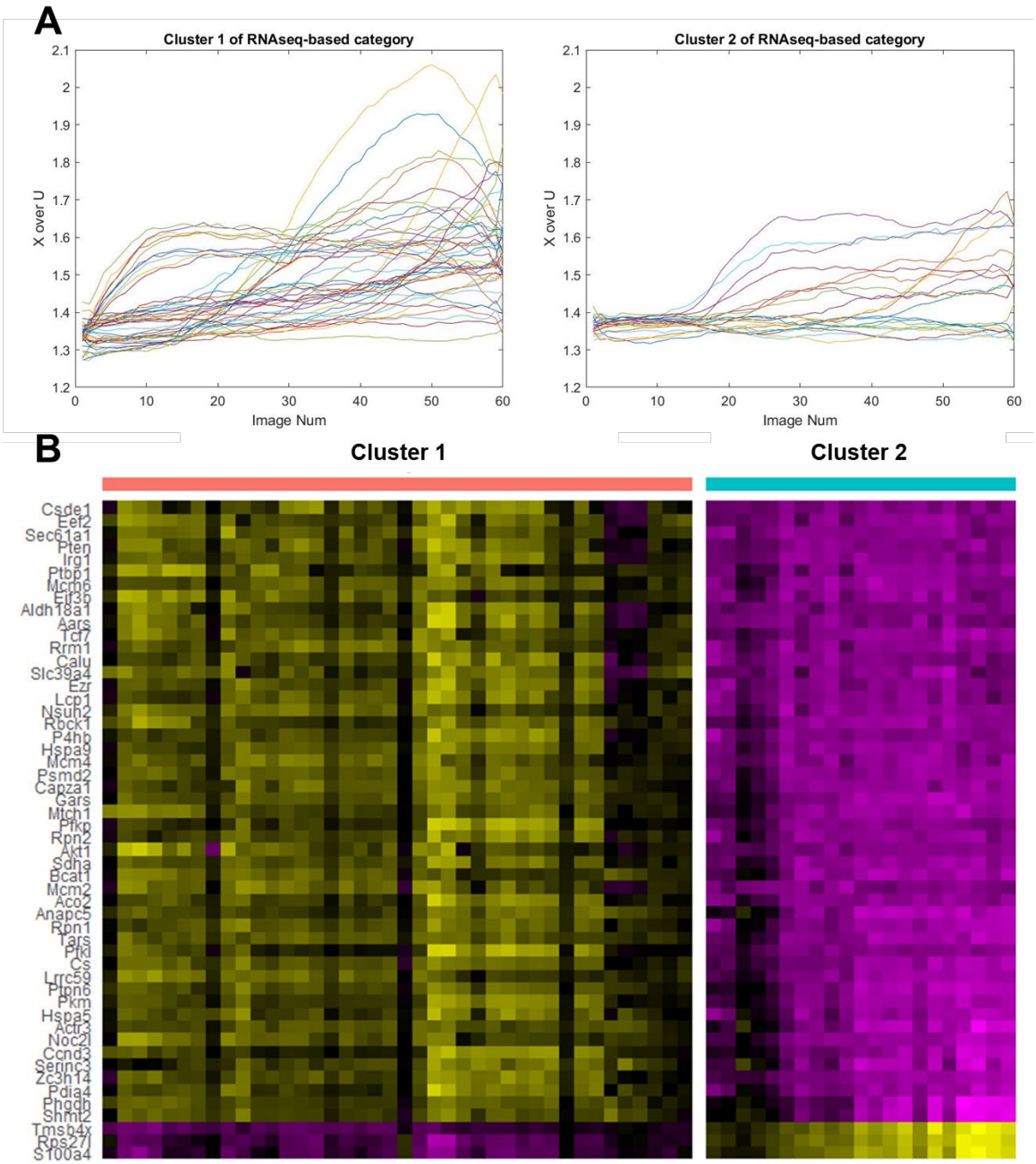

Figure 6.2. Metabolic profiles of clusters, categorized by the gene expression levels and the corresponding heatmap. (A) shows the metabolic profiles of individual cells for their glucose consumption and metabolism, and clusters 1 and 2 are categorized based on their scRNA-seq gene expression levels. The X-axis represents the image number of dynamic observation, which is equivalent to 2 minutes. The Y-axis represents the X over U, a modified Z-score term; it is the top 0.5% intensity within the droplet, the cell's pixel occupancy within the droplet, divided by the median intensity of the droplet. (B) represents the individual clusters' heatmap for the most prominent features.

As shown in **Figure 6.1-(A)**, the single-cell RNA sequencing (scRNA-seq) quality is good overall. The percent mitochondrial count over the exonic count per each sample is calculated, and only one sample is greater than 5% in its percent mitochondrial count. This result suggests that 98.5% of the cells remain healthy and viable throughout long processes of the dynamic observation, metabolic profile analysis and clustering, selective recovery via PHASR device, and the SMART-Seq protocol. It shows that the overall protocol has been optimized for cell viability and again proves the PHASR device's biocompatibility.

Before clustering based on the gene expression profile, all samples' exonic counts are linearly dimension reduced via principal component analysis. Both the Scree plot and the Jackstraw plot are used to determine the number of significant principal components. The Jackstraw plot, shown in **Figure 6.1-(B)**, suggests the first eight principal components are statistically significant; the Scree plot suggested the first nine components. Based on the information from the Scree plot and Jackstraw plot, the first nine principal components are used for the downstream analyses. The features of the principal components are presented in the heatmap in **Figure 6.1-(C)**. Due to the nature of the principal component analysis, the heatmap's orderliness is disturbed as the number of principal components increases or decreases.

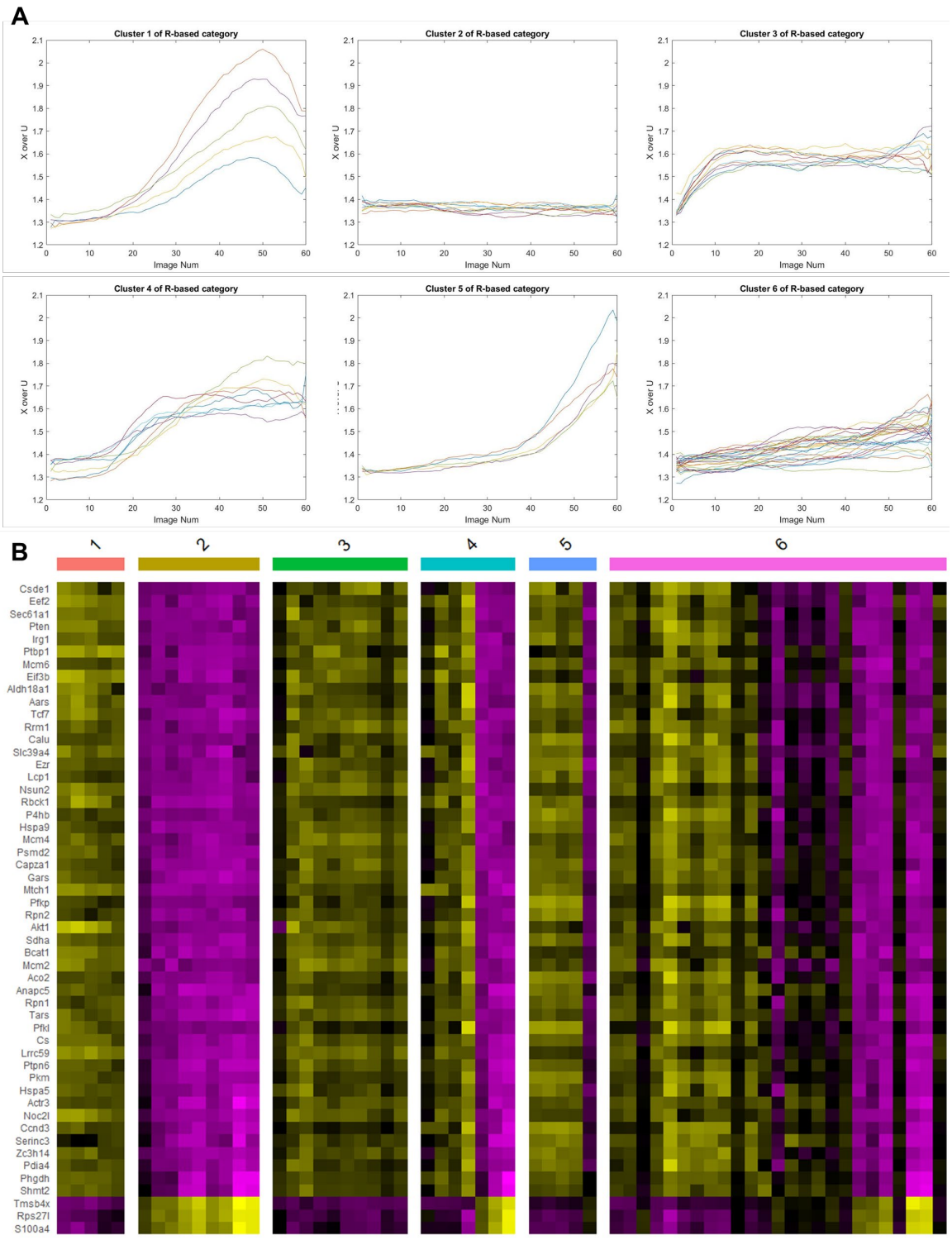

Figure 6.3. Metabolic profiles of clusters and the corresponding heatmap, categorized by the metabolic shapes instead of the gene expression levels. (A) shows the metabolic profiles of individual cells for their glucose consumption and metabolism, and clusters 1 through 6 are categorized based on their metabolic profile

shapes. The X-axis represents the image number of dynamic observation, which is equivalent to 2 minutes. The Y-axis represents the X over U, a modified Z-score term; it is the top 0.5% intensity within the droplet, the cell's pixel occupancy within the droplet, divided by the median intensity of the droplet. (B) represents the individual clusters' heatmap for the most prominent features.

Following gene expression level normalization and linear dimensional reduction using principal component analysis, the scRNA-seq data are clustered based on their gene expression levels. Two clusters are detected when the samples are clustered based on their gene expression levels, as shown in **Figure 6.2-(A)** and **Figure 6.2-(B)**. **Figure 6.2-(A)** shows the two clusters' observed metabolic profiles, and **Figure 6.2-(B)** shows the heatmap of the two clusters' distinctive features. The heatmap shows a more distinct difference in the gene expression levels between clusters 1 and 2, compared to the metabolic profiles. For metabolic profiles, cluster 1 is a heterogeneous mix of various metabolic profiles, whereas cluster 2 is somewhat uniform for the first quarter of the observation time window. The X-axis is the image number of dynamic observation, an increment of which is equivalent to 2 minutes in real-time, and the Y-axis is the X over U, a modified Z-score term. Modified Z-score term is the top 0.5% intensity divided by the median intensity of the same droplet. Cluster 2 shows complete inhibition or restraint in the ratio of glucose uptake and metabolism for the initial 30 minutes.

The Seurat package's clustering is based on the differential analysis added with the thresholding. It makes principal components based on the bulk gene expression profiles, and it may not be a great way to cluster and compare their metabolic profiles in this thesis. The gene expression level clustering is masked by the abundance of the exonic counts to reveal the accurate correlation between transcriptomic and metabolomic. The metabolic profiles are clustered based on their shapes using the

dynamic time warping (DTW) package to enhance the correlation, as shown in **Figure 6.3-(A)**. Compared to the gene expression level based clustering, shape-based DTW clustering shows the more precise categorization of clusters based on the metabolic profiles, which is expected due to the difference in clustering methods. Cluster 1 shows quadratic function-like curves, cluster 2 shows almost perfectly flat lines, and cluster 3 shows logarithmic function-like curves. Cluster 4 seems like a delayed logarithmic function, cluster 5 resembles either an exponential graph or delayed quadratic function, and cluster 6 looks like a low-slope linear function. Clusters 1 and 3 show a similar pattern in their features in the heatmap, and cluster 2 shows the opposite pattern in its features. Clusters 4, 5, and 6 are a mix of pattern in their features within the heatmap, but this is understandable as the heatmap's feature genes are from the gene expression profiles' principal components. To make the correlation more accurate, further manual comparison of the features is necessary as the bulk gene expression profiles are still hindering the divulgence of correlation between transcriptomic and metabolomic.

For an exact comparison of the metabolic profile clusters in terms of their gene expression profile, a bottom-up analysis confined to the glycolysis related genes, is selected. Also, to integrate in kinetic modeling built in **Chapter 4** to the correlation between metabolomics and transcriptomics, this thesis only analyzes and compares the genes related to glycolysis. More specifically, the GLUT1 transport-related genes, glycolysis promotion and suppression genes, and ribosomal proteins crucial to glycolysis are investigated.

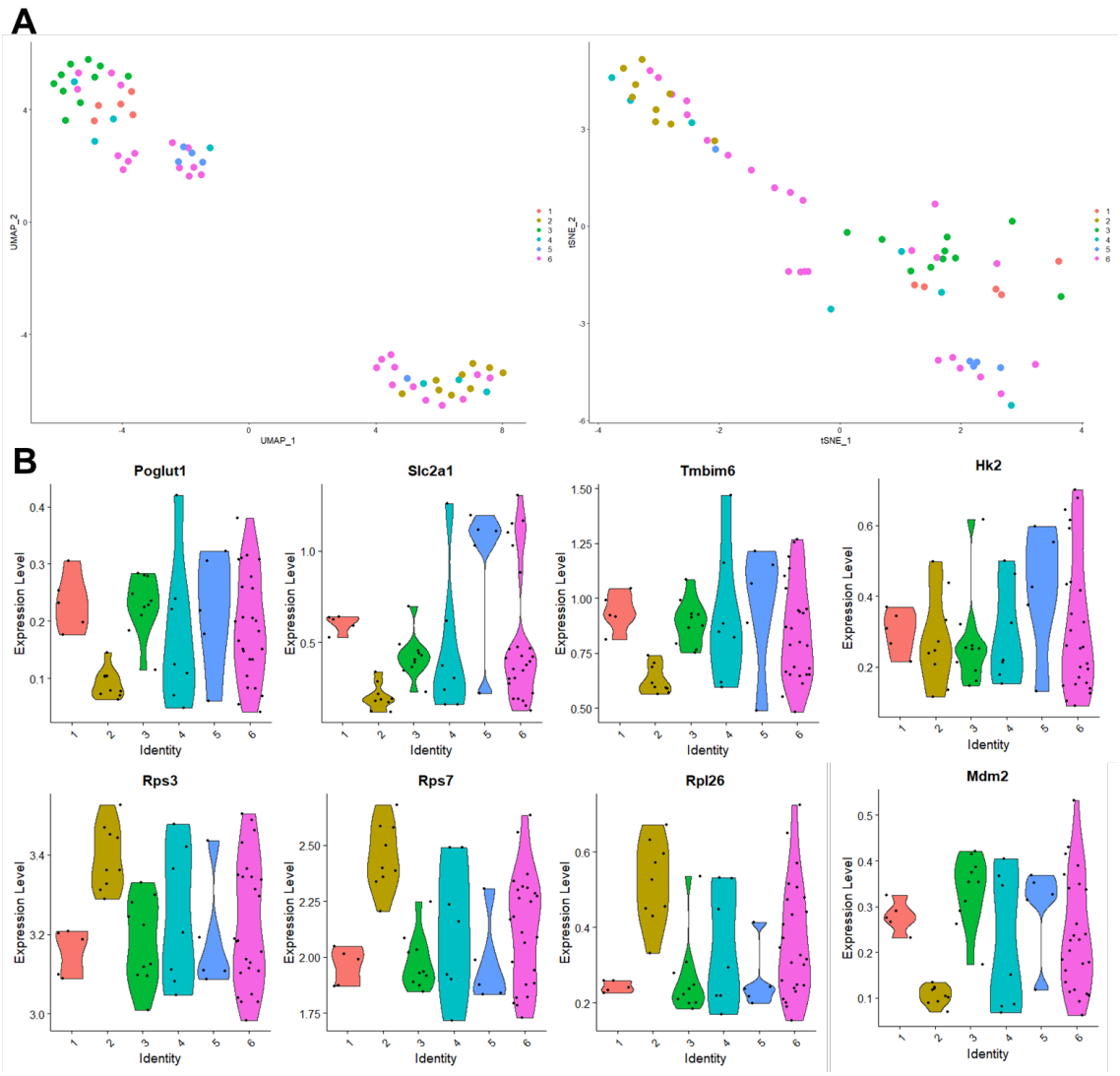

Figure 6.4. Nonlinear dimensional reduction of the gene expression profile and visual projection of the metabolic profile clusters, and bottom-up analysis and comparison of the metabolic profile and the gene expression profile for metabolic profile based clusters. (A) shows the nonlinear dimensional reduced gene expression profile and visual projection of it on the two-dimensional plane; left uses uniform manifold approximation and projection method, and right uses t-distributed stochastic neighbor embedding. Each sample is color-coded with the metabolic profile based clusters. (B) shows violin plots for the bottom-up analysis to correlate metabolomic and transcriptomic. The genes highly related to glycolysis are selected and compared for all metabolic profile based clusters.

Figure 6.4-(A) shows that nonlinear dimension reduced gene expression profiles are projected onto a two-dimensional plane to visualize the cluster subsets. The most

commonly used two nonlinear dimensional reduction methods are used for the visual inspection: uniform manifold approximation and projection (UMAP) and t-distributed stochastic neighbor embedding (tSNE). Similar to the heatmap case from **Figure 6.3-(B)**, clusters that show a clean pattern in the heatmap show well-concentrated cluster dots in both UMAP and tSNE plots in **Figure 6.4-(A)**. However, clusters 4, 5, and 6, which showed a mixed pattern in **Figure 6.3-(B)** heatmap, tend to share region over clusters 1, 2, and 3, and also is widely spread in both UMAP and tSNE plots.

The bottom-up analysis and comparison to establish a correlation between metabolomic and transcriptomic are shown in **Figure 6.4-(B)**. Plotted violin plots are genes that are known to be related to glycolysis. Poglut1 is a gene that provides instruction for the making of protein O-glucosyltransferase 1, which catalyzes the transfer of glucose. Slc2a1 is also a gene that provides instruction for the making of glucose transporter protein type 1 (GLUT1), which is the pathway for glucose uptake into the cell.[27,28] Tmbim6 is still unclear of its exact mechanism, but the knock-out of Tmbim6 showed decreased expression of glycosylation related genes such as Poglut1.[29] Hk2 is a gene that makes enzyme Hexokinase 2 that starts the breakdown of the glucose into glucose 6-phosphate.[30] Slc2a1, Poglut1, and Tmbim6 are directly related to the GLUT1 formation and glucose transport, which are crucial parts of the kinetic modeling system in **Chapter 4**. Besides the genes, ribosomal proteins closely related to the glycolysis is also investigated. Rps3, Rps7, and Rpl26 are recently found to be positively correlated with glycolysis, along with the gene Mdm2, which suppresses glycolysis.[31]

The GLUT1 related genes, Poglut1, Slc2a1, and Tmbim6, all show a distinctive difference in expression level for cluster 2 than the rest of the clusters. Cluster 2 is more distinctive in terms of its metabolic profile than the rest of the clusters in the sense that it

is almost inactive. The GLUT1 related genes show significantly low expression level for cluster 2 compared to the rest. This may suggest the low availability of the GLUT1 pathway on cluster 2 samples, which supports the inactive glucose consumption and uptake pattern observed from the metabolic profile. Hk2 gene expression levels are similar among all clusters, which suggest that the metabolic breakdown capability does not differ from cell to cell. Glycolysis suppression gene, Mdm2, showed distinctively low expression levels in cluster 2. Ribosomal proteins, Rps3, Rps7, and Rpl26, related to glycolysis, also showed significantly high expression levels in cluster 2 than in other clusters. The combined result of ribosomal protein and glycolysis suppression expression levels suggests that cluster 2 is inactive but is actively synthesizing ribosomal proteins to re-establish or repair its glucose uptake pathway so that it can get back on track with glycolysis. Metabolically inactive cluster 2 is potentially not different from the rest of the clusters in its metabolism but is different in its uptake pathway availability.

6.3. DISCUSSION

The comparison between the metabolic profile and its glycolysis-related gene expression level shows a moderate correlation between the two. At least in terms of inactive versus active metabolic profiles, the glycolysis suppression, promotional ribosomal proteins, and uptake pathway expression levels show a significant difference in gene expression level. It is possible that the multiple metabolic profile observations, such as oxygen consumption rate and fatty acid uptake, can enhance the correlation between transcriptomics and metabolomics, because metabolic reprogramming or profile is not limited to the glucose uptake and consumption. Multi-functional probe

observation by mix-and-matching currently available metabolism-related functional probes is also a possibility: for example, microfluidic-chip embedded oxygen sensor, mitochondrial potential probe, fatty acid analogue, pH probe, and glucose analogue. In addition, an in-depth analysis of scRNA-seq data confined only to the metabolism-related genes may enhance the current correlation. This chapter reports that the single-cell level metabolic profiling, selective recovery based on the preceding metabolic profiling followed by single-cell level RNA sequencing, and multi-omics study, transcriptomics, and metabolomics is possible. We also suggest that it can be further developed with more complex metabolic profiling and enhanced scRNA-seq analysis. A moderate correlation between glucose consumption and uptake and glycolysis-related gene expression levels, found in this chapter, can be a vital starting point to, as well as initial guide for, many metabolomics studies in the future.

6.4. METHODS

Reagents

Polydimethylsiloxane (PDMS) was purchased from Dow Corning Corp, MI, USA. HFE-7500 oil containing 2% EA-surfactant (FluoSurf) and HFE-7500 oil containing functionalized SiO2 nanoparticle surfactant (Fluoro-Phase) was purchased from Dolomite Microfluidics, United Kingdom. Trichloro(1H,1H,2H,2H-perfluorooctyl)silane (PFOTS), 1H,1H,2H,2H-Perfluoro-1-octanol (PFO), di(ethylene glycol) Dibenzoate (DEGD), and IR-780 iodide (IR-780) were purchased from Sigma Aldrich, MO, USA. 2-NBDG (2-(N-(7-Nitrobenz-2-oxa-1,3-diazol-4-yl)Amino)-2-Deoxyglucose), Live Cell Imaging Solution (LCIS), RPMI 1640 media, Fetal Bovine Serum (FBS), Penicillin-Streptomycin (10,000U/mL), 100x (4-(2-hydroxyethyl)-1-piperazineethanesulfonic acid)

HEPES, 100x GlutaMAX supplement, 2-Mercaptoethanol, Ficoll and CellTrace Violet, and Qubit™ 1X dsDNA HS Assay Kit (500 assays) were purchased from Thermo Fisher Scientific, MA, USA. EL4 (ATCC TIB-39) mouse lymphoma cell line was purchased from American Type Cell Culture, VA, USA. Fluorinert FC-40 oil was purchased from Sigma Aldrich, MO, USA. 3M Novec 7500 Engineering fluid was purchased from 3M, MN, USA. Agencourt AMPure XP 5ml was purchased from Beckman Coulter Life Sciences, IN, USA. SMART-Seq® HT Kit for 96 reactions and NucleoMag NGS Clean-up and Size Select Kit purchased from Takara Bio US, Inc., CA, USA. Nextera XT DNA Library Preparation Kit (96 samples), NextSeq 500/550 High Output Kit v2.5, and Nextera XT Index Kit v2 Set A (96 indexes, 384 samples) were purchased from Illumina, Inc., CA, USA.

Device Fabrication

The device masks, one for the droplet generator and the other for the observation chamber, are designed using AutoCAD 2020 and printed by CAD/Art Service, Inc., CA, USA. The droplet generator uses a conventional flow-focusing junction design with a single oil inlet, two aqueous phase inlets, and a single outlet. Two aqueous phase channels merge with a low angle (< 20°), roughly 100 μm before the flow-focusing junction. The master mold for the droplet generator is imprinted on a 3-inch silicon wafer (Uniersity Wafer Inc, MA, USA), and the master mold for the droplet observation chamber is imprinted on a 4” silicon wafer, both using the conventional soft lithography technique. The master molds are all fabricated using the cleanroom facility in the Quattrone Nanofabrication Center of the Singh Center of Nanotechnology at the University of Pennsylvania. A positive photoresist SU-8 3050 (Microhem, MA, USA) is used. The molds' thickness is controlled using an appropriate photoresist spin coating

recipe combined with the corresponding UV exposure energy under the mask aligner (SUSS Microtec, Garching, Germany). The droplet generator mold is fabricated via the single-layer soft lithography technique and was targeted for the channel height of 40 μm. The master mold for the droplet observation chamber is fabricated with a multiplayer mold fabrication process; in this process, the initial mold development step is skipped after the initial layer post-bake and directly proceeds with the second layer photoresist deposition and spin coating. The target channel heights for the droplet observation chamber is 60 μm for the initial layer of a flow channel and 50 μm for the second layer of micro-well arrays. Following the fabrications, the master molds are all immediately silanized with trichloro(1H,1H,2H,2H-perfluorooctyl)silane (PFOTS) for the easy detachment of cured polydimethylsiloxane (PDMS) from the master molds.

Polydimethylsiloxane (PDMS) mixture is prepared by mixing the base and curing agents of Sylgard 184 (Dow Corning Corp, MI, USA) in a 10:1 ratio within a disposable plastic cup using a plastic knife. After thorough mixing, the uncured PDMS is degassed within a vacuum chamber for 30 minutes. The droplet generator master mold is placed in a petri dish and then degassed uncured PDMS mixture is poured onto it to fill above 1 mm thickness. For the droplet observation chamber, uncured PDMS is poured minimally just to cover the molds. Onto a separate empty petri dish, uncured PDMS is poured to 1 mm thickness. All the above three are degassed for another 30 minutes to remove any remaining air bubbles between the PDMS and the mold features. Upon complete degassing, the petri dishes with just PDMS and the droplet generator mold are directly baked in a 65 °C oven for 4 hours. For the droplet observation chamber, a transparent moisture-resistant polyester film with a thickness of 0.003-inch is carefully placed on top of the PDMS without trapping any air bubble between the mold and the polyester film. A

2 x 3-inch glass slide is placed both above the polyester film and below the wafer. Using a laboratory 3-prong clamp and binder clips, compressive pressure is applied onto the sandwiched layers of glass slides, polyester film, uncured PDMS, and the wafer. The clamped sandwich complex is left at room temperature for 30 minutes with periodic clamp tightening. This step ensures the open structure of micro-well arrays of the observation chamber. Following room temperature incubation, it is baked in an 80 °C oven for 2 hours. Upon curing, the thin PDMS layer of the observation chamber is carefully peeled off from the wafer; if peel off is not easy, the process can be conducted under ethanol, but the layer must be well dried before the next step. During the peel-off, the polyester film must not be detached from the thin PDMS layer. Following the peel-off, another clean polyester film is placed on the other side of the thin PDMS layer and must be marked with a sharpie; this ensures that the marked polyester film is the bottom side of the observation chamber. The droplet generator and plain PDMS slab can be detached from the mold or the petri dish and cut into desirable sizes, and stored within a closed container along with the thin PDMS layer.

A mixture of four chemicals fabricates the photoresponsive layer for selective recovery of the droplet: polystyrene (PS) of MW 192,000, di(ethylene glycol) dibenzoate (DEGD), IR-780 iodide, and chloroform (Sigma-Aldrich, MO, USA). In 10 ml of chloroform, 5 wt% PS, 1.45 wt% DEGD and 0.1 wt% IR-780 are added and well mixed. Upon mixing, the solution is filtered through a 5 μm PTFE syringe filter. The solution must be stored with minimum light exposure to prevent photobleaching of the photoacoustic dye. A thin photoresponsive layer of approximately 10 μm thickness can be prepared using a flow coater. A clean glass slide is placed on a doctor blade coater (NRT100, ThorLab, NJ, USA), and approximately 2 ml of the photoacoustic solution is

evenly cast on 2 x 3-inch glass slides using a coating speed of 20 mm/sec and acceleration of 1 mm/sec^2. This process generates roughly a 10 – 20 μm thickness photoresponsive layer. The layer is air-dried within the amber container for at least 24 hours to guarantee complete chloroform evaporation.

Under the cleanroom condition, the droplet generator PDMS mold's inlets and outlets are punched using a 1.0 mm disposable biopsy punch (Integra Miltex, NJ, USA). Subsequently, the mold is washed with isopropyl alcohol to wash away any debris and dried with nitrogen gas. Well-dried droplet generator PDMS mold and a clean 1 x 3-inch glass slide are oxygen plasma-treated at 50 Watts for 45 seconds (SCE 110, Anatech Ltd, MI, USA) and bonded together immediately and placed on 80 °C hot plate for 20 minutes. Subsequently, a 5 % PFOTS solution in HFE-7500 is injected through the oil inlet to render the surface of the channel structures hydrophobic. All inlets and outlets of the device are sealed with the scotch tape and stored in a closed container.

For the observation chamber fabrication protocol, a thoroughly dried photoresponsive layer, the thin film observation chamber PDMS layer, and plain PDMS slab of 1 mm thickness are brought into the cleanroom. The photoresponsive layer is gently peeled off from the glass slide, reversed, and fixed onto a glass slide using a Kapton tape; this makes the originally glass-slide-facing photoresponsive layer to be exposed. Subsequently, the layer is oxygen plasma-treated at the same condition and immediately submerged under 5 v/v% (3-Aminopropyl)triethoxysilane (APTES) solution for 20 minutes. After the complete surface modification, the photoresponsive layer is gently washed with DI water and blown with nitrogen gas to remove residual water. Next, plain PDMS slab is oxygen plasma-treated at the same condition and bonded to the APTES-treated side of the photoresponsive layer. The slab-layer complex is left

undisturbed for 1 hour to allow complete bonding. Subsequently, the non-marked polyester film of the thin observation chamber PDMS layer is gently peeled off, and the thin layer is oxygen plasma-treated at the same condition. Immediately following the oxygen plasma treatment, the thin PDMS layer is bonded to the slab-layer complex's photoresponsive layer side. Again, the bonded complex is left undisturbed for 1 hour. After removing the marked polyester film, using the 1.0 mm disposable biopsy punch, inlets and outlets are punched from the complex and gently blown with nitrogen gas to remove residual debris. The thin PDMS layer side of the bonded complex is oxygen plasma-treated and immediately bonded to a 1 x 3-inch glass slide and incubated in a closed amber container for 24 hours to allow complete bonding.

Cell Culture

EL4 (ATCC TIB-39) mouse lymphoma cell line is purchased from American Type Cell Culture, VA, USA. Culturing media for EL4 is made using the following recipe: 869 mL RPMI, 100 mL FBS, 10 mL HEPES, 10 mL GLUTAMAX, 10 ml PennStrep, 1 mL 2-mercaptoethanol. The thawed stock vial of 10M cells/ml concentration is centrifuged down at 50 rcf for 1.5 minutes, and the supernatant was discarded. Subsequently, it was mixed with 10ml of the pre-warmed culture media and incubated at the cell incubator. After 24 hours, the density of cell suspension is measured using the hemacytometer then resuspended into the fresh culture media at the concentration of 200,000 cells/ mL. At passage 3 or 4, the cell suspension was centrifuged and mixed with the freeze stock solution and stored at – 80 °C freezer for future use. The cell suspension is diluted to the fresh culture media every 48 hours at the concentration of 200,000 cells/ mL to ensure healthy cells. After passage 15, the cell suspension is discarded, and the frozen stock is thawed to control the passage number of the cell line.

For the experiment, the cell suspension density is measured using the hemacytometer, and 10M cells are suspended to 1 mL of Live Cell Imaging Solution (LCIS) and stained with the CellTrace Violet. The functional probe is also freshly made for every experiment by mixing the 2-NBDG (2-(N-(7-Nitrobenz-2-oxa-1,3-diazol-4-yl)Amino)-2-Deoxyglucose) with the LCIS to get 100 μM 2-NBDG solution.

Droplet Generation and Trapping

Both the droplet generator and the droplet observation chamber are flushed with neat HFE-7500 oil to fill the channel structure with oil completely; for the observation chamber, 15 minutes of 150 μL/hr flow is recommended to remove air bubbles from the micro-well arrays completely. Four of 1 mL Luer-lock syringes are prepared and loaded with four different solutions: cell suspension, functional probe, 1:1 mixture of HFE-7500 with EA-surfactant and HFE-7500 with functionalized SiO_2 surfactant, and neat FC-40 oil. The device is flushed with the neat HFE-7500 oil before the usage. Using detached syringe needles and PTFE tubings, syringes are connected to the droplet generator. The syringe filled with a 1:1 mixture of HFE-7500 with EA-surfactant and SiO_2 surfactant is connected to the droplet generator's oil inlet. The syringes with functional probe and cell suspension are individually connected to the droplet generator's aqueous inlets. A short PTFE tubing is also connected to the outlet of the droplet generator. Using the syringe pumps (Harvard Apparatus, MA, USA), the flow rates for the oil phase and aqueous phases are set to 300 and 150 μL/hr, respectively. When droplet generation stabilizes, the short PTFE tubing from the droplet generator is connected to the observation chamber for the static droplet array formation. When greater than 60% of the wells are filled within the observation chamber, the droplet generator can be disconnected by pulling out the short PTFE tubing from the observation chamber.

Immediately, FC-40 oil containing syringe must be connected to the observation chamber. Slow FC-40 oil flow is used to fill the rest of the micro-well arrays with the already generated droplets. Once the droplet observation chamber is completely filled, FC-40 oil flow is increased to 1 mL/hr to wash away untrapped droplets from the flow channel. All PTFE tubings are disconnected from the observation chamber, and the inlet and outlet of the chamber are sealed with the SecureSeal™ (Grace BioLabs, OR, USA). The chip is carefully transported to the microscope stage for the dynamic observation.

Dynamic Observation

The observation chamber is securely placed onto the stage of an inverted microscope for the dynamic observation. The microscope specification used in the experiment is as follows: the main body is Zeiss Axio Observer 7 with motorized Z step motor equipped with Zeiss motorized scanning stage 130 x 100 step (X and Y movement), Illuminator microLED 2 transmitted-light illumination condenser with shutter, Colibri 5 Type RGB-UV fluorescence light source with 90 HE LED filter sets, motorized 6x reflector turret with shutter, PlanApo 10x air objective with 0.45 NA with a working distance of 2.0 mm. The main body system is all purchased from Carl Zeiss Microscopy LLC, NY, USA. The main camera is the system is Andor Zyla 4.2 sCMOS, and it was purchased from Oxford Instruments, MA, USA. For temperature, humidity, and carbon dioxide control for optimized cell viability, a digital cage-type microscope incubator was custom-built; it was purchased from Okolab, NA, Italy, and it is equipped with active temperature, CO_2, and humidity control within the gas chamber with built-in 1 x 3-inch glass slide insert. Its control panel separately controls the environmental chamber. It was turned on at least 2 hours before the experimental run to make the chamber optimal for cell viability: 37 ℃, 95% humidity, and 5% CO_2 concentration. The rest of the devices,

camera, stage, light source, shutter, and microscope, are controlled by a microscopy software, MetaMorph. The license for the MetaMorph microscopy automation and image analysis software was purchased from Molecular Devices, LLC., CA, USA. For the data analysis, ImageJ, Python, R, and MATLAB are used, and MATLAB's educational student license was purchased from Mathworks, MA, USA.

Multiple MetaMorph journals were written prior to the dynamic observation for automated stage maneuver, shutter control, and data acquisition. The observation chamber with droplets is locked onto the 1 x 3-inch glass slide insert within the gas chamber, and the environmental chamber is closed and covered with black acrylic plates. Lightsource intensities and exposure times are as follows: for UV, 6% intensity with 10 msec, for brightfield 6% intensity with 10 msec, and for GFP, 15% intensity with 15 msec exposure time. Brightfield and UV loop occur before the GFP loop. With the abovementioned equipment, forty loops of with a single GFP acquisition occupy two hours worth of dynamic observation. The MetaMorph journals take minimal input to allow little flexibility among experiments. Still, the journal's backbone is composed of the precise zig-zag movement of the stage, shutter control, and data acquisition. Journal files can be found in the ***APPENDIX***.

Data Analysis

The data analysis initiates as soon as the data acquisition is complete. As the first step of data analysis, Python code detects the loop's final acquisition and initiates file name reorganization and sorting files via individual positions. Python code can also be found in the ***APPENDIX***. Following the file organization and assortment via Python

code, a modified version of the ImageJ particle analysis is conducted. ImageJ analysis code can also be found in the ***APPENDIX***.

After the ImageJ analysis for the quantitative conversion of dynamic image series into numerical values, MATLAB analysis is initiated to arrange numerical values into specific droplet dynamic dynamics. MATLAB analysis code can also be found in the ***APPENDIX***. During this MATLAB analysis, time series values are sorted, aligned for individual droplets, and single-cell containing droplets are separated from zero-cell containing droplets and multiple-cell containing droplets. To accurately separate the observed metabolomic profiles, the Dynamic Time Warping clustering package from R is deployed. The R code for shape-based metabolomic profile clustering can also be found in the ***APPENDIX***. After R-based clustering, the target droplet for sequential recovery is chosen to have as much as even distribution of various metabolic profiles down into the follow-up sequencing step.

Selective Release of Droplets

Selective recoveries of the target are all conducted at the Vision Research Center (VRC) at the University of Pennsylvania. The main body is Olympus BX61 upright microscope equipped with transmitted light, DIC, and epifluorescence (DAPI, FITC, TRITC filters). It has the capability of simultaneous laser stimulation and imaging via the SIM (SIMultaneous) Scanner system. 10x dry objective and 60x water-immersion objective were used in this study. It has dedicated PMT for laser lines connected with the mode-locked Titanium:Sapphire ($Ti:Al_2O_3$) laser (Cameleon, Coherent, Santa Clara, CA, USA). The laser wavelength is locked at 780 nm for IR-780 based photoresponsive layers, has an output power of 3.37 Joule/s. The laser source is Spectra Physics Mai Tai

HP 1020 pulsed laser, equipped with DeepSee automated group velocity dispersion compensation. The laser repetition rate is 80 MHz at 800 nm wavelength, and the duration of a pulse is less than 100 fsec with the peak power greater than 300 kW. The pass-through percent of the power is calculated to be roughly 20% of the output. With 15% intensity, equal to 221.7 Joule/s·cm^2, scanning speed of 2 µs/pix, scanning resolution of 256 x 256 pixels, and optical zoom of 5x, a 50 µm diameter droplets were released from a 50 µm depth wells. A syringe filled with neat FC-40 oil is connected to the observation chamber's inlet before the droplet recovery. Upon the NIR exposure, the syringe is pushed slowly to generate a constant flow within the flow channel. The droplet pushed out of the well is pushed by the constant flow to the outlet. To ensure the droplet released is accurately retrieved, the field of view follows the droplet from release to recovery. Each droplet is collected in a single 0.2 mL Eppendorf tube and then left in an ice bucket.

Single Cell Recovery from the Droplet

A collected tube contains a single droplet and an excess amount of neat FC-40 oil. The oil is removed from the tube as much as possible without removing the droplet. 1H,1H,2H,2H-Perfluoro-1-octanol (PFOH) of three times the remaining fluid volume is added to the Eppendorf tube. The tube is then gently agitated by tapping the tube to breakdown the droplet and release the cell. The tube is then centrifuged down at 100 rcf for 5 seconds. The top aqueous phase is then carefully pipetted out while tilting the tube at 45°. The aqueous phase should be separated from PFOH as quickly as possible to minimize the cell's damage. The aqueous phase should contain a live cell, and it can be confirmed under DAPI exposure as the CellTrace Violet previously stained the cell. The

cell should be stored in an ice bucket and proceeded to the next step as soon as possible.

cDNA Synthesis from Single Cell and Library Preparation

In order to make cDNA from a single cell, a SMART-Seq kit is used. The SMART-Seq HT Kit User Manual (ver. 060920) is used. Reagents were all thawed on ice except for the One-Step buffer and 10x Lysis buffer. All samples containing a single cell were matched to 10.5 µL volume, then 0.95 µL of 10x Lysis Buffer, 0.05 µL RNase inhibitor, 1 µL of 3' SMART-Seq HT oligonucleotide were added. All samples were mixed by gentle vortexing and centrifuged down briefly. Samples were then incubated at a thermal cycler, pre-heated to 72 °C with a heated lid, for 3 minutes. Samples were placed on ice immediately following the heat incubation for 2 minutes. Then each sample is added with 0.7 µL nuclease-free water, 8 µL One-Step buffer, 1 µL SMART-Seq HT oligonucleotide, 0.5 µL RNase Inhibitor, 0.3 µL SeqAmp DNA Polymerase, and 2 µL SMARTScribe Reverse Transcriptase. Samples were then put into a thermal cycler, pre-heated to 42 °C with a heated lid. The thermal cycler's program is started with the following sequences: 42 °C for 90 min, 95 °C for 1 min, 17x Cycles of [98 °C for 10 sec; 65 °C for 30 sec; 68 °C for 3 min], 72 °C for 10 min, 4 °C for overnight. The sample at 4 °C should only be kept in a thermal cycler for overnight, and it must be stored at -20 °C if it needs extended time of storage before the next step. It is recommended not to exceed two weeks after this step.

PCR-amplified cDNA is purified by NucleoMag NGS Clean-up and Size Select (Takara Bio, CA, USA). To each 50 µL of the sample, 25 µL of NucleoMag beads are added and mixed by vortexing. All samples are incubated at room temperature without

disturbance for 8 minutes then placed on the magnetic separation device for 5 minutes. The supernatants are discarded, and 200 µL of 80% EtOH is added to each sample without disturbing the beads. The supernatants are discarded again, and another clean-up is carried out using 200 µL of 80% EtOH. After the second wash, the supernatant is removed as much as possible, and the samples were air-dried for 2 minutes. 17 µL of elution buffer is added to each sample and then incubated for 2 minutes at room temperature, removed from the magnetic separation device. The samples were again put on the magnetic separation device, and after 2 minutes, the supernatant containing purified cDNA is carefully pipetted out and stored in new 0.2 mL Eppendorf tubes.

cDNA quality and quantity are immediately checked via the Agilent 2100 Bioanalyzer and Agilent's High Sensitivity DNA Kit. The negative control and positive control should also be checked for negative trace and positive trace, respectively. The sample needs to be diluted and re-run on the Bioanalyzer if the peak concentration significantly exceeds the lower and upper marker's top intensity profile for accurate quantification.

The cDNA samples' library preparation is carried out by the Nextera XT DNA Library Prep Reference Guide (ver. 15031942 v05). A 1 ng of individual cDNA sample is the input source for the library preparation. All samples are filled up to 5 µL of volume using the Elution buffer, and 10 µL of the TD and 5 µL of the ATM are added to all samples. After gentle pipetting for mixing, samples were centrifuged down. Samples are placed in a thermal cycler, pre-heated to 55 °C with a heated lid set to 100 °C for 5 minutes. Samples are cooled down to 10 °C in a thermal cycler, then immediately placed in ice, then subsequently added for 5 µL of NT to each well. After gentle vortexing and centrifuge down, samples are incubated at room temperature for 5 minutes. For

multiplexing, an appropriate mixture of 5 µL of i5 adapter and 5 µL of i7 adapter is added to each sample, then 15 µL of NPM is added to all. Upon gentle vortexing and centrifugation, samples are placed in a thermal cycler with a heated lid set to 100 °C. A program with the following sequence is initiated: 72 °C for 3 minutes, 95 °C for 30 sec, 12x Cycles of [95 °C for 10 sec; 55 °C for 30 sec; 72 °C for 30 sec], 72 °C for 5 min, 4 °C for forever. Samples are cleaned up immediately following the amplification protocol. Agentcourt AMPure XP beads are used for the clean-up. To 50 µL of the sample, 30 µL of AMPure XP beads, pre-heated to room temperature, is added and well mixed by vortexing, then centrifuged down. After 5 minutes of room temperature incubation, samples are placed on the magnetic stand, and after 2 minutes of wait, the supernatants are discarded without disturbing the beads. The samples are washed twice with 80% EtOH and air-dried for 15 minutes. Then, 52.5 µL of RSB is added, and samples are vortexed and incubated for 2 minutes away from the magnetic stand. After placed on the magnetic stand for 2 minutes, 50 µL of supernatant containing libraries are transferred to a new 0.2 mL Eppendorf tube. The libraries are checked for their quality and quantity using the Agilent 2100 Bioanalyzer with Agilent High Sensitivity DNA kit. After quantification from 300 bp to 3,000 bp, the samples are mixed in proper dilution factor for even distribution in the mixed volume. Samples are then sequenced using the NextSeq 550 machine.

scRNA-seq Analysis

After sequencing, the sequenced data is transferred to the Kim lab's repository cluster and ran through the Kim lab's proprietary pipeline for demultiplexing, alignment, and exonic count measurements. Using the exonic count and mitochondrial count files of individual samples, downstream single-cell RNA sequencing analysis is carried out. For

the downstream analysis, the Seurat package in R is used. Analysis code is in the Appendix.

6.5. REFERENCES

1. Papalexi E, Satija R. Single-cell RNA sequencing to explore immune cell heterogeneity. *Nat Publ Gr*. 2017;18(1):35-45. doi:10.1038/nri.2017.76

2. McLeod CM, Mauck RL. On the origin and impact of mesenchymal stem cell heterogeneity: New insights and emerging tools for single cell analysis. *Eur Cells Mater*. 2017;34:217-231. doi:10.22203/eCM.v034a14

3. Ackermann M. REVIEWS A functional perspective on phenotypic heterogeneity in microorganisms. *Nat Publ Gr*. 2015;13(8):497-508. doi:10.1038/nrmicro3491

4. Dueck H, Eberwine J, Kim J. Variation is function: Are single cell differences functionally important?: Testing the hypothesis that single cell variation is required for aggregate function. *BioEssays*. 2016;38(2):172-180. doi:10.1002/bies.201500124

5. Sievert SM, Brinkhoff T, Muyzer G, Ziebis W, Kuever J. Spatial heterogeneity of bacterial populations along an environmental gradient at a shallow submarine hydrothermal vent near Milos island (Greece). *Appl Environ Microbiol*. 1999;65(9):3834-3842.

6. Huh D, Paulsson J. Non-genetic heterogeneity from stochastic partitioning at cell division. *Nat Genet*. 2011;43(2):95-100. doi:10.1038/ng.729

7. Chen H, Albergante L, Hsu JY, et al. Single-cell trajectories reconstruction, exploration and mapping of omics data with STREAM. *Nat Commun*. 2019;10(1):1903. doi:10.1038/s41467-019-09670-4

8. Kunz DJ, Gomes T, James KR. Immune cell dynamics unfolded by single-cell technologies. *Front Immunol*. 2018;9(JUN):1-8. doi:10.3389/fimmu.2018.01435

9. Buchholz VR, Flossdorf M. *Single-Cell Resolution of T Cell Immune Responses*. Vol 137. 1st ed. Elsevier Inc.; 2018. doi:10.1016/bs.ai.2017.12.001

10. Trapnell C, Liu S. Single-cell transcriptome sequencing: Recent advances and remaining challenges. *F1000Research*. 2016;5:182. doi:10.12688/f1000research.7223.1

11. O'Neill LAJ, Pearce EJ. Immunometabolism governs dendritic cell and macrophage function. *J Exp Med*. 2016;213(1):15-23. doi:10.1084/jem.20151570

12. Artyomov MN, Van den Bossche J. Immunometabolism in the Single-Cell Era. *Cell Metab*. October 2020. doi:10.1016/j.cmet.2020.09.013

13. O'Neill LAJ, Kishton RJ, Rathmell J. A guide to immunometabolism for immunologists. *Nat Rev Immunol*. 2016;16(9):553-565. doi:10.1038/nri.2016.70

14. Bradley A, Hashimoto T, Ono M. Elucidating T cell activation-dependent mechanisms for bifurcation of regulatory and effector T cell differentiation by multidimensional and single-cell analysis. *Front Immunol*. 2018;9(JUL). doi:10.3389/fimmu.2018.01444

15. Guo X, Zhang Y, Zheng L, et al. Global characterization of T cells in non-small-cell lung cancer by single-cell sequencing. *Nat Med*. 2018;24(7):978-985. doi:10.1038/s41591-018-0045-3

16. Gerlach C, van Heijst JWJ, Swart E, et al. One naive T cell, multiple fates in CD8 + T cell differentiation. *J Exp Med*. 2010;207(6):1235-1246. doi:10.1084/jem.20091175

17. Sarkar S. T Cell Dynamic Activation and Functional Analysis in Nanoliter Droplet Microarray. *J Clin Cell Immunol*. 2015;06(03). doi:10.4172/2155-9899.1000334

18. Zielke C, Pan CW, Gutierrez Ramirez AJ, et al. Microfluidic Platform for the Isolation of Cancer-Cell Subpopulations Based on Single-Cell Glycolysis. doi:10.1021/acs.analchem.9b05738

19. Pavlova NN, Thompson CB. The Emerging Hallmarks of Cancer Metabolism. *Cell Metab*. 2016;23(1):27-47. doi:10.1016/j.cmet.2015.12.006

20. Crotty S, Johnston RJ, Schoenberger SP. Effectors and memories: Bcl-6 and Blimp-1 in T and B lymphocyte differentiation. *Nat Immunol*. 2010;11(2):114-120. doi:10.1038/ni.1837

21. Chang JT, Wherry EJ, Goldrath AW. Molecular regulation of effector and memory T cell differentiation. *Nat Immunol*. 2014;15(12):1104-1115. doi:10.1038/ni.3031

22. Zhang L, Romero P. Metabolic Control of CD8 + T Cell Fate Decisions and Antitumor Immunity. *Trends Mol Med*. 2018;24(1):30-48. doi:10.1016/j.molmed.2017.11.005

23. Pearce EL, Walsh MC, Cejas PJ, et al. Enhancing CD8 T-cell memory by modulating fatty acid metabolism. *Nature*. 2009;460(7251):103-107. doi:10.1038/nature08097

24. Pascual G, Domínguez D, Benitah SA. The contributions of cancer cell metabolism to metastasis. *DMM Dis Model Mech*. 2018;11(8). doi:10.1242/dmm.032920

25. Karabacak NM, Spuhler PS, Fachin F, et al. Microfluidic, marker-free isolation of circulating tumor cells from blood samples. *Nat Protoc*. 2014;9(3):694-710. doi:10.1038/nprot.2014.044

26. Lim H, Back SM, Hwang MH, Lee D-H, Choi H, Nam J. Sheathless High-Throughput Circulating Tumor Cell Separation Using Viscoelastic non-Newtonian

Fluid. *Micromachines*. 2019;10(7):462. doi:10.3390/mi10070462

27. POGLUT1 - Protein O-glucosyltransferase 1 precursor - Homo sapiens (Human) - POGLUT1 gene & protein. https://www.uniprot.org/uniprot/Q8NBL1. Accessed October 27, 2020.

28. SLC2A1 gene: MedlinePlus Genetics. https://medlineplus.gov/genetics/gene/slc2a1/. Accessed October 27, 2020.

29. Kim H-K, Raj Bhattarai K, Patil Junjappa R, et al. TMBIM6/BI-1 contributes to cancer progression through assembly with mTORC2 and AKT activation. doi:10.1038/s41467-020-17802-4

30. HK2 Gene - GeneCards | HXK2 Protein | HXK2 Antibody. https://www.genecards.org/cgi-bin/carddisp.pl?gene=HK2. Accessed October 27, 2020.

31. Deisenroth C, Zhang Y. The ribosomal protein-mdm2-p53 pathway and energy metabolism: Bridging the gap between feast and famine. *Genes and Cancer*. 2011;2(4):392-403. doi:10.1177/1947601911409737

CHAPTER 7

CONCLUSIONS AND FUTURE DIRECTIONS

7.1. OVERVIEW

The overall work presented in this dissertation develops a novel high throughput microfluidic device capable of functional phenotyping and highly selective recovery with an analysis and modeling system that enables single-cell level investigation of combined metabolomics and transcriptomics. **Chapter 1** outlines the importance of the single-cell level study, current approaches for the single-cell level study, and discusses the potential target cell population for single-cell level functional phenotyping. It also briefly describes the current microfluidic approaches for functional phenotyping and the potential areas for improvement. As outlined, single-cell level heterogeneity within a genetically identical population is inevitable, and current state-of-the-art technologies for single-cell level study either are limited to surface phenotyping or lack throughput.[1,2] Dynamic observation-based metabolic profiling is suggested as a valuable investigation method for studying single-cell fate plasticity, and several microfluidic devices have been developed to support this.[3–8] Higher-throughput microfluidic approach with better selective recoverability complemented with analytical systems for the multi-omics study is expected to impact the fields positively. As described in **Chapter 3**, current dynamic observation methods using microfluidics utilize several methods, and most of them possess drawbacks that prevent either high-throughput study or lack of selective recoverability. In addition to the mini-review of the currently available methods, perspectives on implementing each method are posed. This dissertation broadly

overviews the current standings of single-cell functional multi-omics research and expands its methododology. Specifically, novel microfluidics can enhance the throughput of the functional phenotyping and selective recoverability for downstream analysis. Add-on kinetic modeling system and metabolic profiling and clustering system serve as a powerful tool for understanding biological system. Besides, the capability to run a functional multi-omics study expands the current research tools.

Chapter 4 investigates the development of a novel stimuli-responsive layer that allows easy fabrication of a microfluidic device that enables functional phenotyping of single cells with high selectivity. Simple polymer membrane mixed with photoacoustic dye and surface-engineered can serve as a photoresponsive layer that can be actuated easily by externally focused laser for highly selective droplet recovery. **Chapter 5** discusses the kinetic modeling system and the metabolic profiling algorithm following multiple hours-long dynamic observation of single cells. Then complex chain of computational algorithms autonomously operate a microscope to conduct tdynamic observation, run image analysis, quantitatively cluster individual cells' metabolic profiles and analyze kinetic modeling system to demultiplex simple metabolic profile to mechanisms of biological processes. **Chapter 6** establishes the correlations between the glucose metabolic profile and the gene expression profile in individual clusters of samples. The combined technologies from **Chapter 4** and **Chapter 5** enable high-throughput single-cell level glucose metabolic profiling and subsequent scRNA-seq based on their metabolic profiles. Clusters seem to have distinct differences in glucose transport pathway synthesis and the promotion and suppression of active glycolysis.

7.2. SPECIFIC AIM 1

Develop a high-throughput microfluidic device capable of rare cell population detection by functional phenotyping and a coupled system for metabolic profile analysis.

7.2.1. CONCLUSIONS

In this aim, we demonstrate the capability to conduct long time automated dynamic observation within the microfluidic device, add-on system for metabolic profiling of individual cells' glucose uptake and consumption rate, and the separate computational algorithm for kinetic modeling of the cellular metabolic profile to decipher simple metabolic trends to series of closely related biological reactions. Using the droplet microfluidics, we co-encapsulate a single cell and a functional probe into a single droplet. The droplet serves as an isolated, and small chamber that provides a perfect small environment for a single cell's metabolic profiling. Due to the small pico-liter size of the droplet, metabolite measurement is highly sensitive. The complete prevention of cross-talk via a mix of the surfactants ensures accurate signal profiling. As a result, the droplet co-encapsulating single cell and functional probe give high signal-to-noise glucose consumption and uptake rate. The automated microscopy gives the observation time scale flexibility, and a fully automated add-on system for metabolic profiling ensures prompt analysis. The separate computational algorithm for kinetic modeling can be conducted in parallel with the transcriptomic profiling for maximum cell viability. The kinetic modeling system decomposes glucose uptake and consumption signals into four closely related biochemical reactions. Derived from the Michaelis-Menten equation, the four differential equations are fitted to the metabolic profile to reveal its glucose pathway

binding affinity, uptake rate, and metabolic breakdown rate. These rates serve as robust biological definitions of the observed metabolic profiles.

7.2.2. FUTURE DIRECTIONS

Although the kinetic modeling system can distinguish three different rates from a single glucose uptake and consumption signal, it can be implemented to divulge more rates and processes since the actual biological mechanism of cellular metabolism is more complicated. The fluorescent glucose analogue used in this chapter, 2-NBDG, loses its fluorescence when it enters the first glycolysis phase. Therefore, only the hexokinase dependent metabolic breakdown rate can be observed. Suppose the fluorescent glucose analogue can be modified with its fluorophore structure to change its fluorescence emission wavelength at each step. In that case, it can allow us to investigate more granular cycles of the glycolysis. The processing speed for the individual glycolysis cycle can be investigated depending on the specific emission spectrum over the dynamic observation.

Since such modification can be extremely challenging, an alternative approach to investigate cellular metabolism in more detail is multiplexing of functional probes. A fatty acid is also an essential nutrient to all living organisms besides glucose. Multiplexed metabolic profiling, such as a mixture of glucose analogue and fatty acid analogue, can provide a great insight into the metabolic pathway balance. Fatty acid oxidation is a crucial part of metabolic reprogramming for those cells that undergo metabolic pathway switch. Multiplexing can show how much energy is being drawn from each metabolic pathway and whether one pathway is completely shut upon cancer cell differentiation. In addition to the nutrient analogue, ion flux measurement can also add valuable

information to the kinetic modeling system. A combined study of glucose analogue and ion flux measurement probe, such as calcium flux probe, can divulge how the ion concentration affects glycolysis rate or uptake. Multiplexing can be done with more than two functional probes, and as long as these functional probes are metabolism-related, it will add value to the kinetic modeling.

Besides the in-depth signal acquirement, a differential equation solver can be implemented for faster and more precise fitting of the kinetic model to the observed metabolic profiles. This study utilized MATLAB's ODE45 solver, which offers medium accuracy and high speed. Currently, there is no single differential equation solver that maximizes both the accuracy and speed. Furthermore, the differential equation solver often finds local minima instead of the global minima depending on the solver's fine parameter setup. Improved algorithm for the differential equation solver will benefit the kinetic modeling system demonstrated in this work.

7.3. SPECIFIC AIM 2

Develop an innovative microfluidic device with a stationary array that fully supports high-throughput dynamic observation while enabling highly selective recovery of the target.

7.3.1. CONCLUSIONS

In this aim, we demonstrated that the microfluidic devices can conduct the high throughput dynamic observation while enabling highly selective recovery of the droplets using a stimuli-responsive layer. In particular, the photoresponsive layer consisting of

common polymer, polystyrene, and added plasticizer, diethylene glycol dibenzoate, can be easily fabricated. The layer's flexibility and glass transition temperature can be precisely tuned by varying the plasticizer composition. A near-infrared (NIR) region photoacoustic dye, IR-780, is used to minimize potential damage to the encapsulated cells, but it can be swapped with other photoacoustic dyes to enhance its utility. The study demonstrated successful co-encapsulation of probe and cell and biocompatibility of the device by comparing the viability after and before the droplet recovery. The photoresponsive layer is transparent in the visible light spectrum, allowing full flexibility in dye selection for the dynamic observation. The layer can also be embedded into the PDMS microfluidic device by simple surface tuning. The device ultimately allows full functional phenotyping of any time scale. It offers highly selective recoverability of the target with the maximum biocompatibility while requiring only a single focused laser as peripheral equipment. Overall, this work broadens the utility of the microfluidic devices for the single-cell level study.

7.3.2. FUTURE DIRECTIONS

The photoactived selective recovery (PHASR) device offers highly selective recoverability without hindering the visible light spectrum and requires only a single piece of external equipment which is significantly less than multiple peripheral devices that are conventionally needed to recover droplets in the surface acoustic wave system or the pneumatic valve system. However, the near-infrared photoacoustic dye's usage requires the single external laser source to be highly sophisticated and expensive, such as a two-photon titanium sapphire laser. This requirement is due to the short travel

distance of the near-infrared light source. The photoacoustic dye can be replaced with UV responsive or visible light spectrum responsive dyes to simplify the laser light source. Nonetheless, this replacement risks potential damage to the cell and flexibility of functional probe selection. Furthermore, UV light source also requires an expensive UV-transmitted objective.

Structural change of the PHASR device can potentially simplify the light source. If the photoresponsive layer itself can be mechanically tough enough to withstand the high flow pressure from the observation chamber, the top monolithic channel layer can be removed. Removing a millimeters-thick layer can facilitate the focusing of the laser to the photoresponsive layer. With this exposed photoresponsive layer, puncture-based release-up recovery can be achieved more quickly. It may be challenging to balance the photoresponsive layer's thickness and the composition percentage of plasticizer and photoacoustic dye to fabricate a mechanically rigid, optically transparent, and biocompatible layer.

Passive recovery, instead of active recovery, can be another approach for the PHASR device. We show an active recovery of specific droplets of choice, and it requires external stimuli to actively manipulate specific spots of the stimuli-responsive layer. However, passive recovery based on the cellular activity within the droplet does not require external stimuli and can potentially simplify the experimental setup further. There are two potential paths to achieve this: droplets over threshold pushed out of the well or droplets under threshold bind to the well's ceiling. In either case, the stimuli-responsive layer must incorporate additional cellular byproduct responsive materials like a pH-responsive hydrogel or be surface-tuned for passive wetting of the droplets. Cells within the droplet metabolize and release metabolites like acid and carbon dioxide, and a

semi-permeable droplet interface can allow communication between the droplet and the well's ceiling. Depending on the mechanism, the metabolite-responsive hydrogel can swell and push the droplet out of the well, or the metabolite can react with the surface of the well's ceiling to induce the wetting of the droplets. Such a passive recovery method is likely to require extensive labor and time to optimize, but it is most likely to minimize the experimental setup.

7.4. SPECIFIC AIM 3

Investigate the transcriptomic profiles of the metabolic profiled single cells and establish the correlation between metabolomics and transcriptomics.

7.4.1. CONCLUSIONS

In this aim, we demonstrate that we can conduct both metabolic profiling and a single-cell level RNA sequencing using the full-size PHASR device and establish the correlation between the glucose metabolic profile and the glycolysis related gene expression levels. Single-cell level heterogeneity within genetically identical cell populations was discovered less than a few decades ago, and the limitation of population-level study has been revealed. The traditional population-level study cannot provide sufficient resolutions of data to differentiate individual single-cell activities and, moreover, can mask individual heterogeneity and mislead the research. Recently immunologists have been suggesting metabolic plasticity is a crucial parameter of cell fate plasticity. Several cells must undergo several metabolic reprogramming, and the flexibility to adapt is likely to govern the cell fate decision. Glucose uptake and

consumption profiles of multiples of single cells are investigated in this aim, and subsequent RNA sequencing and gene expression level analysis are conducted. We found a distinct difference in expression levels of several glycolysis-related genes between active and inactive metabolic profiles. Gene expression level clustering showed two clusters where either glucose uptake and consumption is restrained for some time or not. Although not all metabolic clusters showed distinctive patterns in the gene expression levels, a slight correlation between metabolomic and transcriptomic of active and inactive cells was discovered. We believe that this can serve as a vital start point for many of the future multi-omics studies.

7.4.2. FUTURE DIRECTIONS

As novel research to conduct metabolic profiling and transcriptomic profiling simultaneously, this work showed a great possibility of a multi-omics study in the future. Nonetheless, there is much more room to strengthen the correlation between transcriptomics and metabolomics. Multiplexing of the functional probe can improve the correlation by providing more resolution in the metabolic profiling aspect. Combinations of various functional probes, such as pH probe, oxygen probe, mitochondrial potential probe, and fatty acid analogue probe, enable in-depth clustering of the metabolic profiles. Cells in a seemingly homogenous population in terms of glucose consumption and uptake may exhibit different oxygen consumption patterns or fatty acid oxidation levels. Since the sequencing gives lots of gene expression levels, metabolic profiling just based on the glucose uptake and consumption is a mismatch. Therefore, the resolution

from the metabolic profiling must be improved in the future study. On the same page, the sample number can also be increased to obtain a higher statistical significance.

The single-cell level RNA sequencing data analysis is still a rapidly developing topic. Although several open-source packages and tools like the Seurat package allow easy analysis of the single-cell RNA sequencing data, it is a streamlined analytical tool and lacks flexibility. Further development in sequencing data analysis, such as confining the exonic counts to specific groups of genes related to a specific function, may further improve the correlation.

7.5. OVERALL SUMMARY

Overall, this dissertation's broad conclusions serve to inform the novel development of a device and a system that enables a simultaneous metabolic and transcriptomic profiling and a correlation between metabolomics and transcriptomics. We developed a novel photoresponsive layer that can be tailored to fit any experimental needs to enable high-throughput and high-selective recovery of the droplets from the closed-space microfluidic devices. We also demonstrate the algorithms for metabolic profiling and the kinetic modeling that can investigate glucose consumption and uptake rate of multiples of cells over an extended time and decompose a single signal into a series of biological reactions. We also show that the correlation between metabolomic and transcriptomic can be established, and that metabolic profiling is a powerful tool for single-cell level study. As more functional probes are developed and better microscopic equipment are invented, enhanced metabolomics study will become possible. As the field of metabolomics and transcriptomics evolve, we hope that the works described in

this thesis will constitute a vital cornerstone for the better single-cell high-throughput functional multi-omics study.

7.6. REFERENCES

1. Dueck HR, Ai R, Camarena A, et al. Assessing characteristics of RNA amplification methods for single cell RNA sequencing. *BMC Genomics*. 2016;17(1). doi:10.1186/s12864-016-3300-3

2. Ackermann M. REVIEWS A functional perspective on phenotypic heterogeneity in microorganisms. *Nat Publ Gr*. 2015;13(8):497-508. doi:10.1038/nrmicro3491

3. Pavlova NN, Thompson CB. The Emerging Hallmarks of Cancer Metabolism. *Cell Metab*. 2016;23(1):27-47. doi:10.1016/j.cmet.2015.12.006

4. Kunz DJ, Gomes T, James KR. Immune cell dynamics unfolded by single-cell technologies. *Front Immunol*. 2018;9(JUN):1-8. doi:10.3389/fimmu.2018.01435

5. Arens R, Schoenberger SP. Plasticity in programming of effector and memory CD8+ T-cell formation. *Immunol Rev*. 2010;235(1):190-205. doi:10.1111/j.0105-2896.2010.00899.x

6. Pan M, Kim M, Blauch L, Tang SKY. Surface-functionalizable amphiphilic nanoparticles for pickering emulsions with designer fluid-fluid interfaces. *RSC Adv*. 2016;6(46):39926-39932. doi:10.1039/c6ra03950b

7. Minakshi P, Kumar R, Ghosh M, et al. Single-cell proteomics: Technology and applications. In: *Single-Cell Omics: Volume 1: Technological Advances and Applications*. Elsevier; 2019:283-318. doi:10.1016/B978-0-12-814919-5.00014-2

8. Ma C, Fan R, Ahmad H, et al. A clinical microchip for evaluation of single immune cells reveals high functional heterogeneity in phenotypically similar T cells. *Nat Med*. 2011;17(6):738-743. doi:10.1038/nm.2375

APPENDIX

Chamber_Acquire_Imaging_V1.JNL


```
<Journal><Description/><Version VersionNumber="2.4"/><CodeBlock><AssignVariableEntry
VariableName="Camera.Digital.Exposure" Expression="CondExpTime_Ac"/><AssignVariableEntry
Disabled="0" VariableName="Device.Illumination.Setting"
Expression="Illumination_acquire"/><FunctionEntry GUID="{0x3cef1e1a-0xe09c-0x11d3-0x93-
0x9a-0x0-0x10-0x5a-0x4-0x2f-0x99}" FunctionName="Select Illumination" Interactive="0"
ApplicationName="mmproc" VersionNumber="1" MissingImage="0" CommandID="1"
MetaJournal="00007FFFA2BED610" IsCurrentVersion="1"
Variables="00007FFFA2BED388"><Variable Type="Logical"
Name="jnlSelectIllum.bUseLegacyDelay" NDimensions="0" Override=""
OverrideVariable="">FALSE</Variable><Variable Type="Integer"
Name="jnlSelectIllum.cMillisecDelay" NDimensions="0" Override=""
OverrideVariable="">100</Variable><Variable Type="String" Name="jnlSelectIllum.stSetting"
NDimensions="0" Override="Variable" OverrideVariable="Illumination_acquire">4
DAPI</Variable></FunctionEntry><AssignVariableEntry Disabled="0"
VariableName="Device.Illumination.Setting"
Expression="Illumination_acquire"/><IfThenElseEntry Expression="Camera.Digital.Exposure
&gt;= 1000"><CodeBlock Condition="true"><FunctionEntry GUID="{0x79f51114-0xe09c-0x11d3-
0x93-0x9a-0x0-0x10-0x5a-0x4-0x2f-0x99}" FunctionName="Assign Variable" Interactive="0"
ApplicationName="mmvar" VersionNumber="1" MissingImage="0" CommandID="2"
MetaJournal="00007FFF961DA0A8" IsCurrentVersion="1"
Variables="00007FFF961D9E08"><Variable Type="ULong" Name="jnlAssign.cbAssignData"
NDimensions="0" Override="" OverrideVariable="">68</Variable><Variable Type="UByte"
Name="jnlAssign.byAssignData" NDimensions="1" Lower1="1" Upper1="68" Override=""
OverrideVariable="">20 0 0 0 153 1 0 0 54 1 0 0 12 0 0 0 36 0 0 0 73 109 103 69 120 112
111 115 117 114 101 0 115 116 114 40 67 97 109 101 114 97 46 68 105 103 105 116 97 108 46
69 120 112 111 115 117 114 101 32 47 32 49 48 48 48 41 0
</Variable></FunctionEntry><AssignVariableEntry VariableName="timeunits"
Expression="&amp;quot;sec&amp;quot;"/></CodeBlock><CodeBlock Condition="false"><FunctionEntry
GUID="{0x79f51114-0xe09c-0x11d3-0x93-0x9a-0x0-0x10-0x5a-0x4-0x2f-0x99}"
FunctionName="Assign Variable" Interactive="0" ApplicationName="mmvar" VersionNumber="1"
MissingImage="0" CommandID="3" MetaJournal="00007FFF961DA0A8" IsCurrentVersion="1"
Variables="00007FFF961D9E08"><Variable Type="ULong" Name="jnlAssign.cbAssignData"
NDimensions="0" Override="" OverrideVariable="">61</Variable><Variable Type="UByte"
Name="jnlAssign.byAssignData" NDimensions="1" Lower1="1" Upper1="61" Override=""
OverrideVariable="">20 0 0 0 153 1 0 0 54 1 0 0 12 0 0 0 29 0 0 0 73 109 103 69 120 112
111 115 117 114 101 0 115 116 114 40 67 97 109 101 114 97 46 68 105 103 105 116 97 108 46
69 120 112 111 115 117 114 101 41 0 </Variable></FunctionEntry><AssignVariableEntry
VariableName="timeunits"
Expression="&amp;quot;msec&amp;quot;"/></CodeBlock></IfThenElseEntry><FunctionEntry
GUID="{0x281ef4a0-0x2b37-0x11d4-0x98-0x53-0x0-0xe0-0x18-0x90-0x87-0x5b}"
FunctionName="Acquire" Interactive="0" ApplicationName="acquire" VersionNumber="20000127"
MissingImage="0" CommandID="4" MetaJournal="00007FFF969BBC08" IsCurrentVersion="1"
Variables="00007FFF969BB968"><Variable Type="Image" Name="jnlAcquire.imDest"
NDimensions="0" Override="" OverrideVariable="">m   0 6 9 17 1 -1 -1 8 Untitled
</Variable></FunctionEntry><FunctionEntry GUID="{0x79f51114-0xe09c-0x11d3-0x93-0x9a-0x0-
0x10-0x5a-0x4-0x2f-0x99}" FunctionName="Assign Variable" ApplicationName="mmvar"
Disabled="0" Interactive="0" VersionNumber="1" MissingImage="0" CommandID="5"
MetaJournal="00007FFF961DA0A8" IsCurrentVersion="1"
Variables="00007FFF961D9E08"><Variable Type="ULong" Name="jnlAssign.cbAssignData"
NDimensions="0" Override="" OverrideVariable="">107</Variable><Variable Type="UByte"
Name="jnlAssign.byAssignData" NDimensions="1" Lower1="1" Upper1="107" Override=""
OverrideVariable="">20 0 0 0 153 1 0 0 54 1 0 0 6 0 0 0 81 0 0 0 105 78 97 109 101 0 40
73 108 108 117 109 105 110 97 116 105 111 110 95 97 99 113 117 105 114 101 32 43 34 95 34
43 80 114 111 98 101 95 65 99 43 34 95 34 43 32 73 109 103 69 120 112 111 115 117 114 101
43 116 105 109 101 117 110 105 116 115 32 43 34 95 34 43 34 105 109 97 103 101 34 43 34
95 34 41 0 </Variable></FunctionEntry><AssignVariableEntry
VariableName="ImageInfo.PlaneIllumSetting"
Expression="Illumination_acquire"/><AssignVariableEntry VariableName="Image.IllumSetting"
Expression="Illumination_acquire"/><FunctionEntry GUID="{0x3cef1eb0-0xe09c-0x11d3-0x93-
0x9a-0x0-0x10-0x5a-0x4-0x2f-0x99}" FunctionName="Setup Sequential File Names"
ApplicationName="mmproc" Disabled="0" Interactive="0" VersionNumber="20060520"
```

MissingImage="0" CommandID="6" MetaJournal="00007FFFA2D54FE8" IsCurrentVersion="1"
Variables="00007FFFA2D54D48"><Variable Type="String" Name="uniqueSetupJNL.baseName"
NDimensions="0" Override="Variable" OverrideVariable="iName">5 trans</Variable><Variable
Type="String" Name="uniqueSetupJNL.stPath" NDimensions="0" Override="Variable"
OverrideVariable="save_driver+save_base_dirc+ Illumination_acquire">43 C:\Users\Kim
Lab\Ellison Project\New images</Variable><Variable Type="Long"
Name="uniqueSetupJNL.number" NDimensions="0" Override=""
OverrideVariable="">1</Variable><Variable Type="Integer" Name="uniqueSetupJNL.imageSave"
NDimensions="0" Override="" OverrideVariable="">3</Variable><Variable Type="Logical"
Name="uniqueSetupJNL.bChangeNameOnSave" NDimensions="0" Override=""
OverrideVariable="">TRUE</Variable><Variable Type="Integer" Name="uniqueSetupJNL.nWidth"
NDimensions="0" Override="" OverrideVariable="">2</Variable><Variable Type="String"
Name="uniqueSetupJNL.stImageType" NDimensions="0" Override="" OverrideVariable="">4
.tif</Variable></FunctionEntry><FunctionEntry GUID="{0x3cef1eb1-0xe09c-0x11d3-0x93-0x9a-
0x0-0x10-0x5a-0x4-0x2f-0x99}" FunctionName="Save Using Sequential File Name"
Interactive="0" ApplicationName="mmproc" VersionNumber="19940603" MissingImage="0"
CommandID="7" MetaJournal="00007FFFA2D55748" IsCurrentVersion="1"
Variables="00007FFFA2D554A8"><Variable Type="Image" Name="uniqueSaveJNL.imSave"
NDimensions="0" Override="" OverrideVariable="">m 1 7 9 0 1 4 0 8 Untitled
</Variable></FunctionEntry><FunctionEntry GUID="{0x3cef1e54-0xe09c-0x11d3-0x93-0x9a-0x0-
0x10-0x5a-0x4-0x2f-0x99}" FunctionName="Close" Interactive="0" ApplicationName="mmproc"
VersionNumber="1" MissingImage="0" CommandID="8" MetaJournal="00007FFFA2C74718"
IsCurrentVersion="1" Variables="00007FFFA2C74478"><Variable Type="Image"
Name="jnlCloseImage.im" NDimensions="0" Override="" OverrideVariable="">m 1 3 9 0 1 -1
-1 8 Untitled </Variable><Variable Type="Logical" Name="jnlCloseImage.bSaveIt"
NDimensions="0" Override=""
OverrideVariable="">FALSE</Variable></FunctionEntry></CodeBlock></Journal>

Chamber_Brightfield_Acquire.JNL

<Journal><Description/><Version VersionNumber="2.4"/><CodeBlock><AssignVariableEntry
Disabled="0" VariableName="SelectDirectory.Path"
Expression="saving_base_directory+"Brightfield\""/><AssignVariableEntry
VariableName="Camera.Digital.Exposure"
Expression="CondExpTime_brightfl"/><AssignVariableEntry Disabled="0"
VariableName="Device.Illumination.Setting"
Expression=""Brightfield""/><AssignVariableEntry
VariableName="Illumination_acquire" Expression=""Brightfield""/><FunctionEntry
GUID="{0x3cef1e1a-0xe09c-0x11d3-0x93-0x9a-0x0-0x10-0x5a-0x4-0x2f-0x99}"
FunctionName="Select Illumination" ApplicationName="mmproc" VersionNumber="1"
CommandID="1" Disabled="0" MissingImage="0" Interactive="0"
MetaJournal="000007FEDC5FD610" IsCurrentVersion="1"
Variables="000007FEDC5FD388"><Variable Type="Logical"
Name="jnlSelectIllum.bUseLegacyDelay" NDimensions="0" Override=""
OverrideVariable="">FALSE</Variable><Variable Type="Integer"
Name="jnlSelectIllum.cMillisecDelay" NDimensions="0" Override=""
OverrideVariable="">100</Variable><Variable Type="String" Name="jnlSelectIllum.stSetting"
NDimensions="0" Override="Variable" OverrideVariable="Illumination_acquire">10
Brighfield</Variable></FunctionEntry><AssignVariableEntry Disabled="0"
VariableName="Component.Zeiss_Filter_Cube.PositionLabel" Expression=""SRmCherry-B-
000""/><AssignVariableEntry VariableName="Component.Zeiss_Trans_Shutter.Position"
Expression="1" Disabled="0"/><IfThenElseEntry Expression="Camera.Digital.Exposure >=
1000"><CodeBlock Condition="true"><FunctionEntry GUID="{0x79f51114-0xe09c-0x11d3-0x93-
0x9a-0x0-0x10-0x5a-0x4-0x2f-0x99}" FunctionName="Assign Variable" Interactive="0"
ApplicationName="mmvar" VersionNumber="1" CommandID="2" MissingImage="0"
MetaJournal="000007FEC92AA0A8" IsCurrentVersion="1"
Variables="000007FEC92A9E08"><Variable Type="ULong" Name="jnlAssign.cbAssignData"
NDimensions="0" Override="" OverrideVariable="">68</Variable><Variable Type="UByte"
Name="jnlAssign.byAssignData" NDimensions="1" Lower1="1" Upper1="68" Override=""
OverrideVariable="">20 0 0 0 153 1 0 0 54 1 0 0 12 0 0 0 36 0 0 0 73 109 103 69 120 112
111 115 117 114 101 0 115 116 114 40 67 97 109 101 114 97 46 68 105 103 105 116 97 108 46
69 120 112 111 115 117 114 101 32 47 32 49 48 48 48 41 0
</Variable></FunctionEntry><AssignVariableEntry VariableName="timeunits"
Expression=""sec""/></CodeBlock><CodeBlock Condition="false"><FunctionEntry
GUID="{0x79f51114-0xe09c-0x11d3-0x93-0x9a-0x0-0x10-0x5a-0x4-0x2f-0x99}"
FunctionName="Assign Variable" Interactive="0" ApplicationName="mmvar" VersionNumber="1"
CommandID="3" MissingImage="0" MetaJournal="000007FEC92AA0A8" IsCurrentVersion="1"

Variables="000007FEC92A9E08"><Variable Type="ULong" Name="jnlAssign.cbAssignData"
NDimensions="0" Override="" OverrideVariable="">61</Variable><Variable Type="UByte"
Name="jnlAssign.byAssignData" NDimensions="1" Lower1="1" Upper1="61" Override=""
OverrideVariable="">20 0 0 0 153 1 0 0 54 1 0 0 12 0 0 0 29 0 0 0 73 109 103 69 120 112
111 115 117 114 101 0 115 116 114 40 67 97 109 101 114 97 46 68 105 103 105 116 97 108 46
69 120 112 111 115 117 114 101 41 0 </Variable></FunctionEntry><AssignVariableEntry
VariableName="timeunits"
Expression=""msec""/></CodeBlock></IfThenElseEntry><FunctionEntry
GUID="{0x281ef4a0-0x2b37-0x11d4-0x98-0x53-0x0-0xe0-0x18-0x90-0x87-0x5b}"
FunctionName="Acquire" Interactive="0" ApplicationName="acquire" VersionNumber="20000127"
CommandID="4" MissingImage="0" MetaJournal="000007FEC9F2BC08" IsCurrentVersion="1"
Variables="000007FEC9F2B968"><Variable Type="Image" Name="jnlAcquire.imDest"
NDimensions="0" Override="" OverrideVariable="">m   0 6 9 17 1 -1 -1 8 Untitled
</Variable></FunctionEntry><AssignVariableEntry Disabled="0"
VariableName="Component.Zeiss_Trans_Shutter.Position" Expression="0"/><FunctionEntry
GUID="{0x79f51114-0xe09c-0x11d3-0x93-0x9a-0x0-0x10-0x5a-0x4-0x2f-0x99}"
FunctionName="Assign Variable" ApplicationName="mmvar" Disabled="0" Interactive="0"
VersionNumber="1" CommandID="5" MissingImage="0" MetaJournal="000007FEC92AA0A8"
IsCurrentVersion="1" Variables="000007FEC92A9E08"><Variable Type="ULong"
Name="jnlAssign.cbAssignData" NDimensions="0" Override=""
OverrideVariable="">94</Variable><Variable Type="UByte" Name="jnlAssign.byAssignData"
NDimensions="1" Lower1="1" Upper1="94" Override="" OverrideVariable="">20 0 0 0 153 1 0 0
54 1 0 0 6 0 0 0 68 0 0 0 105 78 97 109 101 0 40 73 108 108 117 109 105 110 97 116 105
111 110 95 97 99 113 117 105 114 101 32 43 34 95 34 43 32 73 109 103 69 120 112 111 115
117 114 101 43 116 105 109 101 117 110 105 116 115 32 43 34 95 34 43 34 105 109 97 103
101 34 43 34 95 34 41 0 </Variable></FunctionEntry><AssignVariableEntry
VariableName="ImageInfo.PlaneIllumSetting"
Expression="Illumination_acquire"/><AssignVariableEntry VariableName="Image.IllumSetting"
Expression="Illumination_acquire"/><FunctionEntry GUID="{0x3cef1eb0-0xe09c-0x11d3-0x93-
0x9a-0x0-0x10-0x5a-0x4-0x2f-0x99}" FunctionName="Setup Sequential File Names"
ApplicationName="mmproc" Disabled="0" Interactive="0" VersionNumber="20060520"
CommandID="6" MissingImage="0" MetaJournal="000007FEDC764FE8" IsCurrentVersion="1"
Variables="000007FEDC764D48"><Variable Type="String" Name="uniqueSetupJNL.baseName"
NDimensions="0" Override="Variable" OverrideVariable="iName">5 trans</Variable><Variable
Type="String" Name="uniqueSetupJNL.stPath" NDimensions="0" Override="Variable"
OverrideVariable="save_driver+save_base_dirc+ Illumination_acquire">43 C:\Users\Kim
Lab\Ellison Project\New images</Variable><Variable Type="Long"
Name="uniqueSetupJNL.number" NDimensions="0" Override=""
OverrideVariable="">1</Variable><Variable Type="Integer" Name="uniqueSetupJNL.imageSave"
NDimensions="0" Override="" OverrideVariable="">3</Variable><Variable Type="Logical"
Name="uniqueSetupJNL.bChangeNameOnSave" NDimensions="0" Override=""
OverrideVariable="">TRUE</Variable><Variable Type="Integer" Name="uniqueSetupJNL.nWidth"
NDimensions="0" Override="" OverrideVariable="">2</Variable><Variable Type="String"
Name="uniqueSetupJNL.stImageType" NDimensions="0" Override="" OverrideVariable="">4
.tif</Variable></FunctionEntry><FunctionEntry GUID="{0x3cef1eb1-0xe09c-0x11d3-0x93-0x9a-
0x0-0x10-0x5a-0x4-0x2f-0x99}" FunctionName="Save Using Sequential File Name"
Interactive="0" ApplicationName="mmproc" VersionNumber="19940603" CommandID="7"
MissingImage="0" MetaJournal="000007FEDC765748" IsCurrentVersion="1"
Variables="000007FEDC7654A8"><Variable Type="Image" Name="uniqueSaveJNL.imSave"
NDimensions="0" Override="" OverrideVariable="">m 1 7 9 0 1 4 0 8 Untitled
</Variable></FunctionEntry><FunctionEntry GUID="{0x3cef1e54-0xe09c-0x11d3-0x93-0x9a-0x0-
0x10-0x5a-0x4-0x2f-0x99}" FunctionName="Close" Interactive="0" ApplicationName="mmproc"
VersionNumber="1" CommandID="8" MissingImage="0" MetaJournal="000007FEDC684718"
IsCurrentVersion="1" Variables="000007FEDC684478"><Variable Type="Image"
Name="jnlCloseImage.im" NDimensions="0" Override="" OverrideVariable="">m   1 3 9 0 1 -1
-1 8 Untitled </Variable><Variable Type="Logical" Name="jnlCloseImage.bSaveIt"
NDimensions="0" Override=""
OverrideVariable="">FALSE</Variable></FunctionEntry></CodeBlock></Journal>

Chamber_brightfield_capture_movement.JNL

<Journal><Description>New Journal</Description><Version
VersionNumber="2.4"/><CodeBlock><AssignVariableEntry VariableName="pos_X_prev"
Expression="pos_X_1 "/><ForNextLoopEntry LoopVariable="set_being_imaged" StartValue="0"
EndValue="num_chambers_sets" StepValue="1"><CodeBlock><ForNextLoopEntry
LoopVariable="chamber_being_imaged" StartValue="0" EndValue="num_chambers"
StepValue="1"><CodeBlock><IfThenElseEntry Expression="(MOD(chamber_being_imaged, 2)) =

0"><CodeBlock Condition="true"><ForNextLoopEntry Disabled="0"
LoopVariable="in_chamber_pos" StartValue="0" EndValue="length_steps"
StepValue="1"><CodeBlock><AssignVariableEntry VariableName="pos_Y_2" Expression="pos_Y_1
- (chamber_being_imaged*chamber_steps) -
(set_being_imaged*(chamber_set_steps+chamber_steps))"/><AssignVariableEntry Disabled="0"
VariableName="pos_X_2" Expression="pos_X_1 - ((pos_Y_1 -
pos_Y_2)*dxdy_chamber)"/><AssignVariableEntry Disabled="0" VariableName="pos_Z_2"
Expression="pos_Z_BF + ((pos_X_1 - pos_X_2)*dzdx_chamber)"/><AssignVariableEntry
VariableName="pos_X_curr" Expression="pos_X_2 - in_chamber_pos*camera_length"
Disabled="0"/><AssignVariableEntry VariableName="pos_Y_curr" Expression="pos_Y_2 -
((in_chamber_pos*camera_length) * dydx_chamber)" Disabled="0"/><AssignVariableEntry
Disabled="0" VariableName="pos_Z_curr" Expression="pos_Z_2 -
((in_chamber_pos*camera_length) * dzdx_chamber) - (dzdy_chamber * (pos_Y_1 -
pos_Y_curr))"/><FunctionEntry GUID="{0x3cef1e92-0xe09c-0x11d3-0x93-0x9a-0x0-0x10-0x5a-
0x4-0x2f-0x99}" FunctionName="Move Stage to Absolute Position" Interactive="0"
ApplicationName="mmproc" VersionNumber="1" CommandID="1" MissingImage="0"
MetaJournal="000007FEDC71FE68" IsCurrentVersion="1"
Variables="000007FEDC71FBC8"><Variable Type="Double" Name="jnlMoveStageAbs.dpX"
NDimensions="0" Override="Variable" OverrideVariable="pos_X_curr">-
3697.3</Variable><Variable Type="Double" Name="jnlMoveStageAbs.dpY" NDimensions="0"
Override="Variable" OverrideVariable="pos_Y_curr">-4026.8</Variable><Variable
Type="Double" Name="jnlMoveStageAbs.dpZ" NDimensions="0" Override="Variable"
OverrideVariable="pos_Z_curr">18289.4</Variable></FunctionEntry><FunctionEntry
GUID="{0x3cef1e92-0xe09c-0x11d3-0x93-0x9a-0x0-0x10-0x5a-0x4-0x2f-0x99}"
FunctionName="Move Stage to Absolute Position" Interactive="0" ApplicationName="mmproc"
VersionNumber="1" CommandID="2" MissingImage="0" MetaJournal="000007FEDC71FE68"
IsCurrentVersion="1" Variables="000007FEDC71FBC8"><Variable Type="Double"
Name="jnlMoveStageAbs.dpX" NDimensions="0" Override="Variable"
OverrideVariable="pos_X_curr">-3697.3</Variable><Variable Type="Double"
Name="jnlMoveStageAbs.dpY" NDimensions="0" Override="Variable"
OverrideVariable="pos_Y_curr">-4026.8</Variable><Variable Type="Double"
Name="jnlMoveStageAbs.dpZ" NDimensions="0" Override="Variable"
OverrideVariable="pos_Z_curr">18289.4</Variable></FunctionEntry><IfThenElseEntry
Expression="Val(pos_X_prev) - Device.Stage.XPosition = 0"><CodeBlock
Condition="true"><AssignVariableEntry VariableName="pos_Y_2" Expression="pos_Y_1 -
(chamber_being_imaged*chamber_steps) -
(set_being_imaged*(chamber_set_steps+chamber_steps))"/><AssignVariableEntry Disabled="0"
VariableName="pos_X_2" Expression="pos_X_1 - ((pos_Y_1 -
pos_Y_2)*dxdy_chamber)"/><AssignVariableEntry Disabled="0" VariableName="pos_Z_2"
Expression="pos_Z_BF + ((pos_X_1 - pos_X_2)*dzdx_chamber)"/><AssignVariableEntry
VariableName="pos_X_curr" Expression="pos_X_2 - in_chamber_pos*camera_length"
Disabled="0"/><AssignVariableEntry VariableName="pos_Y_curr" Expression="pos_Y_2 -
((in_chamber_pos*camera_length) * dydx_chamber)" Disabled="0"/><AssignVariableEntry
Disabled="0" VariableName="pos_Z_curr" Expression="pos_Z_2 -
((in_chamber_pos*camera_length) * dzdx_chamber) - (dzdy_chamber * (pos_Y_1 -
pos_Y_curr))"/><FunctionEntry GUID="{0x3cef1e92-0xe09c-0x11d3-0x93-0x9a-0x0-0x10-0x5a-
0x4-0x2f-0x99}" FunctionName="Move Stage to Absolute Position" Interactive="0"
ApplicationName="mmproc" VersionNumber="1" CommandID="3" MissingImage="0"
MetaJournal="000007FEDC71FE68" IsCurrentVersion="1"
Variables="000007FEDC71FBC8"><Variable Type="Double" Name="jnlMoveStageAbs.dpX"
NDimensions="0" Override="Variable" OverrideVariable="pos_X_curr">-
3697.3</Variable><Variable Type="Double" Name="jnlMoveStageAbs.dpY" NDimensions="0"
Override="Variable" OverrideVariable="pos_Y_curr">-4026.8</Variable><Variable
Type="Double" Name="jnlMoveStageAbs.dpZ" NDimensions="0" Override="Variable"
OverrideVariable="pos_Z_curr">18289.4</Variable></FunctionEntry><TraceEntry
Expression=""Skipped happened at"+STR(in_chamber_pos)+"chamber position,
at chamber"+STR(chamber_being_imaged)"/><FunctionEntry GUID="{0x79f510e8-0xe09c-
0x11d3-0x93-0x9a-0x0-0x10-0x5a-0x4-0x2f-0x99}" FunctionName="Run Journal" Interactive="0"
ApplicationName="journal" VersionNumber="1" CommandID="4" MissingImage="0"
MetaJournal="000007FEC9726AC8" IsCurrentVersion="1"
Variables="000007FEC9726828"><Variable Type="String"
Name="ExecuteJournalJNL.stExecuteJournal" NDimensions="0" Override=""
OverrideVariable="">57
C:\MM\app\mmproc\journals\Chamber_Brightfield_Acquire.jnl</Variable></FunctionEntry></Cod
eBlock><CodeBlock Condition="false"><FunctionEntry GUID="{0x79f510e8-0xe09c-0x11d3-0x93-
0x9a-0x0-0x10-0x5a-0x4-0x2f-0x99}" FunctionName="Run Journal" Interactive="0"
ApplicationName="journal" VersionNumber="1" CommandID="5" MissingImage="0"
MetaJournal="000007FEC9726AC8" IsCurrentVersion="1"

Variables="000007FEC9726828"><Variable Type="String"
Name="ExecuteJournalJNL.stExecuteJournal" NDimensions="0" Override=""
OverrideVariable="">57
C:\MM\app\mmproc\journals\Chamber_Brightfield_Acquire.jnl</Variable></FunctionEntry></Cod
eBlock></IfThenElseEntry></CodeBlock></ForNextLoopEntry></CodeBlock><CodeBlock
Condition="false"><ForNextLoopEntry Disabled="0" LoopVariable="in_chamber_pos"
StartValue="length_steps" EndValue="0" StepValue="-1"><CodeBlock><TraceEntry
Expression="in_chamber_pos"/><AssignVariableEntry VariableName="pos_Y_2"
Expression="pos_Y_1 - (chamber_being_imaged*chamber_steps) -
(set_being_imaged*(chamber_set_steps+chamber_steps))"/><AssignVariableEntry Disabled="0"
VariableName="pos_X_2" Expression="pos_X_1 - ((pos_Y_1 -
pos_Y_2)*dxdy_chamber)"/><AssignVariableEntry Disabled="0" VariableName="pos_Z_2"
Expression="pos_Z_BF + ((pos_X_1 - pos_X_2)*dzdx_chamber)"/><AssignVariableEntry
VariableName="pos_X_curr" Expression="pos_X_2 - in_chamber_pos*camera_length"
Disabled="0"/><AssignVariableEntry VariableName="pos_Y_curr" Expression="pos_Y_2 -
((in_chamber_pos*camera_length) * dydx_chamber)" Disabled="0"/><AssignVariableEntry
Disabled="0" VariableName="pos_Z_curr" Expression="pos_Z_2 -
((in_chamber_pos*camera_length) * dzdx_chamber) - (dzdy_chamber * (pos_Y_1 -
pos_Y_curr))"/><FunctionEntry GUID="{0x3cef1e92-0xe09c-0x11d3-0x93-0x9a-0x0-0x10-0x5a-
0x4-0x2f-0x99}" FunctionName="Move Stage to Absolute Position" Interactive="0"
ApplicationName="mmproc" VersionNumber="1" CommandID="6" MissingImage="0"
MetaJournal="000007FEDC71FE68" IsCurrentVersion="1"
Variables="000007FEDC71FBC8"><Variable Type="Double" Name="jnlMoveStageAbs.dpX"
NDimensions="0" Override="Variable" OverrideVariable="pos_X_curr">-
3697.3</Variable><Variable Type="Double" Name="jnlMoveStageAbs.dpY" NDimensions="0"
Override="Variable" OverrideVariable="pos_Y_curr">-4026.8</Variable><Variable
Type="Double" Name="jnlMoveStageAbs.dpZ" NDimensions="0" Override="Variable"
OverrideVariable="pos_Z_curr">18289.4</Variable></FunctionEntry><FunctionEntry
GUID="{0x3cef1e92-0xe09c-0x11d3-0x93-0x9a-0x0-0x10-0x5a-0x4-0x2f-0x99}"
FunctionName="Move Stage to Absolute Position" Interactive="0" ApplicationName="mmproc"
VersionNumber="1" CommandID="7" MissingImage="0" MetaJournal="000007FEDC71FE68"
IsCurrentVersion="1" Variables="000007FEDC71FBC8"><Variable Type="Double"
Name="jnlMoveStageAbs.dpX" NDimensions="0" Override="Variable"
OverrideVariable="pos_X_curr">-3697.3</Variable><Variable Type="Double"
Name="jnlMoveStageAbs.dpY" NDimensions="0" Override="Variable"
OverrideVariable="pos_Y_curr">-4026.8</Variable><Variable Type="Double"
Name="jnlMoveStageAbs.dpZ" NDimensions="0" Override="Variable"
OverrideVariable="pos_Z_curr">18289.4</Variable></FunctionEntry><IfThenElseEntry
Expression="Val(pos_X_prev) - Device.Stage.XPosition = 0"><CodeBlock
Condition="true"><AssignVariableEntry VariableName="pos_Y_2" Expression="pos_Y_1 -
(chamber_being_imaged*chamber_steps) -
(set_being_imaged*(chamber_set_steps+chamber_steps))"/><AssignVariableEntry Disabled="0"
VariableName="pos_X_2" Expression="pos_X_1 - ((pos_Y_1 -
pos_Y_2)*dxdy_chamber)"/><AssignVariableEntry Disabled="0" VariableName="pos_Z_2"
Expression="pos_Z_BF + ((pos_X_1 - pos_X_2)*dzdx_chamber)"/><AssignVariableEntry
VariableName="pos_X_curr" Expression="pos_X_2 - in_chamber_pos*camera_length"
Disabled="0"/><AssignVariableEntry VariableName="pos_Y_curr" Expression="pos_Y_2 -
((in_chamber_pos*camera_length) * dydx_chamber)" Disabled="0"/><AssignVariableEntry
Disabled="0" VariableName="pos_Z_curr" Expression="pos_Z_2 -
((in_chamber_pos*camera_length) * dzdx_chamber) - (dzdy_chamber * (pos_Y_1 -
pos_Y_curr))"/><FunctionEntry GUID="{0x3cef1e92-0xe09c-0x11d3-0x93-0x9a-0x0-0x10-0x5a-
0x4-0x2f-0x99}" FunctionName="Move Stage to Absolute Position" Interactive="0"
ApplicationName="mmproc" VersionNumber="1" CommandID="8" MissingImage="0"
MetaJournal="000007FEDC71FE68" IsCurrentVersion="1"
Variables="000007FEDC71FBC8"><Variable Type="Double" Name="jnlMoveStageAbs.dpX"
NDimensions="0" Override="Variable" OverrideVariable="pos_X_curr">-
3697.3</Variable><Variable Type="Double" Name="jnlMoveStageAbs.dpY" NDimensions="0"
Override="Variable" OverrideVariable="pos_Y_curr">-4026.8</Variable><Variable
Type="Double" Name="jnlMoveStageAbs.dpZ" NDimensions="0" Override="Variable"
OverrideVariable="pos_Z_curr">18289.4</Variable></FunctionEntry><TraceEntry
Expression=""Skipped happened at"+STR(in_chamber_pos)+"chamber position,
at chamber"+STR(chamber_being_imaged)"/><FunctionEntry GUID="{0x79f510e8-0xe09c-
0x11d3-0x93-0x9a-0x0-0x10-0x5a-0x4-0x2f-0x99}" FunctionName="Run Journal" Interactive="0"
ApplicationName="journal" VersionNumber="1" CommandID="9" MissingImage="0"
MetaJournal="000007FEC9726AC8" IsCurrentVersion="1"
Variables="000007FEC9726828"><Variable Type="String"
Name="ExecuteJournalJNL.stExecuteJournal" NDimensions="0" Override=""
OverrideVariable="">57

C:\MM\app\mmproc\journals\Chamber_Brightfield_Acquire.jnl</Variable></FunctionEntry></CodeBlock><CodeBlock Condition="false"><FunctionEntry GUID="{0x79f510e8-0xe09c-0x11d3-0x93-0x9a-0x0-0x10-0x5a-0x4-0x2f-0x99}" FunctionName="Run Journal" Interactive="0" ApplicationName="journal" VersionNumber="1" CommandID="10" MissingImage="0" MetaJournal="000007FEC9726AC8" IsCurrentVersion="1" Variables="000007FEC9726828"><Variable Type="String" Name="ExecuteJournalJNL.stExecuteJournal" NDimensions="0" Override="" OverrideVariable="">57
C:\MM\app\mmproc\journals\Chamber_Brightfield_Acquire.jnl</Variable></FunctionEntry></CodeBlock></IfThenElseEntry><AssignVariableEntry VariableName="pos_X_prev" Expression="pos_X_curr"/></CodeBlock></ForNextLoopEntry></CodeBlock></IfThenElseEntry></CodeBlock></ForNextLoopEntry></CodeBlock></ForNextLoopEntry></CodeBlock></Journal>

Chamber_camera_length_input.JNL

<Journal><Description>New Journal</Description><Version VersionNumber="2.4"/><CodeBlock><PromptUserEntry VariableName="window_input_type" PromptType="RadioButton" TitleText="X-movement input type" Constrain="0" PromptText="How should window length by determined?" DialogXPos="743" DialogYPos="322" ItemText="Enter manually Determine by objective"/><IfThenElseEntry Expression="window_input_type = "Enter manually""><CodeBlock Condition="true"><PromptUserEntry VariableName="camera_length_mm" PromptType="Number" TitleText="Please enter camera length in milimeters" Constrain="0" PromptText="1.3312 mm covers entire field in 10X" DialogXPos="743" DialogYPos="322"/><AssignVariableEntry VariableName="camera_length" Expression="camera_length_mm*1000"/></CodeBlock><CodeBlock Condition="false"><PromptUserEntry VariableName="objective_select" PromptType="RadioButton" TitleText="Select magnification" Constrain="0" PromptText="Which magnification will you be using to image?" DialogXPos="743" DialogYPos="322" ItemText="10x 40x   60x   100x   "/><IfThenElseEntry Expression="objective_select = "10x""><CodeBlock Condition="true"><AssignVariableEntry VariableName="camera_length" Expression="1331.2" Disabled="0"/></CodeBlock><CodeBlock Condition="false"><IfThenElseEntry Expression="objective_select = "40x""><CodeBlock Condition="true"><AssignVariableEntry Disabled="0" VariableName="camera_length" Expression="332.8"/></CodeBlock><CodeBlock Condition="false"><IfThenElseEntry Expression="objective_select = "60x""><CodeBlock Condition="true"><AssignVariableEntry Disabled="0" VariableName="camera_length" Expression="221.866"/></CodeBlock><CodeBlock Condition="false"><IfThenElseEntry Expression="objective_select = "100x""><CodeBlock Condition="true"><AssignVariableEntry Disabled="0" VariableName="camera_length" Expression="133.12"/></CodeBlock><CodeBlock Condition="false"/></IfThenElseEntry></CodeBlock></IfThenElseEntry></CodeBlock></IfThenElseEntry></CodeBlock></IfThenElseEntry></CodeBlock></IfThenElseEntry></CodeBlock></Journal>

Chamber_DAPI_Acquire.JNL

<Journal><Description/><Version VersionNumber="2.4"/><CodeBlock><IfThenElseEntry Expression="dapi_capture="Y""><CodeBlock Condition="true"><AssignVariableEntry Disabled="0" VariableName="Illumination_acquire" Expression="Pre_Illumination"/><AssignVariableEntry VariableName="CondExpTime_Ac" Expression="CondExpTime_dapi"/><AssignVariableEntry Disabled="0" VariableName="SelectDirectory.Path" Expression="saving_base_directory+Pre_Illumination+"\""/><AssignVariableEntry VariableName="Camera.Digital.Exposure" Expression="CondExpTime_dapi"/><AssignVariableEntry Disabled="0" VariableName="Device.Illumination.Setting" Expression="Pre_Illumination"/><AssignVariableEntry Disabled="0" VariableName="Device.Illumination.Setting" Expression="Pre_Illumination"/><IfThenElseEntry Expression="Camera.Digital.Exposure >= 1000"><CodeBlock Condition="true"><FunctionEntry GUID="{0x79f51114-0xe09c-0x11d3-0x93-0x9a-0x0-0x10-0x5a-0x4-0x2f-0x99}" FunctionName="Assign Variable" Interactive="0" ApplicationName="mmvar" VersionNumber="1" CommandID="1" MissingImage="0" MetaJournal="000007FEC92AA0A8" IsCurrentVersion="1" Variables="000007FEC92A9E08"><Variable Type="ULong" Name="jnlAssign.cbAssignData" NDimensions="0" Override="" OverrideVariable="">68</Variable><Variable Type="UByte" Name="jnlAssign.byAssignData" NDimensions="1" Lower1="1" Upper1="68" Override="" OverrideVariable="">20 0 0 0 153 1 0 0 54 1 0 0 12 0 0 0 36 0 0 0 73 109 103 69 120 112

111 115 117 114 101 0 115 116 114 40 67 97 109 101 114 97 46 68 105 103 105 116 97 108 46
69 120 112 111 115 117 114 101 32 47 32 49 48 48 48 41 0
</Variable></FunctionEntry><AssignVariableEntry VariableName="timeunits"
Expression=""sec""/></CodeBlock><CodeBlock Condition="false"><FunctionEntry
GUID="{0x79f51114-0xe09c-0x11d3-0x93-0x9a-0x0-0x10-0x5a-0x4-0x2f-0x99}"
FunctionName="Assign Variable" Interactive="0" ApplicationName="mmvar" VersionNumber="1"
CommandID="2" MissingImage="0" MetaJournal="000007FEC92AA0A8" IsCurrentVersion="1"
Variables="000007FEC92A9E08"><Variable Type="ULong" Name="jnlAssign.cbAssignData"
NDimensions="0" Override="" OverrideVariable="">61</Variable><Variable Type="UByte"
Name="jnlAssign.byAssignData" NDimensions="1" Lower1="1" Upper1="61" Override=""
OverrideVariable="">20 0 0 0 153 1 0 0 54 1 0 0 12 0 0 0 29 0 0 0 73 109 103 69 120 112
111 115 117 114 101 0 115 116 114 40 67 97 109 101 114 97 46 68 105 103 105 116 97 108 46
69 120 112 111 115 117 114 101 41 0 </Variable></FunctionEntry><AssignVariableEntry
VariableName="timeunits"
Expression=""msec""/></CodeBlock></IfThenElseEntry><FunctionEntry
GUID="{0x281ef4a0-0x2b37-0x11d4-0x98-0x53-0x0-0xe0-0x18-0x90-0x87-0x5b}"
FunctionName="Acquire" Interactive="0" ApplicationName="acquire" VersionNumber="20000127"
CommandID="3" MissingImage="0" MetaJournal="000007FEC9F2BC08" IsCurrentVersion="1"
Variables="000007FEC9F2B968"><Variable Type="Image" Name="jnlAcquire.imDest"
NDimensions="0" Override="" OverrideVariable="">m 0 6 9 17 1 -1 -1 8 Untitled
</Variable></FunctionEntry><FunctionEntry GUID="{0x79f51114-0xe09c-0x11d3-0x93-0x9a-0x0-
0x10-0x5a-0x4-0x2f-0x99}" FunctionName="Assign Variable" ApplicationName="mmvar"
Disabled="0" Interactive="0" VersionNumber="1" CommandID="4" MissingImage="0"
MetaJournal="000007FEC92AA0A8" IsCurrentVersion="1"
Variables="000007FEC92A9E08"><Variable Type="ULong" Name="jnlAssign.cbAssignData"
NDimensions="0" Override="" OverrideVariable="">94</Variable><Variable Type="UByte"
Name="jnlAssign.byAssignData" NDimensions="1" Lower1="1" Upper1="94" Override=""
OverrideVariable="">20 0 0 0 153 1 0 0 54 1 0 0 6 0 0 0 68 0 0 0 105 78 97 109 101 0 40
73 108 108 117 109 105 110 97 116 105 111 110 95 97 99 113 117 105 114 101 32 43 34 95 34
43 32 73 109 103 69 120 112 111 115 117 114 101 43 116 105 109 101 117 110 105 116 115 32
43 34 95 34 43 34 105 109 97 103 101 34 43 34 95 34 41 0
</Variable></FunctionEntry><AssignVariableEntry
VariableName="ImageInfo.PlaneIllumSetting"
Expression="Pre_Illumination"/><AssignVariableEntry VariableName="Image.IllumSetting"
Expression="Pre_Illumination"/><FunctionEntry GUID="{0x3cef1eb0-0xe09c-0x11d3-0x93-0x9a-
0x0-0x10-0x5a-0x4-0x2f-0x99}" FunctionName="Setup Sequential File Names"
ApplicationName="mmproc" Disabled="0" Interactive="0" VersionNumber="20060520"
CommandID="5" MissingImage="0" MetaJournal="000007FEDC764FE8" IsCurrentVersion="1"
Variables="000007FEDC764D48"><Variable Type="String" Name="uniqueSetupJNL.baseName"
NDimensions="0" Override="Variable" OverrideVariable="iName">5 trans</Variable><Variable
Type="String" Name="uniqueSetupJNL.stPath" NDimensions="0" Override="Variable"
OverrideVariable="save_driver+save_base_dirc+ Illumination_acquire">43 C:\Users\Kim
Lab\Ellison Project\New images</Variable><Variable Type="Long"
Name="uniqueSetupJNL.number" NDimensions="0" Override=""
OverrideVariable="">1</Variable><Variable Type="Integer" Name="uniqueSetupJNL.imageSave"
NDimensions="0" Override="" OverrideVariable="">3</Variable><Variable Type="Logical"
Name="uniqueSetupJNL.bChangeNameOnSave" NDimensions="0" Override=""
OverrideVariable="">TRUE</Variable><Variable Type="Integer" Name="uniqueSetupJNL.nWidth"
NDimensions="0" Override="" OverrideVariable="">2</Variable><Variable Type="String"
Name="uniqueSetupJNL.stImageType" NDimensions="0" Override="" OverrideVariable="">4
.tif</Variable></FunctionEntry><FunctionEntry GUID="{0x3cef1eb1-0xe09c-0x11d3-0x93-0x9a-
0x0-0x10-0x5a-0x4-0x2f-0x99}" FunctionName="Save Using Sequential File Name"
Interactive="0" ApplicationName="mmproc" VersionNumber="19940603" CommandID="6"
MissingImage="0" MetaJournal="000007FEDC765748" IsCurrentVersion="1"
Variables="000007FEDC7654A8"><Variable Type="Image" Name="uniqueSaveJNL.imSave"
NDimensions="0" Override="" OverrideVariable="">m 1 7 9 0 1 3 0 8 Untitled
</Variable></FunctionEntry><FunctionEntry GUID="{0x3cef1e54-0xe09c-0x11d3-0x93-0x9a-0x0-
0x10-0x5a-0x4-0x2f-0x99}" FunctionName="Close" Interactive="0" ApplicationName="mmproc"
VersionNumber="1" CommandID="7" MissingImage="0" MetaJournal="000007FEDC684718"
IsCurrentVersion="1" Variables="000007FEDC684478"><Variable Type="Image"
Name="jnlCloseImage.im" NDimensions="0" Override="" OverrideVariable="">m 1 3 9 0 1 -1
-1 8 Untitled </Variable><Variable Type="Logical" Name="jnlCloseImage.bSaveIt"
NDimensions="0" Override=""
OverrideVariable="">FALSE</Variable></FunctionEntry><IfThenElseEntry
Expression="dapi_capture2 = "Y""><CodeBlock
Condition="true"><AssignVariableEntry Disabled="0" VariableName="Illumination_acquire"
Expression="Pre_Illumination2"/><AssignVariableEntry VariableName="CondExpTime_Ac"
Expression="CondExpTime_dapi2"/><AssignVariableEntry Disabled="0"

VariableName="SelectDirectory.Path"
Expression="saving_base_directory+Pre_Illumination2+"\""/><AssignVariableEntry
VariableName="Camera.Digital.Exposure"
Expression="CondExpTime_dapi2"/><AssignVariableEntry Disabled="0"
VariableName="Component.Zeiss_Filter_Cube.PositionLabel"
Expression="Illumination_acquire"/><FunctionEntry GUID="{0x3cef1e1a-0xe09c-0x11d3-0x93-
0x9a-0x0-0x10-0x5a-0x4-0x2f-0x99}" FunctionName="Select Illumination" Interactive="0"
ApplicationName="mmproc" VersionNumber="1" CommandID="8" MissingImage="0"
MetaJournal="000007FEDC5FD610" IsCurrentVersion="1"
Variables="000007FEDC5FD388"><Variable Type="Logical"
Name="jnlSelectIllum.bUseLegacyDelay" NDimensions="0" Override=""
OverrideVariable="">FALSE</Variable><Variable Type="Integer"
Name="jnlSelectIllum.cMillisecDelay" NDimensions="0" Override=""
OverrideVariable="">100</Variable><Variable Type="String" Name="jnlSelectIllum.stSetting"
NDimensions="0" Override="Variable" OverrideVariable="Illumination_acquire">4
DAPI</Variable></FunctionEntry><AssignVariableEntry Disabled="0"
VariableName="Component.Zeiss_Filter_Cube.PositionLabel"
Expression="Illumination_acquire"/><IfThenElseEntry Expression="Camera.Digital.Exposure
>= 1000"><CodeBlock Condition="true"><FunctionEntry GUID="{0x79f51114-0xe09c-0x11d3-
0x93-0x9a-0x0-0x10-0x5a-0x4-0x2f-0x99}" FunctionName="Assign Variable" Interactive="0"
ApplicationName="mmvar" VersionNumber="1" CommandID="9" MissingImage="0"
MetaJournal="000007FEC92AA0A8" IsCurrentVersion="1"
Variables="000007FEC92A9E08"><Variable Type="ULong" Name="jnlAssign.cbAssignData"
NDimensions="0" Override="" OverrideVariable="">68</Variable><Variable Type="UByte"
Name="jnlAssign.byAssignData" NDimensions="1" Lower1="1" Upper1="68" Override=""
OverrideVariable="">20 0 0 0 153 1 0 0 54 1 0 0 12 0 0 0 36 0 0 0 73 109 103 69 120 112
111 115 117 114 101 0 115 116 114 40 67 97 109 101 114 97 46 68 105 103 105 116 97 108 46
69 120 112 111 115 117 114 101 32 47 32 49 48 48 48 41 0
</Variable></FunctionEntry><AssignVariableEntry VariableName="timeunits"
Expression=""sec""/></CodeBlock><CodeBlock Condition="false"><FunctionEntry
GUID="{0x79f51114-0xe09c-0x11d3-0x93-0x9a-0x0-0x10-0x5a-0x4-0x2f-0x99}"
FunctionName="Assign Variable" Interactive="0" ApplicationName="mmvar" VersionNumber="1"
CommandID="10" MissingImage="0" MetaJournal="000007FEC92AA0A8" IsCurrentVersion="1"
Variables="000007FEC92A9E08"><Variable Type="ULong" Name="jnlAssign.cbAssignData"
NDimensions="0" Override="" OverrideVariable="">61</Variable><Variable Type="UByte"
Name="jnlAssign.byAssignData" NDimensions="1" Lower1="1" Upper1="61" Override=""
OverrideVariable="">20 0 0 0 153 1 0 0 54 1 0 0 12 0 0 0 29 0 0 0 73 109 103 69 120 112
111 115 117 114 101 0 115 116 114 40 67 97 109 101 114 97 46 68 105 103 105 116 97 108 46
69 120 112 111 115 117 114 101 41 0 </Variable></FunctionEntry><AssignVariableEntry
VariableName="timeunits"
Expression=""msec""/></CodeBlock></IfThenElseEntry><FunctionEntry
GUID="{0x281ef4a0-0x2b37-0x11d4-0x98-0x53-0x0-0xe0-0x18-0x90-0x87-0x5b}"
FunctionName="Acquire" Interactive="0" ApplicationName="acquire" VersionNumber="20000127"
CommandID="11" MissingImage="0" MetaJournal="000007FEC9F2BC08" IsCurrentVersion="1"
Variables="000007FEC9F2B968"><Variable Type="Image" Name="jnlAcquire.imDest"
NDimensions="0" Override="" OverrideVariable="">m 0 6 9 17 1 -1 -1 8 Untitled
</Variable></FunctionEntry><FunctionEntry GUID="{0x79f51114-0xe09c-0x11d3-0x93-0x9a-0x0-
0x10-0x5a-0x4-0x2f-0x99}" FunctionName="Assign Variable" ApplicationName="mmvar"
Disabled="0" Interactive="0" VersionNumber="1" CommandID="12" MissingImage="0"
MetaJournal="000007FEC92AA0A8" IsCurrentVersion="1"
Variables="000007FEC92A9E08"><Variable Type="ULong" Name="jnlAssign.cbAssignData"
NDimensions="0" Override="" OverrideVariable="">94</Variable><Variable Type="UByte"
Name="jnlAssign.byAssignData" NDimensions="1" Lower1="1" Upper1="94" Override=""
OverrideVariable="">20 0 0 0 153 1 0 0 54 1 0 0 6 0 0 0 68 0 0 0 105 78 97 109 101 0 40
73 108 108 117 109 105 110 97 116 105 111 110 95 97 99 113 117 105 114 101 32 43 34 95 34
43 32 73 109 103 69 120 112 111 115 117 114 101 43 116 105 109 101 117 110 105 116 115 32
43 34 95 34 43 34 105 109 97 103 101 34 43 34 95 34 41 0
</Variable></FunctionEntry><AssignVariableEntry
VariableName="ImageInfo.PlaneIllumSetting"
Expression="Illumination_acquire"/><AssignVariableEntry VariableName="Image.IllumSetting"
Expression="Illumination_acquire"/><FunctionEntry GUID="{0x3cef1eb0-0xe09c-0x11d3-0x93-
0x9a-0x0-0x10-0x5a-0x4-0x2f-0x99}" FunctionName="Setup Sequential File Names"
ApplicationName="mmproc" Disabled="0" Interactive="0" VersionNumber="20060520"
CommandID="13" MissingImage="0" MetaJournal="000007FEDC764FE8" IsCurrentVersion="1"
Variables="000007FEDC764D48"><Variable Type="String" Name="uniqueSetupJNL.baseName"
NDimensions="0" Override="Variable" OverrideVariable="iName">5 trans</Variable><Variable
Type="String" Name="uniqueSetupJNL.stPath" NDimensions="0" Override="Variable"
OverrideVariable="save_driver+save_base_dirc+ Illumination_acquire">43 C:\Users\Kim

Lab\Ellison Project\New images</Variable><Variable Type="Long"
Name="uniqueSetupJNL.number" NDimensions="0" Override=""
OverrideVariable="">1</Variable><Variable Type="Integer" Name="uniqueSetupJNL.imageSave"
NDimensions="0" Override="" OverrideVariable="">3</Variable><Variable Type="Logical"
Name="uniqueSetupJNL.bChangeNameOnSave" NDimensions="0" Override=""
OverrideVariable="">TRUE</Variable><Variable Type="Integer" Name="uniqueSetupJNL.nWidth"
NDimensions="0" Override="" OverrideVariable="">2</Variable><Variable Type="String"
Name="uniqueSetupJNL.stImageType" NDimensions="0" Override="" OverrideVariable="">4
.tif</Variable></FunctionEntry><FunctionEntry GUID="{0x3cef1eb1-0xe09c-0x11d3-0x93-0x9a-
0x0-0x10-0x5a-0x4-0x2f-0x99}" FunctionName="Save Using Sequential File Name"
Interactive="0" ApplicationName="mmproc" VersionNumber="19940603" CommandID="14"
MissingImage="0" MetaJournal="000007FEDC765748" IsCurrentVersion="1"
Variables="000007FEDC7654A8"><Variable Type="Image" Name="uniqueSaveJNL.imSave"
NDimensions="0" Override="" OverrideVariable="">m   1 7 9 0 1 11 0 8 Untitled
</Variable></FunctionEntry><FunctionEntry GUID="{0x3cef1e54-0xe09c-0x11d3-0x93-0x9a-0x0-
0x10-0x5a-0x4-0x2f-0x99}" FunctionName="Close" Interactive="0" ApplicationName="mmproc"
VersionNumber="1" CommandID="15" MissingImage="0" MetaJournal="000007FEDC684718"
IsCurrentVersion="1" Variables="000007FEDC684478"><Variable Type="Image"
Name="jnlCloseImage.im" NDimensions="0" Override="" OverrideVariable="">m 1 3 9 0 1 -1 -
1 8 Untitled </Variable><Variable Type="Logical" Name="jnlCloseImage.bSaveIt"
NDimensions="0" Override=""
OverrideVariable="">FALSE</Variable></FunctionEntry></CodeBlock><CodeBlock
Condition="false"/></IfThenElseEntry></CodeBlock><CodeBlock
Condition="false"/></IfThenElseEntry><AssignVariableEntry
VariableName="Camera.Digital.Exposure" Expression="CondExpTime_dapi"
Disabled="1"/><AssignVariableEntry
VariableName="Component.Zeiss_Filter_Cube.PositionLabel"
Expression="Illumination_acquire" Disabled="1"/><AssignVariableEntry
VariableName="Illumination_acquire" Expression="Pre_Illumination"
Disabled="1"/><FunctionEntry GUID="{0x3cef1e1a-0xe09c-0x11d3-0x93-0x9a-0x0-0x10-0x5a-0x4-
0x2f-0x99}" FunctionName="Select Illumination" Interactive="0" ApplicationName="mmproc"
VersionNumber="1" MissingImage="0" Disabled="1" CommandID="16"
MetaJournal="000007FEDC5FD610" IsCurrentVersion="1"
Variables="000007FEDC5FD388"><Variable Type="Logical"
Name="jnlSelectIllum.bUseLegacyDelay" NDimensions="0" Override=""
OverrideVariable="">FALSE</Variable><Variable Type="Integer"
Name="jnlSelectIllum.cMillisecDelay" NDimensions="0" Override=""
OverrideVariable="">100</Variable><Variable Type="String" Name="jnlSelectIllum.stSetting"
NDimensions="0" Override="Variable" OverrideVariable="Illumination_acquire">4
DAPI</Variable></FunctionEntry><AssignVariableEntry
VariableName="Component.Zeiss_Filter_Cube.PositionLabel"
Expression="Illumination_acquire" Disabled="1"/><IfThenElseEntry
Expression="Camera.Digital.Exposure >= 1000" Disabled="1"><CodeBlock
Condition="true"><FunctionEntry GUID="{0x79f51114-0xe09c-0x11d3-0x93-0x9a-0x0-0x10-0x5a-
0x4-0x2f-0x99}" FunctionName="Assign Variable" Interactive="0" ApplicationName="mmvar"
VersionNumber="1" MissingImage="0" Disabled="1" CommandID="17"
MetaJournal="000007FEC92AA0A8" IsCurrentVersion="1"
Variables="000007FEC92A9E08"><Variable Type="ULong" Name="jnlAssign.cbAssignData"
NDimensions="0" Override="" OverrideVariable="">68</Variable><Variable Type="UByte"
Name="jnlAssign.byAssignData" NDimensions="1" Lower1="1" Upper1="68" Override=""
OverrideVariable="">20 0 0 0 153 1 0 0 54 1 0 0 12 0 0 0 36 0 0 0 73 109 103 69 120 112
111 115 117 114 101 0 115 116 114 40 67 97 109 101 114 97 46 68 105 103 105 116 97 108 46
69 120 112 111 115 117 114 101 32 47 32 49 48 48 48 41 0
</Variable></FunctionEntry><AssignVariableEntry VariableName="timeunits"
Expression=""sec"" Disabled="1"/></CodeBlock><CodeBlock
Condition="false"><FunctionEntry GUID="{0x79f51114-0xe09c-0x11d3-0x93-0x9a-0x0-0x10-0x5a-
0x4-0x2f-0x99}" FunctionName="Assign Variable" Interactive="0" ApplicationName="mmvar"
VersionNumber="1" MissingImage="0" CommandID="18" MetaJournal="000007FEC92AA0A8"
IsCurrentVersion="1" Variables="000007FEC92A9E08"><Variable Type="ULong"
Name="jnlAssign.cbAssignData" NDimensions="0" Override=""
OverrideVariable="">61</Variable><Variable Type="UByte" Name="jnlAssign.byAssignData"
NDimensions="1" Lower1="1" Upper1="61" Override="" OverrideVariable="">20 0 0 0 153 1 0 0
54 1 0 0 12 0 0 0 29 0 0 0 73 109 103 69 120 112 111 115 117 114 101 0 115 116 114 40 67
97 109 101 114 97 46 68 105 103 105 116 97 108 46 69 120 112 111 115 117 114 101 41 0
</Variable></FunctionEntry><AssignVariableEntry VariableName="timeunits"
Expression=""msec""/></CodeBlock></IfThenElseEntry><FunctionEntry
GUID="{0x281ef4a0-0x2b37-0x11d4-0x98-0x53-0x0-0xe0-0x18-0x90-0x87-0x5b}"
FunctionName="Acquire" Interactive="0" ApplicationName="acquire" VersionNumber="20000127"

MissingImage="0" Disabled="1" CommandID="19" MetaJournal="000007FEC9F2BC08"
IsCurrentVersion="1" Variables="000007FEC9F2B968"><Variable Type="Image"
Name="jnlAcquire.imDest" NDimensions="0" Override="" OverrideVariable="">m 0 6 9 17 1 -1
-1 8 Untitled </Variable></FunctionEntry><FunctionEntry GUID="{0x79f51114-0xe09c-0x11d3-
0x93-0x9a-0x0-0x10-0x5a-0x4-0x2f-0x99}" FunctionName="Assign Variable"
ApplicationName="mmvar" Interactive="0" VersionNumber="1" MissingImage="0" Disabled="1"
CommandID="20" MetaJournal="000007FEC92AA0A8" IsCurrentVersion="1"
Variables="000007FEC92A9E08"><Variable Type="ULong" Name="jnlAssign.cbAssignData"
NDimensions="0" Override="" OverrideVariable="">94</Variable><Variable Type="UByte"
Name="jnlAssign.byAssignData" NDimensions="1" Lower1="1" Upper1="94" Override=""
OverrideVariable="">20 0 0 0 153 1 0 0 54 1 0 0 6 0 0 0 68 0 0 0 105 78 97 109 101 0 40
73 108 108 117 109 105 110 97 116 105 111 110 95 97 99 113 117 105 114 101 32 43 34 95 34
43 32 73 109 103 69 120 112 111 115 117 114 101 43 116 105 109 101 117 110 105 116 115 32
43 34 95 34 43 34 105 109 97 103 101 34 43 34 95 34 41 0
</Variable></FunctionEntry><AssignVariableEntry
VariableName="ImageInfo.PlaneIllumSetting" Expression="Illumination_acquire"
Disabled="1"/><AssignVariableEntry VariableName="Image.IllumSetting"
Expression="Illumination_acquire" Disabled="1"/><FunctionEntry GUID="{0x3cef1eb0-0xe09c-
0x11d3-0x93-0x9a-0x0-0x10-0x5a-0x4-0x2f-0x99}" FunctionName="Setup Sequential File Names"
ApplicationName="mmproc" Interactive="0" VersionNumber="20060520" MissingImage="0"
Disabled="1" CommandID="21" MetaJournal="000007FEDC764FE8" IsCurrentVersion="1"
Variables="000007FEDC764D48"><Variable Type="String" Name="uniqueSetupJNL.baseName"
NDimensions="0" Override="Variable" OverrideVariable="iName">5 trans</Variable><Variable
Type="String" Name="uniqueSetupJNL.stPath" NDimensions="0" Override="Variable"
OverrideVariable="save_driver+save_base_dirc+ Illumination_acquire">43 C:\Users\Kim
Lab\Ellison Project\New images</Variable><Variable Type="Long"
Name="uniqueSetupJNL.number" NDimensions="0" Override=""
OverrideVariable="">1</Variable><Variable Type="Integer" Name="uniqueSetupJNL.imageSave"
NDimensions="0" Override="" OverrideVariable="">3</Variable><Variable Type="Logical"
Name="uniqueSetupJNL.bChangeNameOnSave" NDimensions="0" Override=""
OverrideVariable="">TRUE</Variable><Variable Type="Integer" Name="uniqueSetupJNL.nWidth"
NDimensions="0" Override="" OverrideVariable="">2</Variable><Variable Type="String"
Name="uniqueSetupJNL.stImageType" NDimensions="0" Override="" OverrideVariable="">4
.tif</Variable></FunctionEntry><FunctionEntry GUID="{0x3cef1eb1-0xe09c-0x11d3-0x93-0x9a-
0x0-0x10-0x5a-0x4-0x2f-0x99}" FunctionName="Save Using Sequential File Name"
Interactive="0" ApplicationName="mmproc" VersionNumber="19940603" MissingImage="1"
Disabled="1" CommandID="22" MetaJournal="000007FEDC765748" IsCurrentVersion="1"
Variables="000007FEDC7654A8"><Variable Type="Image" Name="uniqueSaveJNL.imSave"
NDimensions="0" Override="" OverrideVariable="">m 1 7 9 0 1 19 0 8 Untitled
</Variable></FunctionEntry><FunctionEntry GUID="{0x3cef1e54-0xe09c-0x11d3-0x93-0x9a-0x0-
0x10-0x5a-0x4-0x2f-0x99}" FunctionName="Close" Interactive="0" ApplicationName="mmproc"
VersionNumber="1" MissingImage="0" Disabled="1" CommandID="23"
MetaJournal="000007FEDC684718" IsCurrentVersion="1"
Variables="000007FEDC684478"><Variable Type="Image" Name="jnlCloseImage.im"
NDimensions="0" Override="" OverrideVariable="">m 1 3 9 0 1 -1 -1 8 Untitled
</Variable><Variable Type="Logical" Name="jnlCloseImage.bSaveIt" NDimensions="0"
Override="" OverrideVariable="">FALSE</Variable></FunctionEntry></CodeBlock></Journal>

Chamber_dapi_capture_movement.JNL

<Journal><Description>New Journal</Description><Version
VersionNumber="2.4"/><CodeBlock><AssignVariableEntry VariableName="pos_X_prev"
Expression="pos_X_1 "/><ForNextLoopEntry LoopVariable="set_being_imaged" StartValue="0"
EndValue="num_chambers_sets" StepValue="1"><CodeBlock><ForNextLoopEntry
LoopVariable="chamber_being_imaged" StartValue="0" EndValue="num_chambers"
StepValue="1"><CodeBlock><IfThenElseEntry Expression="(MOD(chamber_being_imaged, 2)) =
0"><CodeBlock Condition="true"><ForNextLoopEntry Disabled="0"
LoopVariable="in_chamber_pos" StartValue="0" EndValue="length_steps"
StepValue="1"><CodeBlock><AssignVariableEntry VariableName="pos_Y_2" Expression="pos_Y_1
- (chamber_being_imaged*chamber_steps) -
(set_being_imaged*(chamber_set_steps+chamber_steps))"/><AssignVariableEntry Disabled="0"
VariableName="pos_X_2" Expression="pos_X_1 - ((pos_Y_1 -
pos_Y_2)*dxdy_chamber)"/><AssignVariableEntry Disabled="0" VariableName="pos_Z_2"
Expression="pos_Z_1 + ((pos_X_1 - pos_X_2)*dzdx_chamber)"/><AssignVariableEntry
VariableName="pos_X_curr" Expression="pos_X_2 - in_chamber_pos*camera_length"
Disabled="0"/><AssignVariableEntry VariableName="pos_Y_curr" Expression="pos_Y_2 -
((in_chamber_pos*camera_length) * dydx_chamber)" Disabled="0"/><AssignVariableEntry

Disabled="0" VariableName="pos_Z_curr" Expression="pos_Z_2 -
((in_chamber_pos*camera_length) * dzdx_chamber) - (dzdy_chamber * (pos_Y_1 -
pos_Y_curr))"/><FunctionEntry GUID="{0x3cef1e92-0xe09c-0x11d3-0x93-0x9a-0x0-0x10-0x5a-
0x4-0x2f-0x99}" FunctionName="Move Stage to Absolute Position" Interactive="0"
ApplicationName="mmproc" VersionNumber="1" MissingImage="0" CommandID="1"
MetaJournal="000007FEDC71FE68" IsCurrentVersion="1"
Variables="000007FEDC71FBC8"><Variable Type="Double" Name="jnlMoveStageAbs.dpX"
NDimensions="0" Override="Variable" OverrideVariable="pos_X_curr">-
3697.3</Variable><Variable Type="Double" Name="jnlMoveStageAbs.dpY" NDimensions="0"
Override="Variable" OverrideVariable="pos_Y_curr">-4026.8</Variable><Variable
Type="Double" Name="jnlMoveStageAbs.dpZ" NDimensions="0" Override="Variable"
OverrideVariable="pos_Z_curr">18289.4</Variable></FunctionEntry><FunctionEntry
GUID="{0x3cef1e92-0xe09c-0x11d3-0x93-0x9a-0x0-0x10-0x5a-0x4-0x2f-0x99}"
FunctionName="Move Stage to Absolute Position" Interactive="0" ApplicationName="mmproc"
VersionNumber="1" MissingImage="0" CommandID="2" MetaJournal="000007FEDC71FE68"
IsCurrentVersion="1" Variables="000007FEDC71FBC8"><Variable Type="Double"
Name="jnlMoveStageAbs.dpX" NDimensions="0" Override="Variable"
OverrideVariable="pos_X_curr">-3697.3</Variable><Variable Type="Double"
Name="jnlMoveStageAbs.dpY" NDimensions="0" Override="Variable"
OverrideVariable="pos_Y_curr">-4026.8</Variable><Variable Type="Double"
Name="jnlMoveStageAbs.dpZ" NDimensions="0" Override="Variable"
OverrideVariable="pos_Z_curr">18289.4</Variable></FunctionEntry><IfThenElseEntry
Expression="Val(pos_X_prev) - Device.Stage.XPosition = 0"><CodeBlock
Condition="true"><AssignVariableEntry VariableName="pos_Y_2" Expression="pos_Y_1 -
(chamber_being_imaged*chamber_steps) -
(set_being_imaged*(chamber_set_steps+chamber_steps))"/><AssignVariableEntry Disabled="0"
VariableName="pos_X_2" Expression="pos_X_1 - ((pos_Y_1 -
pos_Y_2)*dxdy_chamber)"/><AssignVariableEntry Disabled="0" VariableName="pos_Z_2"
Expression="pos_Z_1 + ((pos_X_1 - pos_X_2)*dzdx_chamber)"/><AssignVariableEntry
VariableName="pos_Z_2" Expression="pos_Z_BF - ((pos_Y_1 - pos_Y_2)*dzdy_chamber) +
((pos_X_1 - pos_X_2)*dzdx_chamber)" Disabled="1"/><AssignVariableEntry
VariableName="pos_X_curr" Expression="pos_X_2 - in_chamber_pos*camera_length"
Disabled="0"/><AssignVariableEntry VariableName="pos_Y_curr" Expression="pos_Y_2 -
((in_chamber_pos*camera_length) * dydx_chamber)" Disabled="0"/><AssignVariableEntry
Disabled="0" VariableName="pos_Z_curr" Expression="pos_Z_2 -
((in_chamber_pos*camera_length) * dzdx_chamber) - (dzdy_chamber * (pos_Y_1 -
pos_Y_curr))"/><FunctionEntry GUID="{0x3cef1e92-0xe09c-0x11d3-0x93-0x9a-0x0-0x10-0x5a-
0x4-0x2f-0x99}" FunctionName="Move Stage to Absolute Position" Interactive="0"
ApplicationName="mmproc" VersionNumber="1" MissingImage="0" CommandID="3"
MetaJournal="000007FEDC71FE68" IsCurrentVersion="1"
Variables="000007FEDC71FBC8"><Variable Type="Double" Name="jnlMoveStageAbs.dpX"
NDimensions="0" Override="Variable" OverrideVariable="pos_X_curr">-
3697.3</Variable><Variable Type="Double" Name="jnlMoveStageAbs.dpY" NDimensions="0"
Override="Variable" OverrideVariable="pos_Y_curr">-4026.8</Variable><Variable
Type="Double" Name="jnlMoveStageAbs.dpZ" NDimensions="0" Override="Variable"
OverrideVariable="pos_Z_curr">18289.4</Variable></FunctionEntry><TraceEntry
Expression=""Skipped happened at"+STR(in_chamber_pos)+"chamber position,
at chamber"+STR(chamber_being_imaged)"/><FunctionEntry GUID="{0x79f510e8-0xe09c-
0x11d3-0x93-0x9a-0x0-0x10-0x5a-0x4-0x2f-0x99}" FunctionName="Run Journal" Interactive="0"
ApplicationName="journal" VersionNumber="1" MissingImage="0" CommandID="4"
MetaJournal="000007FEC9726AC8" IsCurrentVersion="1"
Variables="000007FEC9726828"><Variable Type="String"
Name="ExecuteJournalJNL.stExecuteJournal" NDimensions="0" Override=""
OverrideVariable="">50
C:\MM\app\mmproc\journals\Chamber_DAPI_Acquire.jnl</Variable></FunctionEntry></CodeBlock>
<CodeBlock Condition="false"><FunctionEntry GUID="{0x79f510e8-0xe09c-0x11d3-0x93-0x9a-
0x0-0x10-0x5a-0x4-0x2f-0x99}" FunctionName="Run Journal" Interactive="0"
ApplicationName="journal" VersionNumber="1" MissingImage="0" CommandID="5"
MetaJournal="000007FEC9726AC8" IsCurrentVersion="1"
Variables="000007FEC9726828"><Variable Type="String"
Name="ExecuteJournalJNL.stExecuteJournal" NDimensions="0" Override=""
OverrideVariable="">50
C:\MM\app\mmproc\journals\Chamber_DAPI_Acquire.jnl</Variable></FunctionEntry></CodeBlock>
</IfThenElseEntry></CodeBlock></ForNextLoopEntry></CodeBlock><CodeBlock
Condition="false"><ForNextLoopEntry Disabled="0" LoopVariable="in_chamber_pos"
StartValue="length_steps" EndValue="0" StepValue="-1"><CodeBlock><TraceEntry
Expression="in_chamber_pos"/><AssignVariableEntry VariableName="pos_Y_2"
Expression="pos_Y_1 - (chamber_being_imaged*chamber_steps) -

(set_being_imaged*(chamber_set_steps+chamber_steps))"/><AssignVariableEntry Disabled="0"
VariableName="pos_X_2" Expression="pos_X_1 - ((pos_Y_1 -
pos_Y_2)*dxdy_chamber)"/><AssignVariableEntry Disabled="0" VariableName="pos_Z_2"
Expression="pos_Z_1 + ((pos_X_1 - pos_X_2)*dzdx_chamber)"/><AssignVariableEntry
VariableName="pos_X_curr" Expression="pos_X_2 - in_chamber_pos*camera_length"
Disabled="0"/><AssignVariableEntry VariableName="pos_Y_curr" Expression="pos_Y_2 -
((in_chamber_pos*camera_length) * dydx_chamber)" Disabled="0"/><AssignVariableEntry
Disabled="0" VariableName="pos_Z_curr" Expression="pos_Z_2 -
((in_chamber_pos*camera_length) * dzdx_chamber) - (dzdy_chamber * (pos_Y_1 -
pos_Y_curr))"/><FunctionEntry GUID="{0x3cef1e92-0xe09c-0x11d3-0x93-0x9a-0x0-0x10-0x5a-
0x4-0x2f-0x99}" FunctionName="Move Stage to Absolute Position" Interactive="0"
ApplicationName="mmproc" VersionNumber="1" MissingImage="0" CommandID="6"
MetaJournal="000007FEDC71FE68" IsCurrentVersion="1"
Variables="000007FEDC71FBC8"><Variable Type="Double" Name="jnlMoveStageAbs.dpX"
NDimensions="0" Override="Variable" OverrideVariable="pos_X_curr">-
3697.3</Variable><Variable Type="Double" Name="jnlMoveStageAbs.dpY" NDimensions="0"
Override="Variable" OverrideVariable="pos_Y_curr">-4026.8</Variable><Variable
Type="Double" Name="jnlMoveStageAbs.dpZ" NDimensions="0" Override="Variable"
OverrideVariable="pos_Z_curr">18289.4</Variable></FunctionEntry><FunctionEntry
GUID="{0x3cef1e92-0xe09c-0x11d3-0x93-0x9a-0x0-0x10-0x5a-0x4-0x2f-0x99}"
FunctionName="Move Stage to Absolute Position" Interactive="0" ApplicationName="mmproc"
VersionNumber="1" MissingImage="0" CommandID="7" MetaJournal="000007FEDC71FE68"
IsCurrentVersion="1" Variables="000007FEDC71FBC8"><Variable Type="Double"
Name="jnlMoveStageAbs.dpX" NDimensions="0" Override="Variable"
OverrideVariable="pos_X_curr">-3697.3</Variable><Variable Type="Double"
Name="jnlMoveStageAbs.dpY" NDimensions="0" Override="Variable"
OverrideVariable="pos_Y_curr">-4026.8</Variable><Variable Type="Double"
Name="jnlMoveStageAbs.dpZ" NDimensions="0" Override="Variable"
OverrideVariable="pos_Z_curr">18289.4</Variable></FunctionEntry><IfThenElseEntry
Expression="Val(pos_X_prev) - Device.Stage.XPosition = 0"><CodeBlock
Condition="true"><AssignVariableEntry VariableName="pos_Y_2" Expression="pos_Y_1 -
(chamber_being_imaged*chamber_steps) -
(set_being_imaged*(chamber_set_steps+chamber_steps))"/><AssignVariableEntry Disabled="0"
VariableName="pos_X_2" Expression="pos_X_1 - ((pos_Y_1 -
pos_Y_2)*dxdy_chamber)"/><AssignVariableEntry Disabled="0" VariableName="pos_Z_2"
Expression="pos_Z_1 + ((pos_X_1 - pos_X_2)*dzdx_chamber)"/><AssignVariableEntry
VariableName="pos_X_curr" Expression="pos_X_2 - in_chamber_pos*camera_length"
Disabled="0"/><AssignVariableEntry VariableName="pos_Y_curr" Expression="pos_Y_2 -
((in_chamber_pos*camera_length) * dydx_chamber)" Disabled="0"/><AssignVariableEntry
Disabled="0" VariableName="pos_Z_curr" Expression="pos_Z_2 -
((in_chamber_pos*camera_length) * dzdx_chamber) - (dzdy_chamber * (pos_Y_1 -
pos_Y_curr))"/><FunctionEntry GUID="{0x3cef1e92-0xe09c-0x11d3-0x93-0x9a-0x0-0x10-0x5a-
0x4-0x2f-0x99}" FunctionName="Move Stage to Absolute Position" Interactive="0"
ApplicationName="mmproc" VersionNumber="1" MissingImage="0" CommandID="8"
MetaJournal="000007FEDC71FE68" IsCurrentVersion="1"
Variables="000007FEDC71FBC8"><Variable Type="Double" Name="jnlMoveStageAbs.dpX"
NDimensions="0" Override="Variable" OverrideVariable="pos_X_curr">-
3697.3</Variable><Variable Type="Double" Name="jnlMoveStageAbs.dpY" NDimensions="0"
Override="Variable" OverrideVariable="pos_Y_curr">-4026.8</Variable><Variable
Type="Double" Name="jnlMoveStageAbs.dpZ" NDimensions="0" Override="Variable"
OverrideVariable="pos_Z_curr">18289.4</Variable></FunctionEntry><TraceEntry
Expression=""Skipped happened at"+STR(in_chamber_pos)+"chamber position,
at chamber"+STR(chamber_being_imaged)"/><FunctionEntry GUID="{0x79f510e8-0xe09c-
0x11d3-0x93-0x9a-0x0-0x10-0x5a-0x4-0x2f-0x99}" FunctionName="Run Journal" Interactive="0"
ApplicationName="journal" VersionNumber="1" MissingImage="0" CommandID="9"
MetaJournal="000007FEC9726AC8" IsCurrentVersion="1"
Variables="000007FEC9726828"><Variable Type="String"
Name="ExecuteJournalJNL.stExecuteJournal" NDimensions="0" Override=""
OverrideVariable="">50
C:\MM\app\mmproc\journals\Chamber_DAPI_Acquire.jnl</Variable></FunctionEntry></CodeBlock>
<CodeBlock Condition="false"><FunctionEntry GUID="{0x79f510e8-0xe09c-0x11d3-0x93-0x9a-
0x0-0x10-0x5a-0x4-0x2f-0x99}" FunctionName="Run Journal" Interactive="0"
ApplicationName="journal" VersionNumber="1" MissingImage="0" CommandID="10"
MetaJournal="000007FEC9726AC8" IsCurrentVersion="1"
Variables="000007FEC9726828"><Variable Type="String"
Name="ExecuteJournalJNL.stExecuteJournal" NDimensions="0" Override=""
OverrideVariable="">50
C:\MM\app\mmproc\journals\Chamber_DAPI_Acquire.jnl</Variable></FunctionEntry></CodeBlock>

```
</IfThenElseEntry><AssignVariableEntry VariableName="pos_X_prev"
Expression="pos_X_curr"/></CodeBlock></ForNextLoopEntry></CodeBlock></IfThenElseEntry></C
odeBlock></ForNextLoopEntry></CodeBlock></ForNextLoopEntry></CodeBlock></Journal>
```


Chamber_Dye_Selection_Capture.JNL


```
<Journal><Description>New Journal</Description><Version
VersionNumber="2.4"/><CodeBlock><IfThenElseEntry Expression="NumofDyes &gt; 0"><CodeBlock
Condition="true"><AssignVariableEntry Disabled="0" VariableName="Illumination_acquire"
Expression="Illumination"/><AssignVariableEntry VariableName="CondExpTime_Ac"
Expression="Cond1ExpTime"/><AssignVariableEntry Disabled="0" VariableName="Probe_Ac"
Expression="Dye_1"/><AssignVariableEntry Disabled="0" VariableName="SelectDirectory.Path"
Expression="saving_base_directory+Illumination+&quot;\&quot;"/><FunctionEntry
GUID="{0x79f510e8-0xe09c-0x11d3-0x93-0x9a-0x0-0x10-0x5a-0x4-0x2f-0x99}" FunctionName="Run
Journal" Interactive="0" ApplicationName="journal" VersionNumber="1" CommandID="1"
MissingImage="0" MetaJournal="00007FFF93606AC8" IsCurrentVersion="1"
Variables="00007FFF93606828"><Variable Type="String"
Name="ExecuteJournalJNL.stExecuteJournal" NDimensions="0" Override=""
OverrideVariable="">56
C:\MM\app\mmproc\journals\Chamber_Acquire_Imaging_V1.jnl</Variable></FunctionEntry><IfThe
nElseEntry Expression="NumofDyes &gt; 1"><CodeBlock Condition="true"><IfThenElseEntry
Expression="TRF = &quot;Y&quot;"><CodeBlock Condition="true"><AssignVariableEntry
Disabled="0" VariableName="Probe_Ac" Expression="Dye_2"/><AssignVariableEntry
Disabled="0" VariableName="Illumination_acquire"
Expression="Illumination2"/><AssignVariableEntry VariableName="CondExpTime_Ac"
Expression="Cond2ExpTime"/><AssignVariableEntry Disabled="0"
VariableName="SelectDirectory.Path"
Expression="saving_base_directory+Illumination2+&quot;\TRF1\&quot;"/><AssignVariableEntry
VariableName="timeunits" Expression="&quot;msec&quot;"/><FunctionEntry GUID="{0xddcbcf00-
0x9656-0x4341-0xa3-0xca-0xea-0x8-0xda-0xac-0x8a-0xf3}" FunctionName="Component Control"
Interactive="0" ApplicationName="mmproc" VersionNumber="1" CommandID="2" MissingImage="0"
MetaJournal="00007FFF98789B98" IsCurrentVersion="1"
Variables="00007FFF987898F8"><Variable Type="String"
Name="jnlComponentControl.stComponentName" NDimensions="0" Override=""
OverrideVariable="">16 Zeiss RL Shutter</Variable><Variable Type="Double"
Name="jnlComponentControl.dPosition" NDimensions="0" Override="" OverrideVariable="">-
1</Variable></FunctionEntry><FunctionEntry GUID="{0xddcbcf00-0x9656-0x4341-0xa3-0xca-
0xea-0x8-0xda-0xac-0x8a-0xf3}" FunctionName="Component Control" Interactive="0"
ApplicationName="mmproc" VersionNumber="1" CommandID="3" MissingImage="0"
MetaJournal="00007FFF98789B98" IsCurrentVersion="1"
Variables="00007FFF987898F8"><Variable Type="String"
Name="jnlComponentControl.stComponentName" NDimensions="0" Override=""
OverrideVariable="">34 Zeiss LED-Module 385nm     Shutter</Variable><Variable
Type="Double" Name="jnlComponentControl.dPosition" NDimensions="0" Override=""
OverrideVariable="">-1</Variable></FunctionEntry><FunctionEntry GUID="{0x79f510e4-0xe09c-
0x11d3-0x93-0x9a-0x0-0x10-0x5a-0x4-0x2f-0x99}" FunctionName="Delay" Interactive="0"
ApplicationName="journal" VersionNumber="1" CommandID="4" MissingImage="0"
MetaJournal="00007FFF93605468" IsCurrentVersion="1"
Variables="00007FFF936051C8"><Variable Type="Double" Name="DelayJNL.dpDelayTime"
NDimensions="0" Override="" OverrideVariable="">20</Variable><Variable Type="Integer"
Name="DelayJNL.nDelayUnits" NDimensions="0" Override=""
OverrideVariable="">1</Variable></FunctionEntry><FunctionEntry GUID="{0xddcbcf00-0x9656-
0x4341-0xa3-0xca-0xea-0x8-0xda-0xac-0x8a-0xf3}" FunctionName="Component Control"
Interactive="0" ApplicationName="mmproc" VersionNumber="1" CommandID="5" MissingImage="0"
MetaJournal="00007FFF98789B98" IsCurrentVersion="1"
Variables="00007FFF987898F8"><Variable Type="String"
Name="jnlComponentControl.stComponentName" NDimensions="0" Override=""
OverrideVariable="">34 Zeiss LED-Module 385nm     Shutter</Variable><Variable
Type="Double" Name="jnlComponentControl.dPosition" NDimensions="0" Override=""
OverrideVariable="">0</Variable></FunctionEntry><FunctionEntry GUID="{0xddcbcf00-0x9656-
0x4341-0xa3-0xca-0xea-0x8-0xda-0xac-0x8a-0xf3}" FunctionName="Component Control"
Interactive="0" ApplicationName="mmproc" VersionNumber="1" CommandID="6" MissingImage="0"
MetaJournal="00007FFF98789B98" IsCurrentVersion="1"
Variables="00007FFF987898F8"><Variable Type="String"
Name="jnlComponentControl.stComponentName" NDimensions="0" Override=""
OverrideVariable="">16 Zeiss RL Shutter</Variable><Variable Type="Double"
Name="jnlComponentControl.dPosition" NDimensions="0" Override=""
```

OverrideVariable="">0</Variable></FunctionEntry><FunctionEntry GUID="{0x79f510e4-0xe09c-0x11d3-0x93-0x9a-0x0-0x10-0x5a-0x4-0x2f-0x99}" FunctionName="Delay" Interactive="0" ApplicationName="journal" VersionNumber="1" CommandID="7" MissingImage="0" MetaJournal="00007FFF93605468" IsCurrentVersion="1" Variables="00007FFF936051C8"><Variable Type="Double" Name="DelayJNL.dpDelayTime" NDimensions="0" Override="" OverrideVariable="">30</Variable><Variable Type="Integer" Name="DelayJNL.nDelayUnits" NDimensions="0" Override="" OverrideVariable="">1</Variable></FunctionEntry><FunctionEntry GUID="{0x79f51114-0xe09c-0x11d3-0x93-0x9a-0x0-0x10-0x5a-0x4-0x2f-0x99}" FunctionName="Assign Variable" Interactive="0" ApplicationName="mmvar" VersionNumber="1" CommandID="8" MissingImage="0" MetaJournal="00007FFF9318A0A8" IsCurrentVersion="1" Variables="00007FFF93189E08"><Variable Type="ULong" Name="jnlAssign.cbAssignData" NDimensions="0" Override="" OverrideVariable="">40</Variable><Variable Type="UByte" Name="jnlAssign.byAssignData" NDimensions="1" Lower1="1" Upper1="40" Override="" OverrideVariable="">20 0 0 0 153 1 0 0 54 1 0 0 12 0 0 0 8 0 0 0 73 109 103 69 120 112 111 115 117 114 101 0 115 116 114 40 51 48 41 0 </Variable></FunctionEntry><FunctionEntry GUID="{0x79f511c0-0xe09c-0x11d3-0x93-0x9a-0x0-0x10-0x5a-0x4-0x2f-0x99}" FunctionName="Acquire Timelapse" Interactive="0" ApplicationName="tlapse" VersionNumber="1" CommandID="9" MissingImage="0" MetaJournal="00007FFF924C7B98" IsCurrentVersion="1" Variables="00007FFF924C78F8"><Variable Type="Single" Name="TimelapseJNL.fpTimeInterval" NDimensions="0" Override="" OverrideVariable="">0.01</Variable><Variable Type="Integer" Name="TimelapseJNL.nTimeIntervalType" NDimensions="0" Override="" OverrideVariable="">2</Variable><Variable Type="Single" Name="TimelapseJNL.fpDuration" NDimensions="0" Override="" OverrideVariable="">0.01</Variable><Variable Type="Integer" Name="TimelapseJNL.nDurationType" NDimensions="0" Override="" OverrideVariable="">2</Variable><Variable Type="Integer" Name="TimelapseJNL.nStorageType" NDimensions="0" Override="" OverrideVariable="">2</Variable><Variable Type="Image" Name="TimelapseJNL.im" NDimensions="0" Override="" OverrideVariable="">m 0 6 9 17 1 -1 -1 8 Untitled </Variable><Variable Type="Integer" Name="TimelapseJNL.nModifier" NDimensions="0" Override="" OverrideVariable="">17</Variable><Variable Type="String" Name="TimelapseJNL.stStorageFile" NDimensions="0" Override="" OverrideVariable="">0 </Variable><Variable Type="Long" Name="TimelapseJNL.lStartFrame" NDimensions="0" Override="" OverrideVariable="">1</Variable><Variable Type="String" Name="TimelapseJNL.stTimelapseJnl" NDimensions="0" Override="" OverrideVariable="">0 </Variable><Variable Type="Logical" Name="TimelapseJNL.bUpdateImage" NDimensions="0" Override="" OverrideVariable="">FALSE</Variable><Variable Type="Logical" Name="TimelapseJNL.bShowLive" NDimensions="0" Override="" OverrideVariable="">FALSE</Variable><Variable Type="Logical" Name="TimelapseJNL.bShowWarning" NDimensions="0" Override="" OverrideVariable="">FALSE</Variable><Variable Type="Logical" Name="TimelapseJNL.bAcquireZSeries" NDimensions="0" Override="" OverrideVariable="">FALSE</Variable><Variable Type="Logical" Name="TimelapseJNL.bPlanesSuperceed" NDimensions="0" Override="" OverrideVariable="">FALSE</Variable><Variable Type="Integer" Name="TimelapseJNL.cPlanes" NDimensions="0" Override="" OverrideVariable="">15</Variable><Variable Type="Double" Name="TimelapseJNL.dpZDistance" NDimensions="0" Override="" OverrideVariable="">0.4</Variable><Variable Type="Integer" Name="TimelapseJNL.nStartAt" NDimensions="0" Override="" OverrideVariable="">1</Variable><Variable Type="Integer" Name="TimelapseJNL.nMoveTo" NDimensions="0" Override="" OverrideVariable="">1</Variable><Variable Type="Integer" Name="TimelapseJNL.nAfter" NDimensions="0" Override="" OverrideVariable="">5</Variable><Variable Type="String" Name="TimelapseJNL.stZSeriesJnl" NDimensions="0" Override="" OverrideVariable="">0 </Variable><Variable Type="String" Name="TimelapseJNL.stShutterName" NDimensions="0" Override="" OverrideVariable="">0 </Variable></FunctionEntry><FunctionEntry GUID="{0x3cef1e29-0xe09c-0x11d3-0x93-0x9a-0x0-0x10-0x5a-0x4-0x2f-0x99}" FunctionName="Acquire Image" Interactive="0" ApplicationName="mmproc" VersionNumber="19980317" CommandID="10" MissingImage="0" Disabled="1" MetaJournal="00007FFF98757778" IsCurrentVersion="1" Variables="00007FFF987574D8"><Variable Type="Image" Name="jnlAcquire.destAcquire" NDimensions="0" Override="" OverrideVariable="">m   0 6 9 17 1 -1 -1 8 Untitled </Variable><Variable Type="Image" Name="jnlAcquire.shadingImage" NDimensions="0" Override="" OverrideVariable="">m 1 2 9 2 1 -1 -1 8 Untitled </Variable><Variable Type="Logical" Name="jnlAcquire.bAcquireSubtraction" NDimensions="0" Override="" OverrideVariable="">FALSE</Variable><Variable Type="Logical" Name="jnlAcquire.bAcquireDivisorField" NDimensions="0" Override="" OverrideVariable="">FALSE</Variable><Variable Type="Logical" Name="jnlAcquire.bAcquireShowLive" NDimensions="0" Override=""

OverrideVariable="">TRUE</Variable><Variable Type="Integer"
Name="jnlAcquire.nAcquireAverage" NDimensions="0" Override=""
OverrideVariable="">1</Variable><Variable Type="Integer"
Name="jnlAcquire.nAcquireDivisor" NDimensions="0" Override=""
OverrideVariable="">1</Variable><Variable Type="UInteger"
Name="jnlAcquire.nAcquireOffset" NDimensions="0" Override=""
OverrideVariable="">0</Variable><Variable Type="Logical" Name="jnlAcquire.bBeep"
NDimensions="0" Override="" OverrideVariable="">FALSE</Variable><Variable Type="Logical"
Name="jnlAcquire.bRecordOnly" NDimensions="0" Override=""
OverrideVariable="">FALSE</Variable><Variable Type="String"
Name="jnlAcquire.stShutterName" NDimensions="0" Override="" OverrideVariable="">0
</Variable></FunctionEntry><FunctionEntry GUID="{0x79f51114-0xe09c-0x11d3-0x93-0x9a-0x0-
0x10-0x5a-0x4-0x2f-0x99}" FunctionName="Assign Variable" ApplicationName="mmvar"
Interactive="0" VersionNumber="1" CommandID="11" MissingImage="0" Disabled="1"
MetaJournal="00007FFF9318A0A8" IsCurrentVersion="1"
Variables="00007FFF93189E08"><Variable Type="ULong" Name="jnlAssign.cbAssignData"
NDimensions="0" Override="" OverrideVariable="">107</Variable><Variable Type="UByte"
Name="jnlAssign.byAssignData" NDimensions="1" Lower1="1" Upper1="107" Override=""
OverrideVariable="">20 0 0 0 153 1 0 0 54 1 0 0 6 0 0 0 81 0 0 0 105 78 97 109 101 0 40
73 108 108 117 109 105 110 97 116 105 111 110 95 97 99 113 117 105 114 101 32 43 34 95 34
43 80 114 111 98 101 95 65 99 43 34 95 34 43 32 73 109 103 69 120 112 111 115 117 114 101
43 116 105 109 101 117 110 105 116 115 32 43 34 95 34 43 34 105 109 97 103 101 34 43 34
95 34 41 0 </Variable></FunctionEntry><AssignVariableEntry
VariableName="ImageInfo.PlaneIllumSetting" Expression="Illumination_acquire"
Disabled="1"/><AssignVariableEntry VariableName="Image.IllumSetting"
Expression="Illumination_acquire" Disabled="1"/><FunctionEntry GUID="{0x3cef1eb0-0xe09c-
0x11d3-0x93-0x9a-0x0-0x10-0x5a-0x4-0x2f-0x99}" FunctionName="Setup Sequential File Names"
ApplicationName="mmproc" Interactive="0" VersionNumber="20060520" CommandID="12"
MissingImage="0" Disabled="1" MetaJournal="00007FFF98874FE8" IsCurrentVersion="1"
Variables="00007FFF98874D48"><Variable Type="String" Name="uniqueSetupJNL.baseName"
NDimensions="0" Override="Variable" OverrideVariable="iName">5 trans</Variable><Variable
Type="String" Name="uniqueSetupJNL.stPath" NDimensions="0" Override="Variable"
OverrideVariable="save_driver+save_base_dirc+ Illumination_acquire+"\TRF1\"">43
C:\Users\Kim Lab\Ellison Project\New images</Variable><Variable Type="Long"
Name="uniqueSetupJNL.number" NDimensions="0" Override=""
OverrideVariable="">1</Variable><Variable Type="Integer" Name="uniqueSetupJNL.imageSave"
NDimensions="0" Override="" OverrideVariable="">3</Variable><Variable Type="Logical"
Name="uniqueSetupJNL.bChangeNameOnSave" NDimensions="0" Override=""
OverrideVariable="">TRUE</Variable><Variable Type="Integer" Name="uniqueSetupJNL.nWidth"
NDimensions="0" Override="" OverrideVariable="">2</Variable><Variable Type="String"
Name="uniqueSetupJNL.stImageType" NDimensions="0" Override="" OverrideVariable="">4
.tif</Variable></FunctionEntry><FunctionEntry GUID="{0x3cef1eb1-0xe09c-0x11d3-0x93-0x9a-
0x0-0x10-0x5a-0x4-0x2f-0x99}" FunctionName="Save Using Sequential File Name"
Interactive="0" ApplicationName="mmproc" VersionNumber="19940603" CommandID="13"
MissingImage="0" Disabled="1" MetaJournal="00007FFF98875748" IsCurrentVersion="1"
Variables="00007FFF988754A8"><Variable Type="Image" Name="uniqueSaveJNL.imSave"
NDimensions="0" Override="" OverrideVariable="">m 1 3 9 0 1 -1 -1 8 Untitled
</Variable></FunctionEntry><FunctionEntry GUID="{0x3cef1e54-0xe09c-0x11d3-0x93-0x9a-0x0-
0x10-0x5a-0x4-0x2f-0x99}" FunctionName="Close" Interactive="0" ApplicationName="mmproc"
VersionNumber="1" CommandID="14" MissingImage="0" Disabled="1"
MetaJournal="00007FFF98794718" IsCurrentVersion="1"
Variables="00007FFF98794478"><Variable Type="Image" Name="jnlCloseImage.im"
NDimensions="0" Override="" OverrideVariable="">m   1 3 9 0 1 -1 -1 8 Untitled
</Variable><Variable Type="Logical" Name="jnlCloseImage.bSaveIt" NDimensions="0"
Override="" OverrideVariable="">FALSE</Variable></FunctionEntry><FunctionEntry
GUID="{0x79f51114-0xe09c-0x11d3-0x93-0x9a-0x0-0x10-0x5a-0x4-0x2f-0x99}"
FunctionName="Assign Variable" Interactive="0" ApplicationName="mmvar" VersionNumber="1"
CommandID="15" MissingImage="0" Disabled="1" MetaJournal="00007FFF9318A0A8"
IsCurrentVersion="1" Variables="00007FFF93189E08"><Variable Type="ULong"
Name="jnlAssign.cbAssignData" NDimensions="0" Override=""
OverrideVariable="">40</Variable><Variable Type="UByte" Name="jnlAssign.byAssignData"
NDimensions="1" Lower1="1" Upper1="40" Override="" OverrideVariable="">20 0 0 0 153 1 0 0
54 1 0 0 12 0 0 0 8 0 0 0 73 109 103 69 120 112 111 115 117 114 101 0 115 116 114 40 51
48 41 0 </Variable></FunctionEntry><FunctionEntry GUID="{0x3cef1e29-0xe09c-0x11d3-0x93-
0x9a-0x0-0x10-0x5a-0x4-0x2f-0x99}" FunctionName="Acquire Image" Interactive="0"
ApplicationName="mmproc" VersionNumber="19980317" CommandID="16" MissingImage="0"
Disabled="1" MetaJournal="00007FFF98757778" IsCurrentVersion="1"
Variables="00007FFF987574D8"><Variable Type="Image" Name="jnlAcquire.destAcquire"

NDimensions="0" Override="" OverrideVariable="">m   0 6 9 17 1 -1 -1 8 Untitled
</Variable><Variable Type="Image" Name="jnlAcquire.shadingImage" NDimensions="0"
Override="" OverrideVariable="">m 1 2 9 2 1 -1 -1 8 Untitled </Variable><Variable
Type="Logical" Name="jnlAcquire.bAcquireSubtraction" NDimensions="0" Override=""
OverrideVariable="">FALSE</Variable><Variable Type="Logical"
Name="jnlAcquire.bAcquireDivisorField" NDimensions="0" Override=""
OverrideVariable="">FALSE</Variable><Variable Type="Logical"
Name="jnlAcquire.bAcquireShowLive" NDimensions="0" Override=""
OverrideVariable="">TRUE</Variable><Variable Type="Integer"
Name="jnlAcquire.nAcquireAverage" NDimensions="0" Override=""
OverrideVariable="">1</Variable><Variable Type="Integer"
Name="jnlAcquire.nAcquireDivisor" NDimensions="0" Override=""
OverrideVariable="">1</Variable><Variable Type="UInteger"
Name="jnlAcquire.nAcquireOffset" NDimensions="0" Override=""
OverrideVariable="">0</Variable><Variable Type="Logical" Name="jnlAcquire.bBeep"
NDimensions="0" Override="" OverrideVariable="">FALSE</Variable><Variable Type="Logical"
Name="jnlAcquire.bRecordOnly" NDimensions="0" Override=""
OverrideVariable="">FALSE</Variable><Variable Type="String"
Name="jnlAcquire.stShutterName" NDimensions="0" Override="" OverrideVariable="">0
</Variable></FunctionEntry><FunctionEntry GUID="{0x79f51114-0xe09c-0x11d3-0x93-0x9a-0x0-
0x10-0x5a-0x4-0x2f-0x99}" FunctionName="Assign Variable" ApplicationName="mmvar"
Disabled="0" Interactive="0" VersionNumber="1" CommandID="17" MissingImage="0"
MetaJournal="00007FFF9318A0A8" IsCurrentVersion="1"
Variables="00007FFF93189E08"><Variable Type="ULong" Name="jnlAssign.cbAssignData"
NDimensions="0" Override="" OverrideVariable="">107</Variable><Variable Type="UByte"
Name="jnlAssign.byAssignData" NDimensions="1" Lower1="1" Upper1="107" Override=""
OverrideVariable="">20 0 0 0 153 1 0 0 54 1 0 0 6 0 0 0 81 0 0 0 105 78 97 109 101 0 40
73 108 108 117 109 105 110 97 116 105 111 110 95 97 99 113 117 105 114 101 32 43 34 95 34
43 80 114 111 98 101 95 65 99 43 34 95 34 43 32 73 109 103 69 120 112 111 115 117 114 101
43 116 105 109 101 117 110 105 116 115 32 43 34 95 34 43 34 105 109 97 103 101 34 43 34
95 34 41 0 </Variable></FunctionEntry><AssignVariableEntry
VariableName="ImageInfo.PlaneIllumSetting"
Expression="Illumination_acquire"/><AssignVariableEntry VariableName="Image.IllumSetting"
Expression="Illumination_acquire"/><FunctionEntry GUID="{0x3cef1eb0-0xe09c-0x11d3-0x93-
0x9a-0x0-0x10-0x5a-0x4-0x2f-0x99}" FunctionName="Setup Sequential File Names"
ApplicationName="mmproc" Disabled="0" Interactive="0" VersionNumber="20060520"
CommandID="18" MissingImage="0" MetaJournal="00007FFF98874FE8" IsCurrentVersion="1"
Variables="00007FFF98874D48"><Variable Type="String" Name="uniqueSetupJNL.baseName"
NDimensions="0" Override="Variable" OverrideVariable="iName">5 trans</Variable><Variable
Type="String" Name="uniqueSetupJNL.stPath" NDimensions="0" Override="Variable"
OverrideVariable="save_driver+save_base_dirc+ Illumination_acquire+"\TRF\"">43
C:\Users\Kim Lab\Ellison Project\New images</Variable><Variable Type="Long"
Name="uniqueSetupJNL.number" NDimensions="0" Override=""
OverrideVariable="">1</Variable><Variable Type="Integer" Name="uniqueSetupJNL.imageSave"
NDimensions="0" Override="" OverrideVariable="">3</Variable><Variable Type="Logical"
Name="uniqueSetupJNL.bChangeNameOnSave" NDimensions="0" Override=""
OverrideVariable="">TRUE</Variable><Variable Type="Integer" Name="uniqueSetupJNL.nWidth"
NDimensions="0" Override="" OverrideVariable="">2</Variable><Variable Type="String"
Name="uniqueSetupJNL.stImageType" NDimensions="0" Override="" OverrideVariable="">4
.tif</Variable></FunctionEntry><FunctionEntry GUID="{0x3cef1eb1-0xe09c-0x11d3-0x93-0x9a-
0x0-0x10-0x5a-0x4-0x2f-0x99}" FunctionName="Save Using Sequential File Name"
Interactive="0" ApplicationName="mmproc" VersionNumber="19940603" CommandID="19"
MissingImage="0" MetaJournal="00007FFF98875748" IsCurrentVersion="1"
Variables="00007FFF988754A8"><Variable Type="Image" Name="uniqueSaveJNL.imSave"
NDimensions="0" Override="" OverrideVariable="">m 1 3 9 0 1 -1 -1 8 Untitled
</Variable></FunctionEntry><FunctionEntry GUID="{0x3cef1e54-0xe09c-0x11d3-0x93-0x9a-0x0-
0x10-0x5a-0x4-0x2f-0x99}" FunctionName="Close" Interactive="0" ApplicationName="mmproc"
VersionNumber="1" CommandID="20" MissingImage="0" MetaJournal="00007FFF98794718"
IsCurrentVersion="1" Variables="00007FFF98794478"><Variable Type="Image"
Name="jnlCloseImage.im" NDimensions="0" Override="" OverrideVariable="">m 1 3 9 0 1 -1 -1
8 Untitled </Variable><Variable Type="Logical" Name="jnlCloseImage.bSaveIt"
NDimensions="0" Override=""
OverrideVariable="">FALSE</Variable></FunctionEntry></CodeBlock><CodeBlock
Condition="false"><AssignVariableEntry Disabled="0" VariableName="Illumination_acquire"
Expression="Illumination2"/><AssignVariableEntry VariableName="CondExpTime_Ac"
Expression="Cond2ExpTime"/><AssignVariableEntry Disabled="0" VariableName="Probe_Ac"
Expression="Dye_2"/><AssignVariableEntry Disabled="0" VariableName="SelectDirectory.Path"
Expression="saving_base_directory+Illumination2+"\""/><FunctionEntry

GUID="{0x79f510e8-0xe09c-0x11d3-0x93-0x9a-0x0-0x10-0x5a-0x4-0x2f-0x99}" FunctionName="Run Journal" Interactive="0" ApplicationName="journal" VersionNumber="1" CommandID="21" MetaJournal="00007FFF93606AC8" IsCurrentVersion="1" Variables="00007FFF93606828" MissingImage="0"><Variable Type="String" Name="ExecuteJournalJNL.stExecuteJournal" NDimensions="0" Override="" OverrideVariable="">56 C:\MM\app\mmproc\journals\Chamber_Acquire_Imaging_V1.jnl</Variable></FunctionEntry></CodeBlock></IfThenElseEntry><IfThenElseEntry Expression="NumofDyes > 2"><CodeBlock Condition="true"><AssignVariableEntry Disabled="0" VariableName="Illumination_acquire" Expression="Illumination3"/><AssignVariableEntry VariableName="CondExpTime_Ac" Expression="Cond3ExpTime"/><AssignVariableEntry Disabled="0" VariableName="Probe_Ac" Expression="Dye_3"/><AssignVariableEntry Disabled="0" VariableName="SelectDirectory.Path" Expression="saving_base_directory+Illumination3+"\""/><FunctionEntry GUID="{0x79f510e8-0xe09c-0x11d3-0x93-0x9a-0x0-0x10-0x5a-0x4-0x2f-0x99}" FunctionName="Run Journal" Interactive="0" ApplicationName="journal" VersionNumber="1" CommandID="22" MetaJournal="00007FFF93606AC8" IsCurrentVersion="1" Variables="00007FFF93606828" MissingImage="0"><Variable Type="String" Name="ExecuteJournalJNL.stExecuteJournal" NDimensions="0" Override="" OverrideVariable="">56 C:\MM\app\mmproc\journals\Chamber_Acquire_Imaging_V1.jnl</Variable></FunctionEntry><IfThenElseEntry Expression="NumofDyes > 3"><CodeBlock Condition="true"><AssignVariableEntry Disabled="0" VariableName="Illumination_acquire" Expression="Illumination4"/><AssignVariableEntry VariableName="CondExpTime_Ac" Expression="Cond4ExpTime"/><AssignVariableEntry Disabled="0" VariableName="Probe_Ac" Expression="Dye_4"/><AssignVariableEntry Disabled="0" VariableName="SelectDirectory.Path" Expression="saving_base_directory+Illumination4+"\""/><FunctionEntry GUID="{0x79f510e8-0xe09c-0x11d3-0x93-0x9a-0x0-0x10-0x5a-0x4-0x2f-0x99}" FunctionName="Run Journal" Interactive="0" ApplicationName="journal" VersionNumber="1" CommandID="23" MetaJournal="00007FFF93606AC8" IsCurrentVersion="1" Variables="00007FFF93606828" MissingImage="0"><Variable Type="String" Name="ExecuteJournalJNL.stExecuteJournal" NDimensions="0" Override="" OverrideVariable="">56 C:\MM\app\mmproc\journals\Chamber_Acquire_Imaging_V1.jnl</Variable></FunctionEntry></CodeBlock><CodeBlock Condition="false"/></IfThenElseEntry></CodeBlock><CodeBlock Condition="false"/></IfThenElseEntry></CodeBlock><CodeBlock Condition="false"/></IfThenElseEntry></CodeBlock><CodeBlock Condition="false"><FunctionEntry GUID="{0x79f510e1-0xe09c-0x11d3-0x93-0x9a-0x0-0x10-0x5a-0x4-0x2f-0x99}" FunctionName="Show Message and Wait" Interactive="0" ApplicationName="journal" VersionNumber="1" CommandID="24" MetaJournal="00007FFF936046F8" IsCurrentVersion="1" Variables="00007FFF93604458" MissingImage="0"><Variable Type="Integer" Name="ShowMessageJNL.nDisplay" NDimensions="0" Override="" OverrideVariable="">1</Variable><Variable Type="Integer" Name="ShowMessageJNL.iTimeout" NDimensions="0" Override="" OverrideVariable="">31</Variable><Variable Type="Logical" Name="ShowMessageJNL.bUseTimeout" NDimensions="0" Override="" OverrideVariable="">TRUE</Variable><Variable Type="String" Name="ShowMessageJNL.stTitle" NDimensions="0" Override="" OverrideVariable="">27 Please Run Pre Z-stack Prep</Variable><Variable Type="String" Name="ShowMessageJNL.stMessage" NDimensions="0" Override="" OverrideVariable="">101 Make sure you run the journal 'Pre Z-stack Prep' to set up settings before running Z-stack Acquire JR</Variable><Variable Type="Integer" Name="ShowMessageJNL.msgX" NDimensions="0" Override="" OverrideVariable="">457</Variable><Variable Type="Integer" Name="ShowMessageJNL.msgY" NDimensions="0" Override="" OverrideVariable="">188</Variable></FunctionEntry></CodeBlock></IfThenElseEntry></CodeBlock></Journal>

Chamber_Imaging_Manual_Start.JNL

<Journal><Description>New Journal</Description><Version VersionNumber="2.4"/><CodeBlock><IfThenElseEntry Expression="VariableExists(device_length)"><CodeBlock Condition="true"><FunctionEntry GUID="{0x3cef1e1a-0xe09c-0x11d3-0x93-0x9a-0x0-0x10-0x5a-0x4-0x2f-0x99}" FunctionName="Select Illumination" ApplicationName="mmproc" VersionNumber="1" Disabled="0" Interactive="0" MissingImage="0" CommandID="1" MetaJournal="00007FF855B6D610" IsCurrentVersion="1" Variables="00007FF855B6D388"><Variable Type="Logical" Name="jnlSelectIllum.bUseLegacyDelay" NDimensions="0" Override="" OverrideVariable="">FALSE</Variable><Variable Type="Integer" Name="jnlSelectIllum.cMillisecDelay" NDimensions="0" Override="" OverrideVariable="">100</Variable><Variable Type="String" Name="jnlSelectIllum.stSetting" NDimensions="0" Override="Variable" OverrideVariable="Illumination">4

DAPI</Variable></FunctionEntry><FunctionEntry VersionNumber="1" GUID="{0x7e1a65f0-0x31b5-0x11d4-0x99-0xfa-0x0-0x10-0x4b-0x98-0xde-0xde}" FunctionName="Acquire - Start Live" ApplicationName="acquire" Interactive="0" ExecuteMode="1" MissingImage="0" CommandID="2" MetaJournal="00007FF86846C920" IsCurrentVersion="1" Variables="00007FF86846C688"></FunctionEntry><PromptUserEntry VariableName="Adjustment2" PromptType="YesNo" TitleText="Re-enter the values again?" Constrain="1" PromptText="Would you llike to re adjust for the values?" DialogXPos="884" DialogYPos="378" Min="4.60877e-312" Max="4.60877e-312"/><IfThenElseEntry Expression="Adjustment2 = "Y""><CodeBlock Condition="true"><FunctionEntry GUID="{0x79f510e1-0xe09c-0x11d3-0x93-0x9a-0x0-0x10-0x5a-0x4-0x2f-0x99}" FunctionName="Show Message and Wait" Interactive="0" ApplicationName="journal" VersionNumber="1" MissingImage="0" CommandID="3" MetaJournal="00007FF84EA346F8" IsCurrentVersion="1" Variables="00007FF84EA34458"><Variable Type="Integer" Name="ShowMessageJNL.nDisplay" NDimensions="0" Override="" OverrideVariable="">3</Variable><Variable Type="Integer" Name="ShowMessageJNL.iTimeout" NDimensions="0" Override="" OverrideVariable="">26</Variable><Variable Type="Logical" Name="ShowMessageJNL.bUseTimeout" NDimensions="0" Override="" OverrideVariable="">FALSE</Variable><Variable Type="String" Name="ShowMessageJNL.stTitle" NDimensions="0" Override="" OverrideVariable="">38 Find Upper-Right hand corner of device</Variable><Variable Type="String" Name="ShowMessageJNL.stMessage" NDimensions="0" Override="" OverrideVariable="">138 Please find the Upper-Right hand corner of the device (it will be the Lower-Left corner in the software). Please 'Continue' when finished.</Variable><Variable Type="Integer" Name="ShowMessageJNL.msgX" NDimensions="0" Override="" OverrideVariable="">168</Variable><Variable Type="Integer" Name="ShowMessageJNL.msgY" NDimensions="0" Override="" OverrideVariable="">190</Variable></FunctionEntry><AssignVariableEntry VariableName="pos_X_1" Expression="Device.Stage.XPosition"/><AssignVariableEntry VariableName="pos_Y_1" Expression="Device.Stage.YPosition"/><AssignVariableEntry VariableName="pos_Z_1" Expression="Device.Focus.CurPos"/><FunctionEntry GUID="{0x79f510e8-0xe09c-0x11d3-0x93-0x9a-0x0-0x10-0x5a-0x4-0x2f-0x99}" FunctionName="Run Journal" Interactive="0" ApplicationName="journal" VersionNumber="1" MissingImage="0" CommandID="4" MetaJournal="00007FF84EA36AC8" IsCurrentVersion="1" Variables="00007FF84EA36828"><Variable Type="String" Name="ExecuteJournalJNL.stExecuteJournal" NDimensions="0" Override="" OverrideVariable="">55 C:\MM\app\mmproc\journals\Chamber_Z_tilt_correction.jnl</Variable></FunctionEntry><FunctionEntry VersionNumber="1" GUID="{0x7e1a65f1-0x31b5-0x11d4-0x99-0xf9-0x0-0x10-0x4b-0x98-0xde-0xde}" FunctionName="Acquire - Stop Live" ApplicationName="acquire" Interactive="0" ExecuteMode="1" MissingImage="0" CommandID="5" MetaJournal="00007FF86846CD70" IsCurrentVersion="1" Variables="00007FF86846CAD8"></FunctionEntry></CodeBlock><CodeBlock Condition="false"/></IfThenElseEntry><PromptUserEntry VariableName="analysis_instant" PromptType="YesNo" TitleText="Start analysis after imaging?" Constrain="0" PromptText="Do you want to start the analysis immediately after imaging?" DialogXPos="0" DialogYPos="0"/><PromptUserEntry VariableName="analysis_loopnum" PromptType="Number" TitleText="What is the loop number?" Constrain="0" PromptText="What is the loop number for the analysis?" DialogXPos="0" DialogYPos="0"/><PromptUserEntry VariableName="analysis_endnum" PromptType="Number" TitleText="What is the end number of image?" Constrain="0" PromptText="What is the end number of image?" DialogXPos="0" DialogYPos="0"/><AssignVariableEntry VariableName="loop_number" Expression="0"/><AssignVariableEntry VariableName="total_position_num" Expression="(num_chambers_sets+1)*(num_chambers+1)*(length_steps+1)"/><FunctionEntry GUID="{0x79f5110a-0xe09c-0x11d3-0x93-0x9a-0x0-0x10-0x5a-0x4-0x2f-0x99}" FunctionName="Loop a Journal" Interactive="0" ApplicationName="journal" VersionNumber="1" MissingImage="0" CommandID="6" MetaJournal="00007FF84EA427E8" IsCurrentVersion="1" Variables="00007FF84EA42548"><Variable Type="Integer" Name="jnlLoop.nLoops" NDimensions="0" Override="" OverrideVariable="">2</Variable><Variable Type="Logical" Name="jnlLoop.bConfirm" NDimensions="0" Override="" OverrideVariable="">FALSE</Variable><Variable Type="String" Name="jnlLoop.stJournal" NDimensions="0" Override="None" OverrideVariable="Journal Name">63 C:\MM\app\mmproc\journals\Chamber_Imaging_Positions_Capture.JNL</Variable><Variable Type="Logical" Name="jnlLoop.bUseInterval" NDimensions="0" Override="" OverrideVariable="">FALSE</Variable><Variable Type="Double" Name="jnlLoop.dpInterval" NDimensions="0" Override="" OverrideVariable="">2</Variable><Variable Type="Integer" Name="jnlLoop.nIntervalUnits" NDimensions="0" Override="" OverrideVariable="">3</Variable><Variable Type="Logical" Name="jnlLoop.bUsePrompt" NDimensions="0" Override="" OverrideVariable="">TRUE</Variable><Variable Type="String" Name="jnlLoop.stPrompt" NDimensions="0" Override="" OverrideVariable="">48 How many times do you want to image the chamber?</Variable><Variable Type="Integer"

Name="jnlLoop.nCurLoop" NDimensions="0" Override=""
OverrideVariable="">0</Variable><Variable Type="Long" Name="jnlLoop.lTime"
NDimensions="0" Override="" OverrideVariable="">0</Variable><Variable Type="Long"
Name="jnlLoop.lLastUpdate" NDimensions="0" Override=""
OverrideVariable="">0</Variable></FunctionEntry><FunctionEntry GUID="{0x3cef1e92-0xe09c-
0x11d3-0x93-0x9a-0x0-0x10-0x5a-0x4-0x2f-0x99}" FunctionName="Move Stage to Absolute
Position" Interactive="0" ApplicationName="mmproc" VersionNumber="1" MissingImage="0"
CommandID="7" MetaJournal="00007FF855C8FE68" IsCurrentVersion="1"
Variables="00007FF855C8FBC8"><Variable Type="Double" Name="jnlMoveStageAbs.dpX"
NDimensions="0" Override="Variable" OverrideVariable="pos_X_1">-
3697.3</Variable><Variable Type="Double" Name="jnlMoveStageAbs.dpY" NDimensions="0"
Override="Variable" OverrideVariable="pos_Y_1">-4026.8</Variable><Variable Type="Double"
Name="jnlMoveStageAbs.dpZ" NDimensions="0" Override="Variable"
OverrideVariable="pos_Z_1">18289.4</Variable></FunctionEntry><IfThenElseEntry
Expression="analysis_instant = "Y""><CodeBlock Condition="true"><FunctionEntry
GUID="{0x79f510e8-0xe09c-0x11d3-0x93-0x9a-0x0-0x10-0x5a-0x4-0x2f-0x99}" FunctionName="Run
Journal" Interactive="0" ApplicationName="journal" VersionNumber="1" MissingImage="0"
CommandID="8" MetaJournal="00007FF84EA36AC8" IsCurrentVersion="1"
Variables="00007FF84EA36828"><Variable Type="String"
Name="ExecuteJournalJNL.stExecuteJournal" NDimensions="0" Override=""
OverrideVariable="">62
C:\MM\app\mmproc\journals\Chamber_analysis_script_analysis.jnl</Variable></FunctionEntry>
</CodeBlock><CodeBlock Condition="false"/></IfThenElseEntry></CodeBlock><CodeBlock
Condition="false"><FunctionEntry GUID="{0x79f510e8-0xe09c-0x11d3-0x93-0x9a-0x0-0x10-0x5a-
0x4-0x2f-0x99}" FunctionName="Run Journal" Interactive="0" ApplicationName="journal"
VersionNumber="1" MissingImage="0" CommandID="9" MetaJournal="00007FF84EA36AC8"
IsCurrentVersion="1" Variables="00007FF84EA36828"><Variable Type="String"
Name="ExecuteJournalJNL.stExecuteJournal" NDimensions="0" Override=""
OverrideVariable="">67
C:\MM\app\mmproc\journals\Chamber_Imaging_Setup_Complete_Script.jnl</Variable></FunctionE
ntry></CodeBlock></IfThenElseEntry></CodeBlock></Journal>

Chamber_Imaging_Positions.JNL

<Journal><Description>New Journal</Description><Version
VersionNumber="2.4"/><CodeBlock><AssignVariableEntry VariableName="camera_length"
Expression="1331.2"/><PromptUserEntry VariableName="device_length" PromptType="Number"
TitleText="Enter the length of the device (down one of the chambers) (mm)" Constrain="1"
PromptText="Enter the length of the device. This is the legnth of one of the chambers in
milimeters (max 44.4082)" DialogXPos="743" DialogYPos="322" Min="2.6624"
Max="44.4082"/><AssignVariableEntry VariableName="length_steps" Expression="CEILING(
(device_length*1000)/camera_length)"/><PromptUserEntry VariableName="num_chambers"
PromptType="Number" TitleText="Please enter the number of chambers" Constrain="1"
PromptText="Enter the number of chambers you wish to image." DialogXPos="743"
DialogYPos="322" Min="1" Max="25"/><AssignVariableEntry VariableName="num_chambers"
Expression="num_chambers - 1"/><PromptUserEntry VariableName="between_chambers"
PromptType="Number" TitleText="Please enter distance between chambers" Constrain="1"
PromptText="Enter distance between chambers in milimeters. (max 12.2269mm)"
DialogXPos="743" DialogYPos="322" Min="2.6624" Max="12.2269"/><FunctionEntry
GUID="{0x79f510e1-0xe09c-0x11d3-0x93-0x9a-0x0-0x10-0x5a-0x4-0x2f-0x99}"
FunctionName="Show Message and Wait" Interactive="0" ApplicationName="journal"
VersionNumber="1" MissingImage="0" CommandID="1" MetaJournal="000007FEC97246F8"
IsCurrentVersion="1" Variables="000007FEC9724458"><Variable Type="Integer"
Name="ShowMessageJNL.nDisplay" NDimensions="0" Override=""
OverrideVariable="">3</Variable><Variable Type="Integer" Name="ShowMessageJNL.iTimeout"
NDimensions="0" Override="" OverrideVariable="">26</Variable><Variable Type="Logical"
Name="ShowMessageJNL.bUseTimeout" NDimensions="0" Override=""
OverrideVariable="">FALSE</Variable><Variable Type="String" Name="ShowMessageJNL.stTitle"
NDimensions="0" Override="" OverrideVariable="">38 Find Upper-Right hand corner of
device</Variable><Variable Type="String" Name="ShowMessageJNL.stMessage" NDimensions="0"
Override="" OverrideVariable="">138 Please find the Upper-Right hand corner of the device
(it will be the Lower-Left corner in the software). Please 'Continue' when
finished.</Variable><Variable Type="Integer" Name="ShowMessageJNL.msgX" NDimensions="0"
Override="" OverrideVariable="">168</Variable><Variable Type="Integer"
Name="ShowMessageJNL.msgY" NDimensions="0" Override=""
OverrideVariable="">190</Variable></FunctionEntry><AssignVariableEntry
VariableName="pos_X_1" Expression="Device.Stage.XPosition"/><AssignVariableEntry

VariableName="pos_Y_1" Expression="Device.Stage.YPosition"/><AssignVariableEntry
VariableName="pos_Z_1" Expression="Device.Focus.CurPos"/><ForNextLoopEntry
LoopVariable="in_chamber_pos" StartValue="0" EndValue="length_steps" StepValue="1"
Disabled="1"><CodeBlock><AssignVariableEntry VariableName="pos_X_curr"
Expression="pos_X_1 - in_chamber_pos*camera_length" Disabled="1"/><AssignVariableEntry
VariableName="pos_Y_curr" Expression="pos_Y_1" Disabled="1"/><AssignVariableEntry
VariableName="pos_Z_curr" Expression="pos_Z_1" Disabled="1"/><FunctionEntry
GUID="{0x3cef1e92-0xe09c-0x11d3-0x93-0x9a-0x0-0x10-0x5a-0x4-0x2f-0x99}"
FunctionName="Move Stage to Absolute Position" Interactive="0" ApplicationName="mmproc"
VersionNumber="1" MissingImage="0" Disabled="1" CommandID="2"
MetaJournal="000007FEDC71FE68" IsCurrentVersion="1"
Variables="000007FEDC71FBC8"><Variable Type="Double" Name="jnlMoveStageAbs.dpX"
NDimensions="0" Override="Variable" OverrideVariable="pos_X_curr">-
3697.3</Variable><Variable Type="Double" Name="jnlMoveStageAbs.dpY" NDimensions="0"
Override="Variable" OverrideVariable="pos_Y_curr">-4026.8</Variable><Variable
Type="Double" Name="jnlMoveStageAbs.dpZ" NDimensions="0" Override="Variable"
OverrideVariable="pos_Z_curr">18289.4</Variable></FunctionEntry><AssignVariableEntry
VariableName="Device.Focus.CurPos" Expression="pos_Z_curr"
Disabled="1"/><AssignVariableEntry VariableName="Device.Focus.Bottom"
Expression="Device.Focus.CurPos" Disabled="1"/><AssignVariableEntry
VariableName="Component.Zeiss_Filter_Cube.PositionLabel" Expression=""GFP""
Disabled="1"/><FunctionEntry GUID="{0x281ef4a0-0x2b37-0x11d4-0x98-0x53-0x0-0xe0-0x18-
0x90-0x87-0x5b}" FunctionName="Acquire" Interactive="0" ApplicationName="acquire"
VersionNumber="20000127" MissingImage="0" Disabled="1" CommandID="3"
MetaJournal="000007FEC9F2BC08" IsCurrentVersion="1"
Variables="000007FEC9F2B968"><Variable Type="Image" Name="jnlAcquire.imDest"
NDimensions="0" Override="" OverrideVariable="">m   0 6 9 17 1 -1 -1 8 Untitled
</Variable></FunctionEntry><AssignVariableEntry VariableName="Camera.Digital.Exposure"
Expression="50" Disabled="1"/><FunctionEntry GUID="{0x79f51061-0xe09c-0x11d3-0x93-0x9a-
0x0-0x10-0x5a-0x4-0x2f-0x99}" FunctionName="Acquire Z Series" ApplicationName="3d"
VersionNumber="20020412" Interactive="0" MissingImage="0" Disabled="1" CommandID="4"
MetaJournal="000007FECA0AA498" IsCurrentVersion="1"
Variables="000007FECA0AA1F8"><Variable Type="Logical" Name="jnlZSeries.bPlanesSuperceed"
NDimensions="0" Override="None" OverrideVariable="Step Size Based On Number Of
Planes">TRUE</Variable><Variable Type="Double" Name="jnlZSeries.dpZDistance"
NDimensions="0" Override="None" OverrideVariable="Step Size">15</Variable><Variable
Type="Integer" Name="jnlZSeries.cPlanes" NDimensions="0" Override="None"
OverrideVariable="Number Of Planes">3</Variable><Variable Type="Integer"
Name="jnlZSeries.nStartAt" NDimensions="0" Override="None" OverrideVariable="Start
At">1</Variable><Variable Type="Integer" Name="jnlZSeries.nMoveTo" NDimensions="0"
Override="None" OverrideVariable="Move To">1</Variable><Variable Type="Integer"
Name="jnlZSeries.nAfter" NDimensions="0" Override="None"
OverrideVariable="After">4</Variable><Variable Type="String" Name="jnlZSeries.stJournal"
NDimensions="0" Override="" OverrideVariable="">0 </Variable><Variable Type="String"
Name="jnlZSeries.stShutterName" NDimensions="0" Override="" OverrideVariable="">3
GFP</Variable><Variable Type="Integer" Name="jnlZSeries.nStorageType" NDimensions="0"
Override="" OverrideVariable="">2</Variable><Variable Type="Image"
Name="jnlZSeries.imDest" NDimensions="0" Override="" OverrideVariable="">m   0 6 9 17 1
-1 -1 8 Untitled </Variable><Variable Type="Integer" Name="jnlZSeries.nModifier"
NDimensions="0" Override="" OverrideVariable="">17</Variable><Variable Type="Long"
Name="jnlZSeries.iOverwritePlane" NDimensions="0" Override="" OverrideVariable="">-
1</Variable><Variable Type="String" Name="jnlZSeries.stStorageFile" NDimensions="0"
Override="" OverrideVariable="">50 E:\Users\JT\10-13-05\cln2_nodox_1-
5min_6_hr183.stk</Variable><Variable Type="Long" Name="jnlZSeries.lStartFrame"
NDimensions="0" Override=""
OverrideVariable="">1</Variable></FunctionEntry></CodeBlock></ForNextLoopEntry><FunctionE
ntry GUID="{0x3cef1e92-0xe09c-0x11d3-0x93-0x9a-0x0-0x10-0x5a-0x4-0x2f-0x99}"
FunctionName="Move Stage to Absolute Position" Interactive="0" ApplicationName="mmproc"
VersionNumber="1" MissingImage="0" Disabled="1" CommandID="5"
MetaJournal="000007FEDC71FE68" IsCurrentVersion="1"
Variables="000007FEDC71FBC8"><Variable Type="Double" Name="jnlMoveStageAbs.dpX"
NDimensions="0" Override="Variable" OverrideVariable="pos_X_1">-
3697.3</Variable><Variable Type="Double" Name="jnlMoveStageAbs.dpY" NDimensions="0"
Override="Variable" OverrideVariable="pos_Y_1">-4026.8</Variable><Variable Type="Double"
Name="jnlMoveStageAbs.dpZ" NDimensions="0" Override="Variable"
OverrideVariable="pos_Z_1">18289.4</Variable></FunctionEntry></CodeBlock></Journal>

Chamber_Imaging_Positions_Capture.JNL

```
<Journal><Description>New Journal</Description><Version
VersionNumber="2.4"/><CodeBlock><IfThenElseEntry Expression="brightf_capture =
&amp;quot;Y&amp;quot;" Disabled="0"><CodeBlock Condition="true"><IfThenElseEntry
Expression="brightf_loop = loop_number" Disabled="0"><CodeBlock
Condition="true"><FunctionEntry GUID="{0x79f510e8-0xe09c-0x11d3-0x93-0x9a-0x0-0x10-0x5a-
0x4-0x2f-0x99}" FunctionName="Run Journal" Interactive="0" ApplicationName="journal"
VersionNumber="1" Disabled="0" CommandID="1" MissingImage="0"
MetaJournal="00007FFA0E556AC8" IsCurrentVersion="1"
Variables="00007FFA0E556828"><Variable Type="String"
Name="ExecuteJournalJNL.stExecuteJournal" NDimensions="0" Override=""
OverrideVariable="">66
C:\MM\app\mmproc\journals\Chamber_brightfield_capture_movement.jnl</Variable></FunctionEn
try></CodeBlock><CodeBlock Condition="false"/></IfThenElseEntry></CodeBlock><CodeBlock
Condition="false"/></IfThenElseEntry><IfThenElseEntry Disabled="0"
Expression="dapi_capture = &amp;quot;Y&amp;quot;"><CodeBlock Condition="true"><IfThenElseEntry
Expression="dapi_loop1 = loop_number" Disabled="0"><CodeBlock
Condition="true"><FunctionEntry GUID="{0x79f510e8-0xe09c-0x11d3-0x93-0x9a-0x0-0x10-0x5a-
0x4-0x2f-0x99}" FunctionName="Run Journal" Interactive="0" ApplicationName="journal"
VersionNumber="1" Disabled="0" CommandID="2" MissingImage="0"
MetaJournal="00007FFA0E556AC8" IsCurrentVersion="1"
Variables="00007FFA0E556828"><Variable Type="String"
Name="ExecuteJournalJNL.stExecuteJournal" NDimensions="0" Override=""
OverrideVariable="">59
C:\MM\app\mmproc\journals\Chamber_dapi_capture_movement.jnl</Variable></FunctionEntry></C
odeBlock><CodeBlock Condition="false"/></IfThenElseEntry></CodeBlock><CodeBlock
Condition="false"/></IfThenElseEntry><AssignVariableEntry VariableName="mod_loop_number"
Expression="loop_number + 1"/><AssignVariableEntry VariableName="spots_already_imaged"
Expression="0"/><IfThenElseEntry Expression="loop_number = 0" Disabled="0"><CodeBlock
Condition="true"><AssignVariableEntry Disabled="0" VariableName="auto_focus_correction"
Expression="&amp;quot;N&amp;quot;"/><AssignVariableEntry VariableName="stg_pos_Z_all"
Expression="&amp;quot;&amp;quot;" Disabled="0"/><AssignVariableEntry
VariableName="stg_pos_Z_all_old" Expression="&amp;quot;&amp;quot;"
Disabled="0"/></CodeBlock><CodeBlock Condition="false"><IfThenElseEntry
Expression="(MOD(mod_loop_number, 30) ) = 0" Disabled="1"><CodeBlock
Condition="true"><AssignVariableEntry VariableName="auto_focus_correction"
Expression="&amp;quot;Y&amp;quot;" Disabled="1"/><AssignVariableEntry
VariableName="stg_pos_Z_all_old" Expression="stg_pos_Z_all"
Disabled="1"/><AssignVariableEntry VariableName="stg_pos_Z_all" Expression="&amp;quot;&amp;quot;"
Disabled="1"/></CodeBlock><CodeBlock Condition="false"><AssignVariableEntry
VariableName="auto_focus_correction" Expression="&amp;quot;N&amp;quot;"/><AssignVariableEntry
VariableName="stg_pos_Z_all_old"
Expression="stg_pos_Z_all"/></CodeBlock></IfThenElseEntry></CodeBlock></IfThenElseEntry><
IfThenElseEntry Expression="loop_number = 180" Disabled="1"><CodeBlock
Condition="true"><AssignVariableEntry VariableName="auto_focus_correction"
Expression="&amp;quot;N&amp;quot;" Disabled="1"/><AssignVariableEntry
VariableName="stg_pos_Z_all_old" Expression="stg_pos_Z_all"
Disabled="1"/></CodeBlock><CodeBlock
Condition="false"/></IfThenElseEntry><AssignVariableEntry VariableName="pos_X_prev"
Expression="pos_X_1 "/><AssignVariableEntry Disabled="0"
VariableName="Illumination_acquire" Expression="Illumination"/><AssignVariableEntry
VariableName="CondExpTime_Ac" Expression="Cond1ExpTime"/><ForNextLoopEntry
LoopVariable="set_being_imaged" StartValue="0" EndValue="num_chambers_sets"
StepValue="1"><CodeBlock><ForNextLoopEntry LoopVariable="chamber_being_imaged"
StartValue="0" EndValue="num_chambers" StepValue="1"><CodeBlock><IfThenElseEntry
Expression="(MOD(chamber_being_imaged, 2) ) = 0"><CodeBlock
Condition="true"><ForNextLoopEntry Disabled="0" LoopVariable="in_chamber_pos"
StartValue="0" EndValue="length_steps" StepValue="1"><CodeBlock><AssignVariableEntry
VariableName="pos_Y_2" Expression="pos_Y_1 - (chamber_being_imaged*chamber_steps) -
(set_being_imaged*(chamber_set_steps+chamber_steps))"/><AssignVariableEntry Disabled="0"
VariableName="pos_X_2" Expression="pos_X_1 - ((pos_Y_1 -
pos_Y_2)*dxdy_chamber)"/><AssignVariableEntry VariableName="pos_Z_2" Expression="pos_Z_1
+ ((pos_X_1 - pos_X_2)*dzdx_chamber)" Disabled="0"/><IfThenElseEntry
Expression="loop_number = 0" Disabled="1"><CodeBlock
Condition="true"><AssignVariableEntry VariableName="pos_Z_2" Expression="pos_Z_1 +
((pos_X_1 - pos_X_2)*dzdx_chamber)" Disabled="1"/></CodeBlock><CodeBlock
```

```
Condition="false"><AssignVariableEntry VariableName="index_first"
Expression="2+9*(spots_already_imaged)"/><AssignVariableEntry VariableName="pos_Z_2"
Expression="MID(stg_pos_Z_all, index_first,
8)"/></CodeBlock></IfThenElseEntry><AssignVariableEntry VariableName="pos_X_curr"
Expression="pos_X_2 - in_chamber_pos*camera_length" Disabled="0"/><AssignVariableEntry
VariableName="pos_Y_curr" Expression="pos_Y_2 - ((in_chamber_pos*camera_length) *
dydx_chamber)" Disabled="0"/><AssignVariableEntry VariableName="pos_Z_curr"
Expression="VAL(pos_Z_2) - ((in_chamber_pos*camera_length) * dzdx_chamber) -
(dzdy_chamber * (pos_Y_1 - pos_Y_curr))" Disabled="0"/><IfThenElseEntry
Expression="loop_number = 0" Disabled="1"><CodeBlock
Condition="true"><AssignVariableEntry VariableName="pos_Z_curr" Expression="VAL(pos_Z_2)
- ((in_chamber_pos*camera_length) * dzdx_chamber) - (dzdy_chamber * (pos_Y_1 -
pos_Y_curr))" Disabled="1"/></CodeBlock><CodeBlock Condition="false"><AssignVariableEntry
Disabled="0" VariableName="pos_Z_curr"
Expression="VAL(pos_Z_2)"/></CodeBlock></IfThenElseEntry><FunctionEntry
GUID="{0x3cef1e92-0xe09c-0x11d3-0x93-0x9a-0x0-0x10-0x5a-0x4-0x2f-0x99}"
FunctionName="Move Stage to Absolute Position" Interactive="0" ApplicationName="mmproc"
VersionNumber="1" CommandID="3" MissingImage="0" MetaJournal="00007FFA1188FE68"
IsCurrentVersion="1" Variables="00007FFA1188FBC8"><Variable Type="Double"
Name="jnlMoveStageAbs.dpX" NDimensions="0" Override="Variable"
OverrideVariable="pos_X_curr">-3697.3</Variable><Variable Type="Double"
Name="jnlMoveStageAbs.dpY" NDimensions="0" Override="Variable"
OverrideVariable="pos_Y_curr">-4026.8</Variable><Variable Type="Double"
Name="jnlMoveStageAbs.dpZ" NDimensions="0" Override="Variable"
OverrideVariable="pos_Z_curr">18289.4</Variable></FunctionEntry><FunctionEntry
GUID="{0x3cef1e92-0xe09c-0x11d3-0x93-0x9a-0x0-0x10-0x5a-0x4-0x2f-0x99}"
FunctionName="Move Stage to Absolute Position" Interactive="0" ApplicationName="mmproc"
VersionNumber="1" CommandID="4" MissingImage="0" MetaJournal="00007FFA1188FE68"
IsCurrentVersion="1" Variables="00007FFA1188FBC8"><Variable Type="Double"
Name="jnlMoveStageAbs.dpX" NDimensions="0" Override="Variable"
OverrideVariable="pos_X_curr">-3697.3</Variable><Variable Type="Double"
Name="jnlMoveStageAbs.dpY" NDimensions="0" Override="Variable"
OverrideVariable="pos_Y_curr">-4026.8</Variable><Variable Type="Double"
Name="jnlMoveStageAbs.dpZ" NDimensions="0" Override="Variable"
OverrideVariable="pos_Z_curr">18289.4</Variable></FunctionEntry><IfThenElseEntry
Expression="Val(pos_X_prev) - Device.Stage.XPosition = 0"><CodeBlock
Condition="true"><AssignVariableEntry VariableName="pos_Y_2" Expression="pos_Y_1 -
(chamber_being_imaged*chamber_steps) -
(set_being_imaged*(chamber_set_steps+chamber_steps))"/><AssignVariableEntry Disabled="0"
VariableName="pos_X_2" Expression="pos_X_1 - ((pos_Y_1 -
pos_Y_2)*dxdy_chamber)"/><AssignVariableEntry VariableName="pos_Z_2" Expression="pos_Z_1
+ ((pos_X_1 - pos_X_2)*dzdx_chamber)" Disabled="0"/><AssignVariableEntry
VariableName="pos_X_curr" Expression="pos_X_2 - in_chamber_pos*camera_length"
Disabled="0"/><AssignVariableEntry VariableName="pos_Y_curr" Expression="pos_Y_2 -
((in_chamber_pos*camera_length) * dydx_chamber)" Disabled="0"/><AssignVariableEntry
VariableName="pos_Z_curr" Expression="VAL(pos_Z_2) - ((in_chamber_pos*camera_length) *
dzdx_chamber) - (dzdy_chamber * (pos_Y_1 - pos_Y_curr))" Disabled="0"/><FunctionEntry
GUID="{0x3cef1e92-0xe09c-0x11d3-0x93-0x9a-0x0-0x10-0x5a-0x4-0x2f-0x99}"
FunctionName="Move Stage to Absolute Position" Interactive="0" ApplicationName="mmproc"
VersionNumber="1" CommandID="5" MissingImage="0" MetaJournal="00007FFA1188FE68"
IsCurrentVersion="1" Variables="00007FFA1188FBC8"><Variable Type="Double"
Name="jnlMoveStageAbs.dpX" NDimensions="0" Override="Variable"
OverrideVariable="pos_X_curr">-3697.3</Variable><Variable Type="Double"
Name="jnlMoveStageAbs.dpY" NDimensions="0" Override="Variable"
OverrideVariable="pos_Y_curr">-4026.8</Variable><Variable Type="Double"
Name="jnlMoveStageAbs.dpZ" NDimensions="0" Override="Variable"
OverrideVariable="pos_Z_curr">18289.4</Variable></FunctionEntry><TraceEntry
Expression="&amp;quot;Skipped happened at&amp;quot;+STR(in_chamber_pos)+&amp;quot;chamber position,
at chamber&amp;quot;+STR(chamber_being_imaged)"/><IfThenElseEntry Disabled="1"
Expression="auto_focus_correction = &amp;quot;Y&amp;quot;"><CodeBlock
Condition="true"><CommentEntry>Z Position List Start</CommentEntry><AssignVariableEntry
VariableName="Camera.Digital.Exposure" Expression="CondExpTime_Ac"/><AssignVariableEntry
Disabled="0" VariableName="Component.Zeiss_Filter_Cube.PositionLabel"
Expression="Illumination_acquire"/><FunctionEntry GUID="{0x79f5106a-0xe09c-0x11d3-0x93-
0x9a-0x0-0x10-0x5a-0x4-0x2f-0x99}" FunctionName="Find Focus" ApplicationName="autofo_s"
Disabled="0" Interactive="0" CommandID="6" VersionNumber="20040226" MissingImage="0"
MetaJournal="00007FFA1AA721F8" IsCurrentVersion="1"
Variables="00007FFA1AA71F58"><Variable Type="Double" Name="jnlFindFocus.dRange"
```

NDimensions="0" Override="" OverrideVariable="">8</Variable><Variable Type="Double"
Name="jnlFindFocus.dAccuracy" NDimensions="0" Override=""
OverrideVariable="">0.5</Variable><Variable Type="Logical"
Name="jnlFindFocus.bDisplayImages" NDimensions="0" Override=""
OverrideVariable="">FALSE</Variable><Variable Type="Logical"
Name="jnlFindFocus.bBacklashCompensation" NDimensions="0" Override=""
OverrideVariable="">FALSE</Variable><Variable Type="Integer"
Name="jnlFindFocus.idxAlgorithm" NDimensions="0" Override=""
OverrideVariable="">2</Variable></FunctionEntry><AssignVariableEntry
VariableName="z_post_after_correction"
Expression="Device.Focus.CurPos"/><AssignVariableEntry Disabled="0"
VariableName="stg_pos_Z_str_temp"
Expression="Str(z_post_after_correction)"/><AssignVariableEntry Disabled="0"
VariableName="Len_z_num"
Expression="LEN(Str(z_post_after_correction))"/><AssignVariableEntry Disabled="0"
VariableName="stg_pos_num_str" Expression="stg_pos_Z_str_temp"/><AssignVariableEntry
VariableName="Len_num" Expression="Len_z_num" Disabled="0"/><AssignVariableEntry
Disabled="0" VariableName="curr_number"
Expression="z_post_after_correction"/><FunctionEntry GUID="{0x79f510e8-0xe09c-0x11d3-
0x93-0x9a-0x0-0x10-0x5a-0x4-0x2f-0x99}" FunctionName="Run Journal" Interactive="0"
ApplicationName="journal" VersionNumber="1" Disabled="0" CommandID="7" MissingImage="0"
MetaJournal="00007FFA0E556AC8" IsCurrentVersion="1"
Variables="00007FFA0E556828"><Variable Type="String"
Name="ExecuteJournalJNL.stExecuteJournal" NDimensions="0" Override=""
OverrideVariable="">62
C:\MM\app\mmproc\journals\Number_correction_Cell_selection.jnl</Variable></FunctionEntry>
<AssignVariableEntry VariableName="stg_pos_Z_str" Expression="stg_pos_num_str"
Disabled="0"/><AssignVariableEntry Disabled="0" VariableName="stg_pos_Z_all"
Expression="stg_pos_Z_all + "," + stg_pos_Z_str"/></CodeBlock><CodeBlock
Condition="false"/></IfThenElseEntry><FunctionEntry GUID="{0x79f510e8-0xe09c-0x11d3-0x93-
0x9a-0x0-0x10-0x5a-0x4-0x2f-0x99}" FunctionName="Run Journal" Interactive="0"
ApplicationName="journal" VersionNumber="1" CommandID="8" MissingImage="0"
MetaJournal="00007FFA0E556AC8" IsCurrentVersion="1"
Variables="00007FFA0E556828"><Variable Type="String"
Name="ExecuteJournalJNL.stExecuteJournal" NDimensions="0" Override=""
OverrideVariable="">59
C:\MM\app\mmproc\journals\Chamber_Dye_Selection_Capture.jnl</Variable></FunctionEntry><As
signVariableEntry VariableName="spots_already_imaged" Expression="spots_already_imaged +
1"/></CodeBlock><CodeBlock Condition="false"><FunctionEntry GUID="{0x79f510e8-0xe09c-
0x11d3-0x93-0x9a-0x0-0x10-0x5a-0x4-0x2f-0x99}" FunctionName="Run Journal" Interactive="0"
ApplicationName="journal" VersionNumber="1" CommandID="11" MissingImage="0"
MetaJournal="00007FFA0E556AC8" IsCurrentVersion="1"
Variables="00007FFA0E556828"><Variable Type="String"
Name="ExecuteJournalJNL.stExecuteJournal" NDimensions="0" Override=""
OverrideVariable="">59
C:\MM\app\mmproc\journals\Chamber_Dye_Selection_Capture.jnl</Variable></FunctionEntry><As
signVariableEntry VariableName="spots_already_imaged" Expression="spots_already_imaged +
1"/></CodeBlock></IfThenElseEntry></CodeBlock></ForNextLoopEntry></CodeBlock><CodeBlock
Condition="false"><ForNextLoopEntry Disabled="0" LoopVariable="in_chamber_pos"
StartValue="length_steps" EndValue="0" StepValue="-1"><CodeBlock><TraceEntry
Expression="in_chamber_pos"/><AssignVariableEntry VariableName="pos_Y_2"
Expression="pos_Y_1 - (chamber_being_imaged*chamber_steps) -
(set_being_imaged*(chamber_set_steps+chamber_steps))"/><AssignVariableEntry Disabled="0"
VariableName="pos_X_2" Expression="pos_X_1 - ((pos_Y_1 -
pos_Y_2)*dxdy_chamber)"/><AssignVariableEntry VariableName="pos_Z_2" Expression="pos_Z_1
+ ((pos_X_1 - pos_X_2)*dzdx_chamber)" Disabled="0"/><AssignVariableEntry
VariableName="pos_X_curr" Expression="pos_X_2 - in_chamber_pos*camera_length"
Disabled="0"/><AssignVariableEntry VariableName="pos_Y_curr" Expression="pos_Y_2 -
((in_chamber_pos*camera_length) * dydx_chamber)" Disabled="0"/><AssignVariableEntry
VariableName="pos_Z_curr" Expression="VAL(pos_Z_2) - ((in_chamber_pos*camera_length) *
dzdx_chamber) - (dzdy_chamber * (pos_Y_1 - pos_Y_curr))" Disabled="0"/><FunctionEntry
GUID="{0x3cef1e92-0xe09c-0x11d3-0x93-0x9a-0x0-0x10-0x5a-0x4-0x2f-0x99}"
FunctionName="Move Stage to Absolute Position" Interactive="0" ApplicationName="mmproc"
VersionNumber="1" CommandID="12" MissingImage="0" MetaJournal="00007FFA1188FE68"
IsCurrentVersion="1" Variables="00007FFA1188FBC8"><Variable Type="Double"
Name="jnlMoveStageAbs.dpX" NDimensions="0" Override="Variable"
OverrideVariable="pos_X_curr">-3697.3</Variable><Variable Type="Double"
Name="jnlMoveStageAbs.dpY" NDimensions="0" Override="Variable"

OverrideVariable="pos_Y_curr">-4026.8</Variable><Variable Type="Double"
Name="jnlMoveStageAbs.dpZ" NDimensions="0" Override="Variable"
OverrideVariable="pos_Z_curr">18289.4</Variable></FunctionEntry><FunctionEntry
GUID="{0x3cef1e92-0xe09c-0x11d3-0x93-0x9a-0x0-0x10-0x5a-0x4-0x2f-0x99}"
FunctionName="Move Stage to Absolute Position" Interactive="0" ApplicationName="mmproc"
VersionNumber="1" CommandID="13" MissingImage="0" MetaJournal="00007FFA1188FE68"
IsCurrentVersion="1" Variables="00007FFA1188FBC8"><Variable Type="Double"
Name="jnlMoveStageAbs.dpX" NDimensions="0" Override="Variable"
OverrideVariable="pos_X_curr">-3697.3</Variable><Variable Type="Double"
Name="jnlMoveStageAbs.dpY" NDimensions="0" Override="Variable"
OverrideVariable="pos_Y_curr">-4026.8</Variable><Variable Type="Double"
Name="jnlMoveStageAbs.dpZ" NDimensions="0" Override="Variable"
OverrideVariable="pos_Z_curr">18289.4</Variable></FunctionEntry><IfThenElseEntry
Expression="Val(pos_X_prev) - Device.Stage.XPosition = 0"><CodeBlock
Condition="true"><AssignVariableEntry VariableName="pos_Y_2" Expression="pos_Y_1 -
(chamber_being_imaged*chamber_steps) -
(set_being_imaged*(chamber_set_steps+chamber_steps))"/><AssignVariableEntry Disabled="0"
VariableName="pos_X_2" Expression="pos_X_1 - ((pos_Y_1 -
pos_Y_2)*dxdy_chamber)"/><AssignVariableEntry Disabled="0" VariableName="pos_Z_2"
Expression="pos_Z_1 + ((pos_X_1 - pos_X_2)*dzdx_chamber)"/><AssignVariableEntry
VariableName="pos_X_curr" Expression="pos_X_2 - in_chamber_pos*camera_length"
Disabled="0"/><AssignVariableEntry VariableName="pos_Y_curr" Expression="pos_Y_2 -
((in_chamber_pos*camera_length) * dydx_chamber)" Disabled="0"/><AssignVariableEntry
VariableName="pos_Z_curr" Expression="VAL(pos_Z_2) - ((in_chamber_pos*camera_length) *
dzdx_chamber) - (dzdy_chamber * (pos_Y_1 - pos_Y_curr))" Disabled="0"/><FunctionEntry
GUID="{0x3cef1e92-0xe09c-0x11d3-0x93-0x9a-0x0-0x10-0x5a-0x4-0x2f-0x99}"
FunctionName="Move Stage to Absolute Position" Interactive="0" ApplicationName="mmproc"
VersionNumber="1" CommandID="14" MissingImage="0" MetaJournal="00007FFA1188FE68"
IsCurrentVersion="1" Variables="00007FFA1188FBC8"><Variable Type="Double"
Name="jnlMoveStageAbs.dpX" NDimensions="0" Override="Variable"
OverrideVariable="pos_X_curr">-3697.3</Variable><Variable Type="Double"
Name="jnlMoveStageAbs.dpY" NDimensions="0" Override="Variable"
OverrideVariable="pos_Y_curr">-4026.8</Variable><Variable Type="Double"
Name="jnlMoveStageAbs.dpZ" NDimensions="0" Override="Variable"
OverrideVariable="pos_Z_curr">18289.4</Variable></FunctionEntry><TraceEntry
Expression=""Skipped happened at"+STR(in_chamber_pos)+"chamber position,
at chamber"+STR(chamber_being_imaged)"/><FunctionEntry GUID="{0x79f510e8-0xe09c-
0x11d3-0x93-0x9a-0x0-0x10-0x5a-0x4-0x2f-0x99}" FunctionName="Run Journal" Interactive="0"
ApplicationName="journal" VersionNumber="1" CommandID="17" MissingImage="0"
MetaJournal="00007FFA0E556AC8" IsCurrentVersion="1"
Variables="00007FFA0E556828"><Variable Type="String"
Name="ExecuteJournalJNL.stExecuteJournal" NDimensions="0" Override=""
OverrideVariable="">59
C:\MM\app\mmproc\journals\Chamber_Dye_Selection_Capture.jnl</Variable></FunctionEntry><As
signVariableEntry VariableName="spots_already_imaged" Expression="spots_already_imaged +
1"/></CodeBlock><CodeBlock Condition="false"><FunctionEntry GUID="{0x79f510e8-0xe09c-
0x11d3-0x93-0x9a-0x0-0x10-0x5a-0x4-0x2f-0x99}" FunctionName="Run Journal" Interactive="0"
ApplicationName="journal" VersionNumber="1" CommandID="20" MissingImage="0"
MetaJournal="00007FFA0E556AC8" IsCurrentVersion="1"
Variables="00007FFA0E556828"><Variable Type="String"
Name="ExecuteJournalJNL.stExecuteJournal" NDimensions="0" Override=""
OverrideVariable="">59
C:\MM\app\mmproc\journals\Chamber_Dye_Selection_Capture.jnl</Variable></FunctionEntry><As
signVariableEntry VariableName="spots_already_imaged" Expression="spots_already_imaged +
1"/></CodeBlock></IfThenElseEntry><AssignVariableEntry VariableName="pos_X_prev"
Expression="pos_X_curr"/></CodeBlock></ForNextLoopEntry></CodeBlock></IfThenElseEntry></C
odeBlock></ForNextLoopEntry></CodeBlock></ForNextLoopEntry><AssignVariableEntry
VariableName="loop_number" Expression="loop_number + 1"/></CodeBlock></Journal>

Chamber_Imaging_Setup_Complete_Script.JNL

<Journal><Description>New Journal</Description><Version
VersionNumber="2.4"/><CodeBlock><CommentEntry>Folder Structure setup
begins</CommentEntry><PromptUserEntry VariableName="Adjustment" PromptType="YesNo"
TitleText="Re-enter the values?" Constrain="1" PromptText="Would you like to re-enter the
values?" DialogXPos="743" DialogYPos="322" Min="4.60877e-312" Max="4.60877e-
312"/><IfThenElseEntry Expression="Adjustment = "Y""><CodeBlock

Condition="true"><PromptUserEntry VariableName="AcqDate" PromptType="String"
TitleText="Date" Constrain="0" PromptText="Please enter the current date (YYYY-MM-DD)"
DialogXPos="884" DialogYPos="378" Disabled="0"/><PromptUserEntry
VariableName="save_driver" PromptType="String" TitleText="Please enter driver letter"
Constrain="0" PromptText="Please enter driver letter where you wish to save your image"
DialogXPos="743" DialogYPos="322"/><AssignVariableEntry VariableName="save_driver"
Expression="save_driver+":"" Disabled="0"/><PromptUserEntry
VariableName="ExpConditions" PromptType="String" TitleText="Experimental Conditions"
Constrain="0" PromptText="Please enter the experimental condition for the set of images"
DialogXPos="884" DialogYPos="378"/><FunctionEntry GUID="{0x5e019877-0x37dc-0x48bd-0x8c-
0x5-0xf9-0xd9-0x32-0xd3-0xba-0x8a}" FunctionName="Create Directory" Interactive="0"
ApplicationName="journal" Disabled="0" VersionNumber="1" CommandID="1" MissingImage="0"
MetaJournal="00007FFF964EBD58" IsCurrentVersion="1"
Variables="00007FFF964EBAB8"><Variable Type="String"
Name="CreateDirectoryJNL.stCreateDirectory" NDimensions="0" Override=""
OverrideVariable="">34 %save_driver%\Syung-
Hun\%AcqDate%\</Variable></FunctionEntry><FunctionEntry GUID="{0x5e019877-0x37dc-0x48bd-
0x8c-0x5-0xf9-0xd9-0x32-0xd3-0xba-0x8a}" FunctionName="Create Directory" Interactive="0"
ApplicationName="journal" Disabled="0" VersionNumber="1" CommandID="2" MissingImage="0"
MetaJournal="00007FFF964EBD58" IsCurrentVersion="1"
Variables="00007FFF964EBAB8"><Variable Type="String"
Name="CreateDirectoryJNL.stCreateDirectory" NDimensions="0" Override=""
OverrideVariable="">49 %save_driver%\Syung-
Hun\%AcqDate%\%ExpConditions%</Variable></FunctionEntry><AssignVariableEntry Disabled="0"
VariableName="SelectDirectory.Path" Expression="save_driver+"\Syung-
Hun\"+AcqDate+"\"+ExpConditions+"\""/><AssignVariableEntry
Disabled="0" VariableName="saving_base_directory" Expression="save_driver+"\Syung-
Hun\"+AcqDate+"\"+ExpConditions+"\""/><AssignVariableEntry
VariableName="len_save_dir" Expression="len(saving_base_directory)-2"
Disabled="0"/><AssignVariableEntry VariableName="save_base_dirc" Expression="RIGHT(
saving_base_directory, len_save_dir)" Disabled="0"/><CommentEntry>Folder Structure setup
ends</CommentEntry><CommentEntry>Experiment settings begin
here</CommentEntry><PromptUserEntry Disabled="0" ItemText="1
2 3 4 " VariableName="NumofDyes" PromptType="Number" TitleText="How many dyes do you
wish to image?" Constrain="1" PromptText="How many dyes do you wish to image?"
DialogXPos="884" DialogYPos="378" Min="1" Max="4"/><PromptUserEntry VariableName="Dye_1"
PromptType="String" TitleText="Enter the highest wavelength dye name" Constrain="0"
PromptText="Enter the highest wavelength dye/probe name first" DialogXPos="884"
DialogYPos="378"/><PromptUserEntry VariableName="Illumination" PromptType="RadioButton"
TitleText="Select Filter" Constrain="0" PromptText="Please Select the 1st Probe
Illumination Setting" DialogXPos="862" DialogYPos="357" ItemText="DAPI
Cy3   GFP   Cy5   TRITC mCherry   "/><PromptUserEntry Disabled="0"
VariableName="Cond1ExpTime" PromptType="Number" TitleText="Select 1st Exposure Time"
Constrain="1" PromptText="Enter exposure time for 1st Probe" DialogXPos="884"
DialogYPos="378" Min="10" Max="100000"/><FunctionEntry GUID="{0x5e019877-0x37dc-0x48bd-
0x8c-0x5-0xf9-0xd9-0x32-0xd3-0xba-0x8a}" FunctionName="Create Directory" Interactive="0"
ApplicationName="journal" VersionNumber="1" Disabled="0" CommandID="3" MissingImage="0"
MetaJournal="00007FFF964EBD58" IsCurrentVersion="1"
Variables="00007FFF964EBAB8"><Variable Type="String"
Name="CreateDirectoryJNL.stCreateDirectory" NDimensions="0" Override=""
OverrideVariable="">64 %save_driver%\Syung-
Hun\%AcqDate%\%ExpConditions%\%Illumination%</Variable></FunctionEntry><IfThenElseEntry
Expression="NumofDyes > 1"><CodeBlock Condition="true"><PromptUserEntry
VariableName="Dye_2" PromptType="String" TitleText="Enter the 2nd highest wavelength
dye/probe name " Constrain="0" PromptText="Enter the 2nd highest wavelength dye/probe
name" DialogXPos="884" DialogYPos="378"/><PromptUserEntry VariableName="TRF"
PromptType="YesNo" TitleText="Would the second dye be in TR-F mode?" Constrain="1"
PromptText="Would the second dye be in TR-F mode?" DialogXPos="743" DialogYPos="322"
Min="4.60877e-312" Max="4.60877e-312"/><IfThenElseEntry Disabled="0" Expression="TRF =
"Y""><CodeBlock Condition="true"><PromptUserEntry Disabled="0"
VariableName="Cond2WaitTime" PromptType="Number" TitleText="Select Initial Wait Exposure
Time of TRF" Constrain="1" PromptText="Enter initial wait exposure time for TRF"
DialogXPos="884" DialogYPos="378" Min="10" Max="100000"/><PromptUserEntry
VariableName="Illumination2" PromptType="RadioButton" TitleText="Select Filter"
Constrain="0" PromptText="Please Select the 2nd Probe Illumination Setting"
DialogXPos="862" DialogYPos="357" ItemText="DAPI
Cy 3   GFP   Cy5   TRITC mCherry   "/><PromptUserEntry Disabled="0"
VariableName="Cond2ExpTime" PromptType="Number" TitleText="Select 2nd Exposure Time"

Constrain="1" PromptText="Enter exposure time for 2nd Probe/Antibody" DialogXPos="884"
DialogYPos="378" Min="10" Max="100000"/><PromptUserEntry Disabled="0"
VariableName="Cond2WaitTimeTRF" PromptType="Number" TitleText="Select Middle Wait
Exposure Time of TRF" Constrain="1" PromptText="Enter middle wait exposure time for TRF"
DialogXPos="884" DialogYPos="378" Min="10" Max="100000"/><PromptUserEntry
VariableName="Illumination2TRF" PromptType="RadioButton" TitleText="Select Filter for
TRF" Constrain="0" PromptText="Please Select the 2nd Probe Illumination Setting"
DialogXPos="862" DialogYPos="357" ItemText="DAPI
Cy 3 GFP Cy5 TRITC mCherry "/><PromptUserEntry Disabled="0"
VariableName="Cond2ExpTimeTRF" PromptType="Number" TitleText="Select 2nd Exposure Time of
TRF" Constrain="1" PromptText="Enter exposure time for 2nd Probe/Antibody"
DialogXPos="884" DialogYPos="378" Min="10" Max="100000"/></CodeBlock><CodeBlock
Condition="false"><PromptUserEntry VariableName="Illumination2" PromptType="RadioButton"
TitleText="Select Filter" Constrain="0" PromptText="Please Select the 2nd Probe
Illumination Setting" DialogXPos="862" DialogYPos="357" ItemText="DAPI Cy 3 GFP Cy5
TRITC mCherry "/><PromptUserEntry Disabled="0" VariableName="Cond2ExpTime"
PromptType="Number" TitleText="Select 2nd Exposure Time" Constrain="1" PromptText="Enter
exposure time for 2nd Probe/Antibody" DialogXPos="884" DialogYPos="378" Min="10"
Max="100000"/></CodeBlock></IfThenElseEntry><FunctionEntry GUID="{0x5e019877-0x37dc-
0x48bd-0x8c-0x5-0xf9-0xd9-0x32-0xd3-0xba-0x8a}" FunctionName="Create Directory"
Interactive="0" ApplicationName="journal" VersionNumber="1" Disabled="0" CommandID="4"
MissingImage="0" MetaJournal="00007FFF964EBD58" IsCurrentVersion="1"
Variables="00007FFF964EBAB8"><Variable Type="String"
Name="CreateDirectoryJNL.stCreateDirectory" NDimensions="0" Override=""
OverrideVariable="">65 %save_driver%\Syung-
Hun\%AcqDate%\%ExpConditions%\%Illumination2%</Variable></FunctionEntry><IfThenElseEntry
Expression="NumofDyes > 2"><CodeBlock Condition="true"><PromptUserEntry
VariableName="Dye_3" PromptType="String" TitleText="Enter the 3rd highest wavelength
dye/probe name " Constrain="0" PromptText="Enter the 3rd highest wavelength dye/probe
name " DialogXPos="884" DialogYPos="378"/><PromptUserEntry VariableName="Illumination3"
PromptType="RadioButton" TitleText="Select Filter" Constrain="0" PromptText="Please
Select the 3rd Probe Illumination Setting" DialogXPos="862" DialogYPos="357"
ItemText="DAPI Cy 3 GFP Cy5 TRITC mCherry "/><PromptUserEntry Disabled="0"
VariableName="Cond3ExpTime" PromptType="Number" TitleText="Select 3rd Exposure Time"
Constrain="1" PromptText="Enter exposure time for 3rd Probe/Antibody" DialogXPos="884"
DialogYPos="378" Min="10" Max="100000"/><FunctionEntry GUID="{0x5e019877-0x37dc-0x48bd-
0x8c-0x5-0xf9-0xd9-0x32-0xd3-0xba-0x8a}" FunctionName="Create Directory" Interactive="0"
ApplicationName="journal" VersionNumber="1" Disabled="0" CommandID="5" MissingImage="0"
MetaJournal="00007FFF964EBD58" IsCurrentVersion="1"
Variables="00007FFF964EBAB8"><Variable Type="String"
Name="CreateDirectoryJNL.stCreateDirectory" NDimensions="0" Override=""
OverrideVariable="">65 %save_driver%\Syung-
Hun\%AcqDate%\%ExpConditions%\%Illumination3%</Variable></FunctionEntry><IfThenElseEntry
Disabled="0" Expression="NumofDyes > 3"><CodeBlock Condition="true"><PromptUserEntry
VariableName="Dye_4" PromptType="String" TitleText="Enter the lowest wavelength dye/probe
name " Constrain="0" PromptText="Enter the lowest wavelength dye/probe name "
DialogXPos="884" DialogYPos="378"/><PromptUserEntry VariableName="Illumination4"
PromptType="RadioButton" TitleText="Select Filter" Constrain="0" PromptText="Please
Select the 4th Probe Illumination Setting" DialogXPos="862" DialogYPos="357"
ItemText="DAPI Cy 3 GFP Cy5 TRITC mCherry "/><PromptUserEntry Disabled="0"
VariableName="Cond4ExpTime" PromptType="Number" TitleText="Select 4th Exposure Time"
Constrain="1" PromptText="Enter exposure time for 4th Probe/Antibody" DialogXPos="884"
DialogYPos="378" Min="10" Max="100000"/><FunctionEntry GUID="{0x5e019877-0x37dc-0x48bd-
0x8c-0x5-0xf9-0xd9-0x32-0xd3-0xba-0x8a}" FunctionName="Create Directory" Interactive="0"
ApplicationName="journal" VersionNumber="1" Disabled="0" CommandID="6" MissingImage="0"
MetaJournal="00007FFF964EBD58" IsCurrentVersion="1"
Variables="00007FFF964EBAB8"><Variable Type="String"
Name="CreateDirectoryJNL.stCreateDirectory" NDimensions="0" Override=""
OverrideVariable="">65 %save_driver%\Syung-
Hun\%AcqDate%\%ExpConditions%\%Illumination4%</Variable></FunctionEntry></CodeBlock><Code
Block Condition="false"/></IfThenElseEntry></CodeBlock><CodeBlock
Condition="false"/></IfThenElseEntry></CodeBlock><CodeBlock
Condition="false"/></IfThenElseEntry><FunctionEntry GUID="{0x79f510e8-0xe09c-0x11d3-0x93-
0x9a-0x0-0x10-0x5a-0x4-0x2f-0x99}" FunctionName="Run Journal" Interactive="0"
ApplicationName="journal" VersionNumber="1" CommandID="7" MissingImage="0"
MetaJournal="00007FFF964E6AC8" IsCurrentVersion="1"
Variables="00007FFF964E6828"><Variable Type="String"
Name="ExecuteJournalJNL.stExecuteJournal" NDimensions="0" Override=""

OverrideVariable="">57
C:\MM\app\mmproc\journals\Chamber_camera_length_input.jnl</Variable></FunctionEntry><Prom
ptUserEntry Disabled="0" VariableName="device_length" PromptType="Number"
TitleText="Enter the length of the device (down one of the chambers) (mm)" Constrain="1"
PromptText="This is the legnth of one of the chambers in milimeters (max 44.4082)"
DialogXPos="743" DialogYPos="322" Min="2.6624" Max="44.4082"/><AssignVariableEntry
VariableName="length_steps" Expression="CEILING((device_length*1000)/camera_length)"
Disabled="0"/><PromptUserEntry Disabled="0" VariableName="num_chambers_sets"
PromptType="Number" TitleText="Please enter the number of chambers sets" Constrain="1"
PromptText="Enter the number of chambers sets you wish to image." DialogXPos="743"
DialogYPos="322" Min="1" Max="25"/><AssignVariableEntry Disabled="0"
VariableName="num_chambers_sets" Expression="num_chambers_sets - 1"/><PromptUserEntry
Disabled="0" VariableName="num_chambers" PromptType="Number" TitleText="Please enter the
number of chambers in a chamber set" Constrain="1" PromptText="Enter the number of
chambers in the chamber sets you wish to image" DialogXPos="743" DialogYPos="322" Min="1"
Max="25"/><AssignVariableEntry VariableName="num_chambers" Expression="num_chambers - 1"
Disabled="0"/><PromptUserEntry VariableName="brightf_capture" PromptType="YesNo"
TitleText="Bright Field Capture?" Constrain="0" PromptText="Do you wish perform a loop
with brightfield illumination?" DialogXPos="743" DialogYPos="322"/><IfThenElseEntry
Expression="brightf_capture = "Y""><CodeBlock Condition="true"><PromptUserEntry
Min="0" Max="12.2269" VariableName="brightf_loop" PromptType="Number" TitleText="When do
you wish to image the bright field loop?" Constrain="0" PromptText="Use 0 to have it be
before the fluorescent first loop" DialogXPos="743" DialogYPos="322"/><PromptUserEntry
Disabled="0" VariableName="CondExpTime_brightfl" PromptType="Number" TitleText="Select
Brightfield Exposure Time" Constrain="1" PromptText="Enter exposure time for brighfield
imaging" DialogXPos="884" DialogYPos="378" Min="10" Max="100000"/><FunctionEntry
GUID="{0x5e019877-0x37dc-0x48bd-0x8c-0x5-0xf9-0xd9-0x32-0xd3-0xba-0x8a}"
FunctionName="Create Directory" Interactive="0" ApplicationName="journal"
VersionNumber="1" Disabled="0" CommandID="8" MissingImage="0"
MetaJournal="00007FFF964EBD58" IsCurrentVersion="1"
Variables="00007FFF964EBAB8"><Variable Type="String"
Name="CreateDirectoryJNL.stCreateDirectory" NDimensions="0" Override=""
OverrideVariable="">61 %save_driver%\Syung-
Hun\%AcqDate%\%ExpConditions%\Brightfield</Variable></FunctionEntry></CodeBlock><CodeBloc
k Condition="false"/></IfThenElseEntry><PromptUserEntry VariableName="dapi_capture"
PromptType="YesNo" TitleText="Fluorescence Capture?" Constrain="0" PromptText="Do you
wish perform a loop with fluorescence illumination?" DialogXPos="743"
DialogYPos="322"/><IfThenElseEntry Expression="dapi_capture = "Y""><CodeBlock
Condition="true"><PromptUserEntry VariableName="Pre_Illumination"
PromptType="RadioButton" TitleText="Select Filter" Constrain="0" PromptText="Please
Select the 1st Probe Illumination Setting" DialogXPos="862" DialogYPos="357"
ItemText="DAPI Cy3 GFP Cy5 TRITC mCherry "/><PromptUserEntry Min="0"
Max="12.2269" VariableName="dapi_loop1" PromptType="Number" TitleText="When do you wish
to image the first fluorescence field loop?" Constrain="0" PromptText="Use 0 to have it
be before the fluorescent first loop" DialogXPos="743" DialogYPos="322"/><PromptUserEntry
Disabled="0" VariableName="CondExpTime_dapi" PromptType="Number" TitleText="Select
fluorescence Exposure Time" Constrain="1" PromptText="Enter exposure time for 1st
fluorescence label imaging" DialogXPos="884" DialogYPos="378" Min="10"
Max="100000"/><PromptUserEntry Min="0" Max="12.2269" VariableName="dapi_loop_num"
Disabled="1" PromptType="Number" TitleText="How many times do you wish to take DAPI
image?" Constrain="0" PromptText="3 for before loop, middle and after loop"
DialogXPos="743" DialogYPos="322"/><IfThenElseEntry Disabled="1"
Expression="dapi_loop_num = 1"><CodeBlock Condition="true"><PromptUserEntry Min="0"
Max="12.2269" VariableName="dapi_loop1" PromptType="Number" TitleText="When do you wish
to image the first fluorescence field loop?" Constrain="0" PromptText="Use 0 to have it
be before the fluorescent first loop" DialogXPos="743"
DialogYPos="322"/></CodeBlock><CodeBlock Condition="false"><IfThenElseEntry
Expression="dapi_loop_num = 2"><CodeBlock Condition="true"><PromptUserEntry Min="0"
Max="12.2269" VariableName="dapi_loop1" PromptType="Number" TitleText="When do you wish
to image the first fluorescence field loop?" Constrain="0" PromptText="Use 0 to have it
be before the fluorescent first loop" DialogXPos="743" DialogYPos="322"/><PromptUserEntry
Min="0" Max="12.2269" VariableName="dapi_loop2" PromptType="Number" TitleText="When do
you wish to image the second fluorescence field loop?" Constrain="0" PromptText="Use 0 to
have it be before the fluorescent first loop" DialogXPos="743"
DialogYPos="322"/></CodeBlock><CodeBlock Condition="false"><IfThenElseEntry
Expression="dapi_loop_num = 3"><CodeBlock Condition="true"><PromptUserEntry Min="0"
Max="12.2269" VariableName="dapi_loop1" PromptType="Number" TitleText="When do you wish
to image the first fluorescence field loop?" Constrain="0" PromptText="Use 0 to have it

be before the fluorescent first loop" DialogXPos="743" DialogYPos="322"/><PromptUserEntry Min="0" Max="12.2269" VariableName="dapi_loop2" PromptType="Number" TitleText="When do you wish to image the second fluorescence field loop?" Constrain="0" PromptText="Use 0 to have it be before the fluorescent first loop" DialogXPos="743" DialogYPos="322"/><PromptUserEntry Min="0" Max="12.2269" VariableName="dapi_loop3" PromptType="Number" TitleText="When do you wish to image the third fluorescence field loop?" Constrain="0" PromptText="Use 0 to have it be before the fluorescent first loop" DialogXPos="743" DialogYPos="322"/></CodeBlock><CodeBlock Condition="false"/></IfThenElseEntry></CodeBlock></IfThenElseEntry></CodeBlock></IfThenElseEntry><FunctionEntry GUID="{0x5e019877-0x37dc-0x48bd-0x8c-0x5-0xf9-0xd9-0x32-0xd3-0xba-0x8a}" FunctionName="Create Directory" Interactive="0" ApplicationName="journal" Disabled="0" VersionNumber="1" CommandID="9" MissingImage="0" MetaJournal="00007FFF964EBD58" IsCurrentVersion="1" Variables="00007FFF964EBAB8"><Variable Type="String" Name="CreateDirectoryJNL.stCreateDirectory" NDimensions="0" Override="" OverrideVariable="">68 %save_driver%\Syung-Hun\%AcqDate%\%ExpConditions%\%Pre_Illumination%</Variable></FunctionEntry></CodeBlock><CodeBlock Condition="false"/></IfThenElseEntry><PromptUserEntry VariableName="dapi_capture2" PromptType="YesNo" TitleText="2nd Fluorescence Capture?" Constrain="0" PromptText="Do you wish perform a loop with 2nd fluorescence illumination?" DialogXPos="743" DialogYPos="322"/><IfThenElseEntry Expression="dapi_capture2 = "Y""><CodeBlock Condition="true"><PromptUserEntry VariableName="Pre_Illumination2" PromptType="RadioButton" TitleText="Select Filter" Constrain="0" PromptText="Please Select the 1st Probe Illumination Setting" DialogXPos="862" DialogYPos="357" ItemText="DAPI Cy3 GFP Cy5 TRITC mCherry "/><PromptUserEntry Min="0" Max="12.2269" VariableName="dapi2_loop1" PromptType="Number" TitleText="When do you wish to image the 2nd fluorescence field loop?" Constrain="0" PromptText="Use 0 to have it be before the fluorescent first loop" DialogXPos="743" DialogYPos="322"/><PromptUserEntry Disabled="0" VariableName="CondExpTime_dapi2" PromptType="Number" TitleText="Select 2nd fluorescence Exposure Time" Constrain="1" PromptText="Enter exposure time for 2nd fluorescence imaging" DialogXPos="884" DialogYPos="378" Min="10" Max="100000"/><PromptUserEntry Min="0" Max="12.2269" VariableName="dapi_loop_num" Disabled="1" PromptType="Number" TitleText="How many times do you wish to take DAPI image?" Constrain="0" PromptText="3 for before loop, middle and after loop" DialogXPos="743" DialogYPos="322"/><IfThenElseEntry Disabled="1" Expression="dapi_loop_num = 1"><CodeBlock Condition="true"><PromptUserEntry Min="0" Max="12.2269" VariableName="dapi_loop1" PromptType="Number" TitleText="When do you wish to image the first fluorescence field loop?" Constrain="0" PromptText="Use 0 to have it be before the fluorescent first loop" DialogXPos="743" DialogYPos="322"/></CodeBlock><CodeBlock Condition="false"><IfThenElseEntry Expression="dapi_loop_num = 2"><CodeBlock Condition="true"><PromptUserEntry Min="0" Max="12.2269" VariableName="dapi_loop1" PromptType="Number" TitleText="When do you wish to image the first fluorescence field loop?" Constrain="0" PromptText="Use 0 to have it be before the fluorescent first loop" DialogXPos="743" DialogYPos="322"/><PromptUserEntry Min="0" Max="12.2269" VariableName="dapi_loop2" PromptType="Number" TitleText="When do you wish to image the second fluorescence field loop?" Constrain="0" PromptText="Use 0 to have it be before the fluorescent first loop" DialogXPos="743" DialogYPos="322"/></CodeBlock><CodeBlock Condition="false"><IfThenElseEntry Expression="dapi_loop_num = 3"><CodeBlock Condition="true"><PromptUserEntry Min="0" Max="12.2269" VariableName="dapi_loop1" PromptType="Number" TitleText="When do you wish to image the first fluorescence field loop?" Constrain="0" PromptText="Use 0 to have it be before the fluorescent first loop" DialogXPos="743" DialogYPos="322"/><PromptUserEntry Min="0" Max="12.2269" VariableName="dapi_loop2" PromptType="Number" TitleText="When do you wish to image the second fluorescence field loop?" Constrain="0" PromptText="Use 0 to have it be before the fluorescent first loop" DialogXPos="743" DialogYPos="322"/><PromptUserEntry Min="0" Max="12.2269" VariableName="dapi_loop3" PromptType="Number" TitleText="When do you wish to image the third fluorescence field loop?" Constrain="0" PromptText="Use 0 to have it be before the fluorescent first loop" DialogXPos="743" DialogYPos="322"/></CodeBlock><CodeBlock Condition="false"/></IfThenElseEntry></CodeBlock></IfThenElseEntry><FunctionEntry GUID="{0x5e019877-0x37dc-0x48bd-0x8c-0x5-0xf9-0xd9-0x32-0xd3-0xba-0x8a}" FunctionName="Create Directory" Interactive="0" ApplicationName="journal" Disabled="0" VersionNumber="1" CommandID="10" MissingImage="0" MetaJournal="00007FFF964EBD58" IsCurrentVersion="1" Variables="00007FFF964EBAB8"><Variable Type="String" Name="CreateDirectoryJNL.stCreateDirectory" NDimensions="0" Override="" OverrideVariable="">68 %save_driver%\Syung-Hun\%AcqDate%\%ExpConditions%\%Pre_Illumination%</Variable></FunctionEntry></CodeBlock><C

odeBlock Condition="false"/></IfThenElseEntry><PromptUserEntry
VariableName="between_chambers" PromptType="Number" TitleText="Please enter distance
between chambers" Constrain="1" PromptText="Enter distance between chambers in
milimeters. (max 12.2269mm)" DialogXPos="743" DialogYPos="322" Min="0"
Max="12.2269"/><AssignVariableEntry VariableName="chamber_steps"
Expression="between_chambers*1000"/><PromptUserEntry VariableName="between_chambers_sets"
PromptType="Number" TitleText="Please enter distance between chambers sets" Constrain="1"
PromptText="Enter distance between chambersets in milimeters. (max 12.2269mm)"
DialogXPos="743" DialogYPos="322" Min="0" Max="12.2269"/><AssignVariableEntry
Disabled="0" VariableName="chamber_set_steps"
Expression="between_chambers_sets*1000"/></CodeBlock><CodeBlock
Condition="false"/></IfThenElseEntry></CodeBlock></Journal>

Chamber_Imaging_Setup_Dyet.JNL

<Journal><Description>New Journal</Description><Version
VersionNumber="2.4"/><CodeBlock><CommentEntry>Folder Structure setup
begins</CommentEntry><PromptUserEntry Disabled="0" ItemText="1 2 3 4 "
VariableName="NumofDyes" PromptType="Number" TitleText="How many dyes do you wish to
image?" Constrain="1" PromptText="How many dyes do you wish to image?" DialogXPos="884"
DialogYPos="378" Min="1" Max="4"/><PromptUserEntry VariableName="Dye_1"
PromptType="String" TitleText="Enter the highest wavelength dye name" Constrain="0"
PromptText="Enter the highest wavelength dye/probe name first" DialogXPos="884"
DialogYPos="378"/><PromptUserEntry VariableName="Illumination" PromptType="RadioButton"
TitleText="Select Filter" Constrain="0" PromptText="Please Select the 1st Probe
Illumination Setting" DialogXPos="862" DialogYPos="357" ItemText="DAPI Cy 3 GFP Cy5
FITC mCherry "/><PromptUserEntry Disabled="0" VariableName="Cond1ExpTime"
PromptType="Number" TitleText="Select 1st Exposure Time" Constrain="1" PromptText="Enter
exposure time for 1st Probe" DialogXPos="884" DialogYPos="378" Min="10"
Max="100000"/><FunctionEntry GUID="{0x5e019877-0x37dc-0x48bd-0x8c-0x5-0xf9-0xd9-0x32-
0xd3-0xba-0x8a}" FunctionName="Create Directory" Interactive="0"
ApplicationName="journal" VersionNumber="1" Disabled="0" MissingImage="0" CommandID="1"
MetaJournal="00007FFA6DB6BD58" IsCurrentVersion="1"
Variables="00007FFA6DB6BAB8"><Variable Type="String"
Name="CreateDirectoryJNL.stCreateDirectory" NDimensions="0" Override=""
OverrideVariable="">64 %save_driver%\Syung-
Hun\%AcqDate%\%ExpConditions%\%Illumination%</Variable></FunctionEntry><IfThenElseEntry
Expression="NumofDyes > 1"><CodeBlock Condition="true"><PromptUserEntry
VariableName="Dye_2" PromptType="String" TitleText="Enter the 2nd highest wavelength
dye/probe name " Constrain="0" PromptText="Enter the 2nd highest wavelength dye/probe
name" DialogXPos="884" DialogYPos="378"/><PromptUserEntry VariableName="Illumination2"
PromptType="RadioButton" TitleText="Select Filter" Constrain="0" PromptText="Please
Select the 2nd Probe Illumination Setting" DialogXPos="862" DialogYPos="357"
ItemText="DAPI Cy 3 GFP Cy5 FITC mCherry "/><PromptUserEntry Disabled="0"
VariableName="Cond2ExpTime" PromptType="Number" TitleText="Select 2nd Exposure Time"
Constrain="1" PromptText="Enter exposure time for 2nd Probe/Antibody" DialogXPos="884"
DialogYPos="378" Min="10" Max="100000"/><FunctionEntry GUID="{0x5e019877-0x37dc-0x48bd-
0x8c-0x5-0xf9-0xd9-0x32-0xd3-0xba-0x8a}" FunctionName="Create Directory" Interactive="0"
ApplicationName="journal" VersionNumber="1" Disabled="0" MissingImage="0" CommandID="2"
MetaJournal="00007FFA6DB6BD58" IsCurrentVersion="1"
Variables="00007FFA6DB6BAB8"><Variable Type="String"
Name="CreateDirectoryJNL.stCreateDirectory" NDimensions="0" Override=""
OverrideVariable="">65 %save_driver%\Syung-
Hun\%AcqDate%\%ExpConditions%\%Illumination2%</Variable></FunctionEntry><IfThenElseEntry
Expression="NumofDyes > 2"><CodeBlock Condition="true"><PromptUserEntry
VariableName="Dye_3" PromptType="String" TitleText="Enter the 3rd highest wavelength
dye/probe name " Constrain="0" PromptText="Enter the 3rd highest wavelength dye/probe
name " DialogXPos="884" DialogYPos="378"/><PromptUserEntry VariableName="Illumination3"
PromptType="RadioButton" TitleText="Select Filter" Constrain="0" PromptText="Please
Select the 3rd Probe Illumination Setting" DialogXPos="862" DialogYPos="357"
ItemText="DAPI Cy 3 GFP Cy5 FITC mCherry "/><PromptUserEntry Disabled="0"
VariableName="Cond3ExpTime" PromptType="Number" TitleText="Select 3rd Exposure Time"
Constrain="1" PromptText="Enter exposure time for 3rd Probe/Antibody" DialogXPos="884"
DialogYPos="378" Min="10" Max="100000"/><FunctionEntry GUID="{0x5e019877-0x37dc-0x48bd-
0x8c-0x5-0xf9-0xd9-0x32-0xd3-0xba-0x8a}" FunctionName="Create Directory" Interactive="0"
ApplicationName="journal" VersionNumber="1" Disabled="0" MissingImage="0" CommandID="3"
MetaJournal="00007FFA6DB6BD58" IsCurrentVersion="1"

Variables="00007FFA6DB6BAB8"><Variable Type="String"
Name="CreateDirectoryJNL.stCreateDirectory" NDimensions="0" Override=""
OverrideVariable="">65 %save_driver%\Syung-
Hun\%AcqDate%\%ExpConditions%\%Illumination3%</Variable></FunctionEntry><IfThenElseEntry
Disabled="0" Expression="NumofDyes > 3"><CodeBlock Condition="true"><PromptUserEntry
VariableName="Dye_4" PromptType="String" TitleText="Enter the lowest wavelength dye/probe
name " Constrain="0" PromptText="Enter the lowest wavelength dye/probe name "
DialogXPos="884" DialogYPos="378"/><PromptUserEntry VariableName="Illumination4"
PromptType="RadioButton" TitleText="Select Filter" Constrain="0" PromptText="Please
Select the 4th Probe Illumination Setting" DialogXPos="862" DialogYPos="357"
ItemText="DAPI Cy 3 GFP Cy5 FITC mCherry "/><PromptUserEntry Disabled="0"
VariableName="Cond4ExpTime" PromptType="Number" TitleText="Select 4th Exposure Time"
Constrain="1" PromptText="Enter exposure time for 4th Probe/Antibody" DialogXPos="884"
DialogYPos="378" Min="10" Max="100000"/><FunctionEntry GUID="{0x5e019877-0x37dc-0x48bd-
0x8c-0x5-0xf9-0xd9-0x32-0xd3-0xba-0x8a}" FunctionName="Create Directory" Interactive="0"
ApplicationName="journal" VersionNumber="1" Disabled="0" MissingImage="0" CommandID="4"
MetaJournal="00007FFA6DB6BD58" IsCurrentVersion="1"
Variables="00007FFA6DB6BAB8"><Variable Type="String"
Name="CreateDirectoryJNL.stCreateDirectory" NDimensions="0" Override=""
OverrideVariable="">65 %save_driver%\Syung-
Hun\%AcqDate%\%ExpConditions%\%Illumination4%</Variable></FunctionEntry></CodeBlock><Code
Block Condition="false"/></IfThenElseEntry></CodeBlock><CodeBlock
Condition="false"/></IfThenElseEntry></CodeBlock><CodeBlock
Condition="false"/></IfThenElseEntry></CodeBlock></Journal>

Chamber_Imaging_Setup_Script.JNL

<Journal><Description>New Journal</Description><Version
VersionNumber="2.4"/><CodeBlock><AssignVariableEntry VariableName="camera_length"
Expression="1331.2"/><PromptUserEntry VariableName="device_length" PromptType="Number"
TitleText="Enter the length of the device (down one of the chambers) (mm)" Constrain="1"
PromptText="Enter the length of the device. This is the legnth of one of the chambers in
milimeters (max 44.4082)" DialogXPos="743" DialogYPos="322" Min="2.6624"
Max="44.4082"/><AssignVariableEntry VariableName="length_steps" Expression="CEILING(
(device_length*1000)/camera_length)"/><PromptUserEntry VariableName="num_chambers"
PromptType="Number" TitleText="Please enter the number of chambers" Constrain="1"
PromptText="Enter the number of chambers you wish to image." DialogXPos="743"
DialogYPos="322" Min="1" Max="25"/><AssignVariableEntry VariableName="num_chambers"
Expression="num_chambers - 1"/><PromptUserEntry VariableName="between_chambers"
PromptType="Number" TitleText="Please enter distance between chambers" Constrain="1"
PromptText="Enter distance between chambers in milimeters. (max 12.2269mm)"
DialogXPos="743" DialogYPos="322" Min="0" Max="12.2269"/><PromptUserEntry
VariableName="between_chambers_sets" PromptType="Number" TitleText="Please enter distance
between chambers sets" Constrain="1" PromptText="Enter distance between chambers in
milimeters. (max 12.2269mm)" DialogXPos="743" DialogYPos="322" Min="0"
Max="12.2269"/><PromptUserEntry VariableName="chambers_in_set" PromptType="Number"
TitleText="How many chambers in a set?" Constrain="0" PromptText="Please enter how many
chambers you have set?" DialogXPos="743" DialogYPos="322"/><AssignVariableEntry
VariableName="chamber_steps" Expression="between_chambers*1000"
Disabled="0"/><AssignVariableEntry VariableName="chamber_set_steps"
Expression="between_chambers*1000" Disabled="0"/></CodeBlock></Journal>

Chamber_Z_tilt_correction.JNL

<Journal><Description>New Journal</Description><Version
VersionNumber="2.4"/><CodeBlock><AssignVariableEntry VariableName="final_distance"
Expression="length_steps*camera_length" Disabled="0"/><AssignVariableEntry
VariableName="final_distance_Y"
Expression="(num_chambers_sets+1)*chamber_steps+num_chambers_sets*chamber_set_steps"
Disabled="0"/><FunctionEntry GUID="{0x3cef1e92-0xe09c-0x11d3-0x93-0x9a-0x0-0x10-0x5a-0x4-
0x2f-0x99}" FunctionName="Move Stage to Absolute Position" Interactive="0"
ApplicationName="mmproc" VersionNumber="1" CommandID="1" Disabled="0" MissingImage="0"
MetaJournal="0C360268" IsCurrentVersion="1" Variables="0C3600BC"><Variable Type="Double"
Name="jnlMoveStageAbs.dpX" NDimensions="0" Override="Variable"
OverrideVariable="pos_X_1">-221.6</Variable><Variable Type="Double"
Name="jnlMoveStageAbs.dpY" NDimensions="0" Override="Variable"
OverrideVariable="pos_Y_1">6.1</Variable><Variable Type="Double"

Name="jnlMoveStageAbs.dpZ" NDimensions="0" Override="Variable"
OverrideVariable="pos_Z_1">16218.5</Variable></FunctionEntry><FunctionEntry
GUID="{0x79f510e1-0xe09c-0x11d3-0x93-0x9a-0x0-0x10-0x5a-0x4-0x2f-0x99}"
FunctionName="Show Message and Wait" Interactive="0" ApplicationName="journal"
VersionNumber="1" CommandID="2" Disabled="0" MissingImage="0" MetaJournal="0D642F40"
IsCurrentVersion="1" Variables="0D642D94"><Variable Type="Integer"
Name="ShowMessageJNL.nDisplay" NDimensions="0" Override=""
OverrideVariable="">3</Variable><Variable Type="Integer" Name="ShowMessageJNL.iTimeout"
NDimensions="0" Override="" OverrideVariable="">26</Variable><Variable Type="Logical"
Name="ShowMessageJNL.bUseTimeout" NDimensions="0" Override=""
OverrideVariable="">FALSE</Variable><Variable Type="String" Name="ShowMessageJNL.stTitle"
NDimensions="0" Override="" OverrideVariable="">29 Make sure chamber is in
focus</Variable><Variable Type="String" Name="ShowMessageJNL.stMessage" NDimensions="0"
Override="" OverrideVariable="">95 Please make sure chamber is in focus under
Brightfield, then press "OK" to record Z-coordinates</Variable><Variable Type="Integer"
Name="ShowMessageJNL.msgX" NDimensions="0" Override=""
OverrideVariable="">539</Variable><Variable Type="Integer" Name="ShowMessageJNL.msgY"
NDimensions="0" Override=""
OverrideVariable="">221</Variable></FunctionEntry><AssignVariableEntry
VariableName="pos_X_1" Expression="Device.Stage.XPosition "
Disabled="0"/><AssignVariableEntry VariableName="pos_Y_1"
Expression="Device.Stage.YPosition " Disabled="0"/><AssignVariableEntry
VariableName="pos_Z_BF" Expression="Device.Focus.CurPos "
Disabled="0"/><AssignVariableEntry VariableName="pos_X_final" Expression="pos_X_1 -
final_distance" Disabled="0"/><FunctionEntry GUID="{0x3cef1e92-0xe09c-0x11d3-0x93-0x9a-
0x0-0x10-0x5a-0x4-0x2f-0x99}" FunctionName="Move Stage to Absolute Position"
Interactive="0" ApplicationName="mmproc" VersionNumber="1" CommandID="3" Disabled="0"
MissingImage="0" MetaJournal="0C360268" IsCurrentVersion="1"
Variables="0C3600BC"><Variable Type="Double" Name="jnlMoveStageAbs.dpX" NDimensions="0"
Override="Variable" OverrideVariable="pos_X_final">-3697.3</Variable><Variable
Type="Double" Name="jnlMoveStageAbs.dpY" NDimensions="0" Override="Variable"
OverrideVariable="pos_Y_1">-4026.8</Variable><Variable Type="Double"
Name="jnlMoveStageAbs.dpZ" NDimensions="0" Override="Variable"
OverrideVariable="pos_Z_1">18289.4</Variable></FunctionEntry><FunctionEntry
GUID="{0x79f510e1-0xe09c-0x11d3-0x93-0x9a-0x0-0x10-0x5a-0x4-0x2f-0x99}"
FunctionName="Show Message and Wait" Interactive="0" ApplicationName="journal"
VersionNumber="1" CommandID="4" Disabled="0" MissingImage="0" MetaJournal="0D642F40"
IsCurrentVersion="1" Variables="0D642D94"><Variable Type="Integer"
Name="ShowMessageJNL.nDisplay" NDimensions="0" Override=""
OverrideVariable="">3</Variable><Variable Type="Integer" Name="ShowMessageJNL.iTimeout"
NDimensions="0" Override="" OverrideVariable="">26</Variable><Variable Type="Logical"
Name="ShowMessageJNL.bUseTimeout" NDimensions="0" Override=""
OverrideVariable="">FALSE</Variable><Variable Type="String" Name="ShowMessageJNL.stTitle"
NDimensions="0" Override="" OverrideVariable="">29 Make sure chamber is in
focus</Variable><Variable Type="String" Name="ShowMessageJNL.stMessage" NDimensions="0"
Override="" OverrideVariable="">77 Please make sure chamber is in focus, then press "OK"
to record Z-coordinates</Variable><Variable Type="Integer" Name="ShowMessageJNL.msgX"
NDimensions="0" Override="" OverrideVariable="">539</Variable><Variable Type="Integer"
Name="ShowMessageJNL.msgY" NDimensions="0" Override=""
OverrideVariable="">221</Variable></FunctionEntry><AssignVariableEntry
VariableName="pos_Z_final_in" Expression="Device.Focus.CurPos "
Disabled="0"/><AssignVariableEntry VariableName="z_tilt" Expression="pos_Z_1 -
pos_Z_final_in" Disabled="0"/><AssignVariableEntry VariableName="z_tilt_rate"
Expression="z_tilt / (device_length*1000)" Disabled="0"/><AssignVariableEntry
VariableName="dzdx_chamber" Expression="z_tilt_rate" Disabled="0"/><FunctionEntry
GUID="{0x79f510e1-0xe09c-0x11d3-0x93-0x9a-0x0-0x10-0x5a-0x4-0x2f-0x99}"
FunctionName="Show Message and Wait" Interactive="0" ApplicationName="journal"
VersionNumber="1" CommandID="5" Disabled="0" MissingImage="0" MetaJournal="0D642F40"
IsCurrentVersion="1" Variables="0D642D94"><Variable Type="Integer"
Name="ShowMessageJNL.nDisplay" NDimensions="0" Override=""
OverrideVariable="">3</Variable><Variable Type="Integer" Name="ShowMessageJNL.iTimeout"
NDimensions="0" Override="" OverrideVariable="">26</Variable><Variable Type="Logical"
Name="ShowMessageJNL.bUseTimeout" NDimensions="0" Override=""
OverrideVariable="">FALSE</Variable><Variable Type="String" Name="ShowMessageJNL.stTitle"
NDimensions="0" Override="" OverrideVariable="">29 Make sure chamber is in
focus</Variable><Variable Type="String" Name="ShowMessageJNL.stMessage" NDimensions="0"
Override="" OverrideVariable="">86 Please make sure chamber is in correct Y-axis, then
press "OK" to record Z-coordinates</Variable><Variable Type="Integer"

Name="ShowMessageJNL.msgX" NDimensions="0" Override=""
OverrideVariable="">539</Variable><Variable Type="Integer" Name="ShowMessageJNL.msgY"
NDimensions="0" Override=""
OverrideVariable="">221</Variable></FunctionEntry><AssignVariableEntry
VariableName="pos_Y_final_in" Expression="Device.Stage.YPosition"
Disabled="0"/><AssignVariableEntry VariableName="y_tilt" Expression="pos_Y_1 -
pos_Y_final_in" Disabled="0"/><AssignVariableEntry VariableName="y_tilt_rate"
Expression="y_tilt / (device_length*1000)" Disabled="0"/><AssignVariableEntry
VariableName="dydx_chamber" Expression="y_tilt_rate" Disabled="0"/><AssignVariableEntry
VariableName="pos_Y_8th" Expression="pos_Y_1 - final_distance_Y"
Disabled="0"/><FunctionEntry GUID="{0x3cef1e92-0xe09c-0x11d3-0x93-0x9a-0x0-0x10-0x5a-0x4-
0x2f-0x99}" FunctionName="Move Stage to Absolute Position" Interactive="0"
ApplicationName="mmproc" VersionNumber="1" CommandID="6" Disabled="0" MissingImage="0"
MetaJournal="0C360268" IsCurrentVersion="1" Variables="0C3600BC"><Variable Type="Double"
Name="jnlMoveStageAbs.dpX" NDimensions="0" Override="Variable"
OverrideVariable="pos_X_1">-3697.3</Variable><Variable Type="Double"
Name="jnlMoveStageAbs.dpY" NDimensions="0" Override="Variable"
OverrideVariable="pos_Y_8th">-4026.8</Variable><Variable Type="Double"
Name="jnlMoveStageAbs.dpZ" NDimensions="0" Override="Variable"
OverrideVariable="pos_Z_1">18289.4</Variable></FunctionEntry><FunctionEntry
GUID="{0x79f510e1-0xe09c-0x11d3-0x93-0x9a-0x0-0x10-0x5a-0x4-0x2f-0x99}"
FunctionName="Show Message and Wait" Interactive="0" ApplicationName="journal"
VersionNumber="1" CommandID="7" Disabled="0" MissingImage="0" MetaJournal="0D642F40"
IsCurrentVersion="1" Variables="0D642D94"><Variable Type="Integer"
Name="ShowMessageJNL.nDisplay" NDimensions="0" Override=""
OverrideVariable="">3</Variable><Variable Type="Integer" Name="ShowMessageJNL.iTimeout"
NDimensions="0" Override="" OverrideVariable="">26</Variable><Variable Type="Logical"
Name="ShowMessageJNL.bUseTimeout" NDimensions="0" Override=""
OverrideVariable="">FALSE</Variable><Variable Type="String" Name="ShowMessageJNL.stTitle"
NDimensions="0" Override="" OverrideVariable="">29 Make sure chamber is in
focus</Variable><Variable Type="String" Name="ShowMessageJNL.stMessage" NDimensions="0"
Override="" OverrideVariable="">77 Please make sure chamber is in focus, then press "OK"
to record Z-coordinates</Variable><Variable Type="Integer" Name="ShowMessageJNL.msgX"
NDimensions="0" Override="" OverrideVariable="">539</Variable><Variable Type="Integer"
Name="ShowMessageJNL.msgY" NDimensions="0" Override=""
OverrideVariable="">221</Variable></FunctionEntry><AssignVariableEntry
VariableName="pos_Z_final_in" Expression="Device.Focus.CurPos "
Disabled="0"/><AssignVariableEntry VariableName="z_tilt" Expression="pos_Z_1 -
pos_Z_final_in" Disabled="0"/><AssignVariableEntry VariableName="z_tilt_rate_y"
Expression="z_tilt / (final_distance_Y)" Disabled="0"/><AssignVariableEntry
VariableName="dzdy_chamber" Expression="z_tilt_rate_y" Disabled="0"/><FunctionEntry
GUID="{0x79f510e1-0xe09c-0x11d3-0x93-0x9a-0x0-0x10-0x5a-0x4-0x2f-0x99}"
FunctionName="Show Message and Wait" Interactive="0" ApplicationName="journal"
VersionNumber="1" CommandID="8" Disabled="0" MissingImage="0" MetaJournal="0D642F40"
IsCurrentVersion="1" Variables="0D642D94"><Variable Type="Integer"
Name="ShowMessageJNL.nDisplay" NDimensions="0" Override=""
OverrideVariable="">3</Variable><Variable Type="Integer" Name="ShowMessageJNL.iTimeout"
NDimensions="0" Override="" OverrideVariable="">26</Variable><Variable Type="Logical"
Name="ShowMessageJNL.bUseTimeout" NDimensions="0" Override=""
OverrideVariable="">FALSE</Variable><Variable Type="String" Name="ShowMessageJNL.stTitle"
NDimensions="0" Override="" OverrideVariable="">29 Make sure chamber is in
focus</Variable><Variable Type="String" Name="ShowMessageJNL.stMessage" NDimensions="0"
Override="" OverrideVariable="">81 Please make sure chamber is in correct X, then press
"OK" to record Z-coordinates</Variable><Variable Type="Integer"
Name="ShowMessageJNL.msgX" NDimensions="0" Override=""
OverrideVariable="">539</Variable><Variable Type="Integer" Name="ShowMessageJNL.msgY"
NDimensions="0" Override=""
OverrideVariable="">221</Variable></FunctionEntry><AssignVariableEntry
VariableName="pos_X_final_in" Expression="Device.Stage.XPosition"
Disabled="0"/><AssignVariableEntry VariableName="x_tilt" Expression="pos_X_1 -
pos_X_final_in" Disabled="0"/><AssignVariableEntry VariableName="x_tilt_rate"
Expression="x_tilt / (final_distance_Y)" Disabled="0"/><AssignVariableEntry
VariableName="dxdy_chamber" Expression="x_tilt_rate" Disabled="0"/><AssignVariableEntry
VariableName="pos_X_curr" Expression="pos_X_1 - final_distance"
Disabled="1"/><AssignVariableEntry VariableName="pos_Y_curr" Expression="pos_Y_1 - ((-
final_distance) * dydx_chamber)" Disabled="1"/><AssignVariableEntry
VariableName="pos_Z_curr" Expression="pos_Z_1 + (dzdx_chamber*(-final_distance)) +
(dzdy_chamber*(pos_Y_1-pos_Y_curr))" Disabled="1"/><FunctionEntry GUID="{0x3cef1e92-

```
0xe09c-0x11d3-0x93-0x9a-0x0-0x10-0x5a-0x4-0x2f-0x99}" FunctionName="Move Stage to
Absolute Position" Interactive="0" ApplicationName="mmproc" VersionNumber="1"
MissingImage="0" Disabled="1" CommandID="9" MetaJournal="0C360268" IsCurrentVersion="1"
Variables="0C3600BC"><Variable Type="Double" Name="jnlMoveStageAbs.dpX" NDimensions="0"
Override="Variable" OverrideVariable="pos_X_curr">-3697.3</Variable><Variable
Type="Double" Name="jnlMoveStageAbs.dpY" NDimensions="0" Override="Variable"
OverrideVariable="pos_Y_curr">-4026.8</Variable><Variable Type="Double"
Name="jnlMoveStageAbs.dpZ" NDimensions="0" Override="Variable"
OverrideVariable="pos_Z_curr">18289.4</Variable></FunctionEntry></CodeBlock></Journal>
```

A01_Automation_Python.py

```
import os
import glob
import shutil
import time

# FIX THIS LINE ##########################
root_directory = "C:/Syung-Hun/2020-06-26/pHrodo_Endo_6NBDG/"
loop = 240
rnd = 40
filebasename1 = "Brightfield_10msec_image_"
filebasename2 = "DAPI_10msec_image_"
filebasename3 = "GFP_GFP_10msec_image_"
filebasename4 = "Cy 3_Cy3_50msec_image_"
##########################################

directory1 = root_directory + "Brightfield/"
directory2 = root_directory + "DAPI/"
directory3 = root_directory + "GFP/"
directory4 = root_directory + "Cy 3/"
# directory path for the files to be sorted out
movedirectory1 = directory1
movedirectory2 = directory2
movedirectory3 = directory3
movedirectory4 = directory4
padding = 5
startnumber = 1

try:
    os.mkdir(root_directory+"Analytical Model Fitting")
except OSError:
    if not os.path.isdir(root_directory+"Analytical Model Fitting"):
        raise
try:
    os.mkdir(root_directory+"Analysis Code")
except OSError:
    if not os.path.isdir(root_directory+"Analysis Code"):
        raise
try:
    os.mkdir(root_directory+"DAPI Analysis")
except OSError:
    if not os.path.isdir(root_directory+"DAPI Analysis"):
        raise
try:
    os.mkdir(root_directory+"DAPI+BF")
except OSError:
    if not os.path.isdir(root_directory+"DAPI+BF"):
        raise
try:
    os.mkdir(root_directory+"GFP ImageJ Analysis")
except OSError:
    if not os.path.isdir(root_directory+"GFP ImageJ Analysis"):
        raise
try:
    os.mkdir(root_directory+"Cy 3 ImageJ Analysis")
except OSError:
```

```
    if not os.path.isdir(root_directory+"Cy 3 ImageJ Analysis"):
        raise

os.chdir(directory1)
while os.path.exists(directory1+filebasename1+str(loop)+".tif") == 0:
    time.sleep(60)
else:
    for file in os.listdir(directory1):
        newname = file.replace(filebasename1, "").replace(".tif", "")
        newname = newname.zfill(padding)
        print(newname)
        new_filename = filebasename1 + newname + ".tif"
        os.rename(os.path.join(directory1, file), os.path.join(directory1, new_filename))
    for x in range(0, loop):
        try:
            os.mkdir(movedirectory1+"Position "+str(x).zfill(3))
        except OSError:
            if not os.path.isdir(movedirectory1+"Position "+str(x).zfill(3)):
                raise
    for file in glob.glob("*.tif"):
        newname = file.replace(filebasename1, "").replace(".tif", "")
        newname = int(newname)
        folder = (newname-startnumber) % loop
        newmovedirectory = movedirectory1+"Position " + str(folder).zfill(3) + "/"
        fullpathold = directory1+file
        fullpathnew = newmovedirectory+file
        print(newname)
        shutil.move(fullpathold, fullpathnew)
    os.chdir(root_directory)
    open('BF_Padding_Locating_Done', 'a').close()

os.chdir(directory2)
while os.path.exists(directory2+filebasename2+str(loop)+".tif") == 0:
    time.sleep(60)
else:
    for file in os.listdir(directory2):
        newname = file.replace(filebasename2, "").replace(".tif", "")
        newname = newname.zfill(padding)
        print(newname)
        new_filename = filebasename2 + newname + ".tif"
        os.rename(os.path.join(directory2, file), os.path.join(directory2, new_filename))
    for x in range(0, loop):
        try:
            os.mkdir(movedirectory2+"Position "+str(x).zfill(3))
        except OSError:
            if not os.path.isdir(movedirectory2+"Position "+str(x).zfill(3)):
                raise
    for file in glob.glob("*.tif"):
        newname = file.replace(filebasename2, "").replace(".tif", "")
        newname = int(newname)
        folder = (newname-startnumber) % loop
        newmovedirectory = movedirectory2+"Position " + str(folder).zfill(3) + "/"
        fullpathold = directory2+file
        fullpathnew = newmovedirectory+file
        print(newname)
        shutil.move(fullpathold, fullpathnew)
    os.chdir(root_directory)
    open('DAPI_Padding_Locating_Done', 'a').close()

os.chdir(directory3)
while os.path.exists(directory3+filebasename3+str(loop*rnd)+".tif") == 0:
    time.sleep(60)
else:
    for file in os.listdir(directory3):
        newname = file.replace(filebasename3, "").replace(".tif", "")
        newname = newname.zfill(padding)
        print(newname)
        new_filename = filebasename3 + newname + ".tif"
```

```
        os.rename(os.path.join(directory3, file), os.path.join(directory3, new_filename))
    for x in range(0, loop):
        try:
            os.mkdir(movedirectory3+"Position "+str(x).zfill(3))
        except OSError:
            if not os.path.isdir(movedirectory3+"Position "+str(x).zfill(3)):
                raise
    for file in glob.glob("*.tif"):
        newname = file.replace(filebasename3, "").replace(".tif", "")
        newname = int(newname)
        folder = (newname-startnumber) % loop
        newmovedirectory = movedirectory3+"Position " + str(folder).zfill(3) + "/"
        fullpathold = directory3+file
        fullpathnew = newmovedirectory+file
        print(newname)
        shutil.move(fullpathold, fullpathnew)
    os.chdir(root_directory)
    open('GFP_Padding_Locating_Done', 'a').close()

os.chdir(directory4)
while os.path.exists(directory4+filebasename4+str(loop*rnd)+".tif") == 0:
    time.sleep(60)
else:
    for file in os.listdir(directory4):
        newname = file.replace(filebasename4, "").replace(".tif", "")
        newname = newname.zfill(padding)
        print(newname)
        new_filename = filebasename4 + newname + ".tif"
        os.rename(os.path.join(directory4, file), os.path.join(directory4, new_filename))
    for x in range(0, loop):
        try:
            os.mkdir(movedirectory4+"Position "+str(x).zfill(3))
        except OSError:
            if not os.path.isdir(movedirectory4+"Position "+str(x).zfill(3)):
                raise
    for file in glob.glob("*.tif"):
        newname = file.replace(filebasename4, "").replace(".tif", "")
        newname = int(newname)
        folder = (newname-startnumber) % loop
        newmovedirectory = movedirectory4+"Position " + str(folder).zfill(3) + "/"
        fullpathold = directory4+file
        fullpathnew = newmovedirectory+file
        print(newname)
        shutil.move(fullpathold, fullpathnew)
    os.chdir(root_directory)
    open('Cy 3_Padding_Locating_Done', 'a').close()
```

A02_ImageJ_Automation.ijm

```
/* This code allows automation of RGB merge, BF_FL overlay and Combine macros after
waiting for certain time*/
macro "Automation"{
   setBatchMode("hide");
   //**********FIX THIS LINE********AND PUT SEMICOLON AT THE END OF ALL***//
   root_directory = "C:/Syung-Hun/2020-06-26/pHrodo_Endo_6NBDG/";
   loop = 240;
   rnd = 40;
   file1 = "Brightfield"
   file2 = "DAPI"
   file3 = "GFP"
   file4 = "Cy 3"
   filebasename1 = file1 + "_10msec_image_";
   filebasename2 = file2 + "_10msec_image_";
   filebasename3 = file3 + "_GFP_10msec_image_";
   filebasename4 = file4 + "_Cy3_50msec_image_";
   //**********FIX THIS LINE********AND PUT SEMICOLON AT THE END OF ALL***//
   directory1 = root_directory + file1 + "/";
```

```
   directory2 = root_directory + file2 + "/";
   directory3 = root_directory + file3 + "/";
   directory4 = root_directory + file4 + "/";
   while (File.exists(root_directory+"BF_Padding_Locating_Done")==0){
      print("Waiting for another 1 min");
      wait(60000);
   }
   print("BF_Padding_Locating_Done Exists");
   while (File.exists(root_directory+file2+"_Padding_Locating_Done")==0){
      print("Waiting for another 1 min");
      wait(60000);
   }
   print(file2+"_Padding_Locating_Done Exists");
   print("BF_FL Overlay ("+file2+" Analysis) started");

   if (File.exists(root_directory+file2+" Analysis/Position "+(loop-1)+"
Outline.jpg")==1){
      analysis = getNumber("Would you like to perform "+file2+" analysis again? If yes,
type 1, if not, type 0",1);
   } else {
      analysis = 1;
   }
   if (analysis == 1){
      masterDir = root_directory+file2+"/";
      masterList = getFileList(masterDir);
      Array.sort(masterList);
      output = root_directory+file2+" Analysis/";
      for (j=0; j<masterList.length; j++){
         subDir=masterDir + masterList[j];
         subList=getFileList(subDir);
         run("Image Sequence...", "open=["+subDir+"] sort");
         name=masterList[j];
         savename=name;
         title=getTitle();
         savename=replace(savename,"/","");
         print(savename);
         run("Subtract Background...", "rolling=10 sliding");
         run("Subtract Background...", "rolling=10 sliding");
         //run("Enhance Contrast...", "saturated=0.1");
         setAutoThreshold("RenyiEntropy dark");
         run("Analyze Particles...", "size=10-Infinity show=Outlines clear include
stack");
         a=getTitle();
         saveAs("Results", output+savename+".csv");
         selectWindow(a);
         a = replace(a,"Drawing of ","");
         a = replace(a,root_directory+file2+"/","");
         b=" Outline.jpg";
         saveAs("Jpeg", output+a+b);
         run("Close");
         run("Red");
         run("Scale Bar...", "width=231 height=15 font=18 color=White background=None
location=[Lower Right] hide overlay label");
         saveAs("Jpeg", output+savename+".jpg");
         run("Close All");
      }
      run("Close All");
   }
   print("BF_FL Overlay ("+file2+" Analysis) completed");

   print("RGB_Merge (BF+"+file2+") started");

   padloop = IJ.pad(loop,5);
   if (File.exists(root_directory+file2+"+BF/"+padloop+padloop+".jpg")==1){
      analysis = getNumber("Would you like to perform "+file2+"+BF again? If yes, type 1,
if not, type 0",1);
   } else {
      analysis = 1;
```

```
   }
   if (analysis == 1){
               masterDir = root_directory+file2+"/";
          masterList = getFileList(masterDir);
      Array.sort(masterList);
      masterDir3 = root_directory+"Brightfield/";
      masterList3 = getFileList(masterDir3);
      Array.sort(masterList3);
      output = root_directory+file2+"+BF/";
         for (j=0; j<masterList.length; j++){
         subDir=masterDir + masterList[j];
         subList=getFileList(subDir);
         subDir3=masterDir3+masterList3[j];
         subList3=getFileList(subDir3);
         for (i=0; i<subList.length; i++){
            subsubDir=masterDir+masterList[j]+subList[i];
            subsubList=getFileList(subsubDir);
            open(subsubDir);
            a=getTitle();
            run("Subtract Background...", "rolling=10");
            run("Enhance Contrast...", "saturated=0.00");
            subsubDir3=masterDir3+masterList3[j]+subList3[i];
            subsubList=getFileList(subsubDir3);
            open(subsubDir3);
            c=getTitle();
            run("Merge Channels...", "c1=["+a+"] c4=["+c+"]");
            a=replace(a,filebasename2,"");
            a=replace(a,".tif","");
            c=replace(c,filebasename1,"");
            c=replace(c,".tif","");
            savename=a+c;
            run("Scale Bar...", "width=231 height=15 font=18 color=White background=None
location=[Lower Right] hide overlay label");
            saveAs("Jpeg", output+savename+".jpg");
            run("Close All");
          }
      run("Close All");
      }
   }
   print("RGB_Merge (BF+"+file2+") completed");
}
```

A03_GFP_Analysis.ijm

```
macro "Histogram"{
   setBatchMode("hide");
   //**********FIX THIS LINE********AND PUT SEMICOLON AT THE END OF ALL***//
   root_directory = "C:/Syung-Hun/2020-06-26/pHrodo_Endo_6NBDG/";
   loop = 240;
   rnd = 40;
   file1 = "Brightfield"
   file2 = "DAPI"
   file3 = "GFP"
   file4 = "Cy 3"
   filebasename1 = file1 + "_10msec_image_";
   filebasename2 = file2 + "_10msec_image_";
   filebasename3 = file3 + "_GFP_10msec_image_";
   filebasename4 = file4 + "_Cy3_50msec_image_";
   time_interval = 461;
   //**********FIX THIS LINE********AND PUT SEMICOLON AT THE END OF ALL***//
   directory1 = root_directory + file1 + "/";
   directory2 = root_directory + file2 + "/";
   directory3 = root_directory + file3 + "/";
   directory4 = root_directory + file4 + "/";
   while (File.exists(root_directory+file3+"_Padding_Locating_Done")==0){
      wait(60000);
      print("Waiting "+file3+" for 1 min...");
```

```
   }
   print(file3+"_Padding_Locating_Done Exists");
   print("Combine "+file3+" (ImageJ Analysis) started");
   if (File.exists(root_directory+file3+" ImageJ Analysis/Position "+(loop-
1)+".avi")==1){
      analysis = getNumber("Would you like to perform "+file3+" ImageJ analysis again? If
yes, type 1, if not, type 0",1);
   } else {
      analysis = 1;
   }
   if (analysis == 1){
      masterDir = root_directory+file3+"/";
      masterList = getFileList(masterDir);
      output = root_directory+file3+" ImageJ Analysis/";
      Array.sort(masterList);
      image_anal_num = rnd;
   }
   for (k=0; k<masterList.length; k++){
      subDir = masterDir + masterList[k];
      subList = getFileList(subDir);
      run("Image Sequence...", "open=["+subDir+"] number=["+image_anal_num+"] sort");
      a = getTitle();
      a = replace(a,filebasename3,"Pos_");
      a = replace(a,".tiff","");
      name=masterList[k];
      csvname=name;
      csvname=replace(csvname,"/","");
      aviname=replace(name,"/",".avi");
      run("Scale Bar...", "width=57.75 height=15 font=18 color=White background=None
location=[Lower Right] hide overlay label");
      run("Label...", "format=00:00:00 starting=0 interval=time_interval x=5 y=20 font=18
text=[] range=1-500 use");
      run("AVI... ", "compression=JPEG frame=5 save=["+output+aviname+"]");
      print(aviname);
      print(output);
      setSlice(image_anal_num);
      setAutoThreshold("Default dark");
      run("Analyze Particles...", "size=1600-30000 clear include stack record");
      saveAs("Results", output+csvname+".csv");
      b = nResults;
      run("Grays");
      run("Clear Results");
      run("Close All");
   }
   print(file3+" Analysis all done");

   while (File.exists(root_directory+file4+"_Padding_Locating_Done")==0){
      wait(60000);
      print("Waiting "+file4+" for 1 min...");
   }
   print(file4+"_Padding_Locating_Done Exists");
   print("Combine "+file4+" (ImageJ Analysis) started");
   if (File.exists(root_directory+file4+" ImageJ Analysis/Position "+(loop-
1)+".avi")==1){
      analysis = getNumber("Would you like to perform "+file4+" ImageJ analysis again? If
yes, type 1, if not, type 0",1);
   } else {
      analysis = 1;
   }
   if (analysis == 1){
      masterDir = root_directory+file4+"/";
      masterList = getFileList(masterDir);
      output = root_directory+file4+" ImageJ Analysis/";
      Array.sort(masterList);
      image_anal_num = rnd;
   }
   for (k=0; k<masterList.length; k++){
      subDir = masterDir + masterList[k];
```

```
      subList = getFileList(subDir);
      run("Image Sequence...", "open=["+subDir+"] number=["+image_anal_num+"] sort");
      a = getTitle();
      a = replace(a,filebasename4,"Pos_");
      a = replace(a,".tiff","");
      name=masterList[k];
      csvname=name;
      csvname=replace(csvname,"/","");
      aviname=replace(name,"/",".avi");
      run("Scale Bar...", "width=57.75 height=15 font=18 color=White background=None
location=[Lower Right] hide overlay label");
      run("Label...", "format=00:00:00 starting=0 interval=time_interval x=5 y=20 font=18
text=[] range=1-500 use");
      run("AVI... ", "compression=JPEG frame=5 save=["+output+aviname+"]");
      print(aviname);
      print(output);
      setSlice(image_anal_num);
      setAutoThreshold("Huang dark");
      run("Analyze Particles...", "size=1600-30000 clear include stack record");
      saveAs("Results", output+csvname+".csv");
      b = nResults;
      run("Grays");
      run("Clear Results");
      run("Close All");
   }
   print(file4+" Analysis all done");
}
```

A05_Bong_0_Analysis.m

```
%% Basic Data Folder Calling
root_directory = "C:\Syung-Hun\2020-06-26\pHrodo_Endo_6NBDG/";
loop = 240;
rnd = 40;
drop_threshold = rnd-5; % important parameter to filter spots with less than certain
image_num
cd(root_directory);
main_image_folder = 'GFP';    % This is in case the MATLAB will be analyzing the tiff
files
image_folder = strcat(root_directory,'/',main_image_folder);
sub_main_image_folder = "Cy 3";    % This is in case the MATLAB will be analyzing the
tiff files
sub_image_folder = strcat(root_directory,'/',main_image_folder);
main_data_folder = 'GFP ImageJ Analysis';    % Change this between ImageJ and Metamorph
Analysis
sub_main_data_folder = 'Cy 3 ImageJ Analysis';    % Change this between ImageJ and
Metamorph Analysis
sub_sub_main_data_folder = 'Cy 3 ImageJ Analysis (new)';    % Change this between ImageJ
and Metamorph Analysis
pop1_folder = 'DAPI Analysis';      %Population marker analysis folder
graph_folder = 'Graph GFP ImageJ Analysis';
if ~exist(graph_folder,'dir')
    mkdir(root_directory,graph_folder);
end
graph_folder2 = 'Graph Cy 3 ImageJ Analysis';
if ~exist(graph_folder2,'dir')
    mkdir(root_directory,graph_folder2);
end
graph_folder3 = 'Graph Combined Analysis';
if ~exist(graph_folder3,'dir')
    mkdir(root_directory,graph_folder3);
end
if contains(main_data_folder,"Metamorph")==1
    z_max = 2;
    add_var = "";
end
if contains(main_data_folder,"ImageJ")==1
```

```
    z_max = 3;
    add_var = "median";
end
disp("Bong analysis 0 is done")
```

A06_Bong_1_Analysis.m

```
%% Calling on the folder for analysis and data conversion
if ~exist(strcat(root_directory,'/',main_data_folder,'/master_data'),'dir')
    mkdir(strcat(root_directory,'/',main_data_folder),'master_data');
end
currentFolder = strcat(root_directory,'/',main_data_folder);
cd(currentFolder);
%% ImageJ Analysis
if contains(main_data_folder,"ImageJ")==1
    list = dir(currentFolder);
    for j = 1:length(list)
        if contains(list(j).name,'Position')==1 && contains(list(j).name,'.csv')==1
            data = readtable(list(j).name);
            assert(height(data)>1000);
            data = data((data.Area>1600) & (data.Area<20000) & (data.Area >
(mean(data.Area)-7*std(data.Area))) &...
                (data.Area < (mean(data.Area)+7*std(data.Area))),:);
            data.Properties.VariableNames({'XM','YM'}) = {'X','Y'};
            list2 = ['X','Y'];
            for type=list2
                data.var = data.(type);
                data = sortrows(data,{'var','X','Y'});
                data.diff = data.Var1 * 0;
                data.diff(1) = NaN;
                data.diff(2:end) = data.var(2:end)-data.var(1:end-1);
                data.add = (data.diff > nanmean(data.diff) + 6 * nanstd(data.diff)) &
isnan(data.diff)==0;
                data.(strcat(type,'_num_temp')) = data.Var1 * 0;
                data.(strcat(type,'_num_temp'))(1) = 1;
                data.check = data.Var1 * 0;
data.(strcat(type,'_num_temp'))(2:end)=cummax(data.(strcat(type,'_num_temp'))(1:end-
1))+cumsum(data.add(2:end));
                for k = 1:max(data.(strcat(type,'_num_temp')))
                   data.check(data.(strcat(type,'_num_temp'))==k) =
sum(data.(strcat(type,'_num_temp'))==k);
                end
                approx = height(data) / max(data.(strcat(type,'_num_temp')));
                data = data(data.check > 0.4 * approx, :);
                data.diff2 = data.Var1 * 0;
                data.diff2(1) = NaN;
                data.diff2(2:end) = data.var(2:end)-data.var(1:end-1);
                data.add2 = (data.diff2 > nanmean(data.diff2) + 8 * nanstd(data.diff2)) &
isnan(data.diff2)==0;
                data.(strcat(type,'_num_temp2')) = data.Var1 * 0;
                data.(strcat(type,'_num_temp2'))(1) = 1;
                data.check2 = data.Var1 * 0;
data.(strcat(type,'_num_temp2'))(2:end)=cummax(data.(strcat(type,'_num_temp2'))(1:end-
1))+cumsum(data.add2(2:end));
                for k = 1:max(data.(strcat(type,'_num_temp2')))
                   data.check2(data.(strcat(type,'_num_temp2'))==k) =
sum(data.(strcat(type,'_num_temp2'))==k);
                end
                approx = height(data) / max(data.(strcat(type,'_num_temp2')));
                data = data(data.check2 > 0.5 * approx, :);
                data.diff3 = data.Var1 * 0;
                data.diff3(1) = NaN;
                data.diff3(2:end) = data.var(2:end)-data.var(1:end-1);
                data.add3 = (data.diff3 > nanmean(data.diff3) + 8 * nanstd(data.diff3)) &
isnan(data.diff3)==0;
                data.(strcat(type,'_num')) = data.Var1 * 0;
```

```
                data.(strcat(type,'_num'))(1) = 1;
data.(strcat(type,'_num'))(2:end)=cummax(data.(strcat(type,'_num'))(1:end-
1))+cumsum(data.add3(2:end));
                if type == 'X'
                    X_max = max(data.(strcat(type,'_num')));
                else
                    Y_max = max(data.(strcat(type,'_num')));
                end
                data.diff = [];
                data.diff2 = [];
                data.diff3 = [];
                data. add = [];
                data.add2 = [];
                data.add3 = [];
                data.check = [];
                data.check2 = [];
                data.(strcat(type,'_num_temp')) = [];
                data.(strcat(type,'_num_temp2')) = [];
            end
            data = sortrows(data,{'X_num','Y_num','Var1'});
            data.image_num = data.Var1 * 0;
            data.image_num(1:end) = cumsum(data.X_num(1:end) ~= 0);
            data.temp = data.Var1 * 0;
            data.temp(2:end) = cummax(data.image_num(2:end) .* ((data.X_num(1:end-1) ~=
data.X_num(2:end)) | (data.Y_num(1:end-1) ~= data.Y_num(2:end))));
            data.image_num(data.temp~=0) = data.image_num(data.temp~=0) -
data.temp(data.temp~=0) + 1;
            data.temp = [];
            data.Var1 = [];

            data_merge_mask = [];
            for i=1:X_max
                for k=1:Y_max
                    testdata=data((data.X_num==i & data.Y_num==k),:);
                    if height(testdata) >= (rnd*0.9)
                        data_merge_mask = vertcat(data_merge_mask,testdata);
                    end
                end
            end
            data = data_merge_mask;

            disp(list(j).name)
            if isempty(data)==0
                crosstab(data.Y_num,data.X_num)
            end
            if isempty(data)==1
            else
data.Properties.VariableNames({'Area','Mean','Min','Max','StdDev','Median'})...
 = {'area','average_intensity','min_intensity','max_intensity','sd_intensity','median'};
                data.zscore_maxintensity1 = (data.max_intensity -
data.average_intensity) ./ data.sd_intensity;
                data.zscore_maxintensity1(abs(data.zscore_maxintensity1)>10) = NaN;
                data.zscore_maxintensity2 = data.image_num * 0;
                data.x_minus_u = (data.max_intensity - data.average_intensity);
                for k = 1:max(data.image_num)
                    count_by_imagenum = sum(data.image_num==k);
                    totavg_by_imagenum = sum(data.average_intensity(data.image_num==k));
                    totsd_by_imagenum = sum(data.sd_intensity(data.image_num==k));
                    data.zscore_maxintensity2(data.image_num==k) = ...
                        (data.max_intensity(data.image_num==k) -
(totavg_by_imagenum/count_by_imagenum)) / (totsd_by_imagenum/count_by_imagenum);
                end
                data.zscore_maxintensity2(abs(data.zscore_maxintensity2)>10) = NaN;
                data.zscore_maxintensity3 = (data.max_intensity - data.median) ./
data.sd_intensity;
                data.zscore_maxintensity3(abs(data.zscore_maxintensity3)>10) = NaN;
```

```
                data.position = data.image_num * 0 +
str2double(strrep(strrep(strrep(list(j).name,".csv",""),"Position ","")...
                    ,"GFP_Data_Chamber_postition_",""),"_data",""));
                saveFolder = strcat(root_directory,'/',main_data_folder,'/master_data');
                writetable(data,
strcat(saveFolder,'/Position_',strrep(strrep(strrep(strrep(list(j).name,".csv",""),"Posit
ion ","")...
                    ,"GFP_Data_Chamber_postition_",""),"_data",""),'.csv'));
            end
        end
    end
end
disp("Bong analysis 1 is done")
```

A07_Bong_2_Analysis.m

```
% 1) POP1 and POP2 data to extract definite cell existence
saveFolder = strcat(root_directory,'/',main_data_folder,'/master_data');
list4 = dir(saveFolder);
cd(saveFolder);
if length(pop1_folder)>3
    if contains(pop1_folder,"Crude")
        max_popu=1;
        pop1_folder_dir = strcat(root_directory,'/',pop1_folder);
        if ~exist(pop1_folder_dir,'dir')
            mkdir(pop1_folder_dir);
        end
        cd(saveFolder);
        data_merge_mask = [];
        zscore_threshold = 1.3;
        for j=1:length(list4)
            if contains(list4(j).name,'Position')==1 &&
contains((list4(j).name),'.csv')==1
                data = readtable(list4(j).name);
                X_max = max(data.X_num); Y_max = max(data.Y_num);
                for q = 1:X_max
                    for p = 1:Y_max
                        testdata=data((data.X_num==q & data.Y_num==p),:);
                        if (max(testdata.zscore_maxintensity1)-
min(testdata.zscore_maxintensity1))>zscore_threshold
                            testdata.cellyes = ones(height(testdata),1);
testdata.object=[];testdata.total_area=[];testdata.PixelArea=[];testdata.area=[];testdata
.RelativeHoleArea=[];testdata.StandardAreaCount=[];testdata.average_intensity=[];testdata
.total_intensity=[];testdata.min_intensity=[];testdata.max_intensity=[];testdata.sd_inten
sity=[];testdata.x=[];testdata.y=[];testdata.RadialDispersion=[];testdata.CentroidX=[];te
stdata.CentroidY=[];testdata.Orientation=[];testdata.shape_factor=[];testdata.shape_lengt
h=[];testdata.shape_breadth=[];testdata.image_num=[];testdata.zscore_maxintensity1=[];tes
tdata.zscore_maxintensity2=[];testdata.x_minus_u=[];testdata=unique(testdata,'rows');
                            data_merge_mask = vertcat(data_merge_mask,testdata);
                        end
                    end
                end
                displayname=strcat("Now processing ",list4(j).name);
                disp(displayname)
            end
        end
        writetable(data_merge_mask, strcat(pop1_folder_dir,'/pop1_label_data.csv'));
    else
    %% Reorganizing Analysis files
        max_popu=1;
        pop1_folder_dir = strcat(root_directory,'/',pop1_folder);
        cd(pop1_folder_dir);
        oldfilefolder = 'Raw file';
        oldfilepath = strcat(pop1_folder_dir,'/',oldfilefolder);
        if ~exist(oldfilefolder,'dir')
            mkdir(pop1_folder_dir,oldfilefolder);
        end
```

```
        list1 = dir(pop1_folder_dir);
        for j = 1:length(list1)
            if contains(list1(j).name,".csv")==1 && contains(list1(j).name," ")==1
                newfile=strrep(list1(j).name," ","_");
                copyfile(list1(j).name,newfile);
                movefile(list1(j).name,oldfilepath);
            end
        end
        if contains(pop2_folder,'Analysis')==1
            max_popu=1;
            pop2_folder_dir = strcat(root_directory,'/',pop1_folder);
            cd(pop2_folder_dir);
            oldfilefolder = 'Raw file';
            oldfilepath = strcat(pop2_folder_dir,'/',oldfilefolder);
            if ~exist(oldfilefolder,'dir')
                mkdir(pop2_folder_dir,oldfilefolder);
            end
            list2 = dir(pop2_folder_dir);
            for j = 1:length(list2)
                if contains(list2(j).name,".csv")==1 && contains(list2(j).name," ")==1
                    newfile=strrep(list2(j).name," ","_");
                    copyfile(list2(j).name,newfile);
                    movefile(list2(j).name,oldfilepath);
                end
            end
        end
        for i = 1:max_popu
            count = 1;
            for j = 1:length(list4)
                cd(saveFolder);
                if contains(list4(j).name,'Position')==1 &&
contains(list4(j).name,'.csv')==1
                    data = readtable(list4(j).name);
                    data = sortrows(data,{'image_num','X_num'});
                    data = data(data.Round > 0.2,:);
                    x_mean = zeros(max(data.X_num),1);
                    y_mean = zeros(max(data.Y_num),1);
                    for k = 1:max(data.X_num)
                        x_mean(k) = mean(data.X(data.X_num==k));
                    end
                    for f = 1:max(data.Y_num)
                        y_mean(f) = mean(data.Y(data.Y_num==f));
                    end
                end
                cd(pop1_folder_dir);
                list1=dir(pop1_folder_dir);
                for k = 1:length(list1)
                    if contains(list1(k).name,'csv')==1
                        if length(list1(k).name)==length(list4(j).name)
                            if list1(k).name==list4(j).name
                                popdata = readtable(list1(k).name);
                                popdata.X_num = popdata.Var1 * 0;
                                popdata.Y_num = popdata.Var1 * 0;
                                for num = 1:max(popdata.Var1)
                                    compareX = abs(popdata.XM(popdata.Var1==num) -
x_mean);
                                    for p = 1:max(data.X_num)
                                        if abs(compareX(p)-min(compareX))<0.1
                                            popdata.X_num(popdata.Var1==num) = p;
                                        end
                                    end
                                    compareY = abs(popdata.YM(popdata.Var1==num) -
y_mean);
                                    for p = 1:max(data.Y_num)
                                        if abs(compareY(p)-min(compareY))<0.1
                                            popdata.Y_num(popdata.Var1==num) = p;
                                        end
                                    end
```

```
                                end
                                popdata.position = popdata.Var1*0 +
str2double(strrep(strrep(list1(k).name,"Position_",""),".csv",""));
                                popdata{:,28}=ones();
                                popdata.Properties.VariableNames({'Var28'})={'multiple'};
                                for i=1:height(popdata)
    if popdata(i,:).Area > 400 && popdata(i,:).Area < 800 && popdata(i,:).Round < 0.75
                                        popdata(i,:).multiple = 2;
                                    end
                                    if popdata(i,:).Area >= 900
                                        popdata(i,:).multiple = 2;
                                    end
                                   if popdata(i,:).Area > 200 && popdata(i,:).Round < 0.7
                                        popdata(i,:).multiple = 2;
                                    end
                                end
popdata.Var1=[];popdata.Area=[];popdata.Mean=[];popdata.StdDev=[];popdata.Min=[];popdata.
Max=[];popdata.XM=[];popdata.YM=[];popdata.Circ_=[];popdata.Feret=[];popdata.IntDen=[];po
pdata.Median=[];popdata.Kurt=[];popdata.x_Area=[];popdata.RawIntDen=[];popdata.Slice=[];p
opdata.FeretX=[];popdata.FeretY=[];popdata.FeretAngle=[];popdata.MinFeret=[];popdata.AR=[
];popdata.Round=[];popdata.Solidity=[];popdata.avgValue=[];
                                if count==1
                                    master_popdata = popdata;
                                else
                                    master_popdata = vertcat(master_popdata,popdata);
                                end
                                count = count+1;
                            end
                        end
                    end
                end
            end
            master_popdata = sortrows(master_popdata,{'X_num','Y_num','position'});
            count = 1;
            for i = 1:max(master_popdata.X_num)
                for j = 1:max(master_popdata.Y_num)
                    for k = 0:max(master_popdata.position)
                        temp_data = master_popdata(master_popdata.X_num == i &
master_popdata.Y_num == j & master_popdata.position == k,:);
                        if height(temp_data) > 1
                            temp_data.multiple = ones(height(temp_data),1)*2;
                        end
                        if count == 1
                            duplicate_master_popdata = temp_data;
                        else
                            duplicate_master_popdata =
vertcat(duplicate_master_popdata,temp_data);
                        end
                        count = count + 1;
                    end
                end
            end
            filtered_master_popdata=unique(duplicate_master_popdata,'rows');
            writetable(filtered_master_popdata,
strcat(pop1_folder_dir,'/pop1_label_data.csv'));
        end
    end
end
disp("Bong analysis 2 is done");
```

A08_Bong_3_Analysis.m

```
%root_directory = "/Users/syunghunhan/Desktop/Sample Data for Matlab/Data 1 (18-09-
07)/Metamorph Analysis/master_data";
master_directory = strcat(root_directory,'/',main_data_folder,'/master_data');
pop_file = readtable(strcat(root_directory,'/',pop1_folder,'/pop1_label_data.csv'));
cd(master_directory);
```

```
list = dir(master_directory);
data = [];
for i=1:length(list)
    if contains(list(i).name,"csv") && contains(list(i).name,"Position")
         temp_data=readtable(strcat(master_directory,'/',list(i).name));
         temp_pop_file = pop_file(pop_file.position == max(temp_data.position),:);
         mergedata_temp = innerjoin(temp_data,temp_pop_file);
         data = vertcat(data, mergedata_temp);
     end
end
savename = char("data.csv");
writetable(data,savename);
disp("Data File Generation Complete");
```

A09_Bong_4_Analysis.m

```
saveFolder = strcat(root_directory,'/',main_data_folder,'/master_data');
data_folder = strcat(root_directory,'/',main_data_folder,'/master_data');
list1 = dir(data_folder);
pop_data = readtable(strcat(root_directory,'/',pop1_folder,'/pop1_label_data.csv'));
data = readtable(strcat(root_directory,'/',main_data_folder,'/master_data/data.csv'));
data.x_over_u = data.avgValue ./ data.median;
for ztype={'x_over_u'}
    tic
    merge_data = double.empty(0,(rnd+4));
    for k=0:max(data.position)
        for i=1:max(data.X_num)
            for j=1:max(data.Y_num)
                data_temp = data(data.X_num == i & data.Y_num == j & data.position ==
k,:);
                if isempty(data_temp)==0
                    data_temp_transposed = data_temp.(string(ztype))';
                    data_temp_temp =
horzcat(data_temp.X_num(1,:),data_temp.Y_num(1,:),data_temp.position(1,:),data_temp_trans
posed);
                    data_temp_temp(1,rnd+4) = data_temp.multiple(1,:);
                    if length(data_temp_temp)<=(4+rnd)
                        merge_data = vertcat(merge_data, data_temp_temp);
                    end
                end
            end
        end
    end

    merge_data = array2table(merge_data);
merge_data.Properties.VariableNames({'merge_data1','merge_data2','merge_data3',strcat('me
rge_data',num2str(4+rnd))})={'X_num','Y_num','position','multiple'};
    toc

    merge_data_single = merge_data(merge_data.multiple == 1,:);
    merge_data_multiple = merge_data(merge_data.multiple > 1,:);
writetable(merge_data_single,strcat(data_folder,"/non_regression_data_",ztype,".csv"));
writetable(merge_data_multiple,strcat(data_folder,"/non_regression_data_for_multiple_cell
s_",ztype,".csv"));
end
disp("Non-regression data generation is done")
for ztype = {'x_over_u'}
    T = readtable(strcat(data_folder,"/non_regression_data_",ztype,".csv"));
    start_column_num = 4;
    end_column_num = rnd+3;
    smoothing_parameter = 0.2;
    T_presmooth = table2array(T(:,start_column_num:end_column_num));
    T_smooth = double.empty((end_column_num - start_column_num + 1),0);
    for i=1:length(T_presmooth)
        T_smooth(i,1:(end_column_num - start_column_num + 1)) =
smooth(T_presmooth(i,:),smoothing_parameter).';
    end
```

```
    T(:,start_column_num:end_column_num) = array2table(T_smooth);
    writetable(T,strcat(data_folder,"/smooth_non_regression_data_",ztype,".csv"));
end
for ztype = {'x_over_u'}
    T =
readtable(strcat(data_folder,"/non_regression_data_for_multiple_cells_",ztype,".csv"));
    start_column_num = 4;
    end_column_num = rnd+3;
    smoothing_parameter = 0.2;
    T_presmooth = table2array(T(:,start_column_num:end_column_num));
    T_smooth = double.empty((end_column_num - start_column_num + 1),0);
    for i=1:length(T_presmooth)
        T_smooth(i,1:(end_column_num - start_column_num + 1)) =
smooth(T_presmooth(i,:),smoothing_parameter).';
    end
    T(:,start_column_num:end_column_num) = array2table(T_smooth);
writetable(T,strcat(data_folder,"/smooth_non_regression_data_for_multiple_cells_",ztype,"
.csv"));
end
for ztype = {'x_over_u'}
    savename = char(strcat("smooth_non_regression_data_",ztype,".csv"));
    pcfdata = readtable(strcat(saveFolder,'/',savename));
    pcfdata = rmmissing(pcfdata);
    pcfdata_original = pcfdata;
    pcfdata = table2array(pcfdata(:,3+1:3+rnd));
    [coeff,score,latent,tsquared,explained] = pca(pcfdata);
    explained_height = length(explained);
    num_of_factors = 0;
    for i = 1:explained_height
        sum_of_explained = sum(explained(1:i));
        if sum_of_explained < 99.9
            num_of_factors = num_of_factors + 1;
        end
    end
    score = score(:,1:num_of_factors);
    floor_Klist = 3;
    ceil_Klist = 10;
    eva1 = evalclusters(score, 'linkage', 'CalinskiHarabasz', 'KList',
[floor_Klist:ceil_Klist]);
    eva2 = evalclusters(score, 'linkage', 'DaviesBouldin', 'KList',
[floor_Klist:ceil_Klist]);
    disp(eva1.OptimalK)
    disp(eva2.OptimalK)
    if eva1.OptimalK == eva2.OptimalK
        clustering_num = eva1.OptimalK;
        clustering_method = 'both';
    else
        if eva1.OptimalK > eva2.OptimalK
            clustering_num = eva1.OptimalK;
            clustering_method = 'CalinskiHarabasz';
        else
            clustering_num = eva2.OptimalK;
            clustering_method = 'DaviesBouldin';
        end
    end
    Z = linkage(score, 'ward');
    T = cluster(Z, 'maxclust', clustering_num);
    for j = 1:clustering_num
        clusterd_num = length(T(T(:,1)==j,:));
        if clusterd_num < 0
            T(T(:,1)==j,:) = NaN;
        end
    end
    pcfdata_original = horzcat(pcfdata_original, array2table(T));
    coeff_data = horzcat(array2table(score),array2table(T));
    savename = char(strcat("clustered_smooth_non_regression_data_",ztype,".csv"));
    writetable(pcfdata_original, strcat(data_folder,'/',savename));
    writetable(coeff_data,strcat(data_folder,"/PCA_",ztype,".csv"));
```

```
end
savedirectory = strcat(root_directory,'/Analytical Model Fitting');
if ~exist(strcat(root_directory,'/Analytical Model Fitting'),'dir')
    mkdir(strcat(root_directory,'/Analytical Model Fitting'));
end
cd(savedirectory);
if ~exist(strcat(savedirectory,"/Cluster Graph"),'dir')
    mkdir(strcat(savedirectory,"/Cluster Graph"));
end
cd(strcat(savedirectory,"/Cluster Graph"));
for ztype = {'x_over_u'}
    if ~exist(strcat(savedirectory,"/Cluster Graph/tSNE"),'dir')
        mkdir(strcat(savedirectory,"/Cluster Graph/tSNE"));
    end
    cd(strcat(savedirectory,"/Cluster Graph/tSNE"));
    savename = char(strcat("smooth_non_regression_data_",ztype,".csv"));
    clustered_data =
readtable(strcat(data_folder,"/clustered_smooth_non_regression_data_",ztype,".csv"));
    T = readtable(strcat(saveFolder,'/',savename));
    Y = tsne(table2array(T(:,4:rnd+3)));
    f=figure('visible','off');
    gscatter(Y(:,1),Y(:,2),table2array(clustered_data(:,rnd+5)));
    set(f,'defaultTextInterpreter','none');
    title(strcat(ztype," tSNE by T1"),'interpreter','none');xlabel("tSNE Component
#1");ylabel("tSNE Component #2");...
        saveas(f,strcat(ztype," tSNE by T1"),'jpg');saveas(f,strcat(ztype," tSNE by
T1"),'fig')
    close();
end
for ztype = {'x_over_u'}
    if ~exist(strcat(savedirectory,"/Cluster Graph/",ztype),'dir')
        mkdir(strcat(savedirectory,"/Cluster Graph/",ztype));
    end
    cd(strcat(savedirectory,"/Cluster Graph/",ztype));
    savename = char(strcat("PCA_",ztype,".csv"));
    coeff_data = readtable(strcat(data_folder,'/',savename));
    list1 = ["score1" "score2" "score3" "score4"];
    C=nchoosek(list1,3);
    for i=1:length(C)
figure('visible','off');gscatter3b(coeff_data.(C(i,1)),coeff_data.(C(i,2)),coeff_data.(C(
i,3)),coeff_data.T);...
            title(strcat(C(i,1)," vs ",C(i,2)," vs ",C(i,3)," by
T1"));xlabel(C(i,1));ylabel(C(i,2));zlabel(C(i,3));saveas(gca,strcat(C(i,1),"_vs_",C(i,2)
,"_vs_",C(i,3),"_T1"),'jpg');saveas(gca,strcat(C(i,1),"_vs_",C(i,2),"_vs_",C(i,3),"_T1"),
'fig');
        close();
    end
    list1 = ["score1" "score2" "score3" "score4"];
    C=nchoosek(list1,2);
    for i=1:length(C)
figure('visible','off');gscatter(coeff_data.(C(i,1)),coeff_data.(C(i,2)),coeff_data.T);...
            title(strcat(C(i,1)," vs ",C(i,2)," by
T1"));xlabel(C(i,1));ylabel(C(i,2));saveas(gca,strcat(C(i,1),"_vs_",C(i,2),"_T1"),'jpg');
saveas(gca,strcat(C(i,1),"_vs_",C(i,2),"_T1"),'fig');
        close();
    end
end
disp("Bong analysis 3&4 without regression is done")
```

A10_Bong_5_Analysis.m

```
saveFolder = strcat(root_directory,'/',main_data_folder,'/master_data');
list3 = dir(saveFolder);
cd(saveFolder);
image_num_max = rnd;
graphlist = {'x_over_u'};
for i=1:length(list3)
```

```
    if contains(list3(i).name,'Position')==1 && contains(list3(i).name,'.csv')==1
        data = readtable(list3(i).name);
        data = sortrows(data,{'image_num','X_num'});
        data.x_over_u = data.max_intensity ./ data.median;
        Y_max = max(data.Y_num);
        X_max = max(data.X_num);

        saveFolder1 = strcat(root_directory,'/',graph_folder);
        saveFolder2 = strcat(saveFolder1,'/',strrep(list3(i).name,".csv",""));
        pop1_folder_dir = strcat(root_directory,'/',pop1_folder);
        popdata = readtable(strcat(pop1_folder_dir,'/pop1_label_data.csv'));
        popdata = popdata(popdata.position==max(data.position),:);
        mergedata=outerjoin(data,popdata);
        mergedata.Properties.VariableNames({'X_num_data','Y_num_data','position_data'}) =
{'X_num','Y_num','position'};
mergedata.X_num_popdata=[];mergedata.Y_num_popdata=[];mergedata.position_popdata=[];
        data = mergedata;

        background = double.empty(rnd,0);
        nocell_data = data(data.multiple ~= 1 & data.multiple ~=2,:);
        for n = 1:max(nocell_data.image_num)
            background(n,1)=mean(nocell_data.x_over_u(nocell_data.image_num==n,:));
        end
        background = flip(background - min(background));
        for j = 1:max(data.X_num)
            for k = 1:max(data.Y_num)
                for ztype={'x_over_u'}
                    if length(data.(string(ztype))(data.X_num == j & data.Y_num ==
k,:))<=(rnd)
                        data.(string(ztype))(data.X_num == j & data.Y_num == k,:) =
smooth(data.(string(ztype))(data.X_num == j & data.Y_num == k,:),0.2) +
background(1:height(data(data.X_num == j & data.Y_num == k,:)),:);
                    end
                end
            end
        end
        if ~exist(saveFolder2,'dir')
            mkdir(saveFolder2);
        end
        zscore3_max = 0;zscore3_min = 0;x_over_u_max = 1;x_over_u_min = 0;
        for var = graphlist
            if var=="zscore_maxintensity3"
                zscore3_max = max(zscore3_max, max(data.(string(var))));zscore3_min =
max(zscore3_min, min(data.(string(var))));
            end
            if var=="x_over_u"
                x_over_u_max = max(x_over_u_max, max(data.(string(var))));x_over_u_min =
max(x_over_u_min, min(data.(string(var))));
            end
            if var=="zscore_maxintensity3"
                ylim = [floor(zscore3_min),zscore3_max*1.1];
            end
            if var=="x_over_u"
                ylim = [floor(x_over_u_min),x_over_u_max*1.1];
            end
            xlim = [1, ceil(image_num_max)];
            master = figure('Position',[0,0,1024,1024],'visible','off');

            ha=tight_subplot(Y_max,X_max,[0.01 0.005],[0.03 0.08],[0.03 0.01]);
            sgtitle(strcat(strrep(var,"_"," ")," of
",strrep(strrep(list3(i).name,".csv",""),"_"," ")),'FontSize',30);
            for k=1:Y_max
                for j=1:X_max
                    if max(data.multiple(data.X_num==j & data.Y_num==k))==1
                        color = 'red';
                    else
                        if max(data.multiple(data.X_num==j & data.Y_num==k))==2
                            color = 'blue';
```

```
                        else
                            color = 'black';
                        end
                    end
                    plot(ha((k-1)*X_max+j),data.image_num(data.X_num==j &
data.Y_num==k),...
                        data.(char(var))(data.X_num==j &
data.Y_num==k),color,'LineWidth',4);
                    set(ha((k-1)*X_max+j),'YLim',ylim);
                    set(ha((k-1)*X_max+j),'XLim',xlim);
                    set(ha((k-1)*X_max+j),'YTickLabelMode','manual');
                    set(ha((k-1)*X_max+j),'XTickLabelMode','manual');
                    set(ha((k-1)*X_max+j),'FontSize',14);
                    if k == Y_max
                        set(ha((k-1)*X_max+j),'XTickLabelMode','auto');
                    end
                    if j == 1
                        set(ha((k-1)*X_max+j),'YTickLabelMode','auto');
                    end
                    grid off;
                end
            end
saveas(master,strcat(saveFolder2,'/',strrep(list3(i).name,".csv",""),"_",var),'jpg');
            close all;
            displayname=strcat("Now processing ",list3(i).name," with ",var);
            disp(displayname)
        end
    end
end
disp("individual grpahing done");
```

A11_Bong_6_Analysis.m

```
saveFolder = strcat(root_directory,'/',main_data_folder,'/master_data');
addpath(strcat(root_directory,'/Analysis Code/Matlab Plug-in M files'));
list3 = dir(saveFolder);
cd(saveFolder);
zscore1_max = 1;zscore1_min = 1;zscore2_max = 1;zscore2_min = 1;zscore3_max =
1;zscore3_min = 1;x_minus_u_max = 0;x_minus_u_min = 0;x_over_u_max = 1;x_over_u_min = 1;
image_num_max = rnd;
data_folder = strcat(root_directory,'/',main_data_folder,'/master_data');
list1 = dir(data_folder);
saveFolder1 = strcat(root_directory,'/',graph_folder,'/');
cd(saveFolder1);
for ztype = {'x_over_u'}
    xlim = [1, ceil(image_num_max)];
    count = 1;
    regression_data =
readtable(strcat(root_directory,'/',main_data_folder,'/master_data/clustered_smooth_non_r
egression_data_',ztype,'.csv'));
    if ztype=="zscore_maxintensity3"
        zscore3_max = max(zscore3_max,
max(max(table2array(regression_data(:,4:rnd+3)))));zscore3_min = min(zscore3_min,
min(min(table2array(regression_data(:,4:rnd+3)))));
    end
    if ztype=="x_over_u"
        x_over_u_max = max(x_over_u_max,
max(max(table2array(regression_data(:,4:rnd+3)))));x_over_u_min = min(x_over_u_min,
min(min(table2array(regression_data(:,4:rnd+3)))));
    end
    mkdir(strcat(saveFolder1,"categorization by ",ztype));
    mkdir(strcat(saveFolder1,"categorization by ",ztype,"/Rescaled"));
    num_cluster = max(regression_data.T);
    for p = 1:num_cluster
        if isempty(regression_data(regression_data.T==p,:))==0
            tempdata = regression_data(regression_data.T==p,:);
            Tr = table2array(tempdata(:,4:3+rnd));
```

```
            [m,n]=size(Tr);
            Tr(Tr==0) = NaN;
            if m > 0
                if ztype=="zscore_maxintensity3"
                    ylim = [floor(zscore3_min),zscore3_max];
                end
                if ztype=="x_over_u"
                    ylim = [floor(x_over_u_min),x_over_u_max];
                end
                f = figure('visible','off');
                plot(Tr');
                title(strcat("Ztype ",ztype," Category
",num2str(p)),'interpreter','none');
                ylabel('Zscore\_MaxIntensity');
                xlabel('Image\_Num');
                set(gca,'XLim',xlim);set(gca,'YLim',ylim);
                saveas(f, strcat(saveFolder1,"categorization by
",ztype,'/Category_',num2str(p)),'jpg');
                saveas(f, strcat(saveFolder1,"categorization by
",ztype,'/Category_',num2str(p)),'fig');
                close all;
            end
        end
        display("Z type "+ztype+" and category "+p+" out of "+num_cluster+" is done")
    end
end
disp("category graphing done");
```

KM_Fitting_Packages – confirm2.m

```
function dpdt2 = confirm2(t,y)
global ksol2;
a=ksol2(7);
b=ksol2(8);
c=ksol2(9);
d=ksol2(10);
e=ksol2(1);
f=ksol2(2);
ee=ksol2(3);
ff=ksol2(4);
eee=ksol2(5);
fff=ksol2(6);
dpdt2 = zeros(4,1);
dpdt2(1) = -a*y(1)*y(2)+b*y(3)+c*y(3)...
    +e*(sech(t-f).^2)+ee*(sech(t-ff).^2)+eee*(sech(t-fff).^2);
dpdt2(2) = -a*y(1)*y(2)+b*y(3)...
    +e*(sech(t-f).^2)+ee*(sech(t-ff).^2)+eee*(sech(t-fff).^2);
dpdt2(3) = a*y(1)*y(2)-b*y(3)-c*y(3);
dpdt2(4) = c*y(3)-d*y(4);
end
```

KM_Fitting_Packages – objectiveFunction2.m

```
function cost2 = objectiveFunction2(k)
global y0_filter;
global tspan;
global xu_filter;
[~,y] = ode45(@(t,y) metdp(t,y,k), tspan, y0_filter);
cost2 = sum((y(:,4) - xu_filter).^2);
end % end function, objectiveFunction
```

KM_Fitting_Packages – metdp.m

```
function dydt = metdp(t,y,k)
a=k(7);
b=k(8);
```

```
c=k(9);
d=k(10);
e=k(1);
f=k(2);
ee=k(3);
ff=k(4);
eee=k(5);
fff=k(6);
dydt = zeros(4,1);
dydt(1) = -a*y(1)*y(2)+b*y(3)+c*y(3)...
    +e*(sech(t-f).^2)+ee*(sech(t-ff).^2)+eee*(sech(t-fff).^2);
dydt(2) = -a*y(1)*y(2)+b*y(3)...
    +e*(sech(t-f).^2)+ee*(sech(t-ff).^2)+eee*(sech(t-fff).^2);
dydt(3) = a*y(1)*y(2)-b*y(3)-c*y(3);
dydt(4) = c*y(3)-d*y(4);
end
```

KM_Fitting_Packages – runOptimization_Global_2.m

```
global xu; global ksol2; global tspan; global y0_filter; global xu_filter;
root_directory = '/home/shan/local/data/km2/2020-06-17/2NBDG_50uM_Trial_3';
savedirectory = strcat(root_directory,'/Analytical Model Fitting');
addpath(savedirectory);
master_data = readtable(strcat(root_directory,'/GFP ImageJ
Analysis/master_data/clustered_smooth_non_regression_data_avgValue.csv'));
simulationfolder = 'Simulation Graphs_5 (without photobleaching)';
simulationsavefolderpath = strcat(savedirectory,'/',simulationfolder);
cd(savedirectory);
if ~exist(simulationsavefolderpath,'dir')
    mkdir(simulationsavefolderpath)
end
addpath(savedirectory);
cd(simulationsavefolderpath);
for i=1:height(master_data)
    pos = master_data.position(i); xnum = master_data.X_num(i); ynum =
master_data.Y_num(i);
    if
exist(strcat(simulationsavefolderpath,'/Pos_',num2str(pos),'_Xnum_',num2str(xnum),'_Ynum_
',num2str(ynum)),'file')==0

fopen(strcat(simulationsavefolderpath,'/Pos_',num2str(pos),'_Xnum_',num2str(xnum),'_Ynum_
',num2str(ynum)),'w+');
        fclose('all');
        display("working on Position "+pos+" Xnum "+xnum+" Ynum "+ynum+".");
        xu =
table2array(master_data(i,3+1:3+(sum(cell2mat(strfind(master_data.Properties.VariableName
s,'merge'))==1))));
        xu = xu(isnan(xu)==0);
        xu_filter = smooth(xu,0.2);
        tspan = linspace(1,length(xu_filter),length(xu_filter));
        y0_filter = [xu_filter(1);xu_filter(1);xu_filter(1);xu_filter(1)];
        k0 = [0.1;0.1;0.1;0.1;0.1;0.1;0.1;0.1;0.1;0.1]; % initial guess
        %% 10 KSOL
        A = [1 0 0 0 0 0 0 0 0 0;-1 0 0 0 0 0 0 0 0 0;...
            0 1 0 0 0 0 0 0 0 0;0 -1 0 0 0 0 0 0 0 0;...
            0 0 1 0 0 0 0 0 0 0;0 0 -1 0 0 0 0 0 0 0;...
            0 0 0 1 0 0 0 0 0 0;0 1 0 -1 0 0 0 0 0 0;...
            0 0 0 0 1 0 0 0 0 0;0 0 0 0 -1 0 0 0 0 0;...
            0 0 0 0 0 1 0 0 0 0;0 0 0 1 0 -1 0 0 0 0;...
            0 0 0 0 0 0 1 0 0 0;0 0 0 0 0 0 -1 0 0 0;...
            0 0 0 0 0 0 0 1 0 0;0 0 0 0 0 0 0 -1 0 0;...
            0 0 0 0 0 0 0 0 1 0;0 0 0 0 0 0 0 0 -1 0;...
            0 0 0 0 0 0 0 0 0 1;0 0 0 0 0 0 0 0 0 -1];
        b = [1000*(1-eps);0-eps;300;0-eps;1000*(1-eps);0-eps;300;-1;1000*(1-eps);0-
eps;300;-1;1000*(1-eps);0-eps;1000*(1-eps);0-eps;1000*(1-eps);0-eps;1000*(1-eps);0-eps;];
1000*(1-eps);0-eps;1000*(1-eps);0-eps;1000*(1-eps);0-eps;1000*(1-eps);0-eps;];
        rng default;
```

```
        opts = optimoptions(@fmincon,'Display','iter','Algorithm','interior-
point','ConstraintTolerance',1.0e-6,...
            'OptimalityTolerance',1.0e-10,'StepTolerance',1.0e-
10,'MaxIter',inf,'MaxFunEvals',inf,'FiniteDifferenceType','central'...
            ,'HessianApproximation','lbfgs');
        [ksol2,fval2,exitflag2,output2] = fmincon(@objectiveFunction2, k0, A,
b,[],[],[],[],[],opts);
        [n,m]=ode45(@confirm2,tspan,y0_filter);
        f=figure('visible','off');
        plot(n,m(:,4),n,xu_filter);
        legend('Analyitcal Model Fit','Smoothed Signal');
        title(strcat("F\_Val=",num2str(fval2)));
saveas(f,strcat(simulationsavefolderpath,'/Pos_',num2str(pos),'_Xnum_',num2str(xnum),'_Yn
um_',...
            num2str(ynum)),'jpg');
        close all;
        savek = [pos,xnum,ynum, ksol2',fval2'];
        savek = array2table(savek);
savek.Properties.VariableNames({'savek1','savek2','savek3','savek4','savek5','savek6','sa
vek7','savek8','savek9','savek10','savek11',...
            'savek12','savek13','savek14'}) =
{'position','X_num','Y_num','e','t','ee','tt','eee','ttt',...
            'k1','k2','k3','k4','f_eval'};
writetable(savek,strcat(simulationsavefolderpath,'/Ksolutions_Pos',num2str(pos),'_Xnum',n
um2str(xnum),'_Ynum',num2str(ynum),'.csv'));
end
end
```

R_Code.R

```
install.packages("dtwclust")
install.packages("TSclust")
library("dtwclust")
library("TSclust")
setwd("D:/Dropbox/Dropbox/Full Protocol Samples for scRNA sequencing/")
data <- read.csv("r_data_sampleonly.csv")
dtw_cluster <- tsclust(data, type="partitional",k=3,
                       distance="sbd",centroid = "shape",
                       seed=1234,trace=T,
                       args = tsclust_args(dist = list(window.size = 50)))

write.csv(dtw_cluster@cluster, file =
"cluster_ID(sbd)_shape_(3categories)_sampleonly.csv", quote = F, row.names = F)
```

syunghun.R

```
install.packages('BiocManager')
BiocManager::install('limma')
install.packages("philentropy")

library(Seurat)
library(patchwork)
library(ggplot2)
library(cowplot)
library(dplyr)
library(magrittr)
library(philentropy)

setwd("D:/Dropbox/Dropbox/Full Protocol Samples for scRNA sequencing")

# From folders each containing mito and exon counts txt files combine all into single txt
file
sample_vector <- dir()
sample_dir <- dir(full.names = T)
master_cnts <- matrix(data = NA, nrow = 23582, ncol = 64)
```

```
for (i in seq(length(sample_vector))) {
        cnts_vector <- dir(sample_dir[i])
        cnts_dir <- dir(sample_dir[i], full.names = T)
        cnts_1 <- read.table(file = cnts_dir[1], header = T, stringsAsFactors = F)
        cnts_2 <- read.table(file = cnts_dir[2], header = T, stringsAsFactors = F)
        cnts <- rbind(cnts_1, cnts_2)
        # Below statement is to create txt file for each samples
        # write.table(file = paste(sample_vector[i], "_cnts.merged.txt", sep = ""), x =
cnts, quote = F, row.names = T)
        assign(x = paste("cnts", sample_vector[i], sep = ""), value = cnts)
        if (i == 1) {
                rownames(master_cnts) <- cnts[,1]
                master_cnts[,1] <- cnts[,2]
                } else {
                master_cnts[,i] <- cnts[,2]
                }
        colnames(master_cnts) <- paste(1:64, "_cnts", sep = "")
}
write.table(file = "all_samples_cnts.merged.txt", x = master_cnts, quote = F, row.names =
T, )

# if calling from the made file
master_cnts <- read.table("D:/Dropbox/Dropbox/Full Protocol Samples for scRNA
sequencing/all_samples_cnts.merged.txt")
master_cnts$X63_cnts <- NULL
master_cnts$X5_cnts <- NULL
master_cnts$X6_cnts <- NULL
master_cnts$X64_cnts <- NULL

# Create Seurat object
mfd.seurat <- CreateSeuratObject(counts = master_cnts, project = "MFD", assay = "RNA")

# Normalize data with log scale
mfd.seurat <- NormalizeData(mfd.seurat, normalization.method = "LogNormalize",
scale.factor = 10000)

# Identifying highly vairable features
mfd.seurat <- FindVariableFeatures(mfd.seurat)

mfd.seurat[["percent.mt"]] <- PercentageFeatureSet(mfd.seurat, pattern = "^mt-")
mfd.seurat <- ScaleData(mfd.seurat, vars.to.regress = "percent.mt")
VlnPlot(mfd.seurat, features = c("nFeature_RNA", "nCount_RNA", "percent.mt"), ncol = 3)
plot1 <- FeatureScatter(mfd.seurat, feature1 = "nCount_RNA", feature2 = "percent.mt")
plot2 <- FeatureScatter(mfd.seurat, feature1 = "nCount_RNA", feature2 = "nFeature_RNA")
plot1 + plot2

# Perform linear dimensional reduction
mfd.seurat <- RunPCA(mfd.seurat, features = VariableFeatures(object = mfd.seurat))
#mfd.seurat <- RunPCA(mfd.seurat, npcs = 50, ndims.print = 1:5, nfeatures.print = 5)

# Plot Elbow plot for determining which PCA values are important
ElbowPlot(mfd.seurat, ndims = 50)

# Determining dimensionality of the dataset by JackStraw Plot (same as Elbow plot)
mfd.seurat <- JackStraw(mfd.seurat, num.replicate = 65)
mfd.seurat <- ScoreJackStraw(mfd.seurat, dims = 1:20)
JackStrawPlot(mfd.seurat, dims = 1:8)

# Dimensional Heat Map generation
VizDimLoadings(mfd.seurat, dims = 1:2, reduction = "pca")
DimPlot(mfd.seurat, reduction = "pca")
#DimHeatmap(mca, dims = c(1:3, 70:75), cells = 500, balanced = TRUE)
DimHeatmap(mfd.seurat, dims = 1, cells = 65, balanced = TRUE, slot = "scale.data",
disp.min = -2.5, disp.max = NULL)

DimHeatmap(mfd.seurat, dims = 1:9, cells = 65, balanced = TRUE)
DimHeatmap(mfd.seurat, dims = 3:9, cells = 65, balanced = TRUE)
```

```
# Cluster the cells
mfd.seurat <- FindNeighbors(mfd.seurat, dims = 1:10)
mfd.seurat <- FindClusters(mfd.seurat, dims.use = 1:9, resolution = 0.5, n.start = 10)
mfd.seurat <- FindClusters(mfd.seurat, dims.use = 2:9)

# Cluster using normal method like hclust
d <- dist( mfd.seurat@reductions[["pca"]]@cell.embeddings, method="euclidean")
sample_cor <- cor( Matrix::t(mfd.seurat@reductions[["pca"]]@cell.embeddings) )
sample_cor <- (1 - sample_cor) / 2
d2 <- as.dist(sample_cor)
h_euclidean <- hclust(d, method="ward.D2")
h_correlation <- hclust(d2, method="ward.D2")
#euclidean distance
mfd.seurat$hc_euclidean_5 <- cutree(h_euclidean,k = 4)
mfd.seurat$hc_euclidean_10 <- cutree(h_euclidean,k = 5)
mfd.seurat$hc_euclidean_15 <- cutree(h_euclidean,k = 6)
#correlation distance
mfd.seurat$hc_corelation_5 <- cutree(h_correlation,k = 4)
mfd.seurat$hc_corelation_10 <- cutree(h_correlation,k = 5)
mfd.seurat$hc_corelation_15 <- cutree(h_correlation,k = 6)
plot_grid(ncol = 3,
DimPlot(mfd.seurat, reduction = "pca", group.by = "hc_euclidean_5", pt.size =
4)+ggtitle("hc_euc_4"),
DimPlot(mfd.seurat, reduction = "pca", group.by = "hc_euclidean_10", pt.size =
4)+ggtitle("hc_euc_5"),
DimPlot(mfd.seurat, reduction = "pca", group.by = "hc_euclidean_15", pt.size =
4)+ggtitle("hc_euc_6"),
DimPlot(mfd.seurat, reduction = "pca", group.by = "hc_corelation_5", pt.size =
4)+ggtitle("hc_cor_4"),
DimPlot(mfd.seurat, reduction = "pca", group.by = "hc_corelation_10", pt.size =
4)+ggtitle("hc_cor_5"),
DimPlot(mfd.seurat, reduction = "pca", group.by = "hc_corelation_15", pt.size =
4)+ggtitle("hc_cor_6"))

# show the cluster number of all cells
head(Idents(mfd.seurat), 65)

# read metadata for separate cluster numbering
metadata <- read.csv("D:/Dropbox/Dropbox/Full Protocol Samples for scRNA
sequencing/meta_data_201012.csv")
# class(mfd.seurat@meta.data)
head(metadata)
# dim(mfd.seurat@meta.data)
mfd.seurat@meta.data <- cbind(mfd.seurat@meta.data, metadata)
head(mfd.seurat@meta.data)
colnames(mfd.seurat@meta.data)[14] <- "metabolic_profile"
head(mfd.seurat@meta.data)

# Run UMAP and plot
mfd.seurat <- RunUMAP(mfd.seurat, dims = 2:9)
DimPlot(mfd.seurat, reduction = "umap", group.by="metabolic_profile", pt.size = 5)
mfd.seurat <- RunUMAP(mfd.seurat, dims = 1:9)
DimPlot(mfd.seurat, reduction = "umap", group.by="metabolic_profile", pt.size = 5)
mfd.seurat <- RunUMAP(mfd.seurat, dims = 2:9)
DimPlot(mfd.seurat, reduction = "umap", pt.size = 5)
mfd.seurat <- RunUMAP(mfd.seurat, dims = 1:9)
DimPlot(mfd.seurat, reduction = "umap", pt.size = 5)


# Run tSNE and plot
mfd.seurat <- RunTSNE(object = mfd.seurat, perplexity = 20, dims = 2:9)
DimPlot(mfd.seurat, reduction = "tsne", group.by = "metabolic_profile", pt.size = 5)
mfd.seurat <- RunTSNE(object = mfd.seurat, perplexity = 20, dims = 1:9)
DimPlot(mfd.seurat, reduction = "tsne", group.by = "metabolic_profile", pt.size = 5)
mfd.seurat <- RunTSNE(object = mfd.seurat, perplexity = 20, dims = 2:9)
DimPlot(mfd.seurat, reduction = "tsne", pt.size = 5)
mfd.seurat <- RunTSNE(object = mfd.seurat, perplexity = 20, dims = 1:9)
DimPlot(mfd.seurat, reduction = "tsne", pt.size = 5)
```

```
# Plot by PCA components for the cluster
mfd.seurat <- FindClusters(mfd.seurat, dims.use = 2:9)
DimPlot(mfd.seurat, reduction = "pca", dim=c(1,2), group.by = "metabolic_profile",
pt.size = 5)
DimPlot(mfd.seurat, reduction = "pca", dim=c(3,4), group.by = "metabolic_profile",
pt.size = 5)
DimPlot(mfd.seurat, reduction = "pca", dim=c(1,2), pt.size = 5)
DimPlot(mfd.seurat, reduction = "pca", dim=c(3,4), pt.size = 5)
mfd.seurat <- FindClusters(mfd.seurat, dims.use = 1:9)
DimPlot(mfd.seurat, reduction = "pca", dim=c(1,2), group.by = "metabolic_profile",
pt.size = 5)
DimPlot(mfd.seurat, reduction = "pca", dim=c(3,4), group.by = "metabolic_profile",
pt.size = 5)
DimPlot(mfd.seurat, reduction = "pca", dim=c(1,2), pt.size = 5)
DimPlot(mfd.seurat, reduction = "pca", dim=c(3,4), pt.size = 5)


# find all markers of cluster 1
cluster1.markers <- FindMarkers(mfd.seurat, ident.1 = 1, min.pct = 0.25)
head(cluster1.markers, n = 5)
# find all markers of cluster 0
cluster0.markers <- FindMarkers(mfd.seurat, ident.1 = 0, min.pct = 0.25)
head(cluster0.markers, n = 5)
# find all markers distinguishing cluster 1 from cluster 0
cluster0.markers <- FindMarkers(mfd.seurat, ident.1 = 0, ident.2 = 1, min.pct = 0.25)
head(cluster0.markers, n = 5)

# Create Violin Plot for visualization of expression level difference in clusters
cluster1.markers <- FindMarkers(mfd.seurat, ident.1 = 0, logfc.threshold = 0.25, test.use
= "roc", only.pos = TRUE)
VlnPlot(mfd.seurat, features = c("Csde1", "Eef2","Sec61a1","Pten","Ptbp1"))
VlnPlot(mfd.seurat, features = c("Calm2", "Polr2g", "0610009D07Rik","Hmgb2","Ranbp1"))

# Create Feature Plot for the same
FeaturePlot(mfd.seurat, features =
c("Csde1","Eef2","Sec61a1","Calm2","Polr2g","0610009D07Rik"))

# Expression heatmap for given cells and features
mfd.seurat.markers <- FindAllMarkers(mfd.seurat, only.pos = TRUE, min.pct = 0.25,
logfc.threshold = 0.25)
mfd.seurat.markers %>% group_by(cluster) %>% top_n(n = 50, wt = avg_logFC)
top10 <- mfd.seurat.markers %>% group_by(cluster) %>% top_n(n = 50, wt = avg_logFC)
DoHeatmap(mfd.seurat, features = top10$gene) + NoLegend()
DoHeatmap(mfd.seurat, features = top10$gene, group.by = "metabolic_profile") + NoLegend()



# manually changing the cluster of active cluster so that we can identify cluster markers
Idents(mfd.seurat) <- "metabolic_profile"
# ident <- as.factor(mfd.seurat@meta.data[14])
# mfd.seurat@active.ident <- mfd.seurat@meta.data[14]
# mfd.seurat@active.ident <- ident
cluster1.markers <- FindMarkers(mfd.seurat, ident.1=1, min.pct = 0.25)
head(cluster1.markers, n = 5)
cluster2.markers <- FindMarkers(mfd.seurat, ident.1=2, min.pct = 0.25)
head(cluster2.markers, n = 5)
cluster3.markers <- FindMarkers(mfd.seurat, ident.1=3, min.pct = 0.25)
head(cluster3.markers, n = 5)
cluster4.markers <- FindMarkers(mfd.seurat, ident.1=4, min.pct = 0.25)
head(cluster4.markers, n = 5)
cluster5.markers <- FindMarkers(mfd.seurat, ident.1=5, min.pct = 0.25)
head(cluster5.markers, n = 5)

cluster1.markers <- FindMarkers(mfd.seurat, ident.1 = 0, ident.2 = 1, min.pct = 0.25)

mfd.seurat.markers <- FindAllMarkers(mfd.seurat, only.pos = TRUE, min.pct = 0.25,
logfc.threshold = 0.25)
```

```
mfd.seurat.markers %>% group_by(cluster) %>% top_n(n = 20, wt = avg_logFC)
top10 <- mfd.seurat.markers %>% group_by(cluster) %>% top_n(n = 20, wt = avg_logFC)
DoHeatmap(mfd.seurat, features = top10$gene) + NoLegend()

VlnPlot(mfd.seurat, features = c("Hk2","Gpi1","Pfkl","Fbp2","Pgk1"), group.by =
"metabolic_profile")
VlnPlot(mfd.seurat, features =
c("Pdha1","Pdhb","Dld","Pdhx","Cs","Aco2","Idh3a","Idh3b","Idh3g","Ogdh","Dlst","Suclg1",
"Suclg2","Sdha","Sdhb","Sdhc","Sdhd","Fh1","Mdh2"), group.by = "metabolic_profile")
VlnPlot(mfd.seurat, features = c("Ucp1","Prdm16"), group.by = "metabolic_profile")
VlnPlot(mfd.seurat, features = c("Elovl3","Tmem26","Dio2","Cidea","Atp2a2","Ryr2"),
group.by = "metabolic_profile")
VlnPlot(mfd.seurat, features =
c("Aldoa","Eno1","Eno2","Hk2","Pdk1","Pfkfb4","Pgm1","Slc2a1","Slc2a3"), group.by =
"metabolic_profile")
VlnPlot(mfd.seurat, features = c("Poglut1","Slc2a1","Tmbim6","Hk2"), group.by =
"metabolic_profile")
VlnPlot(mfd.seurat, features = c("Mdm2","Rps3","Rps7","Rpl26"), group.by =
"metabolic_profile")

DoHeatmap(mfd.seurat, features =
c("Tmem26","Pfkl","Aldoa","Eno1","Pdk1","Pgm1","Slc2a1")) + NoLegend()
```